THE REGULATION OF CHOLESTEROL ABSORPTION:

NUCLEAR HORMONE RECEPTORS AND NIEMANN-PICK C1 LIKE 1

APPROVED BY SUPERVISORY COMMITTEE

Dr. Lourdes Malú Tansey, Ph.D.

Dr. Richard G. W. Anderson, Ph.D.

Dr. Kristen W. Lynch, Ph.D.

Dr. Joyce J. Repa, Ph.D.

Dr. David J. Mangelsdorf, Ph.D.

For Mandy

THE REGULATION OF CHOLESTEROL ABSORPTION:

NUCLEAR HORMONE RECEPTORS AND NIEMANN-PICK C1 LIKE 1

by

MARK ANDREW VALASEK

DISSERTATION

Presented to the Faculty of the Graduate School of Biomedical Sciences

The University of Texas Southwestern Medical Center at Dallas

In Partial Fulfillment of the Requirements

For the Degree of

DOCTOR OF PHILOSOPHY

The University of Texas Southwestern Medical Center at Dallas

Dallas, Texas

August, 2006

ACKNOWLEDGEMENTS

THE REGULATION OF CHOLESTEROL ABSORPTION:

NUCLEAR HORMONE RECEPTORS AND NIEMANN-PICK C1 LIKE 1

Publication No. _____

Mark Andrew Valasek, Ph.D.

The University of Texas Southwestern Medical Center at Dallas, 2006

Supervising Professor: Joyce J. Repa, Ph.D.

Cholesterol plays fundamental roles in cellular physiology, but it is also involved in many pathophysiological processes including atherosclerosis, cholelithiasis, and some forms of neurodegenerative disease. The ability of mammals to selectively absorb cholesterol from the diet while largely excluding plant sterols has been known for more than 75 years, but the precise repertoire of molecular events necessary for this process are just beginning to be elucidated. Recently, several candidates have been put forth as putative intestinal cholesterol "permeases" responsible for cholesterol transport across the intestinal brush border. In addition, members of the nuclear receptor superfamily of

ligand-activated transcription factors are known to modulate expression of genes involved in cholesterol and bile acid homeostasis, and cholesterol absorption. Therefore, we wanted not only to clarify the essential molecular mechanisms by which cholesterol was absorbed, but also to investigate the potential role of nuclear receptors in regulating essential steps in this process. Here, we show that a candidate component of the cholesterol transport machinery, caveolin-1 (CAV1), is neither required for intestinal cholesterol transport or sensitivity to the novel cholesterol absorption blocking agent, ezetimibe. This rules out a critical role for caveolin-1 and lends further support to the contention that Niemann-Pick C1 like 1 (NPC1L1) is the bona fide intestinal cholesterol permease. Therefore to better understand new ways in which nuclear receptors could regulate cholesterol absorption, we studied nuclear receptor regulation of NPC1L1 and determined that several nuclear receptors could modulate its expression in small intestine, including peroxisome proliferator-activated receptor alpha (PPARα) and retinoid X receptor (RXR). Thus, cholesterol absorption can be regulated by nuclear receptor modulation of NPC1L1 expression.

TABLE OF CONTENTS

PRIOR PUBLICATIONS

Xiong, Y., N. Miyamoto, K. Shibata, M. A. Valasek, T. Motoike, R. M. Kedzierski, and M. Yanagisawa. 2004. Short-chain fatty acids stimulate leptin production in adipocytes through the G protein-coupled receptor GPR41. *Proc Natl Acad Sci.* 101: 1045-1050.

Li, H., J. J. Repa, M. A. Valasek, E. Beltroy, S. D. Turley, D. C. German, and J. M. Dietschy. Molecular, anatomical and biochemical events associated with neurodegeneration in mice with Niemann-Pick Type C disease. *J Neuropathol Exp Neurol* 2005 Apr;64(4):323-33.

Valasek, M. A., J. Weng, P. W. Shaul, R. G. W. Anderson, and J. J. Repa. Caveolin-1 is not Required for Murine Intestinal Cholesterol Transport. *J Biol Chem*. 2005 Jul 29;280(30):28103-9. Epub 2005 May 26.

Valasek, M. A., J. J. Repa. The Power of Real-Time PCR. *Adv Physiol Educ.* 2005 Sep;29(3):151-9.

Valasek, M. A., S. L. Clarke, and J. J. Repa. Fenofibrate Reduces Intestinal Cholesterol Absorption via PPARα-dependent Modulation of NPC1L1 Expression in Mouse. (2006) (submitted)

LIST OF FIGURES

LIST OF TABLES

LIST OF ABBREVIATIONS

ABC, ATP-binding cassette transporter

ACAT2, acyl-CoA:cholesterol acyltransferase-2

ACOX1 (or ACO), acyl CoA oxidase 1

ANGPTL3, angiopoietin-like protein 3

ANXA2, annexin-2

AP4, activating enhancer-binding protein 4

APN, aminopeptidase N

ApoA1, apolipoprotein AI

ApoB48, apolipoprotein B48

ApoB100, apolipoprotein B100

AR, androgen receptor

BBB, blood brain barrier

BSEP (or ABCB11), bile salt export pump

CAR, constitutive adrostane receptor

CAV1, caveolin-1

CDCA, chenodeoxycholic acid (FXR agonist)

CE, cholesteryl ester

CYP, cytochrome P450

ChIP, chromatin immunoprecipitation

ChREBP, carbohydrate-responsive element binding protein

CM, chylomicrons

CMr, chylomicron remnant particles

DR4, direct repeat with 4 nucleotide spacer

E47, transcription factor E2a

EBVR, Epstein-Barr virus transcription factor R

ER, endoplasmic reticulum or estrogen receptor

EST, expressed sequence tag

EZ, ezetimibe

FA, fatty acids

FABP6 (or IBABP), fatty acid binding protein 6

FAS, fatty acid synthase

FXR, farnesoid X receptor

GR, glucocorticoid receptor

GW0742, a synthetic PPARδ agonist

HDL, high-density lipoprotein

HMG-CoA, β-hydroxy-β-methylglutaryl-CoA

HMG-CoA Red, β-hydroxy-β-methylglutaryl-CoA reductase

HMG-CoA Syn, β-hydroxy-β-methylglutaryl-CoA synthase

HNF1, hepatic nuclear factor 1

HNF4, hepatocyte nuclear factor 4

HSF, heat shock factor

IBABP (or FABP6), ileal bile acid binding protein

IBAT (or SLC10A2), ileal bile acid transporter

IK3, ikaros 3

INSIG, insulin-induced gene

IR1, inverted repeat with one nucleotide spacer

LCA, lithocholic acid

LCAT, lecithin cholesterol acyltransferase

LDL, low-density lipoprotein

LDLR, low-density lipoprotein receptor

LRH-1, liver receptor homolog 1

LXR, liver X receptor

mpk, mg per kg body weight

MR, mineralocorticoid receptor

MTP, microsomal triglyceride transfer protein

MyoD, myogenic differentiation (determination)

NF-κB, nuclear factor kappa B

NPC, Niemann-Pick Type C

NPC1L1, Niemann-Pick C1 like 1

NTCP, sodium taurocholate cotransporter

OSTα/β, organic solute transporters

PBX, pre B-cell leukemia transcription factor

PCR, polymerase chain reaction

PMF, proton motive force

PPAR, peroxisome proliferator-activated receptor

PR, progesterone receptor

PUFA, polyunsaturated fatty acids

PXR, pregnane X receptor

qRT-PCR (or qPCR), quantitative real-time PCR

RAR, retinoic acid receptor

RND, resistance-nodulation-division

ROS, reactive oxygen species

RORα/β, retinoid-related orphan receptors

RFX, regulatory factor X

RXR, retinoid X receptor

S1P, site 1 protease

S2P, site 2 protease

SCAP, sterol cleavage-activating protein

SCD1, steroyl-CoA desaturase 1

SHP, small heterodimer partner

SLC10A2 (or IBAT), ileal bile acid transporter

SREBP, sterol regulatory element-binding protein

SSD, sterol-sensing domain

STAT, signal transducer and activator of transcription

SR-BI, scavenger receptor class B type I

T0901317, "T-compound" (a synthetic LXR agonist)

T_3, triiodothyronine

T3R (or TR), thyroid hormone receptor

TCF8 (or AREB6), transcription factor 8

TCPOBOP, 1,4-bis[2-(3,5-dichloropyridyloxy)]benzene (CAR agonist)

TG, triglycerides

TM, transmembrane

TTNPB, 4-[(E)-2-(5,6,7,8-tetrahydro-5,5,8,8-tetramethyl-2-naphthalenyl)-1-propenyl]

benzoic acid (RAR agonist)

VDR, vitamin D receptor

VLDL, very low-density lipoprotein

WY-14643, PPARα agonist [[4-chloro-6-[(2,3-dimethylphenyl)amino]-2-

pyrimidinyl]thio]-acetic acid

CHAPTER 1

Introduction

1.1 THE CHOLESTEROL MOLECULE

Cholesterol was first discovered in gallstones in 1784, and has since been found to be important in cellular physiology, serving not only structural roles in cell membranes but also non-structural roles via binding to a variety of proteins. In contrast, cholesterol has also been implicated in cardiovascular disease, cholelithiasis, and several neurodegenerative diseases. Since plasma levels of low-density-lipoprotein (LDL)-cholesterol strongly correlate with incidence of coronary heart disease, much effort has been directed at developing and implementing therapies to lower plasma LDL-cholesterol to ever-lower levels (Grundy et al., 2004). Indeed, genetic evidence suggests that life-long lowering of plasma LDL-cholesterol could be beneficial (Cohen et al., 2006a). Statins, which inhibit the first irreversible reaction in *de novo* synthesis of cholesterol, have become a mainstay for lowering plasma LDL-cholesterol in patients. However, with the increasing need for enhanced reductions in plasma lipids, new therapies that could augment statins are needed. This situation gave impetus for the discovery of a novel cholesterol absorption-blocking agent, ezetimibe. The existence of this potent inhibitor, along with other evidence, suggested that an intestinal cholesterol permease was responsible for uptake of cholesterol into the body. Mammals selectively absorb

1

cholesterol, but the molecular events necessary for this process are just beginning to be elucidated.

1.1.1 Structure of Cholesterol

Cholesterol consists of a four-ring steroid nucleus with an attached hydroxyl group at C3 and an alkyl side chain at C17 (Figure 1.1). Cholesterol is therefore a member of the group of steroids termed sterols, because they contain both the steroid nucleus and an alcohol group. The polar alcohol group allows cholesterol to be amphipathic, although aqueous solubility is extremely poor due to the non-polar steroid nucleus and long alkyl side chain. Because of its amphipathic nature, cholesterol is capable of insinuating into plasma membranes and the surface of lipoprotein particles.

Sterols are present in eukaryotes, while prokaryotes generally lack sterols. Stigmasterol (and other plant sterols) and ergosterol are found in plants and fungi, respectively, while cholesterol is the predominant sterol in animal tissues constituting approximately 25% of the mass of plasma membranes. Mammals synthesize cholesterol and readily absorb cholesterol from the diet, but generally exclude plant sterols from being absorbed. The molecular basis for this observation is discussed later (see Phases and Molecular Mechanisms of Intestinal Cholesterol Absorption).

1.1.2 Biosynthesis of Cholesterol

Cholesterol is a complex small molecule and the biochemical pathway for *de novo* synthesis has been elucidated and involves more than 30 enzymes. Suprisingly, all 27 carbons that make up cholesterol are derived exclusively from acetyl-CoA molecules after their conversion to isoprene subunits. Cholesterol synthesis proceeds by condensation of simple acetyl-CoA units to mevalonate, mevalonate conversion to isoprene, isoprene polymerization to squalene, then squalene cyclization leading to formation of the steroid nucleus and eventually the cholesterol molecule itself.

To begin cholesterol synthesis, 2-carbon acetyl-CoA groups must be obtained by oxidation of fattys acids or other means. Two acetyl-CoA groups are joined by thiolase to form acetoacetyl-CoA, and then another acetyl-CoA is added by β-hydroxy-β-methylglutaryl-CoA (HMG-CoA) synthase to generate HMG-CoA. HMG-CoA reductase catalyzes the first committed (irreversible) step by converting HMG CoA to mevalonate. Statins act by competitively inhibiting this key step. After its formation, mevalonate is triply phosphorylated by enzymes utilizing phosphates from three ATP molecules resulting in 3-phospho-5-pyrophosphomevalonate. This activated form of mevalonate loses both a phosphate and a carboxyl group to form a 5-carbon activated isoprene, called delta-3-isopentenyl pyrophosphate, which can isomerize to dimethylallyl pyrophosphate. In the following steps, six isoprene subunits condense to form squalene. First, prenyl transferase condenses two isoprenes to form geranyl pyrophosphate, and then a third isoprene to form farnesyl pyrophosphate. Second, squalene sythase condenses two 15-carbon farnesyl pyrophosphate molecules to form squalene. To become a sterol, squalene must gain an alcohol and the steroid nucleus. Squalene

monooxygenase uses molecular oxygen (O_2) to add an oxygen atom to squalene in the form of an epoxide creating squalene-2,3-epoxide. This enables cyclization of the steroid nucleus to form lanosterol, which is the direct sterol precursor to cholesterol.

Cholesterol synthesized by the liver (or other tissues) in this way can be utilized directly as a component of cellular membranes or esterified by acyl-CoA:cholesterol acyl transferase 2 (ACAT2), the primary isoform in hepatocytes (Parini et al., 2004), to form non-polar cholesteryl esters. Esterified cholesterol is ideal for storage in lipid droplets or packaging in the core of lipoprotein particles for transport in plasma. In contrast, free or unesterified cholesterol, being amphipathic, is useful in cellular membranes or on the surface of lipoprotein particles, but is very difficult (and detrimental) for the cell to store in this form. Although cholesterol cannot be catabolized *per se*, it can be oxidized to various oxysterols thereby decreasing its hydrophobicity and enhancing its excretion from the cell. Cholesterol can also be converted into bile acids or steroid hormones. Conversion of cholesterol to bile acids is a major pathway for removal of cholesterol from the body. Hepatic cholesterol is exported in one of several ways. Cholesterol can be directly secreted into bile, converted to bile acids for secretion into bile, or esterified and incorporated into very low-density lipoprotein (VLDL) particles for secretion into the circulation.

1.1.3 Regulation of Cholesterol Biosynthesis

Cholesterol biosynthesis occurs primarily in the liver but also in peripheral tissues. Sterol regulatory element-binding protein 2 (SREBP-2) is a transcription factor that controls the transcription of several enzymes in the cholesterol biosynthetic pathway by becoming activated when cellular cholesterol is depleted. Its targets represent at least 15 enzymes in the cholesterol biosynthetic pathway, including HMG-CoA synthase and HMG-CoA reductase (Horton et al., 2002). When cellular cholesterol is replete, sterol cleavage-activating protetin (SCAP) tethers SREBP to insulin-induced gene (Insig) proteins, which act as anchors in the endoplasmic reticulum (ER), causing the entire complex to be retained in the ER (Rawson, 2003). When cholesterol is depleted, SREBP is released from the complex and translocates to the Golgi, where it is sequentially cleaved by two proteases (Site 1 protease (S1P) and S2P) to release a mature transcription factor that can move to the nucleus and perform its function (Brown and Goldstein, 1997).

Cellular cholesterol excess is not only monitored by SCAP to prevent SREBP maturation, but also by HMG-CoA reductase, which is quickly degraded when cellular cholesterol levels are high thereby enabling negative feedback regulation of the first irreversible step of cholesterol biosynthesis (Sever et al., 2003). Excess cholesterol is additionally monitored by a member of the nuclear hormone receptor superfamily of ligand-activated transcription factors, the liver X receptors (LXRs). LXRs respond to cholesterol derivatives, called oxysterols, which bind and activate these nuclear receptors (Janowski et al., 1999; Janowski et al., 1996). LXRs promote expression of transporters that enhance cellular cholesterol efflux (e.g. ATP-binding cassette transporters), enzymes

that convert cholesterol to its derivatives (e.g. CYP7A1, CYP8B1), transcription factors that enhance fatty acid biosynthesis (i.e. SREBP-1c), and steroyl-CoA desaturase 1 (SCD-1) to provide oleic acid for sterol esterification. Therefore, LXR activation enhances the expression of gene products that relieve intracellular cholesterol excess, and synthetic LXR ligands hold promise as drugs for the treatment of atherosclerosis (Jaye, 2003; Peet et al., 1998; Repa et al., 2002a; Repa et al., 2000a; Repa and Mangelsdorf, 2002; Repa et al., 2000c). The potential role(s) of LXRs in direct regulation of cholesterol biosynthesis has not yet been elucidated, however oxysterols themselves seem to prevent maturation of SREBP (Horton et al., 2002).

1.1.4 Endogenously Synthesized Derivatives of Cholesterol

Bile acids are amphipathic molecules, synthesized in the liver from cholesterol, that are crucial for micellar solubilization of fats and fat-soluble molecules in the intestinal lumen prior to absorption. Bile acids are more hydrophilic than cholesterol because of additional polar groups attached to the steroid nucleus or the carbon side chain. The rate-limiting enzyme for the classical pathway of bile acid synthesis is CYP7A1, which is transcriptionally regulated by nuclear receptors.

Steroid hormones are derived from cholesterol, converted to pregnenolone then progesterone, and synthesized primarily in the adrenal gland and gonads. The cortex of the adrenal gland takes up cholesterol esters, primarily by an SR-BI-mediated pathway, and ultimately converts cholesterol into glucocorticoids (i.e. cortisol) or

mineralocorticoids (i.e. corticosterone and aldosterone; Figure 1). The testes synthesize testosterone, although conversion to the more potent dihydroxytestosterone generally occurs in the target tissues. The ovaries and placenta synthesize estradiol.

Oxysterols are present at very low levels relative to cholesterol in mammalian systems. They are derived either from nonezymatic oxygenation of cholesterol by reactive oxygen species (ROS) or conversion of cholesterol by a number of cholesterol oxidases, the most important of which are members of the cytochrome P-450 family (Bjorkhem, 2002). Oxygenation of cholesterol drastically reduces its half-life and enhances its ability to cross cellular membranes for excretion (Lange et al., 1995). Many of these oxygenation reactions are intermediate steps in the synthesis of steroid hormones or bile acids. Several naturally-occurring oxysterols are potent ligands for the liver X receptors (LXRs) including 22(*R*)-hydroxycholesterol, 24(*S*)-hydroxycholesterol, and 24(*S*),25-epoxycholesterol (Janowski et al., 1999; Janowski et al., 1996; Lehmann et al., 1997).
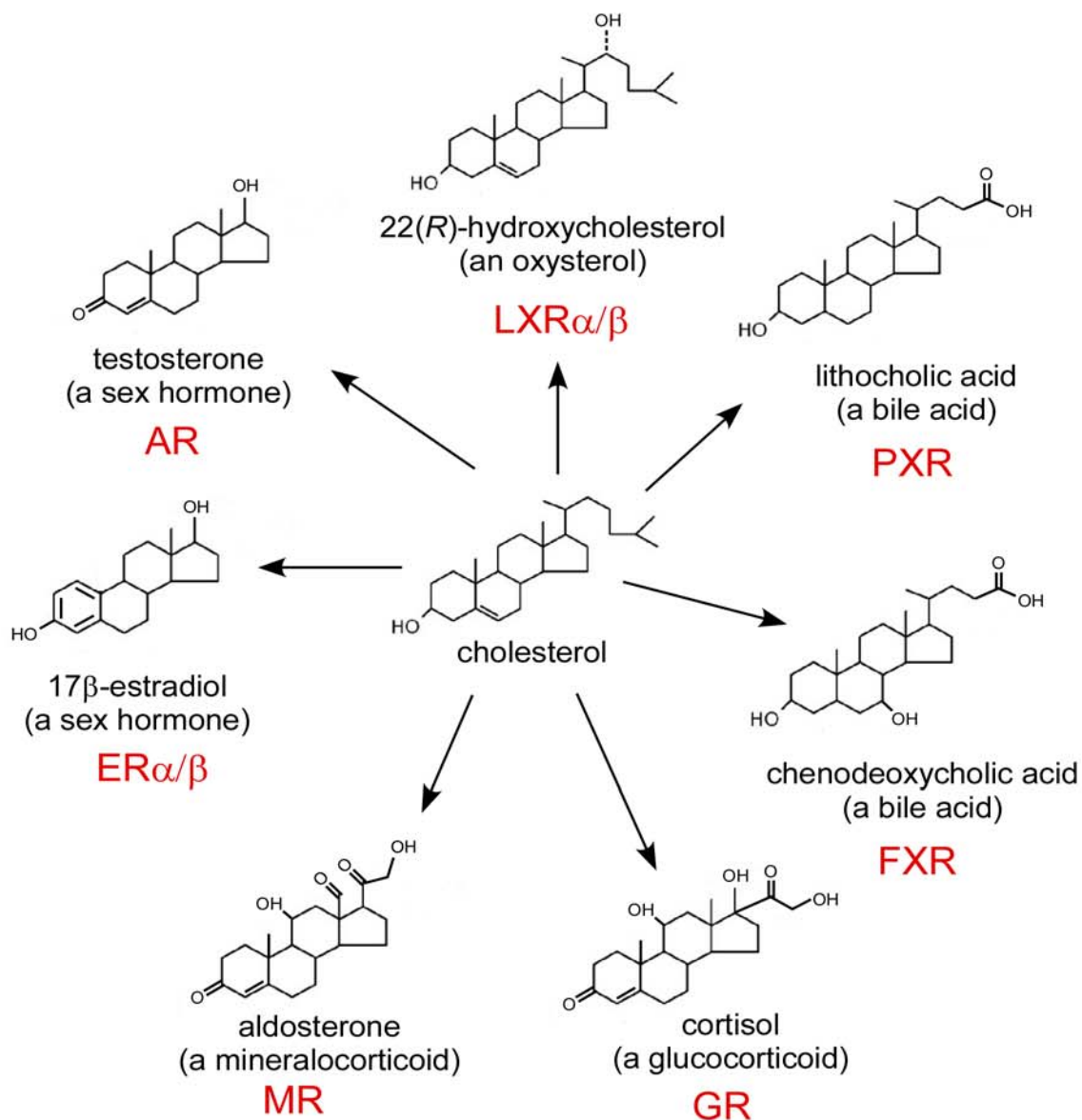
Figure 1.1 Cholesterol derivatives are ligands for nuclear receptors.
Many cholesterol derivatives can function as ligands for nuclear hormone
receptors including sex hormones, mineralocorticoids, glucocorticoids,
oxysterols, and bile acids. Abbreviations denote cognate receptor of
depicted ligands as follows: AR, androgen receptor; ERα/β, estrogen
receptors; FXR, farnesoid X receptor; GR, glucocorticoid receptor;
LXRα/β, liver X receptor; MR, mineralocorticoid receptor, PXR, pregnane
X receptor.

1.2 INTRODUCTION TO CHOLESTEROL ABSORPTION

1.2.1 A Brief History of Cholesterol Absorption

Rudolph Schoenheimer is considered the father of molecular biochemistry and developed the methods which led to radioisotopic labeling of biomolecules to trace their itenerary through the body or synthesis within, thus enabling study of intermediary metabolism. One molecule of particular interest to him was the four-ringed cholesterol molecule, which he discovered to be selectively absorbed in mammals (Klett and Patel, 2004). He also discovered that cholesterol, although a complex molecule, was indeed synthesized and degraded in the body. His general dynamic steady state theory was advanced in the posthumously published (1942) book based on his lecture entitled, "The Dynamic State of Body Constituents," which stood in contrast to the prevailing view of the static constitution of the body. Konrad Bloch, who worked with Schoenheimer, spear-headed elucidation of the cholesterol biosynthetic pathway (see Biosynthesis of Cholesterol), and because of his work shared a Nobel Prize, with Feodor Lynen, in 1964. The molecular basis for understanding the absorption selectivity that Schoenheimer observed would have to wait until after the discovery of the genes responsible for sitosterolemia (Berge et al., 2000) and development of a novel cholesterol absorption blocking agent, ezetimibe (Rosenblum et al., 1998; Van Heek et al., 1997), and discovery of its target (Altmann et al., 2004; Garcia-Calvo et al., 2005).

1.2.2 Cholesterol Absorption and Transport and the Enterohepatic Circulation of Bile Acids

The liver synthesizes bile acids (including cholic acid and chenodeoxycholic acid in humans) from cholesterol and secretes them into the bile via the canalicular bile salt export pump (BSEP, ABCB11; reviewed in (Trauner and Boyer, 2003)). Bile acids can directly enter the duodenum via the hepatic duct, common bile duct, and then the sphincter of Oddi, or can be temporarily stored in the gall bladder by traversing the hepatic duct then the cystic duct. Upon entrance of chyme into the duodenum, cholecystokinin stimulates the smooth muscle of the gall bladder to contract thereby facilitating emptying of bile into the duodenum. In any case, the bile synthesized by the liver enters the intestinal lumen performing the important function of micellar solubilization of fats, cholesterol, and other fat-soluble molecules that facilitates intestinal absorption of these molecules. Bile acids travel along the gastrointestinal tract being partially absorbed, however in the ileum there are active transporters that allow reclamation of approximately 95% of the bile acids present in the intestinal lumen. This active transport process is fulfilled by the apical transporter of bile acids, ileal bile acid transporter (IBAT, Slc10a2), the intracellular binding protein, ileal bile acid binding protein (IBABP, FABP6), and the basolateral bile acid pumps, organic solute transporters α and β (Ostα/β), which may be able to pump bile acids directly into the portal circulation for transport directly back to the liver (Dawson et al., 2005).

The itinerary for cholesterol is more complex than that of bile acids, perhaps because cholesterol is needed by all cells as a component of membranes whereas bile

acids are needed primarily as a means to solubilize fat and cholesterol within the intestine, and indirectly allow for removal of cholesterol from the body. Overall, there is a net movement of cholesterol from peripheral sites of synthesis toward the liver, which is largely responsible for excretion of cholesterol.

On a "normal" Western diet, approximately 300-500 mg of cholesterol is ingested. In addition, 800-1300 mg of biliary cholesterol is secreted into the intestinal lumen (Turley and Dietschy, 2003). Of the total 1100-1800 mg cholesterol present daily in the intestinal lumen, approximately 50% is absorbed, although there are wide inter-individual variations in cholesterol absorption that might possibly be explained by differences in NPC1L1 sequence (Cohen et al., 2006b), a candidate for the intestinal cholesterol permease. Cholesterol (along with large amounts of triacylglycerols (TG)) is packaged into chylomicrons (CMs) within the intestinal epithelial cells for secretion into the lymph. Ultimately, the mesenteric lymphatics anastomose to join the thoracic lymphatic duct, which then connects to the general circulation via the left subclavian vein. CMs then circulate, delivering triacylglycerols to tissues that harbor lipoprotein lipases, which hydrolyze TG to glycerol and fatty acids for uptake and utilization. After the CM is largely depleted of TG, it becomes a CM remnant (CMr) particle, which is recognized and taken up by the liver. The relative atherogenicity of CM and CMr is debated, although there seems to be increasing evidence for its involvement in atherosclerotic lesion formation in the ApoE knockout mouse, a common model of atherosclerosis (Davis et al., 2001a). The liver also takes up cholesterol and cholesteryl esters from LDL and HDL particles, in addition to synthesizing cholesterol from acetyl-

CoA units by the previously described pathway. Cholesterol can then be excreted either by direct secretion into bile via ABCG5/8, or conversion into bile acids via the enzyme CYP7A1, and secretion into bile via BSEP (ABCB11). Biliary cholesterol and dietary cholesterol enter the intestinal lumen where a portion is excreted, thus maintaining cholesterol homeostasis.

There are at least two other pathways by which cholesterol can travel. First, the liver can package cholesterol along with large amounts of TG into VLDL particles to be secreted into the circulation. Depletion of TG within VLDL increases the density of these particles to become LDL. High levels of plasma LDL are strongly associated with coronary heart disease. LDL is taken back up by the liver in a process called "receptor-mediated endocytosis" (reviewed in (Brown and Goldstein, 1986)). A specific receptor in the liver, LDL receptor (LDLR), recognizes a protein component of the LDL particle (i.e. apoB-100) and initiates endocytosis of LDL. The particle is trafficked to the lysosomes in which cholesteryl esters present within LDL are hydrolyzed into unesterified cholesterol and fatty acids. This process for clearance of LDL was discovered by Michael Brown and Joseph Goldstein, and earned them the Nobel Prize in Physiology or Medicine in 1985. Part of the mechanism of action of statins is to cause the upregulation of LDLR in the liver thereby enhancing clearance and lowering plasma concentration of LDL. Second, the liver (and intestine) can generate nascent high-density lipoprotein (HDL) to secrete into the circulation, where it collects free cholesterol from tissues, esterifies it with an enzyme called lecithin-cholesterol acyl transferase (LCAT), then stores it within the core of the particle for return to the liver. The liver takes up

HDL cholesteryl esters via the scavenger receptor BI (SR-BI). This is the major pathway by which cholesterol moves from peripheral tissues to the liver for excretion.

1.2.3 Phases and Molecular Mechanisms of Intestinal Cholesterol Absorption

There are three main phases in the process of intestinal absorption of cholesterol: (1) the intraluminal phase, (2) transmembrane phase (uptake and efflux), and (3) intracellular phase (Figure 1.2). "Intestinal absorption of cholesterol" is defined as the transfer of intraluminal cholesterol into the intestinal or thoracic duct lymph, whereas "uptake of cholesterol" specifically refers to entry of cholesterol into intestinal epithelia (Lammert and Wang, 2005).

1.2.3.1 Intraluminal Phase

The intraluminal phase consists of all the events prior to transfer of cholesterol across the enterocytic apical membrane. Dietary cholesterol largely consists of unesterified cholesterol, however the portion that is esterified is hydrolyzed to cholesterol and fatty acids by pancreatic cholesterol esterase present in pancreatic juice, which is secreted into the duodenum via the common bile duct. As its name implies, bile is also secreted into the duodenum via this duct. Bile contains cholesterol, phospholipids, and bile acids. Because of their amphipathic nature, the bile acids, primarily cholic acid and chenodeoxycholic acid and their taurine- and glycine-conjugated derivatives (Russell,

1999), along with phospholipids promote the micellar solubilization of cholesterol (along with fatty acids and monoacylglycerols). This is a critical step in the absorption process as cholesterol is nearly insoluble in water, and is therefore unable to cross the unstirred water layer that covers the brush border of the intestinal epithelia (Turley and Dietschy, 2003). In contrast, hydrolyzed triacylglycerols (i.e. fatty acids, monoacylglycerols) can cross this barrier more efficiently. Finally, the mixed micelles disaggregate at the brush border membrane to deliver cholesterol to the membrane.

Various intraluminal events can be affected by oral administration of agents to decrease delivery of cholesterol. These agents include cholestyramine, orlistat, olestra, and plant sterols or stanols. Cholestyramine functions as a bile-acid sequestrant which not only decreases micellar solubilization of cholesterol (thereby decreasing delivery to the brush border), but also prevents the reuptake of bile acids in the ileum thereby enhancing bile acid excretion. As bile acids are derived from cholesterol, both of these actions can serve to decrease plasma cholesterol levels. Orlistat is a lipase inhibitor that is used to block triglyceride absorption, while olestra is a poorly absorbed fat substitute. Both of these agents increase the luminal quantity of triglycerides, which could then promote retention of the hydrophobic cholesterol molecule in the small intestinal lumen. Plant sterols and stanols are known to inhibit micellar solubilization of cholesterol (Nissinen et al., 2002), however they may also have effects on other phases of absorption.

In addition to the effects of these inhibitors of cholesterol absorption, genetic manipulation of intraluminal events can influence delivery of cholesterol to the intestinal brush border. For example, mice lacking pancreatic cholesterol esterase show decreased

absorption of esterified cholesterol but not free cholesterol (Howles et al., 1996), demonstrating the importance of this enzyme in hydrolyzing cholesterol esters. Because esterified cholesterol normally makes up only a small portion of the diet, the loss of this gene in a natural setting may only have a minor effect on overall cholesterol absorption. In contrast, *Muc1*-deficient mice, which lack a mucin component of the surface mucous coat beneath the unstirred water layer, display approximately 50 percent decreased cholesterol absorption efficiency (Wang et al., 2004). This adds yet another element to the process of intraluminal events necessary for cholesterol delivery to the brush border, that of passage through the mucous coat.

1.2.3.2 Transmembrane Phase (Uptake and Efflux)

The transmembrane phase should be described as "cholesterol transport" or "uptake of cholesterol," rather than "cholesterol absorption" which refers to the entire process of cholesterol entry into the body. Because of its hydrophobicity, cholesterol has long been believed to diffuse passively across the apical membrane of enterocytes. However, several lines of evidence suggest that cholesterol transport is a protein-mediated process, and thus the existence of an intestinal cholesterol "permease" has been postulated (Turley and Dietschy, 2003). Several candidate proteins have been proposed (see below), however evidence is accumulating that Niemann-Pick C1 Like 1 (NPC1L1) is a critical functional component in cholesterol transport (Altmann et al., 2004; Davies et al., 2005). Also present in the apical membrane are proteins, named ABCG5 and

ABCG8, which oppose cholesterol import by effluxing cholesterol (and plant sterols) back into the intestinal lumen. These proteins are mutated in the disease sitosterolemia (Berge et al., 2000) in which plant sterols are absorbed and plasma levels of plant sterols (and cholesterol) are markedly increased. Studies of mice lacking or overexpressing these genes further confirm the role of ABCG5/8 in cholesterol and plant sterols efflux (Yu et al., 2002a; Yu et al., 2002b). Thus, proteins mediate bidirectional movement of cholesterol across the apical membrane.

One implication of the finding that plant sterol efflux is important to prevent disease is that there must be a plant sterol importer (or some other mechanism) to allow entry in the first place. Small doses of the drug ezetimibe block cholesterol absorption (>90%) at the level of the membrane suggesting not only that this is a protein-mediated process, but that ezetimibe-independent pathways (including passive diffusion) may account for only a small portion of the total amount of cholesterol absorbed. Indeed, ezetimibe can prevent disease in sitosterolemic mice by inhibiting plant sterol absorption (Yu et al., 2005) suggesting that the cholesterol transporter is also responsible for transporting non-cholesterol sterols (i.e. plant sterols). This ezetimibe-dependent pathway likely involves NPC1L1 as knockout mice show greater than 70% reduced cholesterol absorption and are insensitive to ezetimibe (Altmann et al., 2004; Davis et al., 2004). Moreover, NPC1L1-expressing cells specifically bind ezetimibe suggesting that the drug targets this protein to block cholesterol transport (Garcia-Calvo et al., 2005).

1.2.3.3 Intracellular Phase

Many of the events that are necessary for cholesterol trafficking within the enterocyte are well known, however the least understood are those that occur just after the transmembrane phase. In particular, it is not yet clear whether cholesterol moves into the enterocyte via vesicular or non-vesicular transport. What is known is that the cholesterol is delivered to the endoplasmic reticulum (ER) where it is esterified to a fatty acid by the enzyme, ACAT2. Cholesteryl esters can then be incorporated into nascent chylomicrons along with unesterified cholesterol (20-30% of total cholesterol), apolipoprotein-B$_{48}$ and vast amounts of triglyceride. After the nascent chylomicron particle is formed, it is secreted into the lymph for eventual transport to the circulation. Microsomal triglyceride transfer protein (MTP) is crucial for the process of chylomicron maturation in the enterocyte (and VLDL formation in the hepatocyte). A recent study has shown that mice which specifically lack MTP in intestine have massive accumulation of triglycerides in the intestinal parenchyma and also show decreased cholesterol absorption, steatorrhea, and growth arrest (Xie et al., 2006). In addition, both *apolipoprotein-B48 (apo-B48)*-knockout and "apo-B100 only" mice also have decreased cholesterol absorption due to failure to assemble or secrete chylomicrons (Wang and Wang, 2005; Young et al., 1995). In contrast, mice lacking ACAT2 show near normal cholesterol absorption on a basal diet (low cholesterol, low fat) whereas cholesterol absorption is modestly decreased on a lipid-rich diet (Buhman et al., 2000; Repa et al., 2004a).

Unesterified cholesterol is a critical component of the surface of chylomicrons, however mice on a cholesterol-free diet are not growth-arrested and therefore are presumably able to assemble and secrete chylomicrons into the lymph. The explanation may be that enterocytes can synthesize cholesterol from acetate as needed. Studies in mice suggest that rates of sterol synthesis in intestine and liver are responsive to dietary cholesterol (Jolley et al., 1999). It is interesting to note that HMG-CoA reductase inhibitors inhibit cholesterol absorption in rats, rabbits, and humans (Hajri et al., 1995; Nielsen et al., 1993; Vanhanen et al., 1992). This could be due to less efficient synthesis of chylomicrons, or other plieotropic effects of statins (see CHAPTER 3: Discussion).
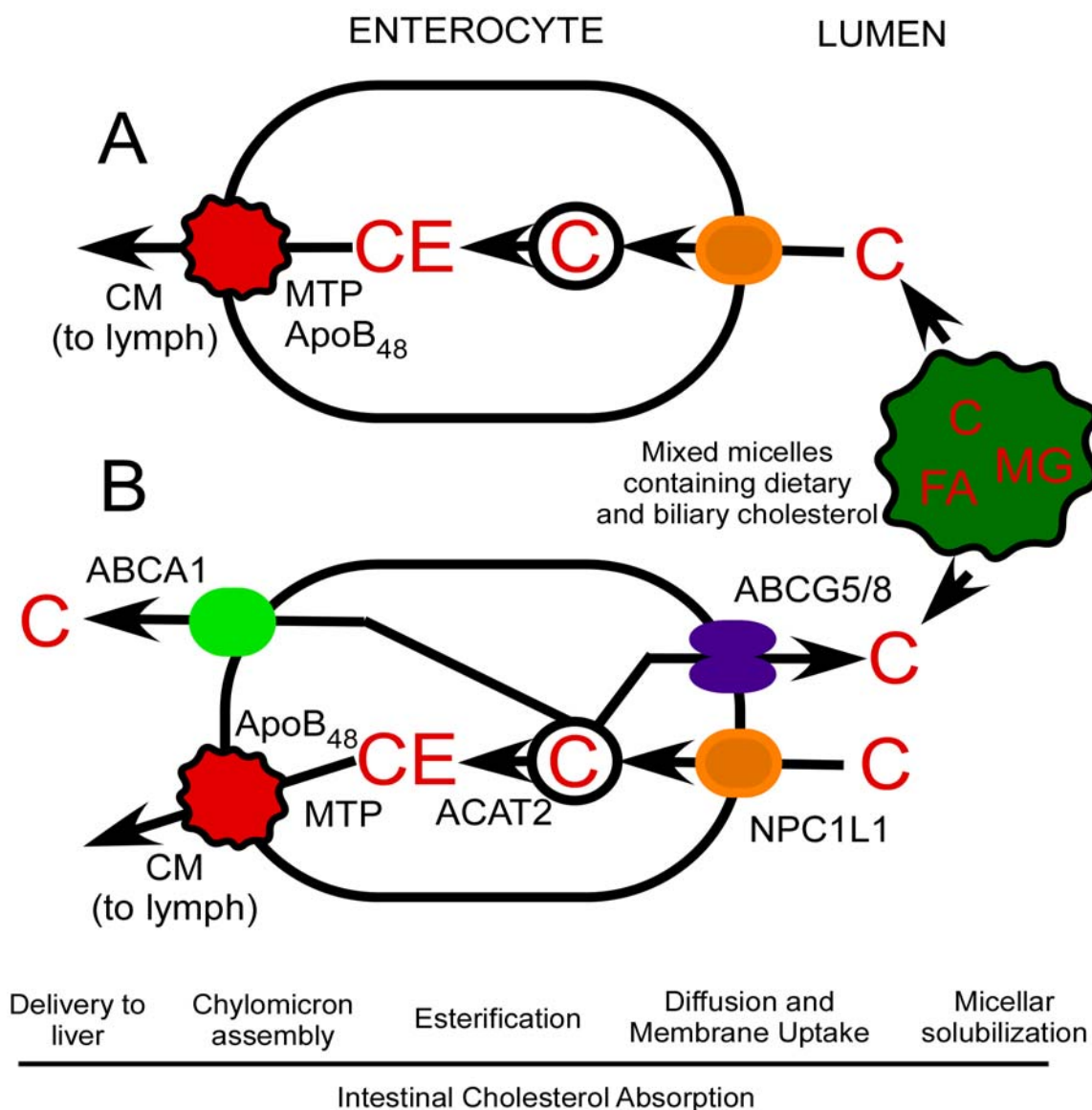
Figure 1.2 Proteins involved in intestinal cholesterol absorption.
Cholesterol (C) solubilized in mixed micelles (with fatty acids (FA) and monoacylglycerol (MG)) diffuses to the enterocyte membrane and is taken up by the enterocyte where it is esterified to form cholesteryl esters (CE) then packaged into chylomicrons (CM). *A*, Depiction of proteins involved in transport known prior to 2000. It was still unclear whether cholesterol was being absorbed passively or via a sterol transporter. *B*, Depiction of proteins involved known to be involved in transport at present. Protein abbreviations used: ABC, ATP-binding cassette transporter; ACAT2, acyl-CoA:cholesterol acyltransferase 2; MTP, microsomal triglyceride transfer protein; NPC1L1, Niemann-Pick C1 Like 1

1.2.4 Nuclear Receptor Regulation of Cholesterol Absorption

1.2.4.1 Classification of Nuclear Hormone Receptors

Nuclear hormone receptors comprise a superfamily of ligand-activated transcription factors consisting of 48 family members in humans (49 in mice). A unified nuclear receptor nomenclature was adopted in 1999, however common names are widely used. These receptors coordinate a variety of biological responses by responding to lipophilic compounds to regulate target genes. This superfamily can be divided into endocrine receptors, orphan receptors, and adopted orphan receptors (Chawla et al., 2001). Endocrine receptors include androgen receptor (AR), estrogen receptors (ER), progesterone receptor (PR), glucocorticoid receptor (GR), mineralocorticoid receptor (MR), vitamin D receptor (VDR), retinoic acid receptors (RAR), and thyroid hormone receptors (TR). These receptors bind their cognate hormonal ligands with high affinity (pM-nM). In contrast, the adopted orphan receptors, including retinoid X receptor (RXR), liver X receptors (LXR), farnesoid X receptors (FXR), peroxisome proliferator-activated receptors (PPAR), pregnane X receptor (PXR), and constitutive androstane receptor (CAR), bind their diet-derived ligands with lower affinity (μM). It is unclear if the remaining orphan receptors are indeed ligand-activated (Benoit et al., 2004). The crystal structures of the ligand binding domain for these orphan receptors suggest that (1) some have no room to harbor a ligand (NURR1, NGF-IB)(Wang et al., 2003b), (2) some appear to "irreversibly" bind a lipid in the pocket (RORα, RORβ, HNF4α, HNF4γ)(Dhe-

Paganon et al., 2002; Kallen et al., 2002; Stehlin et al., 2001; Wisely et al., 2002), and (3) some may have as yet unidentified ligands (LRH-1, SF-1)(Krylova et al., 2005; Li et al., 2005; Ortlund et al., 2005).

Germane commonalities exist between the endocrine and adopted orphan classes of nuclear receptors. First, RXR promiscuously heterodimerizes with not only the adopted orphan receptors, but also RAR, VDR, and TR. A subset of these RXR heterodimers can function permissively. That is, the heterodimer can be stimulated to transactive target genes by addition of an RXR ligand or a ligand for its partner (e.g oxysterols for LXR, bile acids for FXR, fatty acids and derivatives for PPAR, etc); a synergistic effect can be obtained with a combination of both ligands. Second, all of the endocrine receptors (except RAR and TR) along with LXR, FXR, and PXR (lithocholic acid) respond to cholesterol-derived molecules (Figure 1). Thus, it is not suprising that nuclear receptors are intimately involved in cholesterol absorption, conversion of cholesterol to other molecules, and other aspects of cholesterol homeostasis.

1.2.4.2 Nuclear Receptors Important in Cholesterol Absorption

Liver X Receptors (LXRs)

Two LXR isoforms exist in human and mouse genomes, LXRα (NR1H3) and LXRβ (NR1H2). Each of these isoforms responds to oxidized derivatives of cholesterol, called oxysterols, however LXRα and LXRβ show different tissue expression patterns.

Whereas, LXRα mRNA expression is largely restricted to "metabolically active" tissues including liver, kidney, small intestine, and adipose, LXRβ mRNA is more ubiquitously expressed (Lu et al., 2001b). LXRs function as obligate permissive heterodimers with RXR and recognize DNA containing direct hexanucleotide repeats (AGGTCA) with 4 nucleotide spacers (DR4) present in the vicinity of target genes. Because LXR:RXR heterodimers are permissive, ligand-binding to LXR and/or RXR leads to the recruitment of coactivators and induction of transcription.

Because of their responsivity to oxysterols, including 22(R)-hydroxycholesterol, 24(S)-hydroxycholesterol, and 24(S),25-epoxycholesterol (Janowski et al., 1999; Janowski et al., 1996; Lehmann et al., 1997), LXRs are adept at responding to excess cellular cholesterol from the diet or endogenously synthesized sources. Upon activation, LXRs initiate feed-forward mechanisms that promote cellular cholesterol efflux via ABC transporters A1, G1, G5, and G8, conversion of cholesterol to bile acids via CYP7A1 and CYP8B1, or fatty acid synthesis via fatty acid synthase (FAS), SREBP-1c, and other genes (Chawla et al., 2001). Fatty acid synthesis may help prevent cholesterol excess by removing substrate (i.e. acetyl-CoA) for cholesterol biosynthesis, and converting it to fatty acids that can be used to esterify cholesterol for storage thereby decreasing concentrations of free cholesterol.

The liver is the major site for elimination of cholesterol from the body and is responsible for the majority of both LDL- and HDL-cholesterol clearance. Peripheral cells (including macrophages and other tissues) are constantly synthesizing cholesterol. Although cholesterol can be temporarily stored in its esterified form, excess cholesterol

must eventually be removed to maintain homeostasis. To promote storage, LXR upregulates a master regulator of fatty acid synthesis, SREBP-1c (Repa et al., 2000a; Schultz et al., 2000). SREBP-1c is itself a transcription factor (similar to SREBP-2 which controls cholesterol biosythesis) which regulates a variety of lipogenic genes. LXR can also directly regulate FAS and steroyl-CoA desaturase 1 (SCD1) independent of SREBP1c (Liang et al., 2002). A major mechanism of removal of cholesterol from peripheral tissues is efflux of cholesterol by ABCA1 onto Apo-AI-containing lipoprotein particles (HDL) for transport back to the liver for elimination (reverse cholesterol transport).

LXRs regulate key aspects of cholesterol metabolism in the liver and intestine. In rodent liver, activation of LXR upregulates CYP7A1 and CYP8B1 that convert cholesterol to bile acids. Bile acids are then secreted into bile via ABCB11 (or bile-salt export pump, BSEP). Although only 5% of the bile that enters the small intestinal lumen is eventually excreted, this represents a major pathway for cholesterol elimination from the body. Importantly, LXRs upregulate ABCG5/8 in the liver to promote secretion of cholesterol into bile. In the small intestinal lumen, biliary cholesterol joins dietary cholesterol and approximately 50% is absorbed. ABCG5/8 is also present in the intestine and regulated by LXRs. Thus, the enterocyte can respond to elevated cholesterol by inducing expression of ABCG5/8 to efflux cholesterol directly back into the small intestinal lumen. The net effect of LXRs on cholesterol absorption can be seen in LXR-agonist treated wild-type mice (T0901317, 50 mpk/day, 10 days), which display ~60%

decreased fractional cholesterol absorption and a 4-fold elevation in fecal neutral sterol excretion (Repa et al., 2000c).

Farnesoid X Receptor (FXR)

FXR (NR1H4) is expressed primarily in the liver, small intestine, colon, kidneys, and adrenals (Lu et al., 2001b). FXR also forms obligate permissive heterodimers with RXR and responds to various bile acids, especially chenodeoxycholic acid (CDCA) (Makishima et al., 1999; Parks et al., 1999; Wang et al., 1999). Activation of FXR upregulates primary target genes containing inverted hexanucleotide repeats with 1 nucleotide spacer (IR1) or downregulates indirect target genes containing liver receptor homolog 1 (LRH-1) binding sites. Primary target genes of FXR include ABCB11 (or BSEP) which effluxes bile acids across the canalicular membrane into the bile. Indirect targets include CYP7A1 and sodium taurocholate cotransporter (NTCP). FXR accomplishes the repression of indirect targets via a mechanism involving SHP, a nuclear receptor that lacks a DNA-binding domain and acts as a transcriptional repressor (Lu et al., 2000). FXR induces the expression of SHP, which is able to heterodimerize with LRH-1 and recruit co-repressors to diminish transcription of the target gene. Decreased bile acid synthesis leads to a decrease in bile acid pool size and a decrease in the quantity of bile acids present in the small intestinal lumen. This is the key point for the physiology of cholesterol absorption. Decreased bile acid quantity or a change in the composition of bile acids can lead to poor micellar solubilization of cholesterol thereby

decreasing absorption. Thus, mice lacking CYP7A1 or CYP27A1 have markedly reduced bile acid pool size resulting in greatly diminished fractional cholesterol absorption (Repa et al., 2000b; Schwarz et al., 1998).

Bile acids are actively reclaimed (~95%) in the terminal ileum by the ileal bile acid transporter (IBAT) (Dawson et al., 2003). Bile acids are then transported and buffered within the enterocyte by the ileal bile acid binding protein (IBABP) and presumably secreted into the portal circulation by OSTα/β heterodimers (Dawson et al., 2005), although studies in mice lacking *Ostα* or *Ostβ* have not yet been completed. IBABP and Ostα/β are transcriptionally induced by FXR (Dawson et al., 2005), and deletion of IBAT or IBABP leads to massive loss of bile acids and decreased bile acid pool size (Dawson et al., 2003).

Peroxisome Proliferator-activated Receptors (PPARs)

The PPAR nuclear receptor subfamily consists of three isoforms: PPARα (NR1C1), PPARβ/δ (NR1C2), and PPARγ (NR1C3). All three isoforms respond to various fatty acids (especially poly-unsaturated fatty acids (PUFAs)) by binding direct hexanucleotide repeats with 1 nucleotide spacer (DR1) present near target genes. Target genes include those that enhance β-oxidation of fatty acids (e.g. acyl-CoA oxidase (ACOX1)) or binding and transport of fatty acids (e.g. fatty acid-binding protein (FABP)). Fibrates and thiazolidinediones are used clinically to treat hyperlipidemia and diabetes and target PPARα and PPARγ, respectively. Specific synthetic agonists for

PPARδ exist (e.g GW0742), however they are not yet in clinical use. The role of these proteins in cholesterol absorption is just beginning to be assessed. Two tests of importance of these isoforms in cholesterol absorption include assessment of fractional cholesterol absorption in knockout-mice and mice treated with isoform-specific agonists. One study found that PPARβ-selective agonist treatment (GW0742, 0.017% w/w, 8 days) of DBA/1 wild-type mice reduced fractional cholesterol absorption by approximately 50 percent and marginally reduced NPC1L1 mRNA expression in jejunum and ileum, but not duodenum (van der Veen et al., 2005); *Pparβ*-knockout mice were not examined in this study. In Chapter 4, we present data regarding cholesterol absorption and NPC1L1 expression in wild-type and *Pparα*-knockout mice treated with fenofibrate, a clinically utilized fibric acid derivative.

1.2.5 Candidates for the Intestinal Cholesterol Transporter

1.2.5.1 Evidence for an Intestinal Cholesterol Permease

Rather than passive diffusion of cholesterol through lipid bilayers, several lines of evidence suggested that intestinal cholesterol uptake was a protein-mediated process. (1) Plant sterols are much less efficiently absorbed than cholesterol even though they are structurally related, and patients with sitosterolemia lose the ability to distinguish (and therefore exclude) plant sterols (Berge et al., 2000; Lee et al., 2001; Moreau et al., 2002). (2) Cholesterol absorption by small intestinal brush border membranes follows second-

order kinetics and is sensitive to proteases (Thurnhofer and Hauser, 1990). (3) Wide species and interindividual variations in cholesterol absorption are apparent, suggesting that genes and gene products (proteins) have an impact on this process. (4) Potent small molecules were discovered to block cholesterol absorption (see below) and administration of an analog of ezetimibe, SCH 58053, induced gene expression changes that were consistent with blockade of cholesterol entry (Repa et al., 2002c). Taken together, these data strongly suggested that cholesterol absorption was a selective, protein-mediated process. The glaring question that remained was the identity of this protein(s). Because of the importance of ezetimibe to the development of a better understanding of the molecular processes that underlie intestinal cholesterol absorption, highlights of the unconventional manner of its discovery are detailed below.

The development of ezetimibe was prefaced by a desire to identify novel classes of cholesterol-lowering drugs (other than statins) and initiated with a search for compounds that inhibited ACAT activity, as ACAT was known to esterify cholesterol with fatty acids and to play a role in cholesterol absorption in rodents (Clader, 2004). To begin to refine a compound for eventual clinical use, both an in vitro ACAT activity assay and in vivo animal models, especially the cholesterol-fed hamster, were used. In animal models, hepatic cholesteryl ester (CE) levels increase upon cholesterol feeding (and presumably decrease upon inhibition of cholesterol absorption) and could therefore be used as a surrogate for cholesterol absorption. Studies using an intial lead compound and a conformationally constrained variant (Clader et al., 1995; Vaccaro et al., 1996) showed a correlation between IC_{50} of ACAT activity and percent decrease in hepatic

cholesteryl-ester concentration, suggesting that inhibition of ACAT activity was responsible for the inhibition of cholesterol absorption. Over the course of many studies, the structural determinants necessary for ACAT2 inhibition were parsed from those relating to cholesterol absorption (or hepatic cholesteryl-ester accumulation). In particular, a compound was generated which had little to no effect on ACAT activity, but robustly decreased esterified cholesterol accumulation in the hamster and serum cholesterol in cholesterol-fed rat, dog, and monkey. This particular compound also decreased unesterified cholesterol accumulation in the intestine, whereas other ACAT inhibitors did not, suggesting that this compound was acting upstream of cholesteryl-ester formation in the intestine (Clader, 2004). Indeed, later studies using mice with targeted deletion of ACAT2, which is the predominant ACAT isoform in liver and intestine, found only moderate decreases in cholesterol absorption (Buhman et al., 2000; Parini et al., 2004; Repa et al., 2004a). This does not match the >90% reduction often seen upon administration of ezetimibe (Valasek et al., 2005). Another possible explanation for the disparity between ACAT inhibition and cholesteryl-ester formation was that the compounds were being metabolized in the organism to a more (or less) potent species. This question was addressed by a clever experiment (Van Heek et al., 1997). Bile-duct diverted animals were treated with intraduodenal administration of tritiated compound, then bile was collected and called the "metabolite" bile. Bile from vehicle treated animals was collected and spiked with tritiated compound to match the specific activity of the "metabolite" bile. This was called the "parent" bile. Both the "metabolite" and the "parent" bile were administered intraduodenally along with 14C-cholesterol to a second

set of bile-duct diverted animals, then tissue counts of tritium and 14C were measured. The results showed that the "metabolite" bile was more effective than the "parent" bile in decreasing plasma and liver 14C-cholesterol content, arguing that a metabolite(s) might be more effective than the administered compound. Moreover, the "metabolite" bile gave more tritium counts in the lumen and intestinal wall suggesting a metabolite of the compound was accumulating at its proposed site of action more effectively than unmetabolized compound. The strategy then was to distinguish sites of metabolism of the compound that "(1) premetabolize profitable sites of metabolism . . . to improve activity . . . and localize the compound in the intestines and (2) block unprofitable sites of metabolism to maximize activity and limit further oxidative metabolism" (Clader, 2004). In this manner, ezetimibe was generated (Rosenblum et al., 1998) and recently has been shown to act on the NPC1L1 putative cholesterol transporter (Garcia-Calvo et al., 2005). Of critical clinical importance was the realization that upon blockade of intestinal cholesterol absorption by ezetimibe, the liver could compensate by increasing de novo synthesis of cholesterol thereby minimizing therapeutic changes to plasma LDL-cholesterol levels. Since HMG-CoA reductase inhibitors, called statins, can inhibit de novo synthesis of cholesterol, the two classes of drugs might have complementary effects on lowering plasma LDL-cholesterol. This was indeed the case as shown by Davis et al (Davis et al., 2001b).

1.2.5.2 Cholesterol Effluxers

ATP-binding cassette transporter A1 (ABCA1)

As discussed previously, several nuclear receptors are now known to regulate intestinal cholesterol homeostasis. When ABCA1 was first proposed as a potential candidate for the regulation of intestinal cholesterol efflux (Repa et al., 2000c), it was known that LXRα and β, and FXR regulated bile acid production in the rodent liver by transcriptionally inducing or repressing CYP7A1, respectively (Makishima et al., 1999; Peet et al., 1998; Wang et al., 1999). FXR accomplishes the task of CYP7A1 repression by transcriptionally inducing small heterodimer partner (SHP, (Lu et al., 2000)), which inhibits the constitutive transactivation of the CYP7A1 gene by liver receptor homolog 1 (LRH1). Since both LXRs and FXR function as permissive heterodimers with RXR, a highly-specific RXR ligand would activate both pathways. Repa et al (Repa et al., 2000c) determined that administration of an RXR ligand (rexinoid) to mice abolishes cholesterol absorption by two different pathways. They found that rexinoid treatment of mice dramatically reduced cholesterol absorption but not absorption of other lipids. Compensatory upregulation of cholesterol biosynthetic enzymes (HMG-CoA synthase and HMG-CoA reductase) and LDL receptor in the liver and duodenum coincided with increased cholesterol synthesis as determined by tritiated water studies. Since rexinoids decreased CYP7A1 expression and bile acid pool size (presumably by activation of FXR:RXR heterodimers, cholic acid was added to the diet to rescue the bile acid defect and determine if other pathways existed which would inhibit cholesterol absorption. Indeed, cholic acid replacement only recovered the inhibition by approximately 50%

suggesting that pathways independent of FXR existed. Investigation of gene expression in the intestine revealed that ABCA1, the Tangier disease gene (Brooks-Wilson et al., 1999; Orso et al., 2000; Remaley et al., 1999), was markedly upregulated by LG268, and that this was due to LXR activation as the effect was recapitulated by an LXR-selective agonists, 22(R)-hydroxycholesterol and T0901317. In addition, T0901317 alone could decrease cholesterol absorption in wild-type but not Lxrα/β double-knockout mice confirming a novel pathway dependent on LXR and not FXR. These studies did not exclude the possibility that LXR could be influencing gene expression of other proteins involved in cholesterol absorption. Indeed, the action of LXR-agonists on cholesterol absorption was later determined to be more closely related to their ability to increase the novel ABC transporters, ABCG5 and ABCG8 (Plosch et al., 2002; Repa et al., 2002a; Yu et al., 2003). The role of ABCA1 in intestinal cholesterol transport has been unclear as knockout mice show moderate or slight reduction in cholesterol absorption (Drobnik et al., 2001; Temel et al., 2005), and intestinal-specific *Abca1*-knockout mice show no difference in fractional cholesterol absorption but rather a partial (~25%) defect in HDL biosynthesis (Brunham et al., 2006).

ATP-binding cassette transporters G5 and G8 (ABCG5/8)

Further elucidation of intestinal cholesterol absorption came from studies which defined the genes responsible for sitosterolemia, a disease characterized by hyperabsorption of plant sterols and cholesterol resulting in increased plasma levels (>30-

fold increase in phytosterols) (Salen et al., 1992). This causes deposition of cholesterol in the form of xanthomas or atheromas (leading to cardiovascular disease). Interestingly, the brain does not accumulate phytosterols in sitosterolemia (Salen et al., 1985), suggesting that even though there are high levels in the plasma, there is no movement across the blood brain barrier (BBB). Observations of sitosterolemic patients implied that they might be deficient in a gene product that would both inhibit intestinal sterol absorption and enhance biliary secretion of sterols (Berge et al., 2000; Salen et al., 1992). One further insight that was critical toward discovering the defective genes was the hypothesis that they might be regulated by LXR, because it was already known that activation of LXR limits cholesterol absorption and induces ABCA1 (Repa et al., 2000c). Therefore, Berge et al (Berge et al., 2000) treated mice with T0901317 (50mg/kg) and performed microarray studies on liver and intestine. One expressed sequence tag (EST), which was related to *Drosophila* ABC half-transporters, was found to be upregulated approximately 2.5-fold in both liver and intestine. This EST seemed to be a good candidate, as another mouse ABC half-transporter (ABCG1) was already known to transport cholesterol (Klucken et al., 2000; Venkateswaran et al., 2000), and an ABC transporter (ABCA1) was found to be responsible for Tangier disease (Brooks-Wilson et al., 1999; Orso et al., 2000; Remaley et al., 1999), in which there is defective cholesterol metabolism. Using this EST, both mouse and human ABCG5 were cloned, although only one ABCG5 mutation was identified in sitosterolemic patients. Because ABC genes often cluster in the genome, Berge and colleagues looked for nearby ABC genes and found another ABC half-transporter, ABCG8. Indeed, mutations were found in this gene

in patients with sitosterolemia (Berge et al., 2000; Lu et al., 2001a; Patel et al., 1998). They found that ABCG5 and ABCG8 mRNAs were highly expressed in liver and intestine, but not other tissues. Since cholesterol feeding induced ABCG5 and ABCG8, it was likely that this responsivity was dependent on LXRs, as was later demonstrated (Repa et al., 2002a; Yu et al., 2003). In addition, mice lacking one or both of these half-transporters display enhanced sterol uptake (Klett et al., 2004; Plosch et al., 2004; Yu et al., 2002a), and mice overexpressing ABCG5/G8 show diminished sterol absorption (Yu et al., 2002b). Therefore, it seemed that ABCG5 and ABCG8 were ABC half-transporters which might form a heterodimer to efflux sterols from the enterocyte and hepatocyte (Berge et al., 2000). These actions are required to exclude plant sterols from the body and limit cholesterol absorption, and therefore functional impairment of these proteins leads to sitosterolemia.

Thus, these studies continued to shed light on the molecular mechanism by which intestinal cholesterol was selectively absorbed. However, as the ABC transporters were shown to efflux (or export) sterols from cells, it still remained to be determined how cholesterol was imported into enterocytes. Therefore, there was still a necessary component missing, namely the intestinal cholesterol (sterol) permease (or importer).

1.2.5.3 Cholesterol Importers

Scavenger receptor BI (SR-BI)

SR-BI was known to facilitate cellular uptake of cholesterol and cholesteryl ester from high-density lipoprotein (HDL) in both the liver and adrenals. SR-BI was observed to facilitate uptake of cholesterol and cholesterol esters (and phospholipids and triglycerides) into isolated enterocytes in a manner that could be inhibited by application of HDL or Apo-AI (Hauser et al., 1998). This suggested not only that SR-BI could be the intestinal cholesterol permease, but also that HDL (or Apo-AI) could be used as a therapeutic to inhibit cholesterol absorption (Hauser et al., 1998). Other studies had additionally shown that this uptake of cholesterol could be inhibited by ezetimibe (Altmann et al., 2002), strongly suggesting that SR-BI was an ezetimibe-sensitive permease. The critical experiment was to determine the impact of targeted deletion of *Sr-bI* in mice on cholesterol absorption. If SR-BI were a crucial component of the intestinal cholesterol machinery, then knockout mice should show greatly diminished cholesterol absorption. If SR-BI were the target of ezetimibe, the knockouts should be insensitive to the drug. Therefore, Altmann et al measured cholesterol absorption by two methods. First, they determined acute uptake using a 2-h measurement of radiolabeled cholesterol. Second, they utilized the fecal-dual isotope method (at present the most often utilized method to assay cholesterol absorption efficiency) to determine fractional cholesterol absorption. In both cases, the *Sr-bI*-knockout mice absorbed cholesterol similar to wild-type controls. Moreover, ezetimibe was able to diminish cholesterol absorption in the *Sr-bI*-knockout mice similarly to wild-type controls. This clearly demonstrated not only that SR-BI was not critical for cholesterol absorption in vivo, but that it was dispensable for ezetimibe action. The reasons for the discrepancies between *in vitro* (cells and brush-

border membrane vesicles) and *in vivo* behavior of these molecular events remain both unclear and controversial in the field.

It should be additionally noted that, although ezetimibe blocks SR-BI function in enterocytes, it is a "sticky" compound and may be binding to lipid rafts (and resident proteins) non-specifically. This observation could potentially explain the biochemical results obtained by Smart and colleagues showing that CAV-1 and ezetimibe interact (Smart et al., 2004), because CAV-1 is a critical component of a subset of lipid rafts called caveolae. The glucuronide of ezetimibe, its only detectable metabolite, is more potent at blocking cholesterol absorption *in vivo* and does not bind SR-BI *in vitro* (Harry R. Davis, 2006; personal communication). This is further evidence supporting the idea that SR-BI is not crucial for intestinal cholesterol absorption.

Aminopeptidase N (APN)

APN has also been suggested as a putative target for ezetimibe and cholesterol transport based on photoaffinity labeling of a 145-kDa protein with photoreactive ezetimibe analogues (Kramer et al., 2005; Kramer et al., 2000). This protein was determined to be identical to APN, a well-known enzyme and marker for enterocytes. Treatment with ezetimibe did not effect the enzymatic activity of the protein (Kramer et al., 2005), thus it was proposed that other functions of APN like promotion of endocytosis could be involved in cholesterol uptake. To date, *in vitro* or mouse models to test the functional consequences of these interactions have not been developed.

Caveolin 1 (CAV1) and Annexin 2 (ANXA2) Complex

Because CaCo-2 cells, an "enterocytic" cell line derived from a human colon cancer, contained CAV1 mRNA and protein along with detergent-resistant microdomains, Field et al (Field et al., 1998) hypothesized that CAV1 might play a role in intestinal cholesterol transport. Concurrent with the discovery that NPC1L1-deficient mice were insensitive to ezetimibe in terms of cholesterol absorption (Altmann et al., 2004), a different group published that a SDS- and heat-resistant complex containing annexin 2 and caveolin-1 was a target for ezetimibe (Smart et al., 2004). Using whole-mount in situ hybridizations of zebrafish larvae, *cav1* and *anx2b* (the zebrafish orthologes of mouse *cav1* and *anxa2*) transcripts colocalized in the developing intestinal epithelium. ANX2b and CAV1 form a heterodimer (55-kDa complex) in adult fish intestine, whereas this complex does not form in other tissues (e.g. aorta). This suggested a tissue-specific role for the complex within the intestine. Additionally, this complex did not form *in vitro* using a mixture of cell lysates from ANX2b- and CAV1-free embryos that had been injected with morpholinos directed at the respective genes. Anx2b-MO injected zebrafish embryos contained less total cholesterol and cholesteryl ester than their wild-type counterparts, whereas cav1-MO injected zebrafish show developmental abnormalities including defects in somitogenesis. In mice, CAV1/ANXA2 formed a complex which was disrupted by ezetimibe, but only in LDLR-knockout mice or C57Bl/6 mice on a western diet. In addition, CAV1 antibodies were able to immunoprecipitate ezetimibe,

suggesting that in mice ezetimibe binds to CAV1 then disrupts the CAV1/ANXA2 complex. Because, in cultured cells, CAV1 associates with ANXA2 during the cellular uptake of cholesterol, but associates with heat-shock protein 56 during efflux of endogenously synthesized cholesterol (Uittenbogaard et al., 2002; Uittenbogaard et al., 1998), the authors speculated that this tightly bound complex might favor uptake of cholesterol by the intestine.

The striking deficiency of these studies is that the functional consequences of the disruption of this particular complex were not determined. Nevertheless, this study sparked a controversy with the cholesterol absorption field regarding the identity of the intestinal cholesterol permease. Our efforts to determine the importance of this complex in cholesterol absorption by utilizing *Cav1*-knockout mice are described in Chapter 2.

Niemann-Pick C1 Like 1 (NPC1L1)

Prior to implication of NPC1L1 in intestinal cholesterol transport, human NPC1L1 was originally cloned by Davies et al (Davies et al., 2000b) and identified as a relative of NPC1. Mutations in NPC1 protein are known to cause a rare recessively inherited neurodegenerative disorder, Niemann-Pick type C disease (NPC). However, a subset of patients with this disease were found to have intact NPC1 and were termed NPC2 (Steinberg et al., 1994; Vanier et al., 1996), raising the possibility that the newly cloned relative of NPC1 could indeed be NPC2. Therefore, NPC1L1 cDNAs were expressed in fibroblasts from NPC2 patients, and since they failed to complement the

defect in cholesterol trafficking, the cloned cDNAs were aptly named NPC1L1 and not NPC2 (Davies et al., 2000b). The predicted protein for human NPC1L1 was 1359 amino acids encoded by a 5046 base pair cDNA mapping to chromosome 7p13. NPC1L1 predicted protein shared 42% identity and 51% similarity to NPC1 (Davies et al., 2000b). Two motifs are contained in both NPC1 and NPC1L1: the "NPC1 domain" and the "sterol-sensing domain" (SSD, Figure 1.3). NPC1 domains are found in NPC1 orthologs from *Saccharomyces cerevisiae* to *Homo sapiens*, while SSDs are present in several proteins including 3-hydroxy-3-methylglutaryl coenzyme A (HMG CoA) reductase, SCAP, and Patched receptor (Carstea et al., 1997; Johnson et al., 1996).

At least two distinctions could immediately be made between NPC1 and NPC1L1 (Davies et al., 2000b). First, transcriptional regulation of NPC1L1 might differ from NPC1 because the promoter region of NPC1L1 uniquely contains a putative sterol response element (SRE), which could bind SRE binding proteins (SREBP) in response to conditions of cholesterol deprivation (Brown and Goldstein, 1997), and a binding sequence for Ying Yang-1 (YY1; (Shrivastava and Calame, 1994)), which may negatively regulate SREBP1 (Bennett et al., 1999). Second, subcellular targeting signals differ between NPC1 and NPC1L1 proteins. Whereas NPC1 contains a carboxy-terminal dileucine targeting motif (LLNF) that directs it to the endosomal/lysosomal system (Higgins et al., 1999; Neufeld et al., 1999), NPC1L1 instead has an internal YQRL motif (within the SSD), which may serve as a plasma membrane to *trans*-Golgi network transport signal (Bos et al., 1993; Humphrey et al., 1993; Ponnambalam et al., 1994; Rothman and Wieland, 1996). These motifs suggested that NPC1 and NPC1L1 might

have different subcellular localizations and could even conceivably comprise a unified cellular cholesterol transport chain, both serving as "lipid transport facilitators"(Davies et al., 2000b).

NPC1 and NPC1L1 are predicted to be large polytopic glycoproteins having 13 transmembrane domains (TM), with the SSD spanning TM3 through 7 (Ioannou, 2000; Iyer et al., 2005). For NPC1L1, an approximately 300 amino acid amino (N)-terminus and two long internal loops (between TM2 and 3, and TM8 and 9) are predicted to be extracellular (presumably into the intestinal lumen), while the cytoplasmic carboxy (C)-terminus and intracellular loops are shorter. NPC1L1 was found to be enriched in brush border membranes and exhibited N-linked glycosylation, as peptide-*N*-glycanase (PNGase) F shifted the molecular weight ~25 kilodaltons (kDa) by SDS-PAGE (Iyer et al., 2005).

At present, the manner in which NPC1L1 (and NPC1) is arranged in the membrane to perform its cholesterol transport function is unknown and awaits solution of a crystal structure. Current efforts are largely focused on solving the structure of the SSD, which would then have broad applicability to all proteins containing this domain. Nevertheless, there may be clues regarding structure and function from a distantly related family of prokaryotic proteins called the resistance-nodulation-division (RND) permeases (Davies et al., 2000a; Ioannou, 2000; Tseng et al., 1999). These proteins function as molecular pumps which utilize proton motive force (PMF) rather than energy from hydrolysis of ATP as seen for ATP-binding cassette A1 (ABCA1), ABCG5/8, and ABCG1 cholesterol effluxers. Moreover, NPC1 itself displayed the ability to pump

lipophilic molecules, like acriflavone, using PMF when expressed in bacteria (Davies et al., 2000a). A crystal structure of one of the RND permeases, AcrB, has been solved and was shown to form a homotrimer with a large central pore (Murakami et al., 2002) raising the speculation that NPC1L1 may be similarly arranged to transport cholesterol. Another possible connection is that RND permeases can export β-lactam antibiotics (Mazzariol et al., 2000; Srikumar et al., 1998), while the novel cholesterol absorption blocking drug, ezetimibe, also contains a β-lactam moiety (Rosenblum et al., 1998).

Intestinal localization of potent inhibitors of cholesterol absorption (showing structure-activity relationship) strongly argued that there was an intestinal cholesterol permease, especially considering the backdrop of supporting literature. As described several candidate proteins have been proposed to function as intestinal cholesterol transporters including scavenger receptor BI (SR-BI), ATP-binding cassette transporter A1 (ABCA1), ABCG5/8, aminopeptidase N, caveolin-1(CAV1)/annexin-2, and Niemann-Pick C1 like 1 (NPC1L1) (Altmann et al., 2002; Altmann et al., 2004; Field et al., 1998; Hauser et al., 1998; Kramer et al., 2005; Repa et al., 2000c; Smart et al., 2004). With the discovery of the cholesterol absorption blocking agent ezetimibe (Burnett et al., 1994; Rosenblum et al., 1998; Van Heek et al., 1997), new criteria could be used for a candidate intestinal cholesterol transporter. Not only should knockout animals have markedly reduced cholesterol absorption, but they might also be insensitive to ezetimibe. Moreover, in the simplest case, ezetimibe would bind directly to the transporter and inhibit its function. Therefore, the search became one for the ezetimibe-sensitive intestinal cholesterol transporter. Following these criteria several investigations ensued.

Of particular note, both SR-BI and CAV1 knockout mice were found to have similar cholesterol absorption as wild-type their wild-type counterparts and were completely sensitive to ezetimibe (Altmann et al., 2002; Valasek et al., 2005) thereby excluding these proteins as critical for intestinal cholesterol transport.

To accomplish the task of finding novel candidates, Altmann et al (Altmann et al., 2004) utilized a bioinformatics approach. First, they surmised that the putative cholesterol transporter would fulfill three criteria. It would (1) be highly expressed in jejunum, the site of cholesterol absorption, (2) contain common components of transporters (i.e. extracellular signal peptide, transmembrane domains, and N-linked glycosylation sites), and (3) contain known cholesterol interacting motifs (e.g. SSD). Second, they generated EST libraries from rat jejunum, combined these with public ESTs, and then screened them with the above criteria. The result was "only one credible candidate gene," rat NPC1L1 (Altmann et al., 2004). Although NPC1L1 had been cloned earlier (Davies et al., 2000b), very little was known about it beyond its genomic location and relatedness to NPC1, a disease gene involving cellular cholesterol trafficking defects. Altmann and colleagues first determined that NPC1L1 mRNA displays a restricted tissue expression pattern with the highest levels in small intestines of mouse, rat, and human, however humans also express a nearly equivalent amount in liver, as assessed by quantitative microarray (Altmann et al., 2004). Within the intestine, mRNA and protein expression are higher in proximal regions than distal, and was localized to the luminal (or apical) brush border. Critically, they found that targeted deletion of NPC1L1 in mice led to ~70% reduction in fractional cholesterol absorption as assessed by a 24h fecal dual-

isotope method and complete insensitivity to the effects of ezetimibe. These data clearly demonstrated that NPC1L1 was critical for intestinal cholesterol absorption and resided in an ezetimibe-sensitive pathway. This study represents a great leap forward in the understanding of the molecular mechanisms of cholesterol absorption, and affords the opportunity to ask more specific and sophisticated scientific questions about the process. One limitation of this study was its failure to establish NPC1L1 as a direct target of ezetimibe, although a later study gave strong evidence that this was the case ((Garcia-Calvo et al., 2005).

The prediction from studies on sitosterolemic patients and mouse models of the disease was that both cholesterol and plant sterols were taken up by the enterocyte, but primarily plant sterols were effluxed back into the intestinal lumen. In addition, studies of hypercholesterolemic or sitosterolemic patients treated with ezetimibe showed they had markedly reduced plasma plant sterol levels (Salen et al., 2004; Sudhop et al., 2002). Thus, NPC1L1 was tested for its importance in the process of plant sterol absorption. Davis et al (Davis et al., 2004) found that sitosterol absorption was significantly reduced in the *Npc1l1*-knockout mice by 64% compared with wild-type mice as assessed by 4 hour absorption to plasma and liver of radiolabeled sitosterol. Moreover, the plasma levels of two plant sterols, campesterol and sitosterol, were more than 90% lower in the *Npc1l1*-knockout mice. These data demonstrated that NPC1L1 was very important for the absorption of plant sterols in addition to cholesterol.

Another group independently developed *Npc1l1*-knockout mice and assessed their phenotype (Davies et al., 2005), and similarly demonstrated that *Npc1l1*-knockout mice

showed resistance to high-cholesterol diet-induced hypercholesterolemia. However, they were unable to confirm the plasma membrane localization of NPC1L1, and in HepG2 cells found intracellular co-localization with Rab5A. In addition, immortalized neonatal liver fibroblasts from *Npc1l1*-knockout showed defective cholesterol uptake and mislocalization of CAV1.   The authors interpreted this data to be in contrast to the idea that NPC1L1 resides in the apical brush border membrane. The different observations may be explained in part by the fact that there are species differences in the tissue distribution of NPC1L1 (Altmann et al., 2004; Davies et al., 2005), and that NPC1L1 changes its subcellular distribution depending on availability of cholesterol in a hepatoma cell line (Yu et al., 2006).
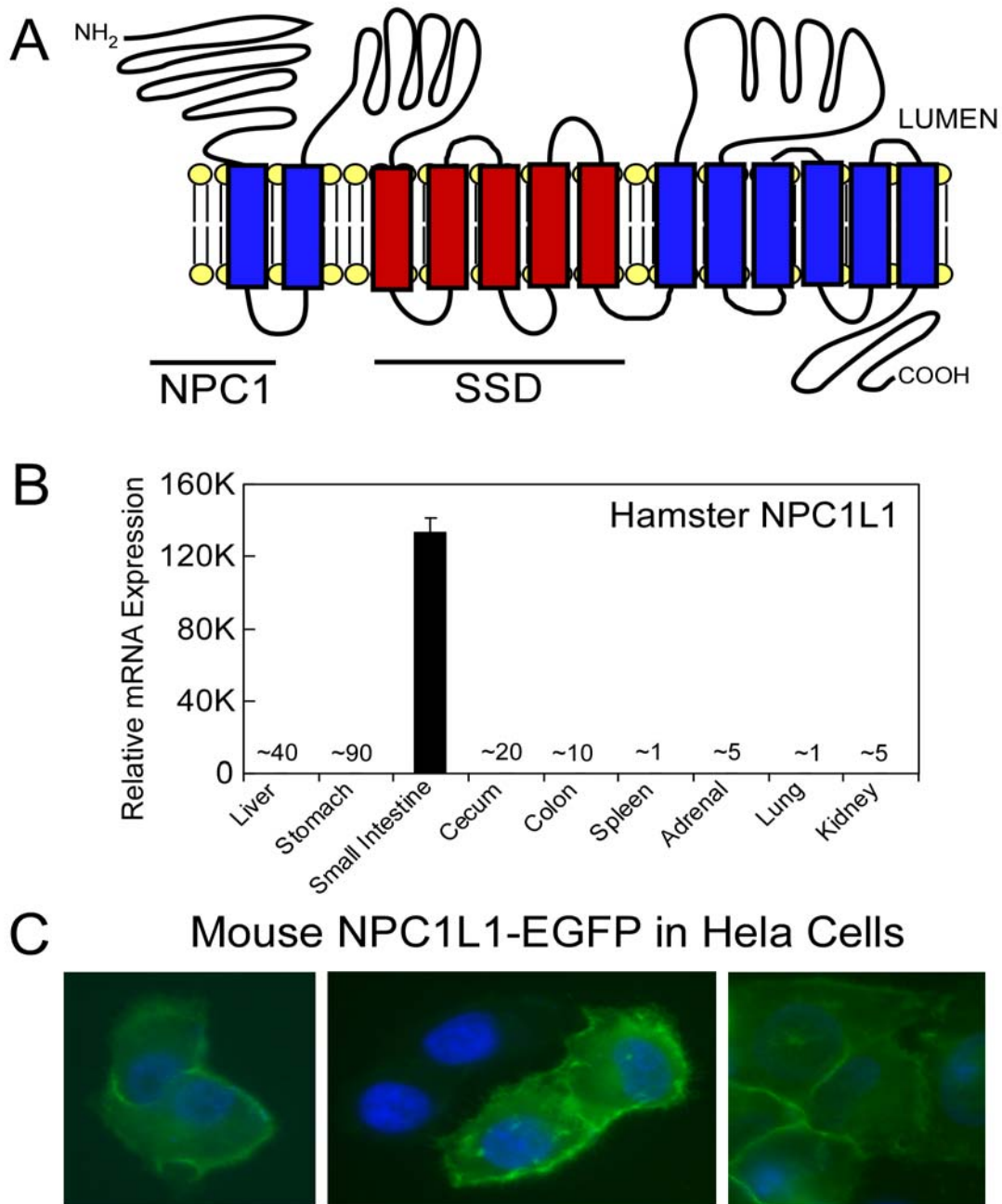
Figure 1.3 NPC1L1 topology, tissue distribution, and subcellular localization.
A, Putative membrane topology consisting of 13 transmembrane domains, a sterol-sensing domain (SSD, red) and an N-terminal NPC1 domain. *B*, Tissue distrubution of NPC1L1 mRNA in the golden Syrian hamster. *C*, NPC1L1 (green) localizes to a "plasma membrane-like" region in Hela cells transfected with mNPC1L1-EGFP (72h). Nuclei were stained with DAPI (blue).

1.3 RATIONALE

Because of the controversies surrounding the nature of the molecular machinery involved in intestinal cholesterol transport and the paucity of information regarding the regulation of this machinery, we wanted not only to clarify the essential molecular mechanisms by which cholesterol was absorbed, but also to investigate the potential role of nuclear receptors in regulating essential steps in this process. Here, we show that a candidate component of the cholesterol transport machinery, caveolin-1(CAV1), is neither required for intestinal cholesterol transport or sensitivity to the novel cholesterol absorption blocking agent, ezetimibe, in the mouse model. This rules out a critical role for caveolin-1 and lends further support to the contention that Niemann-Pick C1 like 1 (NPC1L1) is the *bona fide* intestinal cholesterol permease. Therefore to better understand new ways in which nuclear receptors could regulate cholesterol absorption, we studied nuclear receptor regulation of NPC1L1 and determined that several nuclear receptors could modulate its expression in small intestine, including peroxisome proliferator-activated receptor alpha (PPARα) and retinoid X receptor (RXR). In summary, cholesterol absorption can be regulated by nuclear receptor modulation of NPC1L1 expression.

CHAPTER 2

Caveolin-1 is not Required for Murine Intestinal Cholesterol Transport

2.1 ABSTRACT

Caveolin-1 (CAV1) is the structural protein of the filamentous coat that decorates the cytoplasmic surface of each caveola. Cell culture studies have implicated CAV1 in playing an important role in intracellular cholesterol trafficking. In addition, it has been reported that CAV1 forms a detergent-resistant protein complex with Annexin-2 in enterocytes that can be disrupted by the cholesterol absorption inhibitor ezetimibe, suggesting a possible role for CAV1 in cholesterol absorption. In this report, we have evaluated cholesterol homeostasis in *Cav1*-knockout mice. Deletion of CAV1 does not result in either a compensatory increase of CAV2 or CAV3 in intestine. In addition, *Cav1*-knockout mice display normal mRNA and protein levels of Annexin-2 or the putative cholesterol transport protein Niemann-Pick C1 Like 1 (NPC1L1) in proximal intestinal mucosa. Fractional cholesterol absorption and fecal neutral sterol excretion are statistically similar in *Cav1*-knockout mice and their wild-type littermates. Moreover, oral administration of ezetimibe is equally effective in decreasing cholesterol absorption in *Cav1*-null mice and wild-type controls. The mRNA expression levels of genes sensitive to intracellular cholesterol concentration (ATP-binding cassette transporters ABCA1 and ABCG5, Hydroxy-methylglutaryl CoA Synthase and the LDL Receptor) are

similarly altered in the proximal intestinal mucosa of *Cav1*-null and wild-type mice following ezetimibe treatment. These results demonstrate that CAV1 is not required for cholesterol absorption or ezetimibe sensitivity in the mouse.

2.2 INTRODUCTION

Ezetimibe is a member of the 2-azetidinone class of drugs that has recently been approved for clinical use in reducing plasma cholesterol levels (Sudhop et al., 2005). This drug significantly reduces the uptake of intestinal sterols by a mechanism that has not been fully elucidated. One protein that appears to be involved is NPC1L1 (Altmann et al., 2004). Animals made deficient in NPC1L1 exhibit markedly reduced cholesterol absorption and are unresponsive to ezetimibe (Altmann et al., 2004). While the evidence appears strong that NPC1L1 plays a significant role in sterol absorption (Davis et al., 2004), a direct interaction between NPC1L1 and ezetimibe has yet to be demonstrated. The possibility exists, therefore, that other proteins are required for the inhibitory effects of this drug.

Another protein that has been suggested to be an ezetimibe target is caveolin-1 (CAV1) (Smart et al., 2004). In zebrafish and mice, CAV1 has been shown to tightly associate with annexin-2 to form a complex that is resistant both to high heat and to solubilization by SDS detergent. Treatment of mice with ezetimibe can disrupt this complex, suggesting it may be a molecular target for the drug. Additionally, CAV1 is an attractive candidate target protein because there is considerable evidence for its involvement in intracellular cholesterol transport. Originally discovered as an integral

membrane component of the filamentous coat that decorates the cytoplasmic surface of each caveola (Rothberg et al., 1992), CAV1 is a cholesterol (Murata et al., 1995) and fatty acid (Trigatti et al., 1999) binding protein that is able to move between membrane compartments in the cell (Liu et al., 2002) as a soluble cytoplasmic intermediate (Li et al., 2001b; Uittenbogaard et al., 2002). Importantly, cells lacking CAV1 are defective in transporting cholesterol to caveolae (Fu et al., 2004; Smart et al., 1996). CAV1 also has been linked to cholesterol efflux in animals that are susceptible to gallstones. When these animals are placed on a lithogenic diet, liver CAV1 mRNA and protein appear to be up-regulated (Fuchs et al., 2001). CAV1 expression may also be regulated both by cholesterol and cholesterol efflux in cultured cells.

An important test of protein function is the phenotype of animals that lack the protein. For example, the HDL receptor SR-B1 is clearly involved in efflux and influx of cholesterol (Stangl et al., 1999), yet animals lacking SR-B1 are not defective in intestinal absorption of cholesterol (Mardones et al., 2001) and are fully sensitive to cholesterol absorption inhibition by ezetimibe (Altmann et al., 2002). Likewise, if CAV1 is a target for ezetimibe, then enterohepatic cholesterol transport should be markedly reduced in animals lacking CAV1, and they should be unresponsive to ezetimibe. Here we show that *Cav1*-null mice do not exhibit any defect either in cholesterol transport or in response to ezetimibe.

2.3 EXPERIMENTAL PROCEDURES

2.3.1 Animal studies

Cav1-deficient mice were generated by gene deletion of exon 2 as previously described (Cao et al., 2003). The resulting mouse strain was intercrossed with C57/Bl6 mice for 10 generations to establish a pure C57/Bl6 background. Mouse genotyping was performed by PCR using primers: F1, 5'-ttctgtgtgcaagcctttcc; R1, 5'-gtgtgcgcgtcatacacttg; and R2, 5'-ggggaggagtagaaggtggc to generate a product of 307 bp for the null allele and 260 bp for the wild-type allele (Cao et al., 2003). All studies were carried out with male mice 3 months of age. Although it has been reported that older *Cav1*-null mice are smaller than wild-type mice (Razani et al., 2002), the mice used in these studies showed no difference in body weight (WT: 26.65 ± 2.79g; WT-EZ: 29.48 ± 3.2; *Cav1*-KO: 30.58 ± 1.57; *Cav1*KO-EZ: 30.76 ± 1.59). Animals were housed individually in plastic colony cages containing wood shavings in a 22°C room lit from 7 a.m. to 7 p.m.

Mice were fed ad libitum a cereal-based rodent diet (Teklad Diet #7001, Madison, WI) which contains 0.02% (w/w) cholesterol and 4% total lipid. Mice were fed the powdered form of this diet, which in some experiments was supplemented with ezetimibe to provide 10 mg/day/kg body weight (based on the consumption of 160 g of diet/day/kg body weight). Ezetimibe was provided by Harry R. Davis, Jr. at the Schering-Plough Research Insistute.   Experiments were performed at the end of the dark cycle, and mice were in a fed-state at the time of study. Experiments were approved by the Institutional

Animal Care and Use Committee of the University of Texas Southwestern Medical
Center at Dallas.

2.3.2 Plasma Lipid Analyses

Mice were anesthetized and blood was sampled from the inferior vena cava into
EDTA-containing microfuge tubes (final concentration of EDTA ~2 mM). Plasma was
prepared by low-speed centrifugation (5,000 g) for 10 min at 4°C. For the *lipoprotein
profiles*, equal volumes of plasma from individuals of each group were pooled then
diluted 1:1 (v/v) with PBS and filtered through a 0.22 μm syringe filter (Millipore). One
hundred microliters of diluted sample was injected onto a Superose 6 HR 10/30 gel
filtration column for fractionation by fast-protein liquid chromatography (FPLC,
Pharmacia ÄKTA) at 4°C. Samples were eluted at a flow rate of 0.4 ml/min in buffer
containing 0.05 M phosphate, pH 7.0, and 0.15 M NaCl. Fractions of 0.3 ml were
collected for analysis.

Cholesterol concentrations were measured enzymatically using the Infinity
Cholesterol Reagent (401-500P, Sigma Diagnostics, St. Louis, MO). Plasma non-
esterified fatty acid concentrations were measured enzymatically using a 1:2 ratio of
Color Reagent A to Color Reagent B from NEFA-C kit (994-75409, Wako Chemicals,
Neuss, Germany). Plasma total triglycerides were measured enzymatically with
Triglyceride (GPO-Trinder) Reagents A and B (T2449 and F6428, Sigma Diagnostics, St.
Louis, MO). All kits provided appropriate controls to establish a standard curve for
calculation.

2.3.3 Liver Lipid Analyses

2.3.3.1 Cholesterol

An aliquot of liver was saponified in 3% KOH (in ethanol), and extracted in petroleum ether with added standard (stigmastanol). An aliquot of the PE phase was dried down and resuspended in hexane prior to analysis by gas chromatography (Turley et al., 1994a).

2.3.3.2 Triglyceride

An aliquot of liver (approximately 250 mg) was extracted in 20ml chloroform:methanol (2:1, v/v) in the presence of [^{14}C]triolein (American Radiolabeled Chemicals, Inc., St. Louis, MO). The entire extract was filtered and dried under air and the residue was redissolved in 1 ml of hexane:methyl-t-butyl ether (100:1.5, v/v). This solution was run over a Sep-Pak Vac RC silica cartridge (500 mg, Waters Corporation, Milford, MA). Following elution of the cholesteryl esters, triacylglycerols were eluted with 12ml of hexane:methyl-t-butyl ether (96:4, v/v). The eluate was brought to 100ml with hexane and 2ml aliquots were dried under air and measured for radioactivity using a scintillation counter in order to calculate the percent recovery of the internal standard and triacylglycerol. Separate 2ml aliquots were used for enzymatic determination of triacylglycerol quantity with Infinity Triglycerides Liquid Stable reagent (ThermoTrace, Noble Park, Australia).

2.3.4 Cholesterol balance measurements

2.3.4.1 Absorption

Fractional cholesterol absorption was measured by a fecal dual-isotope ratio method (Turley et al., 1994b). Briefly, mice received a single intragastric dose of MCT oil containing [5,6-^{3}H]sitostanol (2 μCi, American Radiolabeled Chemicals, Inc. St. Louis, MO) and [^{14}C]cholesterol (1 μCi, New England Nuclear, Boston MA). Stools were collected over the following three days. Samples of the dosing mixture and aliquots of stool were extracted, and the ratio of ^{14}C to ^{3}H in each was determined to calculate percent cholesterol absorption (Turley et al., 1994b).

2.3.4.2 Fecal neutral sterol and acidic sterol excretion

Stools were collected from individually housed mice over 3 days. They were dried, weighed, and ground. An aliquot of this material was used to determine bile acid content by an enzymatic method (Turley et al., 1996). A second aliquot was saponified, solvent extracted and amounts of cholesterol, coprostanol, epicoprostanol and cholestanone was quantified by gas chromatography (Schwarz et al., 1998). The amounts measured were adjusted to reflect the daily excretion (based on feces collected over 3 days) per 100 g body weight.

2.3.5 Preparation of samples for RNA and protein measurements

Mice were anesthetized and exsanguinated via the descending vena cava. Small intestines were removed, flushed with ice-cold PBS and cut into three sections of equal length (the proximal third denoted as duodenum). The sections were slit lengthwise, and the mucosae were gently scraped, frozen in liquid nitrogen and stored at −85°C. Whole

livers wer removed and snap-frozen in liquid nitrogen, then crushed to a fine powder with a Besselar Tissue pulverizer and stored at −85°C, thus providing multiple homogenous aliquots for various assays. Total RNA was isolated from tissue samples using RNA STAT-60 (Tel-Test Inc.). Total protein was obtained from the organic phase remaining after RNA isolation by precipitating with isopropanol, consecutively washing with 0.3M guanidine hydrochloride in 95% ethanol and ethanol, then solubilizing the protein pellet in 1% SDS. RNA concentrations were determined by absorbance at 260nm. Protein concentrations were determined using the BCA protein assay kit (Pierce Biotech., Rockford, IL).

2.3.6 Western analysis

Total protein obtained from whole-cell lysates of duodenal mucosa (see above) was size-fractionated on 8% SDS-polyacrylamide gels (60 µg/lane), transferred electrophoretically to PVDF membrane, and incubated with one of the following antisera: CAV1, amino-terminus "pAb1" (N20, Santa Cruz Biotech. Inc, 1:1000); CAV1, central "pAb2" (aa#1-97, BD Bioscience, 1:5000); CAV1, C-terminus "pAb3" (produced in rabbits by injection of the peptide IFSNVRINLQKEI (Ko et al., 1998), 1:500); NPC1L1, kindly provided by Helen Hobbs and Jonathan Cohen (UT-Southwestern Medical Center), generated in rabbits by injection of *E. coli*-expressed recombinant NPC1L1 protein fragments corresponding to aa# 29-250 and 404-611 per GenBank accession number NP_997125. This antiserum recognizes a ~200 kDa protein in intestine samples of wild-type, but not NPC1L1-null, mice (Hobbs and Cohen, personal communication);

ANXA2 (Santa Cruz Biotech., Inc); ERK1/2 (UPSTATE Group LLP, Charlottesville VA). Proteins were visualized by sequential treatment with specific antibodies, HRP-conjugated secondary antibodies, and an ECL kit (Amersham). Signal intensity of bands on autoradiograms was measured by densitometry using a Molecular Dynamics Densitometer Model 300A.

2.3.7 RNA measurements

2.3.7.1 Northern analysis

Equal quantities of total RNA from the samples of each group were pooled and polyA+ RNA was purified using oligo(dT)-cellulose columns (Pharmacia Biotech). mRNA (5 μg/lane) was size fractionated on a 1% formaldehyde agarose gel and transferred to nylon membrane (Zetaprobe, BioRad) for probing with ^{32}P-labeled cDNAs. Probes for ANXA2 and NPC1L1 were generated by reverse transcription-PCR using RNA isolated from mouse duodenum as template and the following primers: ANXA2-F, 5'-gctctcagcgatacgtgc; ANXA2-R, 5'-gagcgaagtctctagaacg (yielding an ANXA2 product consisting of nts 31-1167, GenBank # NM_007585); NPC1L1-F, 5'-agacgagggttatcactagag; NPC1L1-R, 5'-atttataaataccttggccata (yielding full-length mouse NPC1L1 per GenBank #XM_137497, a fragment generated by PstI digestion containing nts 658-1446 was used as a probe). A second cDNA produced against the 3'UTR of NPC1L1 gave identical results by northern analysis and was generated using the same reverse primer and NPC1L1-F2, 5'-aatggagtaggagcttgtc (yielding a product containing nts 4127-4572). HMG CoA Syn cDNA was provided by Michael Brown and Joseph

Goldstein (UTSW, (Shimano et al., 1996)), ABCG5 cDNA was provided by Helen Hobbs (UTSW, (Berge et al., 2000)), and the CAV1 cDNA probe contained the full-length human CAV1 transcript (Machleidt et al., 2000).

2.3.7.2 Quantitiative real-time PCR

qRT-PCR was performed using an Applied Biosystems Prism 7900HT sequence detection system as described (Kurrasch et al., 2004). Briefly, total RNA was treated with DNase I (Rnase-free, Roche Molecular Biochemicals), and reverse-transcribed with random hexamers using SuperScript II (Invitrogen) to generate cDNA. Primers for each gene were designed using Primer Express Software (PerkinElmer Life Sciences) and validated by analysis of template titration and dissociation curves. Each qRT-PCR reaction contained (final volume of 10 µl): 25ng of reverse-transcribed RNA, each primer at 150nM, and 5µl of 2X SYBR Green PCR Master Mix (Applied Biosystems), and each sample was analyzed in triplicate. Results were evaluated by the comparative C_T method (User Bulletin No. 2, PerkinElmer Life Sciences) using cyclophilin as the invariant control gene. RNA levels are expressed relative to those obtained for the wild-type mice fed the basal diet, and reflect the average ± SEM for n=5-6 animals per group.

2.3.8 Statistical Analysis of Data

Data are reported as the mean ± SEM for the specified number of animals. GraphPad Prism software (GraphPad, San Diego, CA) was used to perform all statistical analyses. If unequal variance was indicated by Bartlett's test, log transformation was performed prior to statistical analysis. Two-way ANOVA was used (factors: genotype,

drug).   In no instance was a significant interaction of factors observed, therefore statistical differences for each factor are are fully describe in each figure legend: *, $P<0.05$, **, $P<0.01$, ***$P<0.001$.

2.4 RESULTS

To investigate the role of CAV1 in cholesterol homeostasis, we evaluated a number of metabolic parameters indicative of cholesterol absorption and trafficking in intact mice. In addition, we measured the RNA and protein levels of key transporters, enzymes and trafficking proteins in intestine and liver to corroborate the metabolic changes observed in these mice. *Cav1*-null mice and their wild-type controls were fed for 15 days a standard rodent diet containing 4% total lipid and 0.02% cholesterol. Some mice received this diet supplemented with 10mg ezetimibe /kg body weight. This dose of ezetimibe has previously been established as effective in mice, and results in a greater than 90% decrease in fractional cholesterol absorption (Davis et al., 2001a; Repa et al., 2005). Stool samples were collected from days 7-10 to measure fecal sterol and bile acid excretion, and mice received an intragastric dose of labeled sterols on day 12 to measure cholesterol absorption by the fecal dual isotope method (Turley et al., 1994a; Turley et al., 1994b). After completion of the 15-day dietary regimen, mice were anesthetized and exsanguinated and tissue samples were obtained.

Western blot analyses were performed using whole-cell lysates prepared from the proximal third of the small intestine of individual mice (Figure 2.1). The genotype of mice used in the study was confirmed by the absence of the 22 kDa CAV1 protein

(Rothberg et al., 1992) in samples from the *Cav1*-knockout mice. Importantly, there was no evidence of any immunoreactive CAV1 polypeptide fragment generated in these mice as assessed by a variety of polyclonal antisera that target the amino-terminus (pAb1) through the carboxy-terminus (pAb3). This was necessary, as a truncated CAV1 transcript was still evident by northern analysis in these samples (Figure 2.2C). The absence of invaginated caveolae in vascular endothelial cells (data not shown) further confirm the deletion of this gene product. The inclusion of ezetimibe in the diet had no effect on the CAV1 protein levels measured in the wild-type mice.

NPC1L1 was detected as a large protein (between 150 kDa and 200 kDa) by a novel polyclonal antibody. This protein size is in agreement with that described for rat and human NPC1L1 (Davies et al., 2005; Iyer et al., 2005). The specificity of the NPC1L1 antiserum was confirmed by immunoblotting of intestinal samples from wild-type and *Npc1l1*-knockout mice, with no detected protein in the null animals (H. Hobbs and J. Cohen, personal communication). Protein quantification by densitometry revealed that neither the *Cav1* genotype nor the ezetimibe treatment had a significant effect on NPC1L1 protein levels (WT-control diet: $0.68 \pm .05$ density units relative to loading standard ERK1/2; WT-EZ: 0.80 ± 0.20; CAV1-/-control: $0.56 \pm .09$; CAV1-/-EZ: 0.66 ± 0.15, n=5-6 mice per group).

Blotting with an ANXA2 polyclonal antiserum revealed three protein bands, with the most prominent (~37 kDa) in agreement with previous reports (Smart et al., 1996). The larger molecular weight forms could be a result of ANXA2 ubiquitination as has been observed with extracts from intestinal mucosa (Lauvrak et al., 2005). Densitometric

measurement of the principle ANXA2 band indicated that neither the *Cav1* genotype nor the ezetimibe treatment resulted in altered ANXA2 expression levels (WT-control diet: $0.18 \pm .07$ density units relative to loading standard ERK1/2; WT-EZ: 0.30 ± 0.10; CAV1-/-control: $0.24 \pm .07$; CAV1-/-EZ: 0.19 ± 0.09, n=5-6 mice per group). In summary, the western analyses shown in Figure 2.1 conclusively demonstrate that the absence of CAV1 does not affect the protein levels of NPC1L1 and ANXA2 in the mouse intestine. In addition, treatment of mice with the cholesterol absorption inhibitor ezetimibe does not alter duodenal levels of NPC1L1 and ANXA2 proteins.

Additional evaluation of NPC family members, CAV isoforms, and gene products important for enterocyte cholesterol balance was performed by using quantitative real-time PCR (qRT-PCR) to measure RNA levels (Figure 2.2 A and B). CAV1 RNA was not detected in the *Cav1*-knockout mice by this method. CAV2 and CAV3 levels were unchanged by either genotype or drug treatment. The cycle numbers needed to amplify the CAV PCR products allow for a rough approximation of relative expression of these three isoforms, and suggest that CAV1 is most abundant (C_T=24.8) and CAV3 RNA (C_T=30.9) most sparse in the mouse intestine. This is in agreement with immunoblot analyses that suggest a similar relative expression of these CAV family members in the mouse intestine (Li et al., 2001b). RNA levels of the Niemann-Pick Type C proteins NPC1 and NPC2, involved in the movement of endocytosed LDL-cholesterol from the lysosome/late endosome into the cytosol of cells, were unaffected by the absence of CAV1 or treatment with ezetimibe.

The duodenal mRNA levels for acyl-CoA cholesterol acyltransferase-2 (ACAT2), the principle cholesterol esterifying enzyme of the intestine, and the microsomal triglyceride transfer protein (MTP), a protein essential for chylomicron assembly, were similar in all groups of mice (Figure 2.2B). The scavenger receptor type BI (SR-BI) did not exhibit a change in RNA levels by drug or *Cav1* genotype. Several mRNA species whose expression is under the regulation of sterol-sensing transcription factors exhibited altered levels following ezetimibe administration. The liver X receptors, LXRα and LXRβ, both present in intestine and activated by cholesterol-derived oxysterols, regulate the expression of ABCA1 and ABCG5 (Lu et al., 2001b). Sterol regulatory element-binding protein-2 (SREBP-2) undergoes proteolytic cleavage under low intracellular sterol levels to release its transcription factor to the nucleus to increase transcription of HMG CoA Syn and the LDL-receptor (Horton et al., 2002). The observed gene expression changes (ABCA1, ABCG5, HMG CoA Syn and LDLR) strongly suggest that ezetimibe treatment results in diminished intracellular sterol levels in the enterocyte and agrees with similar observations made using an ezetimibe analog (Repa et al., 2002b). Importantly, these gene changes were observed in both wild-type and *Cav1*-knockout mice.

Northern analysis was performed for selected genes (Figure 2.2C) to detect potential alternative splice variants and to corroborate qRT-PCR results. A truncated CAV1 transcript of 2.5 kb was detected in the knockout mouse intestine. This mRNA was not amplified by qRT-PCR, as one of the PCR primers was directed against exon 2, which was deleted in the targeting vector used to generate this knockout mouse strain.

However, as shown in Figure 1, no detectable CAV1 protein is produced by this aberrant transcript. A single band of 5.2 kilobases was detected for NPC1L1 in intestine (and not in liver, data not shown), allowing it to be easily distinguished from related family members NPC1 (5.8 kb (Loftus et al., 1997)) and NPC2 (1.3 kb (Nakamura et al., 2000)). Northern analyses of ABCG5 showed decreased expression upon treatment with ezetimibe, whereas HMG CoA Syn was increased by drug treatment. These data are consistent with the results obtained by qRT-PCR.

Total plasma cholesterol concentrations were significantly greater in the *Cav1*-null mice, a trend previously observed in male mice of an independently generated strain of *Cav1*-deficient mice (Figure 2.3A) (Razani et al., 2002). The majority of this elevated serum sterol is present in a more buoyant, LDL/IDL-particle (fractions 35-42, Figure 2.3C). Ezetimibe treatment did not evoke a significant decrease in plasma cholesterol, although there appeared to be a trend toward lower values. A reduction in serum cholesterol levels following ezetimibe administration has, to date, only been observed in mouse strains that exhibit hypercholesterolemia, such as *apoE*- or *Ldlr*-knockout mice (Davis et al., 2001a; Repa et al., 2002b; Repa et al., 2005). Hepatic total cholesterol levels did not differ by genotype or drug treatment (Figure 2.3B). Fractional cholesterol absorption was dramatically reduced by ezetimibe treatment (Figure 2.3D), and the values obtained for the C57/Bl6 wild-type mice are nearly identical to those previously reported in this mouse strain at this dose (Davis et al., 2001a). There was no indication that CAV1 plays a critical role in cholesterol absorption as the *Cav1*-knockout mice showed similar cholesterol absorption efficiency in the absence of drug, and responded

similarly to ezetimibe treatment. With this block in cholesterol absorption, fecal excretion of neutral sterols was increased nearly 3-fold in ezetimibe-treated mice (Figure 2.3E). There was no change in fecal bile acid excretion between the wild-type and *Cav1*-null mice, and ezetimibe did not affect bile acid excretion (Figure 2.3F). As bile acid excretion is generally a good indicator of bile acid synthesis, these findings suggest that while ezetimibe has dramatic effects on enterohepatic cholesterol balance, under the conditions of this study bile acid metabolism is unaffected.

Plasma triglyceride levels were elevated in the knockout mice, as reported previously (Figure 2.4A) (Razani et al., 2002), but unaffected by drug treatment. Plasma non-esterified fatty acid concentrations were no different by genotype or ezetimibe administration. Liver mass (as percent of body weight) was modestly, but significantly, greater in *Cav1*-null mice, although this could not be attributed to an increase in hepatic triglyceride levels (no differences among groups, Figure 2.4B) or cholesterol levels (Figure 2.3B). Further evaluation of liver phenotype was performed by qRT-PCR measurement of RNA levels for critical genes (Figure 2.5). CAV1 mRNA is less abundantly expressed in liver ($C_T = 27.8$) than small intestine ($C_T = 24.8$, Figure 2.2A), in agreement with reports on relative protein levels in these two mouse tissues (Li et al., 2001b). CAV2 RNA levels were modestly, but significantly, reduced in the *Cav1*-null mice. This is consistent with previous reports that CAV2 protein levels are diminished upon the loss of CAV1 in other tissues (lung, adipose, heart) of the *Cav1*-knockout mouse (Cao et al., 2003; Razani et al., 2002). CAV3 mRNA was undetectable ($C_T > 35$ cycles) in liver. These results suggest that the mild to absent hepatic phenotype in the

Cav1-null mouse is not due to a compensatory increase of another caveolin family member. Among the other RNA species measured, only HMG-CoA Syn showed a significant change, an increase in ezetimibe-treated mice. The decreased delivery of cholesterol from intestine to liver in the ezetimibe-treated mouse is accompanied by a compensatory increase in hepatic cholesterol synthesis (Repa et al., 2002b; Repa et al., 2005). In the chow-fed mice, it appears that this newly synthesized sterol is sufficient to restore basal hepatic concentrations (Figure 2.3B), and no further changes in sterol-sensitive gene expression (i.e. LXR target genes, ABCG5, ANGPTL3, SREBP-1c, ChREBP) are observed in the liver.

2.5 DISCUSSION

Cholesterol homeostasis is maintained by a fine balance between cholesterol acquisition (synthesis and absorption) and cholesterol elimination (fecal excretion of cholesterol and bile acids) (Dietschy and Turley, 2001). A wide variety of agents have been identified that affect these processes to ultimately reduce serum LDL-cholesterol (LDL-C) levels with the goal of lowering the incidence of atherogenesis and coronary events. Statins clearly reduce cholesterol biosynthesis, decrease LDL-C levels, and reduce mortality and morbidity associated with coronary heart disease (Nguyen, 1998). Several additional agents have been identified that reduce cholesterol absorption, and the elucidation of the mechanisms of action for these absorption inhibitors has identified key proteins involved in the processes that move free cholesterol

from the lumen of the intestine into the enterocyte, where it is esterified by ACAT2 and ultimately packaged into chylomicrons for delivery into the lymphatic circulation.

Several ACAT inhibitors have been characterized and have demonstrated the critical role of this enzyme in sterol absorption in animal models (Homan and Krause, 1997). Furthermore, the deletion of *Acat2* in mice results in decreased cholesterol absorption (Buhman et al., 2000; Repa et al., 2004b). Agonists of the nuclear hormone receptors RXR and LXR are potent cholesterol absorption inhibitors (Repa et al., 2000c), and the search for the receptor target genes responsible for this effect revealed the ABC transporters ABCG5 and ABCG8 (Berge et al., 2000; Repa et al., 2002a), which reside on the apical membrane of enterocytes to efflux free cholesterol back into the lumen, thereby reducing cholesterol absorption efficiency. Overexpression of ABCG5/G8 results in decreased cholesterol absorption efficiency (Yu et al., 2002b) and deletion of *Abcg5/g8* is associated with decreased fecal excretion of sterols (Yu et al., 2002a). Finally, ezetimibe, a potent cholesterol absorption inhibitor, has been found to act in the enterocyte by a mechanism involving NPC1L1 (Altmann et al., 2004). Mice lacking *Npc1l1* exhibit diminished cholesterol absorption efficiency (Davies et al., 2005; Davis et al., 2004) and fail to respond to ezetimibe (Altmann et al., 2004).

Additional proteins involved in cellular cholesterol trafficking in the intestine could also be important in cholesterol absorption. Caveolin-1 is such a candidate as it is expressed in the intestine, binds cholesterol, and is known to move among cellular compartments. It has also been reported that the behavior of caveolin-1 is altered in the intestine of zebrafish and mice after exposure to ezetimibe (Smart et al., 2004). A

detergent-resistant complex of CAV1 and annexin-2 is disrupted by prior treatment of these animals with ezetimibe, strongly suggesting that CAV1 and/or annexin-2 could play a role in cholesterol absorption. The studies described in this report demonstrate that the absence of CAV1 does not affect the intestinal expression of NPC1L1, ACAT2, ABCG5/G8 or other previously identified proteins involved in cholesterol absorption. Nor does the deletion of CAV1 result in a compensatory change in CAV2 or CAV3. In response to ezetimibe, similar changes in expression were observed in *Cav1*-knockout mice and wild-type controls. NPC1L1 and ANXA2 levels remained unchanged upon treatment of mice with ezetimibe, unlike SREBP target genes (i.e. HMG CoA Syn, LDLR) or LXR target genes (i.e. ABCA1, ABCG5), which showed increased or decreased expression, respectively. This suggests that NPC1L1 and ANXA2 expression may be dependent upon other mechanisms than the SREBP or LXR sterol-sensing pathways. Interestingly, we found that treatment with ezetimibe completely eliminated cholesterol absorption (fractional absorption was approximately zero), suggesting that the ezetimibe-sensitive pathway could account for all, or nearly all, intestinal cholesterol absorption under these conditions. Ultimately, mice devoid of CAV1 show normal fractional cholesterol absorption and are fully sensitive to ezetimibe. These findings demonstrate that caveolin-1 is not required for intestinal cholesterol absorption in the mouse model.

2.6 ACKNOWLEDGEMENTS

Figure 2.1 NPC1L1 and Annexin-2 protein levels are unaltered in Cav1 null mice and unaffected by ezetimibe feeding.
Wild-type (+) and *Cav1-/-*(-) mice were fed a powdered basal diet with or without ezetimibe (to provide 10 mg/ kg body weight per day) for 15 days. Protein was isolated from mucosa of the proximal third of the mouse small intestine. 60µg of total protein was loaded in each lane, and analyzed by western blot analysis using polyclonal antisera specific for CAV1 (pAb1 targets the amino-terminus, pAb2 detects the central region of the protein, and pAb3 detects carboxy-terminal amino acids), NPC1L1, and annexin-2 (ANXA2). ERK1/2 protein levels were used to assess equal sample loading. Shown are the representative results for 3 (of 6 analyzed) mice per group.
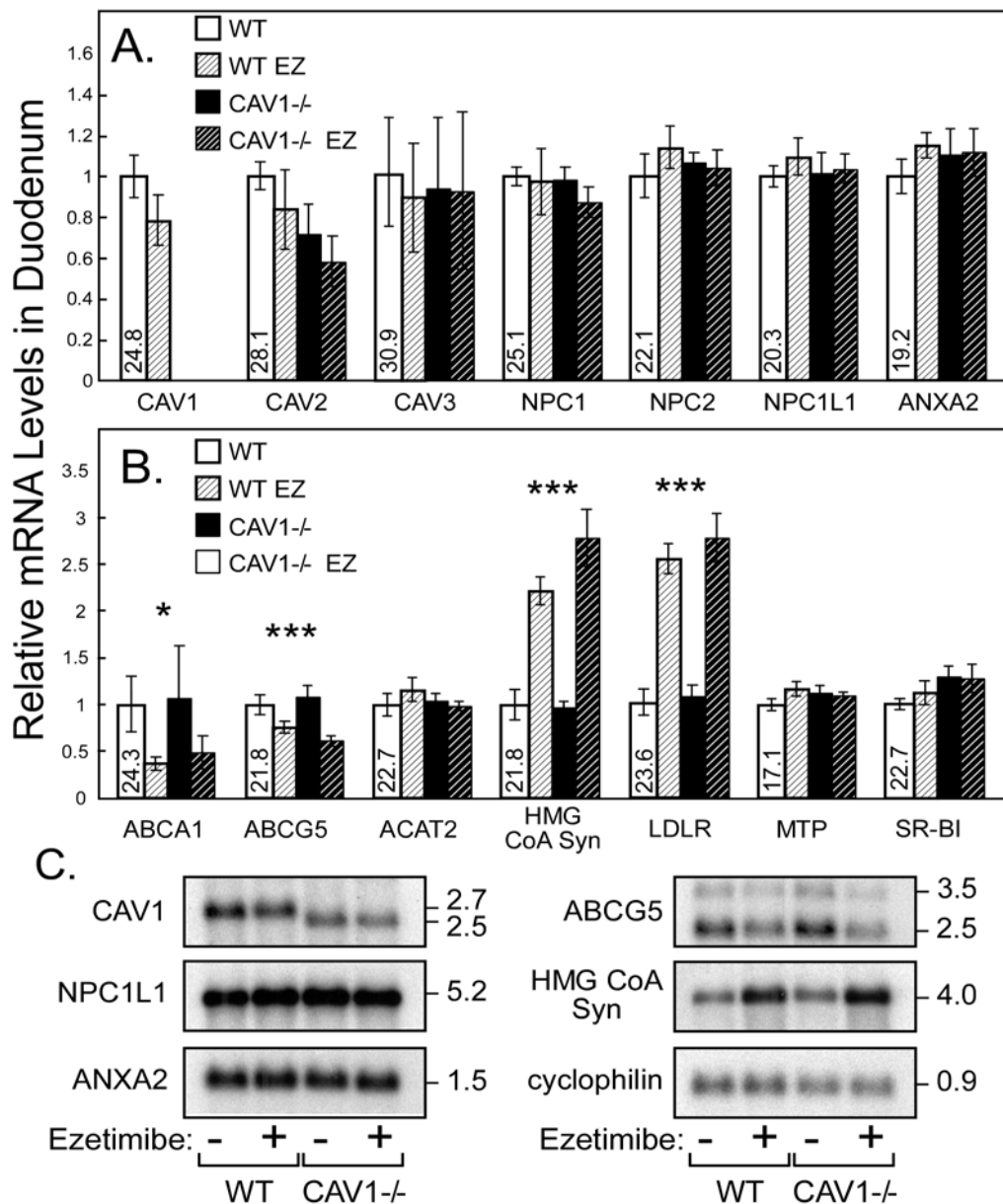
Figure 2.2 Relative expression of various genes involved with cholesterol handling in the duodenum.
Wild-type and *Cav1-/-* mice were fed a powdered basal diet with or without ezetimibe (to provide 10 mg/ kg body weight per day) for 15 days. RNA was isolated from mucosa of the proximal third of the mouse small intestine. *A* and *B*, mRNA levels were determined for duodenum of individual mice by quantitative real-time PCR. Values represent the mean ± SEM of data from 5-6 mice per group. The asterisks denote significant difference due to ezetimibe treatment: *P<0.05, ***P<0.0001. *C*, Northern analysis for selected mRNAs was also performed using 5 μg polyA+ RNA/lane purified from a pooled sample obtained from 5-6 mice per treatment.
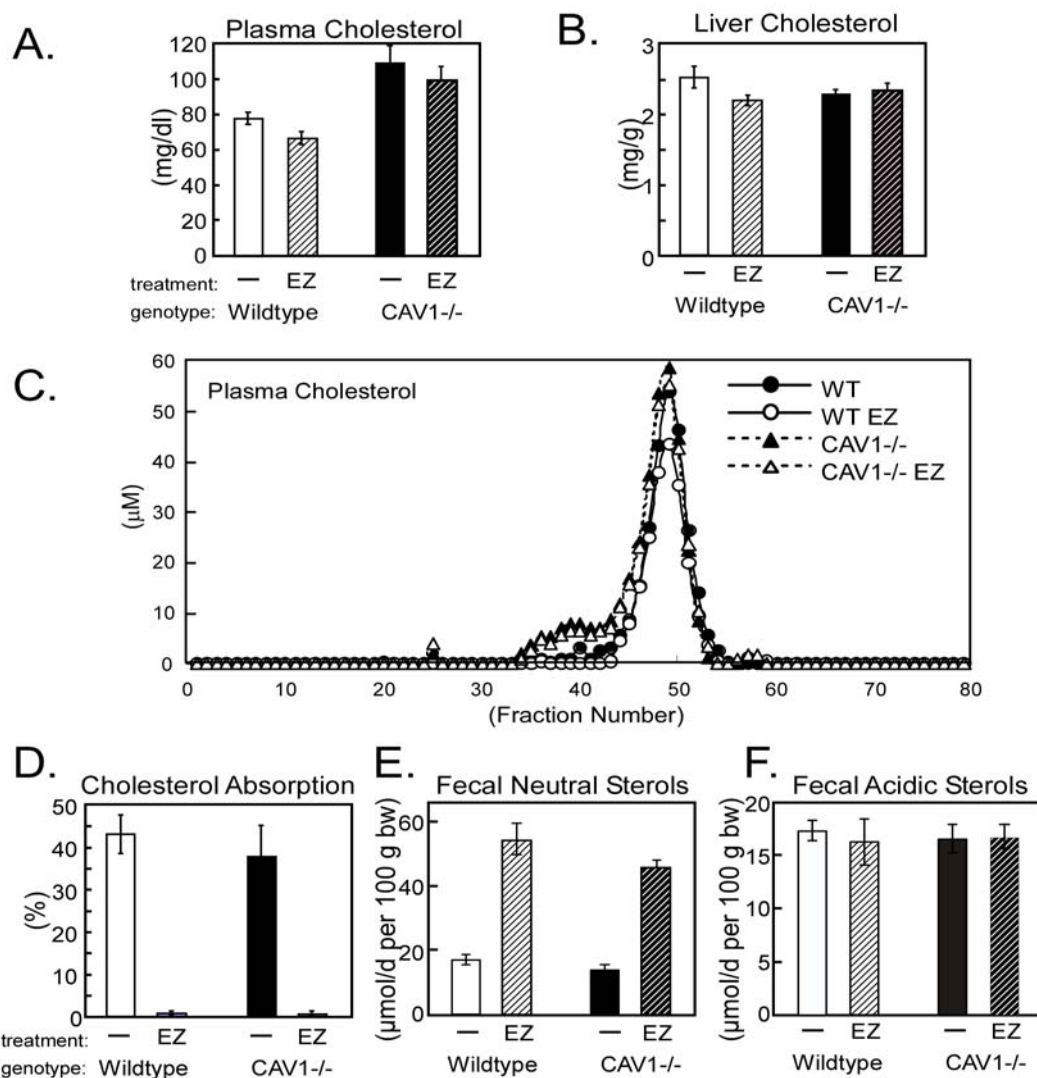
Figure 2.3 Sterol metabolism in wild-type and caveolin-1 knockout mice is similar, and ezetimibe works comparably to block cholesterol absorption. Male mice at 3 months of age were fed a basal rodent diet with or without added ezetimibe to provide 10 mg/kg body weight daily for 15 days. *A*, Plasma cholesterol was greater in *Cav1-/-* mice than wild-type mice (P<0.01). Ezetimibe treatment had no significant effect on plasma cholesterol. *B*, Liver total cholesterol levels did not differ by genotype or ezetimibe treatment. *C*, Plasmas from the 6 mice per group were pooled and fractionated by fast protein liquid chromatography using a Superose 6 column. The cholesterol content of each fraction was determined. *D*, Cholesterol absorption efficiency was determined by the fecal dual-isotope method and found to be similar in wild-type and knockout mice. Ezetimibe caused a significant decrease in absorption (P<0.001), regardless of genotype. *E*, Fecal neutral sterol excretion was greater in mice treated with ezetimibe (P<0.001). *F*, Fecal bile acid excretion was similar in all groups.
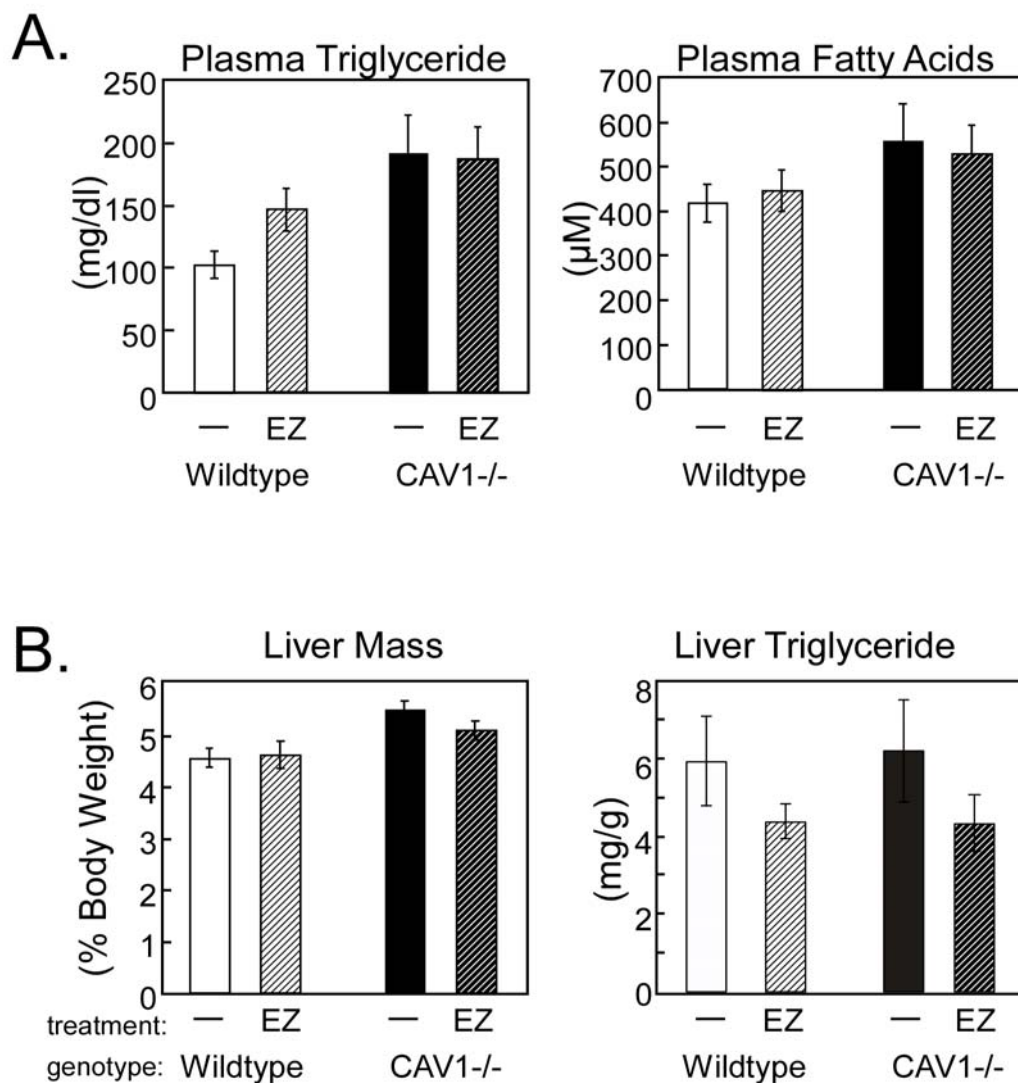
Figure 2.4 Plasma and liver lipid profiles show similar patterns in wild-type and *Cav1-/-* given ezetimibe.
Mice were fed a powdered basal diet with or without ezetimibe (to provide 10 mg/ kg body weight per day) for 15 days. *A*, Plasma triglyceride levels were significantly greater in Cav1-knockout mice (P<0.005), but no effect of ezetimibe was observed. Plasma non-esterified fatty acid levels were similar in all groups. *B*, Liver mass was statistically greater in Cav1-/- mice than wild-type (P<0.01). There was no significant effect of ezetimibe. Liver triglyceride concentration (expressed as mg/g wet liver weight) was not different among groups. Values represent the mean ± SEM of data from 5-6 mice per group. Statistical analyses were performed by 2-way ANOVA.
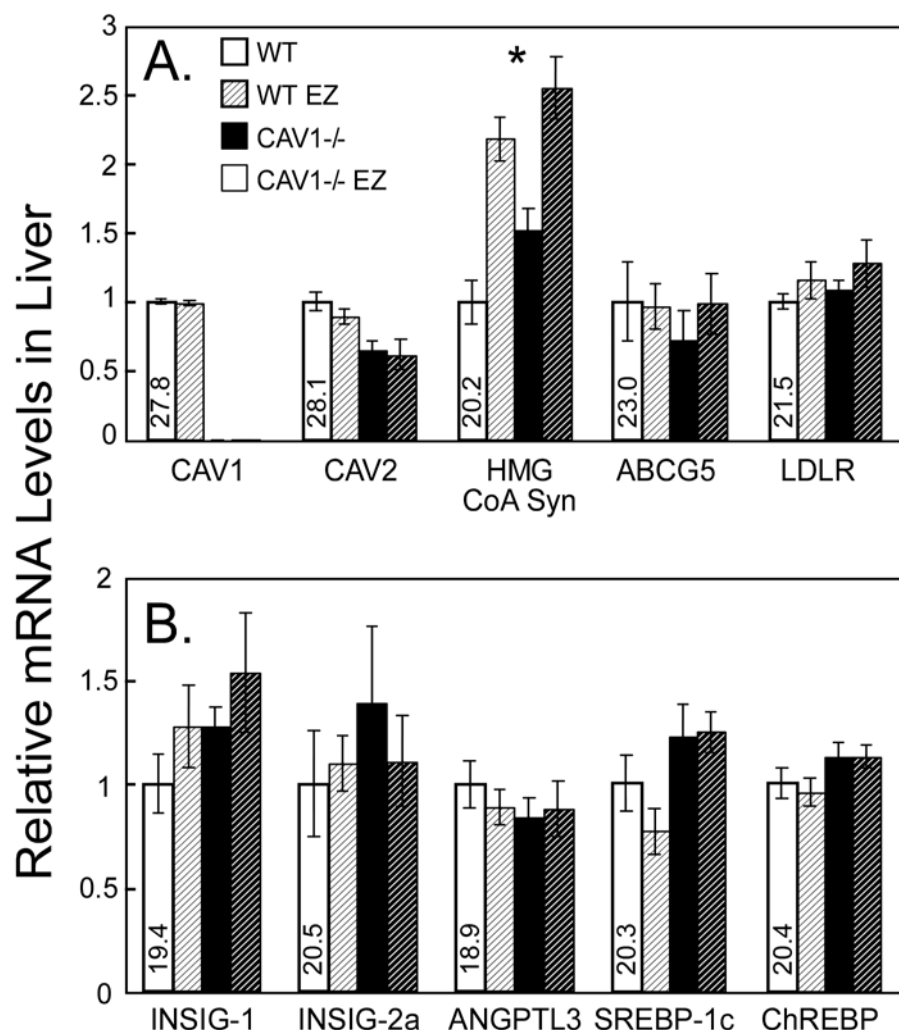
Figure 2.5 Relative expression of various genes of hepatic lipid metabolism.
Wild-type and *Cav1-/-* mice were fed a powdered basal diet with or without
ezetimibe (to provide 10 mg/ kg body weight per day) for 15 days. *A* and *B*,
mRNA levels were determined for liver of individual mice by quantitative real-time
PCR using SYBR green chemistry with gene-specific primers and calculated by
the comparative CT method using cyclophilin as the invariant control. The aver-
age cycle number at threshold for the control group (wild-type mice, basal diet) is
provided for each gene to allow for an approximate comparison of relative abun-
dance of different RNAs (note, cyclophilin CT = 19.2). Values represent the mean
± SEM of data from 5-6 mice per group. Statistical analyses were performed by
2-way ANOVA with genotype and ezetimibe treatment as the two factors. No sig-
nificant interaction of drug and genotype was observed for any mRNA species
measured. The only statistically significant differences observed were CAV2
mRNA reduction due to Cav1 deletion (*P<0.05), and elevated HMG CoA Syn
expression in mice treated with ezetimibe (*P<0.05).

CHAPTER 3

Retinoid X Receptor acutely Modulates Niemann-Pick C1 Like 1 Expression in Mouse Small Intestine

3.1 ABSTRACT

Niemann-Pick C1 Like 1 (NPC1L1) was recently identified as a protein critical for cholesterol uptake across the brush border of the enterocyte and as the molecular target of the novel cholesterol absorption blocking drug, ezetimibe. Since nuclear receptors are known to regulate cholesterol and lipid metabolism, we hypothesized that NPC1L1 expression might be modulated by this family of transcription factors. Using a library of nuclear receptor agonists, we treated animals for ~12h then measured intestinal mRNA expression of NPC1L1 by quantitative real-time PCR. Surprisingly, only the retinoid X receptor (RXR) specific agonist, LG268, modulated NPC1L1, whereas agonists for heterodimeric partners of RXR failed to recapitulate this effect. In addition, RXR repression of NPC1L1 occurs in the proximal intestine, the physiological site of cholesterol absorption, but not in the ileum. *In situ* hybridization revealed that NPC1L1 mRNA expression is reduced in jejunal enterocytes. Because intestinal cell lines fail to express NPC1L1 mRNA at levels comparable to intact small intestine and also fail to regulate expression in a similar manner by LG268, we have developed an intestinal explant system. In this system, we demonstrate not only that NPC1L1 mRNA expression is retained, but also that intestinal RXR activation is able to repress NPC1L1 gene

expression via a mechanism requiring a transcriptional and translational step, as both actinomycin D and cycloheximide block repression in LG268-treated intestinal explants. Cross-referencing of genes upregulated by LG268 in intestine with *in silico* analysis of NPC1L1 5' flanking region revealed putative regulatory networks involved in regulation of NPC1L1 expression including a modulator of signal transducer and activator of transcription (STAT) and nuclear factor kappa B (NF-κB) activity. Therefore, these results demonstrate that RXR can inhibit NPC1L1 gene transcription via an indirect mechanism, and suggest that hormones, cytokines, and other pro- or anti-inflammatory factors could influence NPC1L1 expression.

3.2 INTRODUCTION

Because of the strong correlation between coronary heart disease and plasma levels of LDL-cholesterol, much effort has been focused on development of agents that can decrease plasma cholesterol including inhibitors of *de novo* cholesterol synthesis (i.e. statins) or intestinal uptake (e.g. ezetimibe, cholestyramine, plant stanols, etc). The biochemical pathways governing endogenous cholesterol synthesis and the mechanism of action of statins (to competitively inhibit β-hydroxy-β-methylglutaryl-CoA (HMG-CoA) reductase) have been established. In contrast, the precise molecular mechanisms responsible for selective intestinal uptake of cholesterol have only begun to be elucidated. The discovery that NPC1L1 is critical for the uptake of cholesterol and non-cholesterol sterols (Altmann et al., 2004; Davies et al., 2005; Davis et al., 2004) provides a necessary functional component for understanding cholesterol physiology within the enterocyte.

NPC1L1 seems to act as an intestinal sterol permease, and, therefore in conjunction with the sterol effluxers adenosine triphosphate-binding cassette transporter G5 (ABCG5) and ABCG8 (Berge et al., 2000) govern movement of cholesterol between the enterocyte and the intestinal lumen.

Members of the nuclear receptor superfamily of ligand-activated transcription factors are known to regulate cholesterol absorption. Liver X receptors (LXRs) are thought to respond to endogenous metabolites of cholesterol, oxysterols (Janowski et al., 1999; Janowski et al., 1996) to upregulate feed-forward mechanisms to correct a cellular excess of cholesterol (Chawla et al., 2001). In the liver of mice, LXRs enhance conversion of cholesterol to bile acids by transactivation of CYP7A1, the rate-limiting enzyme in bile acid biosynthesis (Peet et al., 1998; Russell and Setchell, 1992). LXRs upregulate ABCG5/8 to efflux sterols across the canalicular membrane of hepatocytes into bile, and in the intestine to efflux sterols across the apical membrane of enterocytes into the intestinal lumen (Repa et al., 2002a; Yu et al., 2003). Farnesoid X receptor (FXR) responds to bile acids in the liver and represses CYP7A1 to provide negative feed-back regulation of bile acid production via induction of the transcriptional repressor SHP (Lu et al., 2000). Thus, activation of FXR indirectly leads to decreased intestinal cholesterol absorption because of decreased synthesis of bile acids, which are important for the micellar solubilization of luminal cholesterol prior to absorption in the intestine. Interestingly, both LXRs and FXR along with other nuclear receptors that act as "lipid sensors" for the body function as heterodimers with the retinoid X receptor (RXR).

Therefore, agonists of RXR can activate both LXR:RXR and FXR:RXR to robustly decrease cholesterol absorption via activation of two pathways (Repa et al., 2000c).

Since nuclear receptors are known to regulate cholesterol and lipid metabolism, we hypothesized that NPC1L1 expression might be modulated by this family of transcription factors. In this manner, nuclear receptors could alter the efficiency of cholesterol transport across the intestinal brush border through transcriptional regulation of NPC1L1. Here, we show that specific activation of RXR, but not other nuclear receptors known to heterodimerize with RXR, acutely modulates NPC1L1 mRNA and protein expression in the proximal small intestine. Moreover, RXR-mediated repression occurs through an indirect mechanism. *In silico* analysis of the promoter suggests hypothetical pathways by which nuclear receptors and other factors may alter NPC1L1 expression. These data suggest a novel mechanism by which RXR can influence cholesterol absorption.

3.3 EXPERIMENTAL PROCEDURES

3.3.1 Animal Experiments

Knockout mice for the following genes were generated previously as described: Acat2 (Buhman et al., 2000), Abca1 (Christiansen-Weber et al., 2000), Ibat (Dawson et al., 2003), Cyp7a1 (Ishibashi et al., 1996), Npc1 (Loftus et al., 1997), Cyp46 (Lund et al., 2003), Pparα (Peters et al., 1997), Cyp27a1 (Rosen et al., 1998), Fxr (Sinal et al., 2000), Lxr (Peet et al., 1998; Repa et al., 2000c), and Sr-b1 (Varban et al., 1998). Mice were maintained on a cereal-based rodent diet (Teklad Diet #7001, Madison, WI) which

contains 0.02% (w/w) cholesterol and 4% total lipid. For some experiments, mice were fed the powdered form of this diet with or without supplementation of various nuclear receptor agonists, including: 30 mg/kg/day LG268 [retinoid X receptor (RXR)], 0.5% (wt/wt) fenofibrate (PPAR-α), 150 mg/kg/day troglitazone (PPAR-γ), 0.05% (wt/wt) prenenolone-16α-carbonitrile [pregnane X receptor (PXR)], 3 mg/kg/day TCPOBOP (constitutive androstane receptor), 0.5% (wt/wt) chenodeoxycholic acid (farnesoid X receptor), 50 mg/kg/day T1317 [liver X receptor (LXR)], or 30 mg/kg/day LG268 + 50 mg/kg/day T1317 (RXR+LXR). The calculated quantities of dietary drug supplement assume a food consumption rate of 160 g of diet/day/kg body weight. Other agonists were administered by oral gavage as a suspension in 1% methylcellulose 1% Tween-80 and dosed twice over 14h. These include: 5 mg/kg GW0742 (PPARβ/δ), 1 mg/kg triiodothyronine (T_3) [thyroid hormone receptor (TR)], 50μg/kg 4-[(E)-2-(5,6,7,8-tetrahydro-5,5,8,8-tetramethyl-2-naphthalenyl)-1-propenyl] benzoic acid (TTNPB) [retinoic acid receptor (RAR)], and 75 μg/kg 1α,25-dihydroxyvitamin D_3 [vitamin D receptor (VDR)]. Mice were housed in a temperature-controlled environment with 12 hour light/dark cycles with free access to food and water. Unless otherwise specified, mice were sacrificed and tissues harvested at the end of the dark cycle, thus mice were in a fed-state at the time of study. Experiments were approved by the Institutional Animal Care and Use Committee of the University of Texas Southwestern Medical Center at Dallas.

3.3.2 Cholesterol Absorption

Fractional cholesterol absorption was measured by a fecal dual-isotope ratio method (Turley et al., 1994b). Three days before sacrifice, mice received a single intragastric dose of medium-chain triglyceride oil containing [5,6-^{3}H]sitostanol (2 μCi, American Radiolabeled Chemicals, Inc. St. Louis, MO) and [^{14}C]cholesterol (1 μCi, New England Nuclear, Boston MA). Stools were collected over the following 3 days. Samples of the dosing mixture and aliquots of stool were extracted, and the ratio of ^{14}C to ^{3}H in each was determined to calculate percent cholesterol absorption (Turley et al., 1994b).

3.3.3 Preparation of samples for RNA and protein measurements

Mice were anesthetized and exsanguinated via the descending vena cava. Small intestines were removed, flushed with ice-cold PBS and cut into three sections of equal length. The proximal, medial, and distal third were denoted duodenum, jejunum, and ileum, respectively. The sections were slit lengthwise, and the mucosae were gently scraped, frozen in liquid nitrogen and stored at –85°C. Total RNA was isolated from tissue samples using RNA STAT-60 (Tel-Test Inc.). Total protein was obtained from the organic phase remaining after RNA isolation by precipitating with isopropanol, consecutively washing with 0.3M guanidine hydrochloride in 95% ethanol and ethanol, then solubilizing the protein pellet in 1% SDS, 50mM Tris-Cl pH 8.8 (Banerjee et al., 2003). RNA concentrations were determined by absorbance at 260nm. Protein concentrations were determined using the BCA protein assay kit (Pierce Biotech., Rockford, IL).

3.3.4 Quantitiative real-time PCR (qRT-PCR)

qRT-PCR was performed using an Applied Biosystems Prism 7900HT sequence detection system as described (Kurrasch et al., 2004). Briefly, total RNA was treated with DNase I (RNase-free, Roche Molecular Biochemicals), and reverse-transcribed with random hexamers using SuperScript II (Invitrogen) to generate cDNA. Primers for each gene were designed using Primer Express Software (PerkinElmer Life Sciences) and validated by analysis of template titration and dissociation curves. Primers sequences for all assayed genes are provided in Table 3.1. Both sets of NPC1L1 primers gave identical results. Each qRT-PCR reaction contained (final volume of 10 μl): 25ng of reverse-transcribed RNA, each primer at 150nM, and 5μl of 2X SYBR Green PCR Master Mix (Applied Biosystems), and each sample was analyzed in triplicate. Results were evaluated by the comparative C_T method (User Bulletin No. 2, PerkinElmer Life Sciences) using cyclophilin as the invariant control gene. Similar results were obtained when villin was used as the housekeeping gene, suggesting that the changes observed were not the result of altered expression of our calibrator.

3.3.5 Western analysis

Total protein samples obtained from whole-cell lysates of the proximal third of small intestine were size-fractionated on 6% SDS-polyacrylamide gels (40 μg/lane), transferred electrophoretically to nitrocellulose membrane, and incubated with either polyclonal antisera for actin (sc-1616, Santa Cruz Biotech., Inc) or NPC1L1 (provided by Helen Hobbs (Valasek et al., 2005)). Proteins were visualized by exposure to film after

sequential treatment with specific primary antibodies, appropriate HRP-conjugated secondary antibodies, and a standard ECL kit (Amersham). Signal intensity of bands was determined by scanning then analyzing images with OptiQuant v3.1 (Packard Biosciences).

3.3.6 In Situ Hybridization

Segments of jejunum (13-18 cm from pyloric sphincter) were harvested and fixed overnight in 4% paraformaldehyde. Segments were paraffin-embedded, sectioned, then *in situ* hybridization was performed by using ^{35}S-labeled sense and antisense riboprobes as previously described (Shelton et al., 2000) using an NPC1L1 specific probe that recognizes the 3' untranslated region (nucleotides 4127-4572; GenBank Accession #XM_137497). Slides were exposed at 4°C for 2 weeks. Sections hybridized with the sense probe revealed no signal above background (data not shown).

3.3.7 Oligonucleotide Array Analysis

Total RNA was isolated from scraped mucosae from a segment of jejunum (corresponding to 8 – 16 cm from pyloric sphincter) of male A129/SvJ mice treated with vehicle or LG268 (30mpk/day) for 12 hours (n=4 per group). Total RNA was pooled then subjected to gel electrophoresis to confirm integrity of the RNA (data not shown). Expression was analyzed and compared using the Affymetrix GeneChip Mouse Expression Set 430A with a threshold value of 1.87-fold by Ruth Yu and Michael Downes of the NURSA signaling atlas (http://www.nursa.org). Genes up- or down-

regulated by LG268 are shown in Supplemental Table 3.1 and Supplemental Table 3.2, respectively.

3.3.8 Intestinal Explant Culture

Intestinal explants were cultured for ~8-24 hours using a combination of features from methods previously described (Armbrecht et al., 2002; Ferland and Hugon, 1979a, b; Mallordy et al., 1993). Briefly, mice were anesthetized then small intestines were removed, flushed with PBS, and a proximal small intestinal segment was obtained by cutting transversely at 8 and 16 cm distal to the pyloric sphincter. This segment was slit lengthwise and then cut to make small rectangular explants (approximately 2 mm x 5 mm). Explants were placed villi upward on Millicell culture plate inserts (Millipore, 30 mm diameter, 0.45 μm pore size) in 6-well culture plates containing 1.5 ml of explant media in the lower chamber. Explant media consisted of the following in a 8:1:1 ratio: high-glucose Dulbecco's modified Eagle's medium (DMEM) containing L-glutamine (Sigma), HEPES (25 mM, pH 7.4); NCTC-135 (Sigma); lipoprotein-deficient serum (LPDS, Intracel). In addition, penicillin/streptomycin was added to prevent bacterial overgrowth. After explants were placed on filters, a 500 μl cocktail containing soybean trypsin inhibitor, leupeptin, insulin (to a final concentration of 50 μg/ml, 25 μg/ml, and 10 μg/ml, respectively) was gently added dropwise onto the explants. In addition, LG268 (1 μM final concentration), actinomycin D (10 or 20 μM), cycloheximide (500 μM), dexamethasone (300 nM) and/or appropriate vehicle controls (matching volume of DMSO, methanol:ethanol (1:1), and/or water) was added to the cocktails. Fluid levels

generally equilibrated after several minutes such that a thin film remained above the insert without immersing the explants. Explants were immediately gassed with 95% O_2/ 5% CO_2 in a sealed chamber and incubated at 35°C for 24 hours. Explants from each well (3 explants/well) were pooled for RNA isolation; each treatment group consisted of three wells per experiment.

3.3.9 In Vivo Chromatin Immunoprecipitation Assay

Frozen mucosae from proximal intestine were crushed to a fine powder with a Besselar Tissue pulverizer then crosslinked in 1% formaldehyde for 15 minutes at room temperature. Reactions were stopped by addition of 0.1x volume 1.25 M glycine. Samples were washed twice with PBS supplemented with 1 mM phenylmethanesulfonyl fluoride (PMSF, Sigma) and complete protease inhibitor cocktail (Roche). Resuspended samples were subjected to 7 strokes of a Dounce homogenizer then centrifuged at 500 g for 2 minutes to pellet cells. Cells were resuspended in 2 mL SDS lysis buffer (1%SDS, 5 mM EDTA, 50 mM Tris-Cl pH 8.1) then incubated with rotation for 15 minutes at 4°C and sonicated with 20 15-second pulses to shear DNA to an average of approximately 400 base pairs. Debris was removed by centrifuging samples at 10,000 x g for 10 minutes and collecting the supernatant. Protein concentration was assayed using BCA (Pierce). The following steps utilized reagents from the Acetyl-Histone H3 Immunoprecipitation (ChIP Assay Kit (#17-245, Upstate)) and were performed according to the manufacturers protocol. Briefly, samples were diluted to 0.5 μg protein/μl (approximately 1:8) using ChIP Dilution Buffer and precleared with protein A agarose

incubation for at 4°C for 30 minutes. 5 µg anti-acetylated histone-H3 antibody was added to 500 µg protein aliquots and incubated at 4°C overnight with rotation. Protein A agarose was used to collect the antibody/histone complex, the pellet was washed and eluted according to manufacturer's instructions. Recovered DNA was analyzed by qRT-PCR against a standard titration curve, corrected by 10% input value, and then normalized to the background region (internal control). Primer sets were designed using Primer Express Software to generate amplicons of approximately 80 base pairs. Primers sets are shown in Table 3.2. The distance of each primer set from the putative transcriptional start site is represented as the distance of the central base pair of the amplicon and plotted on the x-axis. Relative expression for each primer set is plotted on the y-axis as fold over background region (defined as the average value for points -3911,-3612,-3455, and -2921). This average was previously determined to correlate with non-specific binding of a foreign plasmid (e.g. tk-LUC).

3.3.10 *In Silico* Analysis of Mouse NPC1L1 Promoter Region

Mouse cDNA sequence (Genbank Accession # XM_137497) was blasted against the mouse genome. 2000 bp upstream of exon 1 (corresponding to Genbank Accession # NT_039515; nt 3132251-3130252) was aligned with human sequence using zPicture (http://zpicture.dcode.org) then directly submitted for rVista 2.0 analysis (http://rvista.dcode.org) using only high-specificity matrices optimized for function within the vertebrate TRANSFAC professional library to identify conserved transcription factor binding sites. Results are summarized in Table 3.3.

3.3.11 Statistical Analysis of Data

Data are reported as the mean ± SEM for the specified number of animals. GraphPad Prism 4 or InStat 3 software (GraphPad, San Diego, CA) was used to perform all statistical analyses. If unequal variance was indicated by Bartlett's test, log transformation of data was performed prior to statistical analysis. For most studies, a 2-way analysis of variance (ANOVA) was performed, using genotype and treatment as factors. If a statistical interaction was observed between factors, comparison of all 4 groups was performed by Newman-Keuls post-hoc comparison. If only two groups were being compared, then two-tailed p-values were determined by Student's t-test. Statistical significance is denoted by asterisks: $*p<0.05$, $**p<0.01$, and $***p<0.001$.

3.4 RESULTS

To better understand if alterations in lipid or bile acid handling might influence NPC1L1 expression, thereby giving clues into metabolic regulation of this gene, duodenal expression of NPC1L1 mRNA in various gene-deficient mice was assessed by real-time quantitative PCR (Figure 3.1). Relative expression of ABCA1 and HMG-CoA synthase were also assessed to determine the impact on LXR and SREBP sterol-sensing pathways, respectively. Targeted deletion of ACAT2, LXRs, LXRs/FXR, or SRBI led to increased duodenal ABCA1 expression compared to wild-type controls, whereas deletion of CYP7A1 or IBAT decreased ABCA1 expression. HMG-CoA synthase was significantly decreased in ACAT2 deficient mice and increased in CYP7A1, CYP27A1, and IBAT deficient mice. In contrast, NPC1L1 mRNA expression is not significantly

altered by any of the genotypes suggesting that it is constitutively expressed and largely recalcitrant to these metabolic alterations. Thus in these particular mouse models, alterations in NPC1L1 expression are unlikely to attenuate or exacerbate the observed phenotypes, at least under these conditions. In addition, the observed expression pattern suggests that even though NPC1L1 contains a putative sterol regulatory element (SRE, (Davies et al., 2000b)), it may be regulated differently than HMG-CoA synthase, perhaps with less sensitivity. Moreover, NPC1L1 does not follow a similar pattern as ABCA1, suggesting it is not a direct target of LXR.

To determine if NPC1L1 expression is acutely regulated by nuclear receptors, we treated male A129/SvJ mice with a panel of nuclear receptor agonists supplemented in the diet including: 30 mg/kg/day LG268 [retinoid X receptor (RXR)], 0.5% (wt/wt) fenofibrate (PPAR-α), 150 mg/kg/day troglitazone (PPAR-γ), 0.05% (wt/wt) prenenolone-16α-carbonitrile [pregnane X receptor (PXR)], 3 mg/kg/day TCPOBOP (constitutive androstane receptor), 0.5% (wt/wt) chenodeoxycholic acid (farnesoid X receptor), 50 mg/kg/day T1317 [liver X receptor (LXR)], 30 mg/kg/day LG268 + 50 mg/kg/day T1317 (RXR+LXR); or given intragastically including: 5 mg/kg GW0742 (PPARβ/δ), 1 mg/kg triiodothyronine (T$_3$) [thyroid hormone receptor (TR)], 50μg/kg 4-[(E)-2-(5,6,7,8-tetrahydro-5,5,8,8-tetramethyl-2-naphthalenyl)-1-propenyl] benzoic acid (TTNPB) [retinoic acid receptor (RAR)], and 75 μg/kg 1α,25-dihydroxyvitamin D$_3$ [vitamin D receptor (VDR)]. These particular nuclear receptors were chosen because they are ligand-activated "lipid" sensors that heterodimerize with RXR (Shulman et al.,

2004). Some of these heterodimers are considered "permissive," meaning ligands for either RXR or its partner can transactivate target genes (e.g. CAR, FXR, LXR, PPAR, PXR). Others are considered "conditionally permissive," meaning ligands for RXR can further enhance transactivation if the ligand for its partner is already bound (e.g RAR), or "non-permissive," meaning RXR ligands cannot induce the heterodimer for coactivator recruitment and transactivation irrespective of ligand binding to its partner (e.g. T3R and VDR). For each of the treatments positive control genes were assessed to ensure delivery of drug. In addition to nuclear receptor agonists, we also treated mice with either ezetimibe for 12 days or statins (lovastatin or simvastatin) for 4 days because of their known cholesterol-reducing effects in patients and animal models. Relative mRNA abundance in duodenum was determined for NPC1L1, ABCA1, and HMG-CoA synthase (Figure 3.2). As expected, ABCA1 is robustly upregulated by agonists for RXR, LXR, or the combination (5-, 33-, and 65-fold, respectively). In addition, ABCA1 was upregulated approximately 4-fold by acute administration of triiodothyronine (T3), although it has been reported previously that TR may repress ABCA1 transcription *in vitro* (Huuskonen et al., 2004). In addition, ABCA1 expression was reduced by administration of ezetimibe as observed previously (Valasek et al., 2005), but unchanged by statins. In contrast to ABCA1, HMG-CoA synthase was unchanged by any of the nuclear receptor agonists tested under these acute conditions, however HMG-CoA synthase was induced by both ezetimibe and statins, suggesting the treatments were able to decrease cellular cholesterol within the enterocyte, as expected. Whereas HMG CoA

synthase was induced by both cholesterol-lowering agents, NPC1L1 mRNA abundance was not changed by administration of ezetimibe and even reduced by administration of statins. Suprisingly, NPC1L1 mRNA was reduced in duodenum of mice treated with an RXR-specific agonist, LG268, by itself, or in combination with an LXR agonist, T1317. Since the LXR agonist alone did not statistically effect the expression of NPC1L1 mRNA as compared to vehicle-treated controls, we conclude that the repression of NPC1L1 is due to the specific activation of RXR. Because RXR is known to promiscuously heterodimerize with a subset of nuclear receptors to transactivate target genes (Chawla et al., 2001; Mangelsdorf and Evans, 1995), we expected one of the other nuclear receptor agonists to recapitulate repression of NPC1L1 expression in a similar manner as the RXR-specific agonist thereby revealing the heterodimer responsible for induction. However, the other nuclear receptor agonists tested did not reduce NPC1L1 expression in the duodenum. These data suggest a novel mechanism for RXR-mediated repression of NPC1L1.

Although NPC1L1 seems to be almost exclusively expressed in small intestine of the mouse (Altmann et al., 2004), its distribution along the length of the small intestine is not known in this model organism. Because we wanted to determine the distribution not only of NPC1L1 but also its repression by RXR, we treated mice for 12 hours with or without LG268 (30 mg/kg/day) supplemented in the diet then determined NPC1L1 gene expression along the length of the small intestine. Figure 3.3A shows NPC1L1 expression in mucosae from each fifth of the intestine from the pyloric sphincter to ileo-

cecal junction. NPC1L1 was significantly reduced in the proximal 3/5 of the small intestine (~50% reduced), but not in the distal 2/5 of the small intestine, although a trend toward lower values was observed. *In situ* hybridization of jejunum using a riboprobe to specifically target the 3'UTR of NPC1L1 (nt 4127-4572, Genbank Accession# NM_137497) reveals a distribution pattern consistent with expression in enterocytes (Figure 3.3B). LG268 administration reduced NPC1L1 expression along most of the villus with retention of expression at the villus tips. This suggests that activation of RXR may be reprogramming immature enterocytes and/or mature enterocytes are recalcitrant to RXR activation. Longer term studies could address this question. To effect a meaningful biological change, the RXR-mediated repression of NPC1L1 mRNA expression in the proximal intestine must lead to significant changes in protein. Equal quantities of whole cell protein extracts obtained from proximal intestinal mucosae were size-fractionated by SDS-PAGE and subjected to immunoblot using polyclonal antibodies for NPC1L1 or actin (Figure 3.3C). NPC1L1 protein expression from 3 individual animals in each group was quantified with actin as a loading control and showed that LG268 significantly decreases NPC1L1 protein in proximal intestine. Because LG268 decreases both NPC1L1 mRNA and protein in the proximal small intestine, RXR regulation of NPC1L1 could have physiological importance as the bulk of cholesterol is absorbed in this location.

To better understand the mechanism by which RXR regulates NPC1L1 expression in intestine, we wanted to develop an in vitro system using enterocytic cell lines to better

assess gene expression and promoter activity. Unfortunately, the cell lines tested not only failed to express NPC1L1 at levels comparable to small intestine, they failed to exhibit acute regulation by RXR. These cell lines include HT29, T84, CaCo-2, IEC-6, IEC-18 (Mark Valasek, unpublished observation). To obtain a system that better approximates the intact small intestine, we developed an intestinal explant system similar to others that have been published (Armbrecht et al., 2002; Ferland and Hugon, 1979a, b; Mallordy et al., 1993). Intestinal explants cultured for 24 hours retain NPC1L1 expression as compared to uncultured small intestine (Figure 3.4A, C_T ~19). Under these culture conditions, a marker for enterocytes, villin, is highly expressed (C_T ~17) although marginally reduced over the 24-hour period. ABCA1 is modestly increased in these samples (C_T ~21). To determine if RXR could regulate NPC1L1 in intestinal explants, we treated explants with 1μM LG268 or dimethylsulfoxide (DMSO) control for 22-24 hours. As shown in Figure 3.4, LG268 significantly decreases NPC1L1 in intestinal explants, and increases ABCA1, acetyl-CoA carboxylase beta (ACCβ), and sterol regulatory element binding protein 1c (SREBP1c), and malic enzyme (ME). This suggests not only that RXR can be activated in this system, as evidenced by robust induction of control genes, but also that activation of intestine-resident RXR is sufficient to repress NPC1L1 expression. To determine if a transcriptional step were required for RXR-mediated repression of NPC1L1, intestinal explants were pretreated with an RNA polymerase II inhibitor, actinomycin D (10μM), for 2 hours before addition of LG268 (1μM), then incubated for 22 hours. Preatment with 10μM actinomycin D severely

blunted, but did not totally prevent, the induction of control genes by LG268. Similar results were obtained using co-treatment with 20µM actinomycin D (data not shown). Actinomycin D prevented repression of NPC1L1 by LG268, suggesting that a transcriptional step was required (Figure 3.4B). This is consistent with the fact that nuclear receptors generally act by influencing transcription. To determine if a translational step were required, intestinal explants were treated simultaneously with cycloheximide (500µM) and LG268 (1µM). Cycloheximide prevented the repression of NPC1L1 by LG268, suggesting that an intermediate protein was being generated to cause NPC1L1 repression. Although it is possible that cycloheximide may be blunting the effects of LG268 because of non-specific toxicity, this is unlikely to be the case as primary LXR target genes are robustly induced even in the presence of this dose of cycloheximide, while indirect target genes are blocked as expected (e.g. ME, GPAT, data not shown). Thus, RXR is likely to be transactivating expression of an intermediate protein that is responsible for NPC1L1 repression.

To identify potential intermediates, we undertook cDNA microarray studies to determine those genes regulated by RXR in the proximal small intestine using the samples depicted in Figure 3.3A (Segment B). The microarray results included 346 regulated genes total with 148 upregulated and 198 downregulated genes (using 1.87-fold threshold, Supplementary Tables 3.1 and 3.2). Included in the upregulated genes were many known targets of various RXR heterodimers. LXR:RXR target genes included SREBP1c (increased 5.19-fold) and ABCA1 (increased 4.84-fold) along with others.

PPAR:RXR target genes were also induced as compared to vehicle-treated animals: ACCβ (9.19-fold), stearoyl Coenzyme A desaturase 2 (SCD2, 6.73- and 6.5-fold), PPARα (5.46-fold), pyruvate dehydrogenase kinase 4 (Pdk4, 4.92-fold), and SCD1 (2.64-fold). In addition, peroxisomal structural proteins and enzymes are upregulated (Pex11a, Pxmp4, Decr2, and Peci), although peroxisomal proliferation itself has not been assessed in intestine and is generally thought to occur is response to peroxisome proliferators only in the rodent liver. FXR upregulates small heterodimeric partner (SHP, Nr0b2; 1.93-fold). Because of the prevalence of expected genes changes, it can be inferred that the microarray dataset has reasonable fidelity. Nevertheless, several genes were assessed by qPCR to give further validation of the array results (data not shown). Although many genes were down-regulated, of special interest were the upregulated genes as one of them could represent the intermediate which regulated NPC1L1 mRNA expression.

As changes in transcription factor activation or DNA binding often lead to alterations in histone acetylation, we performed *in vivo* chromatin-immunoprecipitation analysis of the 5' flanking region of NPC1L1 using acetylated histone-H3 antibodies to immunoprecipitate histone from formaldehyde cross-linked duodenal samples. Primer sets used to quantify immunoprecipitated DNA are shown in Table 3.2. Figure 3.5A shows enrichment of acetylated histone-H3 in the proximal promoter region. Moreover, acute administration of LG268 (~14h; 30 mg/kg) causes a decrease in histone-H3 acetylation in a discrete region. To determine which pathways might be important for transcriptional regulation of NPC1L1, we compared the mouse promoter region

(encompassing 2kb upstream) to human sequence to determine conserved transcription factor binding sites (TFBS) using rVista 2.0 (Loots and Ovcharenko, 2004). This type of analysis reduces the number of false positives by including only those TFBS that are conserved between species. The analysis reveals 9 non-overlapping sites (Table 3.3) ranging from −28 to −1608 which contain conserved binding sites for at least 16 transcription factors including: AP4, activating enhancer-binding protein 4; E47, transcription factor E2a; EBVR, Epstein-Barr virus transcription factor R; HNF1, hepatic nuclear factor 1; HNF4, hepatocyte nuclear factor 4; HSF, heat shock factor; IK3, ikaros 3; LXR, liver X receptor; MyoD, myogenic differentiation (determination); NF-κB, nuclear factor kappa B; PBX, pre B-cell leukemia transcription factor; RFX, regulatory factor X; STAT, signal transducer and activator of transcription; TCF8, transcription factor 8 (AREB6). Although any number of these sites may be important for regulated or tissue-specific expression of NPC1L1, we wanted to further reduce the number of sites likely to be specifically involved in RXR-mediated repression. To do this, we performed literature searches of the Medline database by cross-referencing upregulated genes on the array (with known gene names) with transcription factors known to bind the conserved TFBS. The resulting literature was predominated by articles concerning suppressor of cytokine signaling 3 (SOCS3) and its impact on various STAT proteins. In addition, SOCS3 may inhibit NF-κB signaling (Karlsen et al., 2004; Wang et al., 2003a). Therefore, we validated SOCS3 mRNA expression using qRT-PCR. Indeed, SOCS3 was induced ~3-fold in proximal intestine (Segment B, 8-16 cm from pyloric sphincter) by

administration of LG268 (30mg/kg/day) for 12h (Figure 3.5B), suggesting it may be a primary target gene of RXR. Thus, we were able to develop a hypothetical model pathway involved in regulation of NPC1L1 (Figure 5C). Specifically, activation of RXR by LG268 induces SOCS3 expression, SOCS3 inhibits the function of STATs or NF-kB to transactivate NPC1L1, and then NPC1L1 protein levels decrease causing decreased cholesterol absorption. If indeed STATs and NF-kB regulate NPC1L1 expression, other factors that regulate these proteins could also alter cholesterol absorption.

One prediction of this model is that agents that decrease STAT or NF-kB activity (e.g. anti-inflammatory agents) would also decrease NPC1L1 expression. Therefore, we hypothesized that dexamethasone, a synthetic glucocorticoid which acts as an anti-inflammatory and immunosuppressant by binding the glucocorticoid receptor (GR), would decrease NPC1L1 expression in the small intestine. To test this, we treated intestinal explants for 8h with vehicle or 300nM dexamethasone. As shown in Figure 3.6, dexamethasone significantly reduced NPC1L1 expression. This observation suggests that anti-inflammatory agents can reduce NPC1L1 expression.

3.5 DISCUSSION

Because of the magnitude of the impact of cardiovascular disease on industrialized countries, there has been much impetus to develop novel cholesterol-lowering agents. Recently a cholesterol absorption blocking drug, ezetimibe, has been approved for use in combination with statins (HMG-CoA reductase inhibitors) or as a monotherapy to decrease plasma LDL-cholesterol concentrations. Ezetimibe potently

inhibits cholesterol absorption in several species by targeting NPC1L1 (Garcia-Calvo et al., 2005). In mice, the species for which ezetimibe is the least potent, the IC_{50} of cholesterol absorption for ezetimibe is approximately 0.5 mpk/day (Garcia-Calvo et al., 2005), while cholesterol absorption is completely blocked at 10 mpk/day (for example (Valasek et al., 2005)). Selective activation of RXR also has profound effects on cholesterol absorption with similar potency as ezetimibe. In mice, the IC_{50} of cholesterol absorption for LG268 is approximately 1 mpk/day, while cholesterol absorption is completely blocked at 14 mpk/day (Repa et al., 2000c). In contrast to ezetimibe, which blocks NPC1L1 activity, LG268 activates RXR to effect a number of pathways which together robustly reduce cholesterol absorption. First, LG268 activates FXR:RXR heterodimers to down-regulate CYP7A1 (Makishima et al., 1999), the rate-limiting step in the classical pathway of bile acid biosynthesis, via a mechanism involving small heterodimer partner (SHP, (Lu et al., 2000)). Decreased bile acid synthesis decreases bile acid pool size and lumenal content of bile acids, thus inhibiting the requisite process of micellar solubilization of cholesterol prior to absorption. Second, LG268 activates LXR:RXR heterodimers thereby transactivating target genes, including ABCG5/8, in the liver and intestine to promote efflux of cholesterol into the bile or the intestinal lumen, respectively (Repa et al., 2002a; Repa et al., 2000c). Here, we have discovered a third pathway in which LG268 reduces cholesterol absorption, namely by reduction of NPC1L1 expression in the proximal small intestine.

RXR-mediated reduction of NPC1L1 expression is likely to be independent of the FXR and LXR pathways for a number of reasons. First, cholesterol absorption is reduced by LG268 in *Lxrα/β-*, *Fxr-*, and *Lxrα/β/Fxr*-knockout mice demonstrating the existence of other pathways (Amy Liverman and David Mangelsdorf, unpublished observation). Second, acute administration of FXR (chenodeoxycholate) or LXR (T0901317) agonists does not recapitulate the repression seen by acute administration of LG268 (Figure 3.2). Third, manipulation of the bile acid pool size by targeted-deletion of various genes involved in bile acid synthesis, trafficking, and homeostasis has no significant effect on NPC1L1 mRNA expression in duodenum (Figure 3.1). Fourth, cholesterol supplementation (0.2-2.0% w/w) of a basal low-fat diet generally does not reduce NPC1L1 mRNA expression more than ~20% ((Valasek, 2006), data not shown), suggesting the general effect of LXR might be minimal under these conditions. Nevertheless, assessment of NPC1L1 expression in *Lxrα/β/Fxr*-knockout mice acutely treated with LG268 may be necessary to conclusively rule-out involvement of these pathways in the RXR-mediated regulation of NPC1L1.

It is also possible that the effects of RXR are simply due to activation of permissive heterodimers with PPARα or β, which have already been implicated in the modulation of NPC1L1. It has been shown that PPARα agonist treatment (fenofibrate, 800 mpk/day, 10 days) of A129 wild-type reduces duodenal NPC1L1 mRNA expression by approximately 40 percent (Valasek et al, 2006), and PPARβ/δ agonist treatment (GW610742, 0.017% w/w, 8 days) of DBA/1 wild-type mice reduces NPC1L1 mRNA

expression in jejunum and ileum, but not duodenum (van der Veen et al., 2005). Our data suggest that RXR can modulate NPC1L1 independently of these interactions, as LG268 can significantly reduce NPC1L1 mRNA in duodenum and jejunum after acute treatment (~12h), whereas agonists for PPARs and other nuclear receptors fail to do so in this short period (Figure 3.2).

RXR is also known to heterodimerize with NURR1 or NGF-IB, which lack ligand-binding pockets. These heterodimers could theoretically be involved in regulation of NPC1L1. Alternatively, since RXR homodimers are able to regulate PPAR target genes *in vivo* (A et al., 2004), it may be possible that RXR homodimers could regulate distinct genes as well.

LG268 represses NPC1L1 exclusively in the proximal intestine, the physiologic site of cholesterol absorption, but not in the ileum (Figure 3.3A). It is possible that the pharmacological intervention to specifically activate RXR is mimicking a physiological event by which elements of the diet contribute to a decrease in cholesterol absorption. However, it is unclear at present what signals RXR itself may be responding to in the small intestine. Putative endogenous ligands for RXRs include 9-*cis*-retinoic acid (Heyman et al., 1992), docosahexanoic acid (de Urquiza et al., 2000), and phytanic acid (Lemotte et al., 1996). Moreover, activated RXR is detectable during embryonic development (Luria and Furlow, 2004; Solomin et al., 1998). The microarray results strongly suggest that activation of RXR leads to a upregulation of genes (and their gene products) which promote handling of lipids, especially fats. While this can be explained

largely by the fact that RXR is signaling through PPARs, the question regarding the character of bona-fide endogenous (or exogenous) physiologically relevant ligands for RXR remains. It is interesting to note here that acute administration of medium-chain triglycerides (MCT) also decreases NPC1L1 expression (data not shown). MCT could be signaling through RXR (by promoting production of an endogenous ligand) or could be acting in a parallel fashion by altering metabolism similar to RXR activation (e.g. promoting β-oxidation) to eventually impact NPC1L1 expression. Determining the proximate factors that can regulate NPC1L1 expression will aid in investigating the signaling networks that regulate NPC1L1.

To better understand the mechanism by which RXR activation leads to a reduction in NPC1L1 expression, we developed an intestinal explant system. Intestinal explants treated with LG268 (1 μM, ~24h) show a reduction in NPC1L1 expression that is blocked by actinomycin D and cycloheximide (Figure 3.4). These data suggest not only that selective activation of RXR resident in the intestine is sufficient for repression of NPC1L1, but also that this repression is indirect, relying on both RNA polymerase II transcription and new protein synthesis. The most parsimonious explanation is that RXR enhances transcription of an intermediate that is responsible for reducing steady-state levels of NPC1L1 mRNA either by reducing transcription or changing transcript stability.

In vivo, acute administration of LG268 (~14h; 30 mg/kg) causes a decrease in duodenal histone-H3 acetylation in a discrete region of the NPC1L1 promoter in which we found TFBS that were conserved between mouse and human. This suggested that

these sites might be important for transcriptional regulation and might possibly be involved in RXR-mediated repression of transcription. To determine the sites that could be altered by RXR action in the intestine, we performed literature searches of the Medline database to find articles containing both a gene upregulated by LG268 (from array data) and a transcription factor known to bind one of the conserved sites. Because many of the articles concerned SOCS3 regulation of STAT proteins, we tested SOCS3 gene expression by qRT-PCR and found that it was indeed upregulated ~3-fold by LG268 administration. SOCS3 is known to inhibit STAT signaling downstream of a number of gp130-linked receptors which lack intrinsic tyrosine-kinase activity, rather relying on janus kinases (JAKs) to phosphorylate STAT proteins. In addition, SOCS3 may inhibit NF-κB signaling (Karlsen et al., 2004; Wang et al., 2003a). In each of these cases, an increased quantity of SOCS3 protein would be predicted to decrease activity of STATs or NF-κB and therefore NPC1L1 expression. Thus, a hypothetical model can be proposed in which modulators of STAT or NF-κB activity could impact NPC1L1 expression and cholesterol absorption. This model predicts that certain cytokines, growth factors, or pro-inflammatory factors could increase NPC1L1 expression, whereas cellular inhibitors of STATs or NF-κB (e.g. SOCS, IκB) or anti-inflammatory factors could decrease NPC1L1 expression. To further test this hypothesis, we treated intestinal explants with dexamethasone, a potent anti-inflammatory agent, and found that it quickly decreased NPC1L1 expression. This model may also provide an explanation for the ability of statins to decrease NPC1L1 expression (Figure 3.2), as they are known to have

anti-inflammatory properties. The ability of statins to decrease cellular cholesterol levels may not be important for regulation of NPC1L1 expression, because treatment with ezetimibe to likewise diminish cellular sterol levels had no effect on expression.

In summary, acute activation of RXR decreases NPC1L1 mRNA and protein expression in the proximal small intestine via an indirect mechanism. Investigation of pathways likely to be responsible for transcriptional regulation of NPC1L1 reveals that modulation of STAT or NF-kB activity by cytokines, growth factors, inflammation, or other factors might influence both NPC1L1 expression and cholesterol absorption.

3.6 ACKNOWLEDGEMENTS
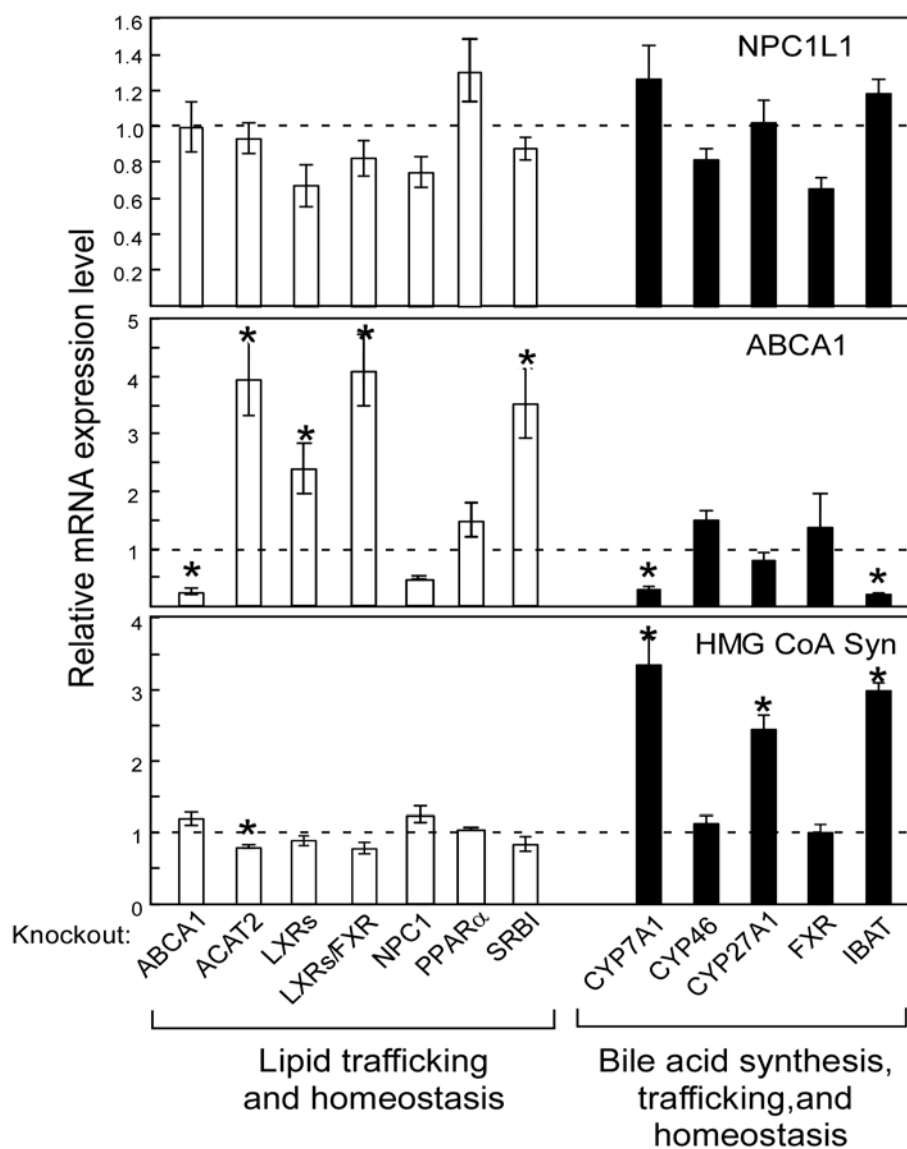
Figure 3.1 NPC1L1 mRNA expression in proximal small intestine is not altered by targeted deletion of various genes in lipid and bile acid homeostasis.
NPC1L1, ABCA1, and HMG-CoA synthase mRNA levels were measured in the proximal intestine of various knockout mice and compared to their gender-, age-, and background-matched controls while on a basal diet. Relative mRNA levels were measured using SYBR green chemistry with gene-specific primers (Table 1) and calculated by the comparative CT method using cyclophilin as the housekeeping control gene. Values represent the mean ± SEM of data from 4-6 mice per group. Statistical analyses were performed by two-tailed Student's t-test; asterisks indicate statistical difference from wild-type controls on the same genetic background: *, $p < 0.05$.
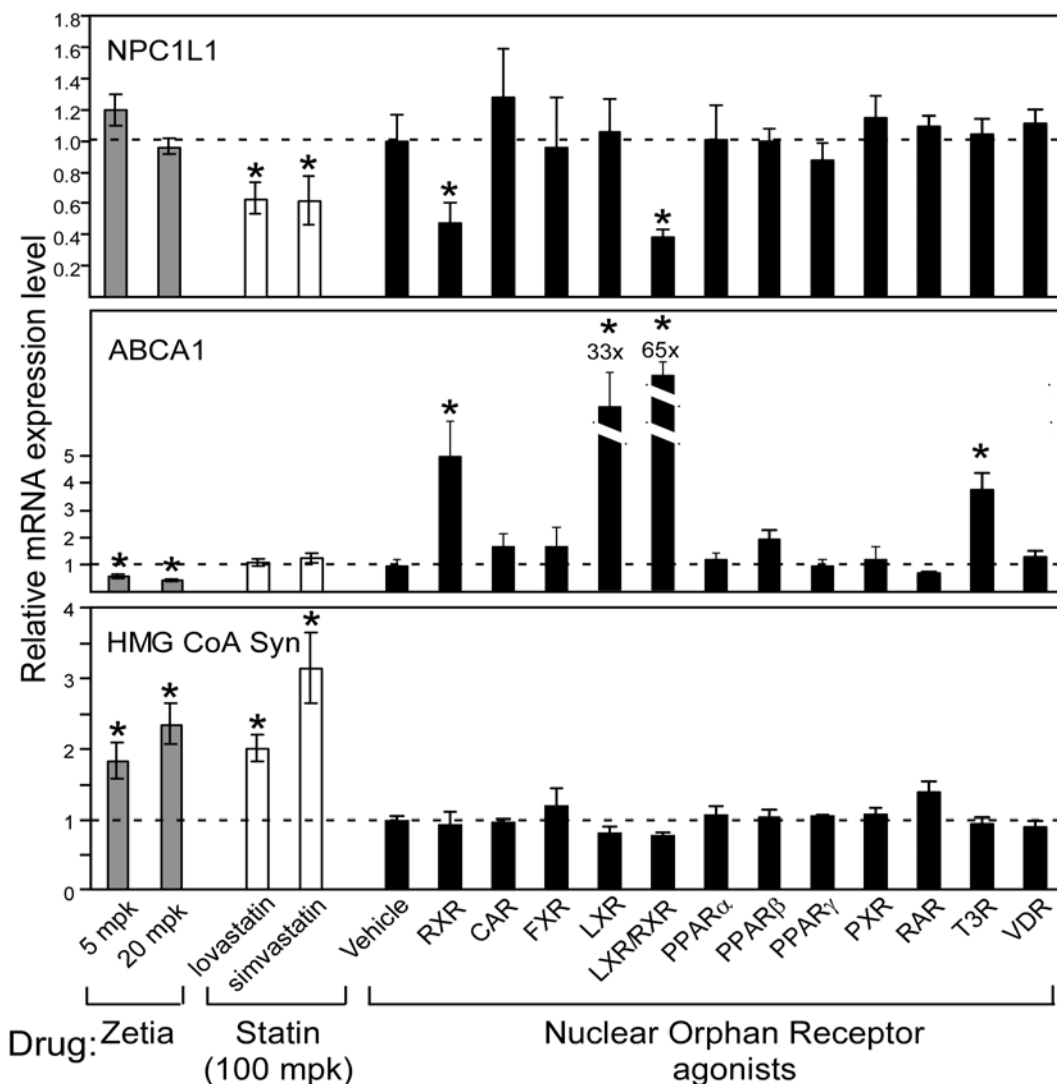
Figure 3.2 NPC1L1 mRNA expression in proximal small intestine is reduced by an RXR-specific agonist and statins, but not by agonists for heterodimeric partners of RXR or ezetimibe.
NPC1L1, ABCA1, and HMG-CoA Synthase mRNA levels were measured in the duodenum of various drug-treated male A129/SvJ mice and compared to vehicle controls. Nuclear receptor agonists were administered in diet or by oral gavage (see Experimental Procedures) for ~12-14h, statins were administered in diet for 4 days at 100 mpk/day, and ezetimibe (Zetia) was administered for 12 days at 5 or 20 mpk/day. Relative mRNA levels were measured using SYBR green chemistry with gene-specific primers (Table 1) and calculated by the comparative C_T method using cyclophilin as the housekeeping control gene. Values represent the mean ± SEM of data from 4-6 mice per group. Statistical analyses were performed by two-tailed Student's t-test; asterisks indicate statistical difference from vehicle-treated controls: *, $p < 0.05$.
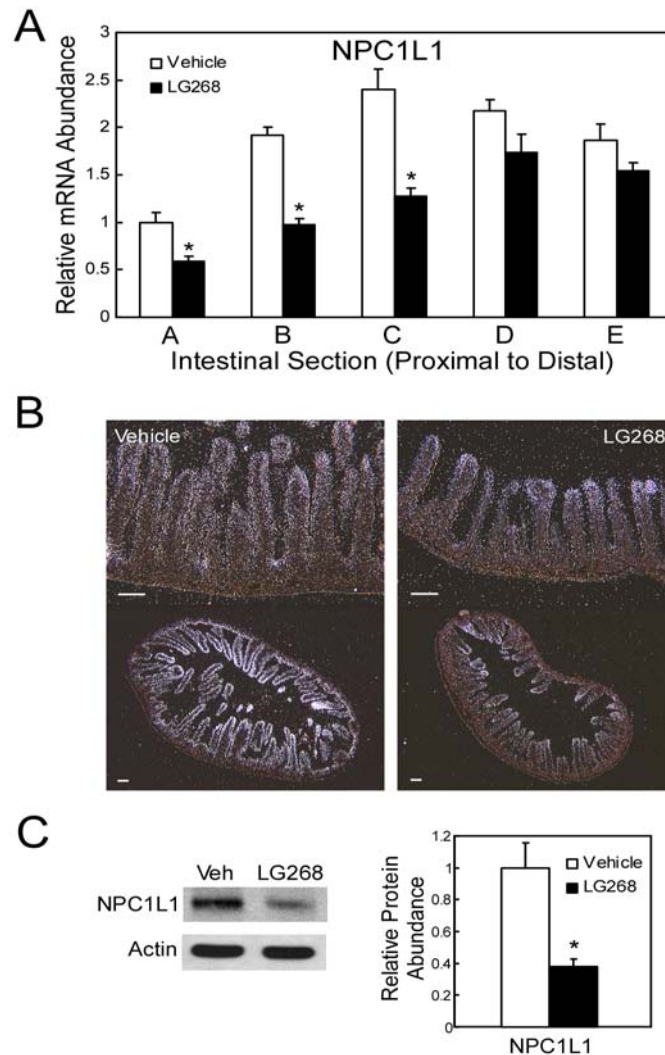
Figure 3.3 LG268 reduces NPC1L1 mRNA and protein in proximal small intestine. *A*, Relative mRNA expression of NPC1L1 along the entire length of small intestine. Small intestines were divided into fifths from vehicle- and LG268-treated (30 mpk/day; 12h diet) male A129/SvJ mice then assayed for gene expression by qRT-PCR. *B*, *In situ* hybridization of jejunal sections using a probe directed at the 3' UTR of NPC1L1 shows reduced expression in female mice given two intragastric doses of 30 mpk LG268 over 14h. Sense controls gave no signal above background (Scale Bar: 100µm) *C*, Whole-cell protein was isolated from mucosa of the proximal third of small intestine of each individual animal. 40µg protein was loaded in each lane and resolved by SDS-PAGE, then immunoblotted with NPC1L1 and actin polyclonal antisera. Representative immunoblots and NPC1L1 protein quantification using OptiQuant v3.1 software with actin as a loading control. Values represent the mean ± SEM of data from 3-4 mice per group. Statistical analyses were performed by two-tailed Student's t-test; asterisks indicate statistical difference from vehicle controls: *, p<0.05.
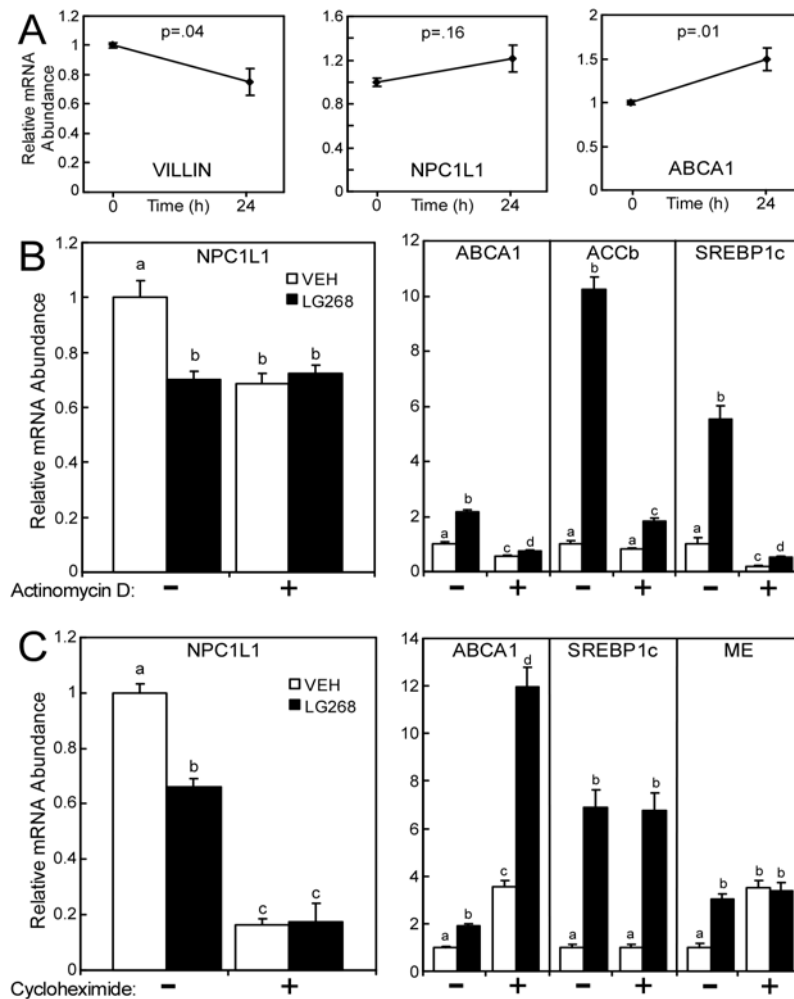
Figure 3.4 Reduction of NPC1L1 mRNA expression by LG268 is blocked by actinomycin D and cycloheximide in intestinal explants. Intestinal explants were harvested from 2-3 month old female A129/SvJ mice. *A*, NPC1L1 mRNA expression is maintained in intestinal explant culture. Explants were either immediately frozen on liquid nitrogen (t = 0h) or cultured for 24 hours (t = 24h) in 95% O_2/ 5% CO_2 at 35°C, then RNA was isolated and qRT-PCR was performed. *B*, Actinomycin D blocks repression of NPC1L1 by LG268. Explants were pretreated with 10 µM actinomycin D or vehicle (methanol:ethanol, 1:1 ratio) for 2 hours in 95% O_2/ 5% CO_2 at 35°C, then LG268 (1 µM final concentration) or vehicle (DMSO) was added dropwise to the explants and incubated for 22 hours in 95% O_2/ 5% CO_2 at 35°C. *C*, Cycloheximide blocks repression of NPC1L1 by LG268. Explants were co-treated with 500 µM cycloheximide, 1 µM LG268, and/or vehicles (H2O, DMSO) for 24 hours in 95% O_2/ 5% CO_2 at 35°C. Values represent the mean ± SEM of data from two independent experiments done in triplicate. Statistical analyses were performed by two-tailed Student's t-test to determine p-values, or by one-way ANOVA with post-hoc test (different letters indicate statistically different groups, $p < 0.05$).
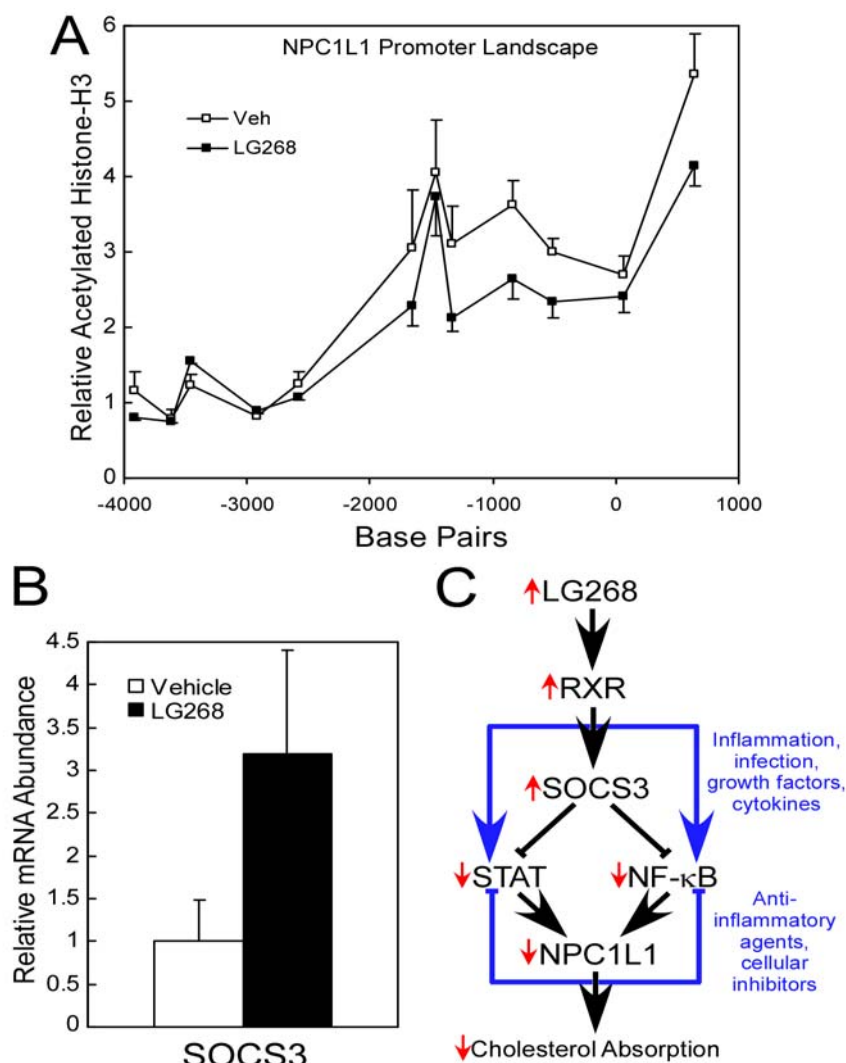
Figure 3.5 Putative transcriptional pathways involved in the regulation of NPC1L1 expression. *A*, Histone-H3 acetylation is diminished at the NPC1L1 locus in duodenum. Formaldehyde cross-linked protein/DNA complexes from duodena of vehicle or LG268-treated mice (n=3 per group) was sheared to approximately 400bp then immunoprecipitated with acetylated histone-H3 antibodies. Quantitation of immunoprecipitated DNA was performed by qRT-PCR using the primers listed in Table 3.2. Data was normalized to the background region (average of points -3911,-3612,-3455, and -2921), which was previously determined to correlate with non-specific binding of a foreign plasmid (e.g. tk-LUC). *B*, SOCS3 is upregulated by LG268 in the proximal small intestine (Section B, Figure 3.3A) as assessed by qRT-PCR (n=4 per group). *C*, Cross-referencing of SOCS3 and transcription factor binding sites conserved in the NPC1L1 promoter (see Table 3.3) yields possible pathways by which RXR and other factors may influence NPC1L1 gene expression. Values represent the mean ± SEM of data from 3-4 mice per group.
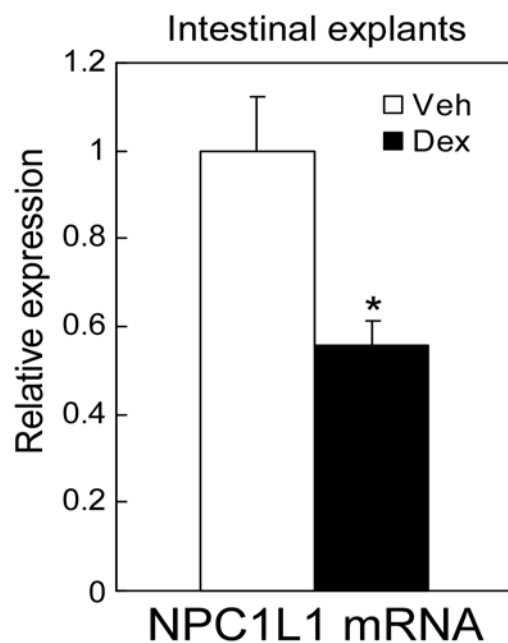
Figure 3.6 Dexamethasone reduces NPC1L1 mRNA expression in intestinal explants.
Intestinal explants were harvested from 2-3 month old female A129/SvJ mice and cultured (see Experimental Procedures). Explants were treated with vehicle or 300 nM dexamethasone for 8 hours in 95% O_2/ 5% CO_2 at 35°C. Values represent the mean ± SEM of data from triplicate wells per treatment. Statistical analyses were performed by two-tailed Student's t-test; asterisks indicate statistical difference from vehicle-treated controls: *, $p < 0.05$.

TABLE 3.1

Primer sequences used for the measurement of mouse intestinal RNA levels
by quantitative real-time PCR.

Gene	Common name	GenBank #	Primer sequences
ABCA1	ATP-binding cassette transporter A1	NM_013454	F: 5'-cgtttccgggaagtgtccta R: 5'-gctagagatgacaaggaggatgga
ACCβ	Acetyl-CoA carboxylase beta	XM_132282	F: 5'-cccagccgagtttgtcact R: 5'-ggcgatgagcaccttctcta
Cyclo	Cyclophilin	M60456	F: 5'-tggagagcaccaagacagaca R: 5'-tgccggagtcgacaatgat
HMG CoA Syn	β-hydroxy-β-methylglutaryl-CoA synthase	NM_145942	F: 5'-gccgtgaactgggtcgaa R: 5'-gcatatatagcaatgtctcctgcaa
ME	Malic enzyme	NM_008615	F: 5'-gccggctctatcctcctttg R: 5'-tttgtatgcatcttgcacaatcttt
NPC1L1 5' set	Niemann Pick type C1-like 1	NM_207242	F: 5'-tggactggaaggaccatttcc R: 5'-gacaggtgccccgtagtca
NPC1L1 3' set	Niemann Pick type C1-like 1	NM_207242	F: 5'-ggcatgaacgccatttgc R: 5'-gcaatagccacataagactgattagg
SOCS3	Suppressor of cytokine signaling 3	NM_007707	F: 5'-cacctggactcctatgagaaagtg R: 5'-gagcatcatactgatccaggaact
SREBP-1c	Sterol regulatory element binding protein 1c	NM_011480	F: 5'-ggagccatggattgcacatt R: 5'-ggcccgggaagtcactgt
Villin	Villin	NM_009509	F: 5'-agtcccccatcttccaacaac R: 5'-tcaaacttcacctgttccacctt

Primer sequences are designed and optimized for use with the Applied Biosystems real-time PCR system (ABI7900HT).

TABLE 3.2

Primer sequences used for the measurement by qRT-PCR
of mouse NPC1L1 genomic DNA fragments following
chromatin immunoprecipitation with acetylated histone-H3 antibody.

Set#	Median nt# relative to transcriptional start site	Amplified Segment per GenBank# NT_039515	Primer sequences
1 (distal)	-3911	3134208-3134116	F: 5'-ctgtcatttcttcttttgcaatatatgtag R: 5'-aaaacctagcaatccaaatgtgtgt
2	-3612	3133905-3133820	F: 5'-gtggtggctcatacctgcaa R: 5'-ccctgtgtatcccacagatgact
3	-3455	3133746-3133665	F: 5'-agaaagaatggaaggaaggtcaga R: 5'-acatctcatccagcagtcacaaa
4	-2921	3133215-3133129	F: 5'-tgaggcaaggcgctacact R: 5'-aagttggcctgaaaaattctatgg
5	-2576	3132883-3132771	F: 5'-gcacaagaggtgggcaagac R: 5'-gctgaccaccgtgcatgtc
6	-1656	3131945-3131868	F: 5'-ggcaaccagcccgatttt R: 5'-ccatgtttatttggaattatcatcca
7	-1464	3131752-3131678	F: 5'-ccccacacaggcagtgatg R: 5'-gaagcccccaaaagcatga
8	-1326	3131617-3131537	F: 5'-ctggacagccctcgtgaga R: 5'-gccacatgaaaaccccaaga
9	-838	3131147-3131030	F: 5'-tggcatccagggagcaa R: 5'-gctcgggtgggctcaga
10	-520	3130821-3130721	F: 5'-ccaggttgggtgggacttg R: 5'-ctcctcatgcccgttctatcc
11	61	3130224-3130158	F: 5'-agctgccttaatgtgcaaactca R: 5'-ggaccaggccttggagaca
12 (proximal)	637	3129652-3129578	F: 5'-tgacagcaataaaggtcgctatct R: 5'-gtgatccaatagagtgtggctttaaa

Primer sequences are designed and optimized for use with the Applied Biosystems real-time PCR system (ABI7900HT).

TABLE 3.3

Conserved sites (mouse vs human) within proximal promoter region of NPC1L1 gene
(NT_039515; nt 3132251-3130252) as determined by rVista 2.0 analysis using
TRANSFAC database(Loots and Ovcharenko, 2004).

Site#	Non-overlapping site range (nt relative to tss)	Transcription factor(s) at each site	Mouse Site Sequence (5' – 3')
1	-28 to -48	HNF1	GAAAATAAATTATTAACCAGT
2	-351 to -359	RFX	CAGTTGCTA
3	-568 to -588	EBVR, TCF8	TGAACCATGTACCTGGGCCCA
4	-727 to -745	AP4, E47, MyoD	CTCCCTGCAGCTGTCTCAA
5	-1004 to -1021	LXR*	TGTCGTCACCTGAAGTCA
6	-1180 to -1199	STAT1/5A/5B, NF-κB, HSF, IK3	CTATTCCAGGAATGTCCTCA
7	-1362 to -1377	CP2, AP4	TCTGGGGACAGCTGGA
8	-1395 to -1403	HNF4*	CTGGACCTC
9	-1597 to -1608	PBX	GATTGAGGGCAA

Abbreviations used include: AP4, activating enhancer-binding protein 4; E47,
transcription factor E2a; EBVR, Epstein-Barr virus transcription factor R; HNF1, hepatic
nuclear factor 1; HNF4, hepatocyte nuclear factor 4; HSF, heat shock factor; IK3, ikaros
3; LXR, liver x receptor; MyoD, myogenic differentiation; NF-κB, nuclear factor kappa
B; PBX, pre B-cell leukemia transcription factor; RFX, regulatory factor X; STAT, signal
transducer and activator of transcription; TCF8, transcription factor 8 (AREB6).
*NUBISCAN analysis to determine putative binding sites for LXR (i.e. DR4) or HNF4
(i.e. DR1) did not corroborate these sites, suggesting they may be false positives or
reflect insufficiently specific matrices.

SUPPLEMENTARY TABLE 3.1

Genes upregulated by LG268 (30 mpk; 12 hours) in proximal small intestine.

ProbeSet	Avg Ratio	Unigene	Title	Gene Symbol
1429790_at	23.43	Mm.265415	RIKEN cDNA 6330569O16 gene	6330569O16Rik
1443147_at	13.69	Mm.23581	Mus musculus transcribed sequences	---
1448894_at	10.74	Mm.5378	aldo-keto reductase family 1, member B8	Akr1b8
1441237_at	10.2	Mm.102593	Mus musculus transcribed sequences	---
1427052_at	9.19	Mm.81793	acetyl-Coenzyme A carboxylase beta	Acacb
1425137_a_at	7.73	Mm.88795	histocompatibility 2, Q region locus 10	H2-Q10
1415822_at	6.73	Mm.193096	stearoyl-Coenzyme A desaturase 2	Scd2
1415823_at	6.5	Mm.193096	stearoyl-Coenzyme A desaturase 2	Scd2
1449051_at	5.46	Mm.1373	peroxisome proliferator activated receptor alpha	Ppara
1431833_a_at	5.37	Mm.10633	3-hydroxy-3-methylglutaryl-Coenzyme A synthase 2	Hmgcs2
1422997_s_at	5.37	Mm.45431	mitochondrial acyl-CoA thioesterase 1	Mte1-pending
1426690_a_at	5.19	Mm.214958	sterol regulatory element binding factor 1	Srebf1
1423858_a_at	5.1	Mm.10633	3-hydroxy-3-methylglutaryl-Coenzyme A synthase 2	Hmgcs2
1449065_at	5.1	Mm.1978	cytosolic acyl-CoA thioesterase 1	Cte1
1417273_at	4.92	Mm.10283	pyruvate dehydrogenase kinase, isoenzyme 4	Pdk4
1421840_at	4.84	Mm.369	ATP-binding cassette, sub-family A (ABC1), member 1	Abca1
1424853_s_at	4.44	Mm.10742	cytochrome P450, family 4, subfamily a, polypeptide 10	Cyp4a10
1417148_at	4.44	Mm.4146	platelet derived growth factor receptor, beta polypeptide	Pdgfrb
1425409_at	4.29	Mm.57350	cholinergic receptor, nicotinic, alpha polypeptide 2 (neuronal)	Chrna2
1457721_at	4.21	Mm.18935	Mus musculus transcribed sequences	---
1424439_at	3.93	Mm.45641	RIKEN cDNA 1810065E05 gene (PLA2i)	1810065E05Rik
1439675_at	3.8	Mm.212789	Mus musculus adult male testis cDNA	---
1439478_at	3.54	---	---	---
1426785_s_at	3.48	Mm.194795	monoglyceride lipase	Mgll
1421011_at	3.42	Mm.254439	retinal short-chain dehydrogenase/reductase 2	Retsdr2-pending
1447845_s_at	3.36	Mm.27154	vanin 1	Vnn1
1435173_at	3.31	Mm.216321	arginine-tRNA-protein transferase 1	Ate1
1448964_at	3.31	Mm.6891	calbindin 3, (vitamin D-dependent calcium binding protein)	Calb3
1421031_a_at	3.25	Mm.45161	RIKEN cDNA 2310016C08 gene	2310016C08Rik
1423619_at	3.19	Mm.3903	RAS, dexamethasone-induced 1	Rasd1
1424451_at	3.14	Mm.224885	3-ketoacyl-CoA thiolase B	MGC29978
1421183_at	3.14	Mm.78133	testis expressed gene 12	Tex12
1417231_at	3.08	Mm.117068	claudin 2	Cldn2
1415824_at	3.08	Mm.193096	stearoyl-Coenzyme A desaturase 2	Scd2
1416946_a_at	3.08	Mm.205266	acetyl-Coenzyme A acyltransferase 1	Acaa1
1416576_at	3.08	Mm.3468	suppressor of cytokine signaling 3	Socs3
1417130_s_at	2.98	Mm.196189	angiopoietin-like 4	Angptl4
1422996_at	2.98	Mm.45431	mitochondrial acyl-CoA thioesterase 1	Mte1-pending

1448700_at	2.93	Mm.3283	G0/G1 switch gene 2	G0s2
1421134_at	2.93	Mm.8039	amphiregulin	Areg
1444518_at	2.88	Mm.100170	Mus musculus transcribed sequences	---
1450391_a_at	2.88	Mm.194795	monoglyceride lipase	Mgll
1421517_at	2.88	Mm.89194	sialyltransferase 7	Siat7a
1455025_at	2.83	Mm.30771	RIKEN cDNA 1700020G04 gene	1700020G04Rik
1417568_at	2.78	Mm.135621	DNA segment, Chr 15, ERATO Doi 412, expressed	D15Ertd412e
1435135_at	2.73	Mm.24576	RIKEN cDNA B230106I24 gene	B230106I24Rik
1428309_s_at	2.64	Mm.12746	RIKEN cDNA 1110004D19 gene	1110004D19Rik
1419104_at	2.64	Mm.181473	RIKEN cDNA 0610041D24 gene	0610041D24Rik
1415965_at	2.64	Mm.267377	stearoyl-Coenzyme A desaturase 1	Scd1
1428386_at	2.64	Mm.27944	fatty acid Coenzyme A ligase, long chain 3	Facl3
1456212_x_at	2.64	Mm.3468	suppressor of cytokine signaling 3	Socs3
1436321_at	2.64	Mm.86467	UDP-GlcNAc:betaGal beta-1,3-N-acetylglucosaminyltransferase 7	B3gnt7
1436169_at	2.59	Mm.151485	RIKEN cDNA C730029A08 gene	C730029A08Rik
1417109_at	2.59	Mm.15801	lipocalin 7	Lcn7
1455227_at	2.59	Mm.24576	RIKEN cDNA B230106I24 gene	B230106I24Rik
1455899_x_at	2.59	Mm.3468	suppressor of cytokine signaling 3	Socs3
1426603_at	2.55	Mm.259254	ribonuclease L (2', 5'-oligoisoadenylate synthetase-dependent)	Rnasel
1460235_at	2.55	Mm.259568	scavenger receptor class B, member 2	Scarb2
1452771_s_at	2.55	Mm.27944	fatty acid Coenzyme A ligase, long chain 3	Facl3
1449709_s_at	2.51	Mm.216321	arginine-tRNA-protein transferase 1	Ate1
1448382_at	2.51	Mm.288363	RIKEN cDNA 1300002P22 gene	1300002P22Rik
1448318_at	2.51	Mm.381	adipose differentiation related protein	Adfp
1429822_at	2.46	Mm.178280	RIKEN cDNA 4633401B06 gene	4633401B06Rik
1419365_at	2.46	Mm.20615	peroxisomal biogenesis factor 11a	Pex11a
1442622_at	2.46	Mm.218768	Mus musculus transcribed sequences	---
1424268_at	2.46	Mm.29763	spermine oxidase	Smox
1448747_at	2.46	Mm.40466	F-box only protein 32	Fbxo32
1453836_a_at	2.42	Mm.194795	monoglyceride lipase	Mgll
1449442_at	2.42	Mm.20615	peroxisomal biogenesis factor 11a	Pex11a
1431028_a_at	2.42	Mm.24742	pantothenate kinase 1	Pank1
1458083_at	2.38	Mm.102553	Mus musculus transcribed sequences	---
1422603_at	2.38	Mm.175173	ribonuclease, RNase A family 4	Rnase4
1428164_at	2.38	Mm.241484	nudix (nucleoside diphosphate linked moiety X)-type motif 9	Nudt9
1458496_at	2.34	Mm.117566	Mus musculus transcribed sequences	---
1416632_at	2.34	Mm.148155	malic enzyme, supernatant	Mod1
1436168_at	2.34	Mm.151485	RIKEN cDNA C730029A08 gene	C730029A08Rik
1415806_at	2.34	Mm.154660	plasminogen activator, tissue	Plat
1426594_at	2.34	Mm.27789	RIKEN cDNA 6030440G05 gene	6030440G05Rik
1454704_at	2.34	Mm.39288	RIKEN cDNA 9330185J12 gene	9330185J12Rik
1424214_at	2.34	Mm.44208	RIKEN cDNA 9130213B05 gene	9130213B05Rik

1457824_at	2.3	Mm.14627	phospholipid scramblase 1	Plscr1
1416947_s_at	2.3	Mm.205266	acetyl-Coenzyme A acyltransferase 1	Acaa1
1418715_at	2.3	Mm.24742	pantothenate kinase 1	Pank1
1430697_at	2.26	Mm.143724	Ammecr1	Ammecr1
1437667_a_at	2.26	Mm.233944	BTB and CNC homology 2	Bach2
1415964_at	2.26	Mm.267377	stearoyl-Coenzyme A desaturase 1	Scd1
1454883_at	2.26	Mm.286806	expressed sequence AI987692	AI987692
1416840_at	2.26	Mm.29429	RIKEN cDNA 3110038L01 gene	3110038L01Rik
1419031_at	2.26	Mm.38901	fatty acid desaturase 2	Fads2
1449553_at	2.26	Mm.46513	RIKEN cDNA 2610200G18 gene	2610200G18Rik
1458599_at	2.22	Mm.156831	Mus musculus transcribed sequences	---
1454632_at	2.22	Mm.18957	RIKEN cDNA 6330442E10 gene	6330442E10Rik
1447585_s_at	2.22	Mm.26865	mitochondrial ribosomal protein S6	Mrps6
1418486_at	2.22	Mm.27154	vanin 1	Vnn1
1435484_at	2.22	Mm.288678	Mus musculus transcribed sequences	---
1455506_at	2.18	Mm.101716	Mus musculus transcribed sequences	---
1419550_a_at	2.18	Mm.198414	serine/threonine kinase 39, STE20/SPS1 homolog (yeast)	Stk39
1452011_a_at	2.18	Mm.201248	UDP-glucuronate decarboxylase 1	Uxs1
1433600_at	2.18	Mm.235195	adrenergic receptor, alpha 2a	Adra2a
1455438_at	2.18	Mm.24673	peroxisomal membrane protein 4	Pxmp4
1436970_a_at	2.18	Mm.4146	platelet derived growth factor receptor, beta polypeptide	Pdgfrb
1419591_at	2.18	Mm.83284	melanoma-derived leucine zipper, extra-nuclear factor	Mlze
1436515_at	2.18	Mm.88186	RIKEN cDNA E030004N02 gene	E030004N02Rik
1434897_a_at	2.14	Mm.16228	solute carrier family 25, member 4	Slc25a4
1426275_a_at	2.14	Mm.201248	UDP-glucuronate decarboxylase 1	Uxs1
1426856_at	2.14	Mm.26772	RIKEN cDNA 2610207I16 gene	2610207I16Rik
1438169_a_at	2.14	Mm.27789	RIKEN cDNA 6030440G05 gene	6030440G05Rik
1423495_at	2.14	Mm.35760	2-4-dienoyl-Coenzyme A reductase 2, peroxisomal	Decr2
1424211_at	2.14	Mm.41877	RIKEN cDNA 5730438N18 gene	5730438N18Rik
1459344_at	2.11	Mm.218534	RIKEN cDNA 9630019E01 gene	9630019E01Rik
1441971_at	2.11	Mm.25647	Mus musculus transcribed sequences	---
1460674_at	2.07	Mm.142343	membrane progestin receptor alpha	Mpra-pending
1434866_x_at	2.07	Mm.18522	carnitine palmitoyltransferase 1, liver	Cpt1a
1438156_x_at	2.07	Mm.18522	carnitine palmitoyltransferase 1, liver	Cpt1a
1422780_at	2.07	Mm.24673	peroxisomal membrane protein 4	Pxmp4
1448942_at	2.07	Mm.25547	guanine nucleotide binding protein (G protein), gamma 11	Gng11
1452008_at	2.03	Mm.1622	RIKEN cDNA 9130422G05 gene	9130422G05Rik
1457254_x_at	2.03	Mm.18957	RIKEN cDNA 6330442E10 gene	6330442E10Rik
1436499_at	2.03	Mm.220936	RIKEN cDNA 9530058O11 gene	9530058O11Rik
1434382_at	2.03	Mm.45132	RIKEN cDNA 2310004K20 gene	2310004K20Rik
1421262_at	2.03	Mm.55113	lipase, endothelial	Lipg
1438313_at	2	Mm.124117	Mus musculus transcribed sequences	---

1455229_x_at	2	Mm.227366	silencer-associated factor (Saf) pseudogene	LOC260345
1426604_at	2	Mm.259254	ribonuclease L (2', 5'-oligoisoadenylate synthetase-dependent)	Rnasel
1446228_at	2	Mm.267131	DNA segment, Chr 19, Wayne State University 12, expressed	D19Wsu12e
1448229_s_at	2	Mm.3141	cyclin D2	Ccnd2
1415776_at	2	Mm.4210	aldehyde dehydrogenase family 3, subfamily A2	Aldh3a2
1450018_s_at	2	Mm.46067	RIKEN cDNA 4933433D23 gene	4933433D23Rik
1430307_a_at	1.97	Mm.148155	malic enzyme, supernatant	Mod1
1418337_at	1.97	Mm.17905	ribose 5-phosphate isomerase A	Rpia
1431688_at	1.97	Mm.203971	RIKEN cDNA 4833407H14 gene	4833407H14Rik
1454045_a_at	1.97	Mm.28864	RIKEN cDNA 4933424M23 gene	4933424M23Rik
1448325_at	1.97	Mm.4048	myeloid differentiation primary response gene 116	Myd116
1437277_x_at	1.93	Mm.18843	transglutaminase 2, C polypeptide	Tgm2
1420651_at	1.93	Mm.216321	arginine-tRNA-protein transferase 1	Ate1
1426857_a_at	1.93	Mm.26772	RIKEN cDNA 2610207I16 gene	2610207I16Rik
1439018_at	1.93	Mm.27654	hypothetical protein 6330505N24	6330505N24
1454046_x_at	1.93	Mm.28864	RIKEN cDNA 4933424M23 gene	4933424M23Rik
1449854_at	1.93	Mm.34209	nuclear receptor subfamily 0, group B, member 2	Nr0b2
1430641_at	1.93	Mm.42327	RIKEN cDNA 9030605I04 gene	9030605I04Rik
1431922_at	1.9	Mm.158735	RIKEN cDNA 9130012O13 gene	9130012O13Rik
1431012_a_at	1.9	Mm.28883	peroxisomal delta3, delta2-enoyl-Coenzyme A isomerase	Peci
1423108_at	1.9	Mm.29666	solute carrier family 25, member 20	Slc25a20
1423952_a_at	1.9	Mm.30142	keratin complex 2, basic, gene 7	Krt2-7
1433428_x_at	1.87	Mm.18843	transglutaminase 2, C polypeptide	Tgm2
1448391_at	1.87	Mm.25306	RAB9, member RAS oncogene family	Rab9
1418739_at	1.87	Mm.26462	serum/glucocorticoid regulated kinase 2	Sgk2
1417369_at	1.87	Mm.3195	hydroxysteroid (17-beta) dehydrogenase 4	Hsd17b4

SUPPLEMENTARY TABLE 3.2

Genes downregulated by LG268 (30 mpk; 12 hours) in proximal small intestine.

ProbeSet	Avg Ratio	Unigene	Title	Gene Symbol
1455882_x_at	-10.37	Mm.134437	RIKEN cDNA A930041G11 gene	A930041G11Rik
1453505_a_at	-7.86	Mm.23375	eukaryotic translation initiation factor 2 alpha kinase 3	Eif2ak3
1438439_at	-7.73	Mm.123648	RIKEN cDNA F730001G15 gene	F730001G15Rik
1418857_at	-7.59	Mm.57258	solute carrier family 13, member 2	Slc13a2
1421637_at	-7.46	Mm.154797	solute carrier family 5, member 4a	Slc5a4a
1433578_at	-7.34	Mm.253661	hypothetical protein E130304D01	E130304D01
1422974_at	-6.96	Mm.31676	5' nucleotidase, ecto	Nt5e
1437755_at	-6.84	Mm.277148	expressed sequence AI315119	AI315119
1420970_at	-6.5	Mm.288206	adenylate cyclase 7	Adcy7
1436667_at	-6.5	Mm.41963	X transporter protein 3	Xtrp3
1456123_at	-6.17	Mm.277148	expressed sequence AI315119	AI315119
1443137_at	-5.86	Mm.187830	Mus musculus 0 day neonate lung cDNA	---
1426990_at	-4.59	Mm.2735	cubilin (intrinsic factor-cobalamin receptor)	Cubn
1422899_at	-4.59	Mm.41963	X transporter protein 3	Xtrp3
1419339_at	-4.36	Mm.103703	neuraminidase 3	Neu3
1439617_s_at	-4.36	Mm.42246	phosphoenolpyruvate carboxykinase 1, cytosolic	Pck1
1422757_at	-4.21	Mm.155678	solute carrier family 5, member 4b	Slc5a4b
1426199_x_at	-4.21	Mm.240437	immunoglobulin heavy chain (J558 family)	Igh-VJ558
1427851_x_at	-4.21	Mm.240437	immunoglobulin heavy chain (J558 family)	Igh-VJ558
1419727_at	-4.21	Mm.34044	decay accelerating factor 2	Daf2
1451681_at	-3.93	Mm.214923	cis-retinol/3alpha hydroxysterol short-chain dehydrogenase-like	CRAD-L
1418979_at	-3.73	Mm.26838	RIKEN cDNA 9030611N15 gene	9030611N15Rik
1417828_at	-3.67	Mm.9970	aquaporin 8	Aqp8
1425668_a_at	-3.61	Mm.2793	sialyltransferase 4C (beta-galactoside alpha-2,3-sialyltransferase)	Siat4c
1422217_a_at	-3.54	Mm.14089	cytochrome P450, family 1, subfamily a, polypeptide 1	Cyp1a1
1426849_at	-3.36	Mm.192303	Mus musculus activated spleen cDNA	---
1427860_at	-3.31	Mm.104747	immunoglobulin kappa chain variable 8 (V8)	Igk-V8
1451964_at	-3.31	Mm.213215	melanoma inhibitory activity 2	Mia2
1450348_at	-3.25	Mm.261542	solute carrier family 19 (sodium/hydrogen exchanger), member 3	Slc19a3
1423439_at	-3.25	Mm.42246	phosphoenolpyruvate carboxykinase 1, cytosolic	Pck1
1452536_s_at	-3.19	Mm.104747	immunoglobulin kappa chain variable 8 (V8)	Igk-V8
1455454_at	-3.19	Mm.22832	Mus musculus transcribed sequence	---
1434917_at	-3.19	Mm.22847	cordon-bleu	Cobl
1425738_at	-3.14	Mm.196407	immunoglobulin kappa chain variable 21 (V21)	Igk-V21
1452270_s_at	-3.14	Mm.2735	cubilin (intrinsic factor-cobalamin receptor)	Cubn
1445583_x_at	-3.14	Mm.80916	Mus musculus transcribed sequences	---

1436368_at	-3.08	Mm.186778	RIKEN cDNA 2610103N14 gene	2610103N14Rik
1434592_at	-3.08	Mm.268429	Mus musculus transcribed sequence	---
1427797_s_at	-3.03	---	---	---
1448975_s_at	-3.03	Mm.220955	renin 1 structural	Ren1
1455561_at	-3.03	Mm.23278	carnosinase 1	Cn1-pending
1437021_at	-2.98	Mm.96833	RIKEN cDNA C530009C10 gene	C530009C10Rik
1427798_x_at	-2.93	---	---	---
1431102_at	-2.93	Mm.260247	RIKEN cDNA 6430546F08 gene	6430546F08Rik
1427735_a_at	-2.88	Mm.214950	actin, alpha 1, skeletal muscle	Acta1
1438673_at	-2.88	Mm.258893	solute carrier family 4, sodium bicarbonate cotransporter, member 7	Slc4a7
1424811_at	-2.88	Mm.46315	camello-like 5	Cml5
1448607_at	-2.83	Mm.202727	pre-B-cell colony-enhancing factor	Pbef-pending
1428547_at	-2.83	Mm.31676	5' nucleotidase, ecto	Nt5e
1431261_at	-2.83	Mm.37666	chloride intracellular channel 5	Clic5
1425871_a_at	-2.78	Mm.104747	immunoglobulin kappa chain variable 8 (V8)	Igk-V8
1433959_at	-2.78	Mm.125242	RIKEN cDNA 9630048M01 gene	9630048M01Rik
1430999_a_at	-2.78	Mm.24763	short coiled-coil protein	Scoc
1428719_at	-2.78	Mm.271192	RIKEN cDNA 2010309G21 gene	2010309G21Rik
1451019_at	-2.73	Mm.29561	cathepsin F	Ctsf
1426584_a_at	-2.69	Mm.104920	sorbitol dehydrogenase 1	Sdh1
1419520_at	-2.69	Mm.154782	camello-like 4	Cml4
1422017_s_at	-2.69	Mm.24593	RIKEN cDNA 4833439L19 gene	4833439L19Rik
1425739_at	-2.69	Mm.260972	phospholipase D1	Pld1
1456043_at	-2.69	Mm.30602	ubiquitin specific protease 22	Usp22
1449907_at	-2.64	Mm.117119	beta-carotene 15, 15'-dioxygenase 1	Bcdo1
1427610_at	-2.64	Mm.219579	Mus musculus, clone IMAGE:4983756, mRNA, partial cds	---
1451418_a_at	-2.64	Mm.33268	SPRY domain-containing SOCS box 4	Ssb4-pending
1437863_at	-2.64	Mm.8073	butyrylcholinesterase	Bche
1420450_at	-2.59	Mm.14126	matrix metalloproteinase 10	Mmp10
1451787_at	-2.59	Mm.14177	cytochrome P450, family 2, subfamily b, polypeptide 20	Cyp2b20
1432436_a_at	-2.59	Mm.196067	adenylate kinase 3 alpha-like	Ak3l
1440844_at	-2.59	Mm.259673	transducer of ErbB-2.1	Tob1
1424576_s_at	-2.59	Mm.26457	cDNA sequence BC034834	BC034834
1456494_a_at	-2.59	Mm.277377	Mus musculus cDNA clone MGC:68284 IMAGE:5035734, complete cds	---
1424592_a_at	-2.59	Mm.38470	deoxyribonuclease I	Dnase1
1448723_at	-2.59	Mm.6696	retinol dehydrogenase 7	Rdh7
1431213_a_at	-2.55	---	---	---
1438446_x_at	-2.55	Mm.1458	putative phosphatase	Pps
1415893_at	-2.55	Mm.200373	sphingosine phosphate lyase 1	Sgpl1
1457271_at	-2.55	Mm.20167	Mus musculus transcribed sequence	---
1425994_a_at	-2.51	Mm.104900	N-acylsphingosine amidohydrolase 2	Asah2
1453416_at	-2.51	Mm.11982	RIKEN cDNA 8430435B07 gene	8430435B07Rik

1447918_x_at	-2.51	Mm.182172	Mus musculus transcribed sequences	---
1460650_at	-2.51	Mm.20869	ATPase, H+ transporting, lysosomal V0 subunit a isoform 1	Atp6v0a1
1427512_a_at	-2.51	Mm.42012	laminin, alpha 3	Lama3
1431721_a_at	-2.46	Mm.118345	protein Z, vitamin K-dependent plasma glycoprotein	Proz
1425732_a_at	-2.46	Mm.2154	Max interacting protein 1	Mxi1
1428720_s_at	-2.46	Mm.271192	RIKEN cDNA 2010309G21 gene	2010309G21Rik
1431530_a_at	-2.46	Mm.31927	transmembrane 4 superfamily member 9	Tm4sf9
1448348_at	-2.42	Mm.1098	GPI-anchored membrane protein 1	Gpiap1
1456940_at	-2.42	Mm.11186	cDNA sequence BC042513	BC042513
1450379_at	-2.42	Mm.138876	moesin	Msn
1448678_at	-2.42	Mm.154444	RIKEN cDNA 3110048E14 gene	3110048E14Rik
1424453_at	-2.42	Mm.209300	phosphate cytidylyltransferase 1, choline, alpha isoform	Pcyt1a
1422749_at	-2.42	Mm.215096	lymphocyte antigen 6 complex, locus G6C	Ly6g6c
1425576_at	-2.42	Mm.220328	S-adenosylhomocysteine hydrolase-like 1	Ahcyl1
1427960_at	-2.42	Mm.221171	expressed sequence AI788959	AI788959
1457528_at	-2.42	Mm.254581	Mus musculus 12 days embryo spinal ganglion cDNA	---
1436417_at	-2.42	Mm.261542	solute carrier family 19 (sodium/hydrogen exchanger), member 3	Slc19a3
1434969_at	-2.42	Mm.276234	Mus musculus cDNA clone IMAGE:5683160, partial cds	---
1422975_at	-2.42	Mm.38931	membrane metallo endopeptidase	Mme
1456080_a_at	-2.42	Mm.4962	tumor differentially expressed 1	Tde1
1421259_at	-2.42	Mm.8359	pyruvate kinase liver and red blood cell	Pklr
1423436_at	-2.42	Mm.88367	glial cell line derived neurotrophic factor family receptor alpha 1	Gfra1
1438183_x_at	-2.38	Mm.104920	sorbitol dehydrogenase 1	Sdh1
1435477_s_at	-2.38	Mm.10809	Fc receptor, IgG, low affinity IIb	Fcgr2b
1421448_at	-2.38	Mm.154667	tuberin-like protein 1	Tulip1-pending
1453589_a_at	-2.38	Mm.213005	RIKEN cDNA 2610005L07 gene	2610005L07Rik
1421989_s_at	-2.38	Mm.27646	3'-phosphoadenosine 5'-phosphosulfate synthase 2	Papss2
1420715_a_at	-2.38	Mm.3020	peroxisome proliferator activated receptor gamma	Pparg
1454247_a_at	-2.38	Mm.46357	glycoprotein A33 (transmembrane)	Gpa33
1417574_at	-2.38	Mm.465	chemokine (C-X-C motif) ligand 12	Cxcl12
1430634_a_at	-2.34	Mm.108076	phosphofructokinase, platelet	Pfkp
1426441_at	-2.34	Mm.1304	solute carrier family 11, member 2	Slc11a2
1435691_at	-2.34	Mm.259334	RIKEN cDNA C630028N24 gene	C630028N24Rik
1458381_at	-2.34	Mm.37666	chloride intracellular channel 5	Clic5
1421218_at	-2.34	Mm.8073	butyrylcholinesterase	Bche
1452997_at	-2.3	Mm.213005	RIKEN cDNA 2610005L07 gene	2610005L07Rik
1425853_s_at	-2.3	Mm.2752	prolactin receptor	Prlr
1435665_at	-2.3	Mm.277377	Mus musculus cDNA clone MGC:68284 IMAGE:5035734, complete cds	---
1456873_at	-2.3	Mm.37666	chloride intracellular channel 5	Clic5
1417066_at	-2.3	Mm.38330	chaperone, ABC1 activity of bc1 complex like (S. pombe)	Cabc1
1422095_a_at	-2.26	Mm.1676	thymidylate kinase family LPS-inducible member	Tyki
1420966_at	-2.26	Mm.200907	solute carrier family 25, member 15	Slc25a15

1416229_at	-2.26	Mm.7013	RIKEN cDNA 0610038L10 gene	0610038L10Rik
1421258_a_at	-2.26	Mm.8359	pyruvate kinase liver and red blood cell	Pklr
1421283_at	-2.22	Mm.11958	bone morphogenetic protein 5	Bmp5
1455980_a_at	-2.22	Mm.11982	RIKEN cDNA 8430435B07 gene	8430435B07Rik
1422002_at	-2.22	Mm.1329	Max dimerization protein	Mad
1430130_at	-2.22	Mm.169261	RIKEN cDNA 1300015B04 gene	1300015B04Rik
1422257_s_at	-2.22	Mm.218749	cytochrome P450, family 2, subfamily b, polypeptide 10	Cyp2b10
1451963_at	-2.22	Mm.240437	immunoglobulin heavy chain (J558 family)	Igh-VJ558
1427302_at	-2.18	Mm.194888	ectonucleotide pyrophosphatase/phosphodiesterase 3	Enpp3
1427303_at	-2.18	Mm.194888	ectonucleotide pyrophosphatase/phosphodiesterase 3	Enpp3
1458849_at	-2.18	Mm.207258	Mus musculus transcribed sequences	---
1451547_at	-2.18	Mm.24153	RIKEN cDNA 0610009A07 gene	0610009A07Rik
1442544_at	-2.18	Mm.259062	immunoglobulin heavy chain 4 (serum IgG1)	Igh-4
1421866_at	-2.18	Mm.268617	nuclear receptor subfamily 3, group C, member 1	Nr3c1
1427221_at	-2.18	Mm.27208	RIKEN cDNA A730081N20 gene	A730081N20Rik
1421338_at	-2.18	Mm.36808	cDNA sequence BC042423	BC042423
1416209_at	-2.14	Mm.10600	glutamate dehydrogenase	Glud
1437244_at	-2.14	Mm.11982	RIKEN cDNA 8430435B07 gene	8430435B07Rik
1425799_at	-2.14	Mm.215258	flavin containing monooxygenase 4	Fmo4
1421987_at	-2.14	Mm.27646	3'-phosphoadenosine 5'-phosphosulfate synthase 2	Papss2
1448364_at	-2.14	Mm.3527	cyclin G2	Ccng2
1450214_at	-2.14	Mm.40740	adenosine A2b receptor	Adora2b
1424600_at	-2.14	Mm.7190	amiloride binding protein 1 (amine oxidase, copper-containing)	Abp1
1439153_at	-2.14	Mm.95695	cDNA sequence BC025007	BC025007
1425645_s_at	-2.11	Mm.14177	cytochrome P450, family 2, subfamily b, polypeptide 20	Cyp2b20
1426699_at	-2.11	Mm.206206	expressed sequence AU040320	AU040320
1426546_at	-2.11	Mm.227059	testis-specific kinase 2	Tesk2
1434354_at	-2.11	Mm.241656	monoamine oxidase B	Maob
1431537_at	-2.11	Mm.249243	RIKEN cDNA 2010001E11 gene	2010001E11Rik
1416639_at	-2.11	Mm.260220	solute carrier family 2 (facilitated glucose transporter), member 5	Slc2a5
1450006_at	-2.11	Mm.275762	nuclear receptor coactivator 4	Ncoa4
1438716_at	-2.11	Mm.277377	Mus musculus cDNA clone MGC:68284 IMAGE:5035734, complete cds	---
1425606_at	-2.11	Mm.77381	solute carrier family 5 (iodide transporter), member 8	Slc5a8
1430523_s_at	-2.11	Mm.780	immunoglobulin lambda chain, variable 1	Igl-V1
1421832_at	-2.07	Mm.10153	twisted gastrulation homolog 1 (Drosophila)	Twsg1
1423596_at	-2.07	Mm.143818	NIMA (never in mitosis gene a)-related expressed kinase 6	Nek6
1452384_at	-2.07	Mm.194888	ectonucleotide pyrophosphatase/phosphodiesterase 3	Enpp3
1429040_at	-2.07	Mm.213005	RIKEN cDNA 2610005L07 gene	2610005L07Rik
1448814_at	-2.07	Mm.24573	growth factor receptor bound protein 2-associated protein 1	Gab1
1419622_at	-2.07	Mm.29157	UDP-glucuronosyltransferase 2 family, member 5	Ugt2b5
1449434_at	-2.07	Mm.300	carbonic anhydrase 3	Car3
1426511_at	-2.07	Mm.31096	RIKEN cDNA 1200011D11 gene	1200011D11Rik

1417179_at	-2.07	Mm.31927	transmembrane 4 superfamily member 9	Tm4sf9
1426165_a_at	-2.07	Mm.34405	caspase 3, apoptosis related cysteine protease	Casp3
1438325_at	-2.07	Mm.56965	ecotropic viral integration site 1	Evi1
1442031_at	-2.07	Mm.69732	RIKEN cDNA 2010012O16 gene	2010012O16Rik
1447181_s_at	-2.03	Mm.142455	solute carrier family 7, member 7	Slc7a7
1449067_at	-2.03	Mm.18443	solute carrier family 2 (facilitated glucose transporter), member 2	Slc2a2
1423244_at	-2.03	Mm.44084	cytochrome P450, family 2, subfamily c, polypeptide 40	Cyp2c40
1445643_at	-2.03	Mm.55061	Mus musculus transcribed sequences	---
1430984_at	-2.03	Mm.6775	ornithine decarboxylase antizyme inhibitor	Oazin
1416230_at	-2.03	Mm.7013	RIKEN cDNA 0610038L10 gene	0610038L10Rik
1426161_at	-2	Mm.104747	immunoglobulin kappa chain variable 8 (V8)	Igk-V8
1445695_at	-2	Mm.139937	Mus musculus transcribed sequences	---
1425850_a_at	-2	Mm.143818	NIMA (never in mitosis gene a)-related expressed kinase 6	Nek6
1431233_at	-2	Mm.155669	cyclin M4	Cnnm4
1423718_at	-2	Mm.196067	adenylate kinase 3 alpha-like	Ak3l
1431061_s_at	-2	Mm.28957	pellino 1	Peli1
1417042_at	-2	Mm.30087	glucose-6-phosphatase, transport protein 1	G6pt1
1455961_at	-2	Mm.38931	membrane metallo endopeptidase	Mme
1432212_at	-2	Mm.87538	RIKEN cDNA 1810073H04 gene	1810073H04Rik
1445128_at	-2	Mm.99973	Mus musculus transcribed sequences	---
1427837_at	-1.97	Mm.104747	immunoglobulin kappa chain variable 8 (V8)	Igk-V8
1453054_at	-1.97	Mm.201455	secretory carrier membrane protein 1	Scamp1
1424968_at	-1.97	Mm.26580	RIKEN cDNA 2210023G05 gene	2210023G05Rik
1436858_at	-1.97	Mm.28651	muscleblind-like 2	Mbnl2
1417777_at	-1.97	Mm.34497	leukotriene B4 12-hydroxydehydrogenase	Ltb4dh
1427034_at	-1.97	Mm.754	angiotensin converting enzyme	Ace
1417642_at	-1.93	Mm.140988	aldehyde dehydrogenase family 1, subfamily A3	Aldh1a3
1420709_s_at	-1.93	Mm.20115	D-amino acid oxidase	Dao1
1425281_a_at	-1.93	Mm.22216	glucocorticoid-induced leucine zipper	Gilz
1420896_at	-1.93	Mm.30197	synaptosomal-associated protein 23	Snap23
1426201_at	-1.9	Mm.104747	immunoglobulin kappa chain variable 8 (V8)	Igk-V8
1434657_at	-1.9	Mm.268503	Mus musculus, clone IMAGE:6432957, mRNA	---
1455508_at	-1.9	Mm.76212	RIKEN cDNA A530082C11 gene	A530082C11Rik
1448253_at	-1.87	Mm.10600	glutamate dehydrogenase	Glud
1448568_a_at	-1.87	Mm.16757	solute carrier family 20, member 1	Slc20a1
1427961_s_at	-1.87	Mm.221171	expressed sequence AI788959	AI788959

CHAPTER 4

Peroxisome Proliferator-activated Receptor Alpha Reduces Cholesterol Absorption Via Modulation of Niemann-Pick C1 Like 1 Expression

4.1 ABSTRACT

Peroxisome proliferator-activated receptor alpha (PPARα) is a member of the nuclear receptor superfamily known to regulate lipid metabolism by acting as a molecular sensor for a variety of fatty acids. Treatment with PPARα agonists enhances fatty acid oxidation, decreases plasma triglycerides, and may promote reverse cholesterol transport. In addition, PPARα agonist administration reduces cholesterol absorption in humans and rodents, however the mechanism for this effect is largely unknown. Here, we show that fenofibrate-treated wild-type mice (800 mg/day/kg body weight; 10 days) not only have decreased fractional cholesterol absorption (35-47% decrease) and increased fecal neutral sterol excretion (51-83% increase), but also have decreased relative expression of Niemann-Pick C1 Like 1 (NPC1L1) mRNA (38-55% decrease) and protein (66% decrease) in the proximal small intestine. These effects of fenofibrate treatment are dependent on PPARα, as knockout mice fail to respond like their wild-type littermates. Fenofibrate impacts the ezetimibe-sensitive pathway, and retains the ability to decrease cholesterol absorption and NPC1L1 mRNA expression in liver X receptor α/β (*Lxrα/β*)-double-knockout mice and high-cholesterol (0.2% w/w) fed wild-type mice. Taken

together, these data suggest that PPARα acts at the level of regulation of NPC1L1 expression to decrease cholesterol absorption.

4.2 INTRODUCTION

Peroxisome proliferator-activated receptor alpha (PPARα, NR1C1) is a member of the nuclear receptor superfamily and acts as a ligand-activated transcription factor in response to a variety of fatty acids (Desvergne and Wahli, 1999; Willson et al., 2000). As such, it regulates expression of genes involved in lipid metabolism, especially fatty acid oxidation and transport. Fibric acid derivatives, including fenofibrate and gemfibrozil, are known to function largely by binding and activating PPARα. These drugs are especially useful in treating hypertriglyceridemia, and may also moderately lower plasma LDL cholesterol while raising plasma HDL (for example (Adkins and Faulds, 1997)), although the magnitude of positive impact on coronary event outcomes is uncertain (Frick et al., 1987; Keech et al., 2005; Rubins et al., 1999).

Several candidate proteins have been proposed to function as intestinal cholesterol transporters including scavenger receptor BI (SR-BI), ATP-binding cassette transporter A1 (ABCA1), ABCG5/8, aminopeptidase N, caveolin-1(CAV1)/annexin-2, and Niemann-Pick C1 like 1 (NPC1L1) (Altmann et al., 2002; Altmann et al., 2004; Field et al., 1998; Hauser et al., 1998; Kramer et al., 2005; Repa et al., 2000c; Smart et al., 2004). With the discovery of the cholesterol absorption blocking agent ezetimibe (Burnett et al., 1994; Rosenblum et al., 1998), new criteria could be used to define and characterize a candidate intestinal cholesterol transporter. Not only should knockout animals have

markedly reduced cholesterol absorption, but they might also be insensitive to ezetimibe. Moreover, in the simplest case, ezetimibe would bind directly to the transporter and inhibit its function. Along these lines, *Sr-bI*, and *Cav1*-knockout mice have similar cholesterol absorption as wild-type mice and are sensitive to ezetimibe (Altmann et al., 2002; Valasek et al., 2005), thereby excluding these proteins as critical for intestinal cholesterol transport. The role of ABCA1 in intestinal cholesterol transport has been less clear as knockout mice show moderate or slight reduction in fractional cholesterol absorption (Drobnik et al., 2001; Temel et al., 2005), whereas intestinal-specific *Abca1*-knockout mice show no difference in cholesterol absorption but rather a partial defect in HDL biosynthesis (Brunham et al., 2006). Liver X receptor (LXR) agonists are potent cholesterol absorption inhibitors and inducers of ABCA1 (Repa et al., 2000c), however their action was found to be independent of ABCA1 and related to their ability to increase expression of ABCG5 and ABCG8 (Plosch et al., 2002; Repa et al., 2002a; Yu et al., 2003). Studies have revealed that ABCG5/8 functions as a heterodimer on the apical membrane of enterocytes to efflux free cholesterol and plant sterols back into the intestinal lumen (Berge et al., 2000). Transgenic mice with ABCG5/8 overexpressed in liver and intestine have decreased fractional cholesterol absorption (Yu et al., 2002b) thus ABCG5/8 seems to function in the opposite direction as the putative cholesterol transporter. In contrast, mice lacking *Npc1l1* have decreased fractional cholesterol absorption (Altmann et al., 2004; Davies et al., 2005; Davis et al., 2004) and are insensitive to ezetimibe (Altmann et al., 2004). In addition, NPC1L1-expressing cells

show specific binding to ezetimibe and increased cholesterol uptake (Garcia-Calvo et al., 2005; Yu et al., 2006).

Because PPARα agonists are known to reduce cholesterol absorption in humans and rodents (Knight et al., 2003; McNamara et al., 1980; Rubins et al., 1999; Vanhanen and Miettinen, 1995), we hypothesized that activation of PPARα might influence the expression of the putative intestinal sterol transporter, NPC1L1, thereby limiting cholesterol absorption at the level of cholesterol transport across the apical membrane of the enterocyte. Here, we report that mice treated with fenofibrate indeed show decreased NPC1L1 mRNA and protein expression in the small intestine that correlates with decreased fractional cholesterol absorption and increased fecal neutral sterol excretion. This suggests that PPARα can influence cholesterol absorption by altering expression of NPC1L1.

4.3 EXPERIMENTAL PROCEDURES

4.3.1 Animal Experiments

Lxrα/β-double-knockout mice were generated previously as described (Lee et al., 1995; Peet et al., 1998; Repa et al., 2000c), and maintained on a mixed-strain background (C57Bl/6*A129/SvJ) as were age- and gender-matched wild-type controls. *Pparα*-null mice on a 129S4/SvJae genetic background were kindly provided by Frank Gonzalez. Mice were maintained on a cereal-based rodent diet (Wayne Lab Blox, No. 8604; Harlan Teklad, Madison, WI) which contains 0.02% (w/w) cholesterol and approximately 4%

total lipid. For most experiments mice were fed the powdered form of this diet for a period of 7-10 days. In some experimental groups, the diet was supplemented with fenofibrate (2-[4-(4-chlorobenzoyl)phenoxy]-2-methylpropanoic acid isopropyl ester) to provide 800 mg/day/kg body weight (mpk/day), ezetimibe (10 mpk/day), or cholesterol (0.2%, w/w). The calculated quantities of dietary drug supplement assume a food consumption rate of 160 g of diet/day/kg body weight. For oral gavage dosing, fenofibrate or GW7647 were administered once daily as a suspension in 1% methylcellulose, 1% Tween-80. Fenofibrate was purchased from Sigma, ezetimibe was provided by Harry R. Davis, Jr. at the Schering-Plough Research Institute, and GW7647 was generously provided by Timothy Willson at GlaxoSmithKline-Research, Triangle Park, NC. Mice were housed in a temperature-controlled environment with 12 hour light/dark cycles with free access to food and water. Unless otherwise specified, mice were sacrificed and tissues harvested at the end of the dark cycle, thus mice were in a fed-state at the time of study. Experiments were approved by the Institutional Animal Care and Use Committee of the University of Texas Southwestern Medical Center at Dallas.

4.3.2 Cholesterol Balance Measurements

4.3.2.1 Intestinal Absorption

Fractional cholesterol absorption was measured by a fecal dual-isotope ratio method (Turley et al., 1994b). Three days before sacrifice, mice received a single intragastric dose of medium-chain triglyceride oil containing [5,6-^{3}H]sitostanol (2 μCi, American Radiolabeled Chemicals, Inc. St. Louis, MO) and [4-^{14}C]cholesterol (1 μCi,

Perkin Elmer Life Sciences, Boston MA). Stools were collected over the following 3 days. Samples of the dosing mixture and aliquots of stool were extracted, and the ratio of ^{14}C to ^{3}H in each was determined to calculate percent cholesterol absorption (Turley et al., 1994b).

4.3.2.2 Fecal Neutral Sterol Excretion

Stools were collected from individually housed mice over the final 3 days of each experiment. They were dried, weighed, and ground. An aliquot was saponified, solvent extracted and amounts of cholesterol, coprostanol, epicoprostanol and cholestanone were quantified by gas chromatography (Schwarz et al., 1998). The measured sterols were added together to represent total neutrol sterols then adjusted to reflect the daily excretion (based on feces collected over 3 days) per 100 g body weight.

4.3.2.3 Biliary Cholesterol Concentration

Gallbladder bile was harvested from mice that had been fasted for 4 h and the concentration of cholesterol was measured as previously described (Schwarz et al., 1998; Turley et al., 1991).

4.3.3 Preparation of Samples for RNA and Protein Measurements

Mice were anesthetized and exsanguinated via the descending vena cava. Small intestines were removed, flushed with ice-cold PBS and cut into three sections of equal length (the proximal third was utilized in these studies). The sections were slit lengthwise, and the mucosae were gently scraped, frozen in liquid nitrogen and stored at –85°C. Total RNA was isolated from tissue samples using RNA STAT-60 (Tel-Test

Inc.). Total protein was obtained from the organic phase remaining after RNA isolation by precipitating with isopropanol, consecutively washing with 0.3M guanidine hydrochloride in 95% ethanol and ethanol, then solubilizing the protein pellet in 1% SDS, 50mM Tris-Cl pH 8.8 (Banerjee et al., 2003). RNA concentrations were determined by absorbance at 260nm. Protein concentrations were determined using the BCA protein assay kit (Pierce Biotech., Rockford, IL).

4.3.4 Quantitiative real-time PCR

Quantitative real-time PCR (qRT-PCR) was performed using an Applied Biosystems Prism 7900HT sequence detection system as described (Kurrasch et al., 2004). Briefly, total RNA was treated with DNase I (RNase-free, Roche Molecular Biochemicals), and reverse-transcribed with random hexamers using SuperScript II (Invitrogen) to generate cDNA. Primers for each gene were designed using Primer Express Software (PerkinElmer Life Sciences) and validated by analysis of template titration and dissociation curves. Primers sequences for all assayed genes are provided in Table 4.1. Both sets of NPC1L1 primers gave identical results. Each qRT-PCR reaction contained (final volume of 10 μl): 25ng of reverse-transcribed RNA, each primer at 150nM, and 5μl of 2X SYBR Green PCR Master Mix (Applied Biosystems), and each sample was analyzed in triplicate. Results were evaluated by the comparative C_T method (User Bulletin No. 2, PerkinElmer Life Sciences) using cyclophilin as the invariant control gene. Similar results were obtained when villin was used as the housekeeping

gene, suggesting that the changes observed were not the result of altered expression of our calibrator.

4.3.5 Western Analysis

Total protein obtained from whole-cell lysates of the proximal third of small intestine were size-fractionated on 6% SDS-polyacrylamide gels (40 μg/lane), transferred electrophoretically to nitrocellulose membrane, and incubated with either polyclonal antisera for actin (sc-1616, Santa Cruz Biotech., Inc) or NPC1L1 (provided by Helen Hobbs (Valasek et al., 2005)). Proteins were visualized by exposure to film after sequential treatment with specific primary antibodies, appropriate HRP-conjugated secondary antibodies, and a standard ECL kit (Amersham). Signal intensity of bands was determined by analyzing scanned images with OptiQuant v3.1 (Packard Biosciences).

4.3.6 *In Situ* Hybridization

Segments of jejunum (13-18 cm from pyloric sphincter) were harvested and fixed overnight in 4% paraformaldehyde. Segments were paraffin-embedded, sectioned, then *in situ* hybridization was performed by using ^{35}S-labeled sense and antisense riboprobes as previously described (Shelton et al., 2000) using an NPC1L1 specific probe that recognizes the 3' untranslated region (nucleotides 4127-4572; GenBank Accession #XM_137497). Slides were exposed at 4°C for 2 weeks. Sections hybridized with the sense probe revealed no signal above background (data not shown).

4.3.7 *In Vivo* Chromatin Immunoprecipitation Assay

Frozen mucosae from proximal intestine were crushed to a fine powder with a Besselar Tissue pulverizer then crosslinked in 1% formaldehyde for 15 minutes at room temperature. Reactions were stopped by addition of 0.1x volume 1.25 M glycine. Samples were washed twice with PBS supplemented with 1 mM phenylmethanesulfonyl fluoride (PMSF, Sigma) and complete protease inhibitor cocktail (Roche). Resuspended samples were subjected to 7 strokes of a Dounce homogenizer then centrifuged at 500 g for 2 minutes to pellet cells. Cells were resuspended in 2 mL SDS lysis buffer (1%SDS, 5 mM EDTA, 50 mM Tris-Cl pH 8.1) then incubated with rotation for 15 minutes at 4°C and sonicated with 20 15-second pulses to shear DNA to an average of approximately 400 base pairs. Debris was removed by centrifuging samples at 10,000 x *g* for 10 minutes and collecting the supernatant. Protein concentration was assayed using BCA (Pierce). The following steps utilized reagents from the Acetyl-Histone H3 Immunoprecipitation (ChIP Assay Kit (#17-245, Upstate)) and were performed according to the manufacturers protocol. Briefly, samples were diluted to 1 μg protein/μl (approximately 1:4) using ChIP Dilution Buffer and precleared with protein A agarose incubation for at 4°C for 30 minutes. 5 μg anti-acetylated histone-H3 antibody was added to 500 μg protein aliquots and incubated at 4°C overnight with rotation. Protein A agarose was used to collect the antibody/histone complex, the pellet was washed and eluted according to manufacturer's instructions. Recovered DNA was analyzed by qRT-PCR against a standard titration curve, corrected by 10% input value, and then

normalized to the background region (internal control). Primer sets were designed using Primer Express Software to generate amplicons of approximately 80 base pairs. Primers sets are provided in Table 4.2.   The distance of each primer set from the putative transcriptional start site is represented as the distance of the central base pair of the amplicon and plotted on the x-axis. Relative expression for each primer set is plotted on the y-axis as fold over background region (defined as the average value for points -3911,-3612,-3455, and -2921). This average was previously determined to correlate with non-specific binding of a foreign plasmid (e.g. tk-LUC).

4.3.8 Statistical Analysis of Data

Data are reported as the mean $\pm$ SEM for the specified number of animals. GraphPad Prism 4 or InStat 3 software (GraphPad, San Diego, CA) were used to perform all statistical analyses.   If unequal variance was indicated by Bartlett's test, log transformation of data was performed prior to statistical analysis. For most studies, a 2-way analysis of variance (ANOVA) was performed, using genotype and treatment as factors. If a statistical interaction was observed between factors, comparison of all 4 groups was performed by Newman-Keuls post-hoc comparison.   If only two groups were being compared, then two-tailed p-values were determined by Student's t-test. Statistical significance is denoted by asterisks: $*p<0.05$, $**p<0.01$, and $***p<0.001$.

4.4 RESULTS

To better understand how PPARα agonists influence cholesterol absorption, we treated male wild-type and *Ppara*-knockout mice with the PPARα agonist, fenofibrate, supplemented in the diet (800 mpk/day; 10 days). We measured fractional cholesterol absorption using the fecal dual isotope method, collecting samples from day 7 to day 10 just prior to sacrificing animals. Figure 4.1A shows that fenofibrate decreases fractional cholesterol absorption relative to vehicle controls (35% decrease; vehicle v. fenofibrate, $57.4 \pm 4.7\%$ v. $37.6 \pm 2.8\%$, respectively). This confirms reports that administration of other PPARα agonists, namely WY-14643 and gemfibrozil, decreases cholesterol absorption in rodents (Knight et al., 2003; Umeda et al., 2001). To our knowledge, these studies represent the first assessment of cholesterol absorption in mice treated with fenofibrate. In contrast, *Ppara*-knockout mice fail to respond to fenofibrate. This finding is critical as it distinguishes a PPARα-dependent mechanism and rules out potential cross-reactivity with PPARβ/δ, which has recently been reported to regulate cholesterol absorption (van der Veen et al., 2005). Consistent with the decrease in fractional cholesterol absorption is a concomitant increase in fecal neutral sterol excretion (Figure 4.1B, 83% increase; 10.4 ± 0.9 vs 19.0 ± 1.8 μmol/day/100 g bw), which does not occur in *Ppara*-null mice. We hypothesized that activation of PPARα might influence the expression of the putative intestinal cholesterol transporter, NPC1L1, thereby limiting cholesterol absorption at the level of cholesterol transport across the apical membrane of the enterocyte. To test this, we measured NPC1L1 mRNA expression by two methods: quantitative real-time PCR (qRT-PCR) and *in situ* hybridization. As shown in Figure

4.1C, qRT-PCR analysis of mucosae from proximal small intestine reveals a reduction in relative expression of NPC1L1 mRNA in fenofibrate-treated wild-type mice (55% reduction) but not *Pparα*-knockouts. The housekeeping gene used in these studies (cyclophilin) did not differ between treatment groups (data not shown). *In situ* hybridization was carried out on transverse and longitudinal sections of segments of jejunum (13-18cm from pyloric sphincter) using an antisense RNA probe directed at the 3' untranslated region of NPC1L1 mRNA previously determined to be specific to NPC1L1 (without cross-reacting with NPC1) by northern analysis (Valasek et al., 2005). As shown in Figure 4.1D, NPC1L1 shows a distribution pattern along the entire villus length consistent with expression in enterocytes. Fenofibrate-treated animals have markedly reduced expression of NPC1L1 in jejunal enterocytes. Sense controls gave no signal above background (data not shown). It was additionally observed that fenofibrate-treated jejuna seemed to have longer villi (n=2 each for vehicle and fenofibrate treatment), although additional studies will be required to further address this observation. Thus activation of PPARα decreases cholesterol absorption and NPC1L1 mRNA expression, and may potentially have trophic effects on intestinal cells.

To exert a biological effect on cholesterol absorption, the change in NPC1L1 mRNA must result in a change in protein level. Therefore, we prepared whole-cell lysates from proximal intestinal mucosae and immunoblotted with polyclonal antisera for NPC1L1 and actin. Figure 4.2A depicts immunoblots of protein of one animal from each experimental group. Quantification of 4-6 animals from each group (Figure 2B) was

calculated by dividing NPC1L1 by actin signal intensity as determined using OptiQuant v3.1 software. The data were then transformed so that the vehicle group was set to a value of 1. NPC1L1 protein levels show a marked reduction by fenofibrate (66% reduction) in wildtype mice but not *Pparα*-knockouts.

To determine whether other target genes could be involved in the PPARα-dependent reduction of cholesterol absorption, we measured the mRNA levels in proximal small intestine of several proteins thought to function in cholesterol absorption and homeostasis. We wanted to characterize the relative levels of PPAR and LXR isoforms in the proximal small intestine. In qRT-PCR, the cycle times (C_T) inversely relate to the approximate quantity of mRNA in the sample so that more abundantly expressed genes have lower C_T values. Based on the average C_T (wild-type vehicle-treated group; Figure 4.3A) the rank order for abundance of PPAR and LXR isoforms in untreated proximal intestine is PPARβ > PPARα > PPARγ and LXRα > LXRβ. PPARα was the only isoform induced by fenofibrate (4.12 ± 0.52 fold as compared to vehicle). Note that the PPARα expression detected in *Pparα*-knockouts represents recognition of an aberrant transcript. PPARα target gene ACOX1 is induced by fenofibrate in a PPARα-dependent fashion (2.68 ± 0.15 fold). This establishes that PPARα is present in proximal small intestine, and responds to fibrate treatment by increasing expression of known target genes, acyl CoA oxidase 1 (ACOX1) and PPARα itself (Pineda Torra et al., 2002; Tugwood et al., 1992). In addition PPARα activation has no effect on the mRNA levels of LXRα and β, transcription factors previously implicated in the regulation of

cholesterol absorption (Repa et al., 2000c). As shown in Figure 4.3B, ABCA1 mRNA levels are significantly increased (3.07 ± 0.56 fold) by fenofibrate treatment in wild-type mice but not *Pparα*-knockouts. Although initially considered to be a candidate for the cholesterol transporter (Repa et al., 2000c), evidence suggests that ABCA1 is localized to the abluminal surface of the enterocyte (Wellington et al., 2002) and may have minimal impact on fractional cholesterol absorption (Brunham et al., 2006; Temel et al., 2005). In addition, *Abca1*-knockout mice treated with fenofibrate show reduced fractional cholesterol absorption and expression of NPC1L1 mRNA, similar to wild-type controls (data not shown). These data suggest that although PPARα activation results in an induction of ABCA1 expression in the small intestine, it is unlikely to substantially alter cholesterol absorption and is not required for PPARα- mediated repression of cholesterol absorption. In contrast to ABCA1, both ABCG5 and ABCG8 show no change in mRNA expression level by fenofibrate administration. ABCG5 and ABCG8 are thought to function as heterodimeric sterol transporters which efflux cholesterol and plant sterols back into the intestinal lumen (Berge et al., 2000; Yu et al., 2002b; Yu et al., 2003). Thus enhanced expression of ABCG5 and/or ABCG8 would have a net effect of decreasing cholesterol absorption and enhancing fecal neutral sterol excretion. SR-BI and CAV1 have previously been considered as candidates for performing intestinal cholesterol permease functions (Altmann et al., 2002; Field et al., 1998; Hauser et al., 1998; Smart et al., 2004; Werder et al., 2001). Neither SR-BI nor CAV1 mRNA expression was

significantly altered by treatment (Figure 4.3B). In contrast, NPC1L1 is downregulated (55% decrease) which correlates with a decrease in cholesterol absorption (Figure 4.1).

As it has previously been proposed that PPARα activation may decrease cholesterol absorption by activating LXRs (Knight et al., 2003), we wanted to conclusively determine if LXRs were involved in PPARα-mediated reduction of NPC1L1 expression and cholesterol absorption. Therefore, we treated *Lxrα/β*-double-knockout mice with or without fenofibrate for 7 days. Figure 4.4 shows that NPC1L1 mRNA expression is significantly reduced by fenofibrate treatment in both wild-type mice and *Lxrα/β*-double-knockouts. This change in NPC1L1 positively correlates with fractional cholesterol absorption (Figure 4.4B) and negatively correlates with fecal neutral sterol excretion (Figure 4.4C). Interestingly, LXR deletion itself leads to lower basal cholesterol absorption and higher fecal neutral sterol excretion, most likely due to derepression of target genes ABCG5 and ABCG8 resulting in increased expression ((Repa et al., 2002a); data not shown). Since LXR deletion has no significant effect on NPC1L1 expression (although there is a slight trend toward lower values), the lower fractional cholesterol absorption may potentially reflect a change in the ratio of NPC1L1 to ABCG5/8 heterodimers. Thus, LXRα and LXRβ are both present in the proximal small intestine, but are not required for fenofibrate-induced modulation of NPC1L1 expression or cholesterol absorption.

Ezetimibe is a cholesterol-lowering drug which functions by blocking intestinal cholesterol absorption. It has been shown to bind to NPC1L1 (Garcia-Calvo et al., 2005)

and block its critical function in cholesterol absorption (Altmann et al., 2004). To determine if fenofibrate is acting on the ezetimibe-sensitive cholesterol absorption pathway, we treated animals with 10 mpk/day ezetimibe (a dose well above the EC_{50} of 0.5mpk/day for mice (Garcia-Calvo et al., 2005)), 800 mpk/day fenofibrate, or both for a period of 10 days. As shown in Figure 4.5, ezetimibe potently decreases cholesterol absorption relative to vehicle controls (~92% decreased, 45.1 ± 7.3 to $3.8 \pm 0.5\%$). Fenofibrate moderately decreases fractional cholesterol absorption (42% decreased, 45.1 ± 7.3 to $26.2 \pm 2.5\%$) as observed in other animal studies using PPARα agonists (Fig. 4.1, 4.5; ref. 23). There was no significant difference between ezetimibe-treated and dual-treated groups, although a trend toward lower values for the both-treated group was observed (3.8 ± 0.5 vs $2.6 \pm 0.9\%$). This suggests not only that the ezetimibe-insensitive pathway seems to be a minor pathway comprising only a small fraction (approx. 10% or less) of the total amount of cholesterol absorbed as seen in other studies (Repa et al., 2005), but also that fenofibrate does not substantially impact the ezetimibe-insensitive pathway. To determine the impact of fenofibrate on the "ezetimibe-sensitive" pathway, we subtracted the fractional cholesterol absorption for the ezetimibe-treated group from vehicle-treated group. This difference represents the "ezetimibe-sensitive" fractional cholesterol absorption under basal conditions. Similarly, to determine the "ezetimibe-sensitive" fractional cholesterol absorption during fenofibrate treatment, we subtracted the fractional cholesterol absorption value for the dual-treated (ezetimibe and fenofibrate) group from the fenofibrate-treated group. The calculation shows that fenofibrate

significantly reduces the "ezetimibe-sensitive" fractional cholesterol absorption (43% reduced, $41.3 \pm 7.3\%$ to $23.6 \pm 2.7\%$). Thus, fenofibrate may act to reduce cholesterol absorption by modulating the ezetimibe-sensitive pathway. This is consistent with the idea that fenofibrate is changing cholesterol absorption by decreasing expression of NPC1L1. Finally, NPC1L1 expression was reduced by fenofibrate administration regardless of ezetimibe treatment. This suggests that cholesterol flux from the intestinal lumen into the enterocyte does not affect NPC1L1 mRNA levels. If the putative sterol regulatory element (SRE) identified in the promoter of this gene (Davies et al., 2000b) were responsive under these conditions, the ezetimibe-treated animals should have shown increased NPC1L1 expression, as observed for β-hydroxy-β-methylglutaryl-CoA (HMG-CoA) synthase and the low-density lipoprotein receptor (LDLR) under these conditions (Altmann et al., 2004; Valasek et al., 2005).

PPARs may also play a role in biliary secretion of cholesterol and bile acids, at least in humans, as fibrates are understood to have negative effects on biliary lipid composition by increasing cholesterol concentrations (Grundy and Vega, 1987). One way to blunt the potential effects of alterations in biliary cholesterol secretion is to provide animals with excess dietary cholesterol. We fed mice a "low" (0.02% w/w) or "high" (0.2%) cholesterol diet and supplemented with or without fenofibrate (800 mpk/day) for 10 days. On both a low- and high- cholesterol diet, fenofibrate reduces fractional cholesterol absorption compared to appropriate vehicle controls (Figure 4.6A; LOW 47% reduced, HIGH 46% reduced). NPC1L1 mRNA expression displays a similar

pattern as fractional cholesterol absorption, with values being statistically reduced by fenofibrate on either low or high cholesterol (Figure 4.6B). The addition of cholesterol itself caused a decrease in both fractional cholesterol absorption and NPC1L1 expression. Thus, excess cholesterol may modestly regulate NPC1L1 mRNA expression, whereas depletion of cholesterol with ezetimibe has no effect on NPC1L1 mRNA expression (Figure 4.5C, (Valasek et al., 2005)). Female mice treated with 800 mpk/day fenofibrate for 30 days show no increase in biliary cholesterol concentration, rather a decrease (data not shown). These data suggest that the observed changes in fractional cholesterol absorption are not likely due to dilution of radiolabeled cholesterol by enhanced biliary secretion of cholesterol, but rather an alteration in intestinal cholesterol transport.

To better understand the molecular mechanism by which PPARα activation leads to a reduction in NPC1L1 expression, we determined the time-course of PPARα agonist-mediated repression of NPC1L1 mRNA. Animals treated with PPARα agonists for 3, 7, or 10 days show reduced NPC1L1 mRNA levels relative to vehicle controls (Figure 4.7A). In contrast, 12h treatment with fenofibrate fails to reduce NPC1L1 expression in small intestine. Thus "chronic" activation of PPARα seems necessary to inhibit expression of NPC1L1. Because of the observed time course, PPARα is likely to be influencing NPC1L1 indirectly, perhaps by altering the metabolic or signaling milieu in the proximal small intestine, or by changing humoral factors.

To further evaluate possible transcriptional regulation of the NPC1L1 gene, we assessed the histone acetylation status of the proximal promoter. Because recruitment of

cofactors during transcription often leads to alterations in histone acetylation, we hypothesized that acetylation of chromatin at the NPC1L1 locus might be altered by metabolic or signaling changes induced by PPARα. As shown in Figure 4.7B, histone-H3 acetylation is increased (up to ~9-fold) in regions of the NPC1L1 promoter closest to the transcriptional start site (designated as base pair 0). Fenofibrate treatment, however, does not significantly alter histone-H3 acetylation at any of the points assayed.

4.5 DISCUSSION

Fenofibrate is known to bind PPARα to enhance fatty acid oxidation and decrease serum triglycerides in patients and may also give additional beneficial effects on plasma lipoproteins when combined with statins (for example (Grundy et al., 2005)). Studies also suggest that clofibrate reduces cholesterol absorption efficiency in humans (McNamara et al., 1980; Vanhanen and Miettinen, 1995). The pleiotropic effects of fibrates (and other PPARα agonists) on cholesterol absorption, however, are poorly understood. Using the mouse model, the present work suggests that specific activation of PPARα with fenofibrate decreases cholesterol absorption via an inhibitory effect on NPC1L1 expression in the small intestine. The fenofibrate effect requires PPARα and not other PPAR isoforms, as *Pparα*-knockout mice fail to respond similarly in terms of fractional cholesterol absorption, fecal neutral sterol excretion, or NPC1L1 mRNA and protein expression in small intestine (Figures 4.1 and 4.2). In the mouse this effect on NPC1L1 expression is likely restricted to the small intestine, as NPC1L1 is not expressed at appreciable levels in liver (Altmann et al., 2004; Calpe-Berdiel et al., 2005; Davies et

al., 2005; Valasek et al., 2005). However, in humans and non-human primates, NPC1L1 is expressed in liver and small intestine (Altmann et al., 2004; Davies et al., 2005; Yu et al., 2006). This raises the question of whether fibrates alter NPC1L1 expression in human intestine and/or liver. If so, one could predict that administration of fibrates might lead to a decrease of intestinal cholesterol transport and an increase in biliary secretion of cholesterol due to reduced reclamation of cholesterol across the canalicular membrane of hepatocytes, the proposed site of NPC1L1 in liver (Yu et al., 2006). Thus, the enhancement of biliary cholesterol secretion seen in patients treated with fibrates (Grundy and Vega, 1987; Palmer, 1985) may be potentially explained, at least in part, by changes in hepatic NPC1L1 expression.

The present studies are consistent with the idea that NPC1L1 is an intestinal sterol transporter, as modulation of its expression correlates with cholesterol absorption. It is possible, however, that other factors are involved in PPARα-mediated reduction of cholesterol absorption. Analysis of mRNA expression in proximal small intestine of fenofibrate-treated mice (Figure 4.3) reveals that other known players in cholesterol metabolism (including ABCG5/8 and SR-BI) are unlikely to contribute to PPARα action as their expression levels are unchanged or changed in a direction opposite from those expected to decrease cholesterol absorption. Although ABCA1 was induced by fenofibrate, recent evidence suggests that ABCA1 may have minimal impact on cholesterol absorption (Brunham et al., 2006; Temel et al., 2005). In addition, ABCA1 knockout mice treated with fenofibrate show reduced fractional cholesterol absorption

and expression of NPC1L1 mRNA similar to wild-type controls (data not shown). These data suggest that although PPARα activation results in an induction of ABCA1 expression in the small intestine, it is unlikely to substantially alter cholesterol absorption and is not required for PPARα mediated repression of cholesterol absorption.

In addition to the modulation of intestinal NPC1L1 expression in a PPARα-dependent fashion, the observation that fenofibrate continues to reduce cholesterol absorption on a high cholesterol diet (0.2% w/w) is indirect evidence to suggest the effect of fenofibrate is not primarily a product of changes in biliary cholesterol secretion, but rather could be a result in alterations of enterocytic cholesterol transport. The cholesterol diet itself slightly reduces fractional cholesterol absorption (Figure 4.5A) but not to the extent of fenofibrate. Thus, biliary secretion of cholesterol would have to increase to a quantity greater than 10-fold of the normal dietary cholesterol contribution to exert an effect similar to that of fenofibrate. However, in contrast to humans, it is unlikely that fenofibrate increases biliary cholesterol in rodents, because mice treated for 30 days have decreased biliary cholesterol content (data not shown), and hamsters treated for 9 days have a decreased rate of hepatic cholesterol biosynthesis, as determined by reduced activities of HMG-CoA synthase and HMG-CoA reductase, and reduced incorporation of radiolabeled acetate into cholesterol (Guo et al., 2001). Other theoretical possibilities that could contribute to a reduction in cholesterol absorption include a decrease in secretion of bile acids into bile or in the overall size of bile acid pool. However, it has been observed in mice treated with fenofibrate that the rate of bile acid secretion increases (Chianale et

al., 1996), bile flow increases in clofibrate-treated mice (Kok et al., 2003), and bile acid pool size is unchanged in clofibrate-treated rats (Turley and Dietschy, 1980).

Fenofibrate seems to impact the "ezetimibe-sensitive" pathway. Figure 4.5 shows that fenofibrate has no significant effect on the ezetimibe-insensitive pathway, although a trend toward lower values was observed. In contrast, the calculated "ezetimibe-sensitive" fractional cholesterol absorption is significantly reduced by fenofibrate (43% reduced, $41.3 \pm 7.3\%$ to $23.6 \pm 2.7\%$). This corresponds to the change in NPC1L1 mRNA expression (38-55% reduction) and protein expression (66% reduction) observed in these studies. Thus, fenofibrate may act to reduce cholesterol absorption by modulating the "ezetimibe-sensitive pathway." Of course, cholesterol absorption pathways acting independently of the ezetimibe-sensitive pathway may exist, although they would seem to be responsible for only a small fraction (less than 10%) of the cholesterol absorbed.

Because fenofibrate seems to be reducing cholesterol absorption through downregulation of NPC1L1, which is also important for uptake of phytosterols (Davis et al., 2004), it would be interesting to test whether fenofibrate administration would decrease phytosterol absorption and plasma levels in *Abcg5/8*-knockout mice, a model of sitosterolemia. The disease in these mice is prevented by administration of ezetimibe (Yu et al., 2005).

Traditionally, the liver has been understood to be the primary target of fibrates. Indeed, when wild-type mice are given PPAR agonists, there is hepatomegaly resulting

from increased peroxisome proliferation. Fortunately, peroxisome proliferation does not occur in humans. Here, we show not only that PPARα is expressed in intestine, but also that administration of a PPARα agonist alters gene expression and function in the intestine. Our results are consistent with the idea that activation of PPARα resident within the intestinal epithelium is responsible for the physiological changes we observe, however they do not rule out the possibility that PPARα agonists may be acting at a distant site and then influence the intestine via humoral, metabolic, or other factors. Further investigation of the precise role(s) of PPARα in the intestine is warranted.

Although our data suggest that PPARα is reducing cholesterol absorption by decreasing expression of NPC1L1 in the intestine, they do not fully define the precise molecular mechanisms downstream of PPARα activation which lead to altered expression of NPC1L1. It was previously proposed that administration of a PPARα agonist could decrease cholesterol absorption by activating LXRs (Knight et al., 2003), which are themselves known to play a role in cholesterol efflux and absorption (Chawla et al., 2001). Our data indicate that fenofibrate is able to reduce cholesterol absorption and NPC1L1 expression independently of LXRs, as *Lxrα/β*-double-knockout mice still respond to fenofibrate similar to their wild-type controls. In addition, short-term treatment of wild-type mice with fenofibrate reveals no repression of NPC1L1 mRNA expression, whereas longer treatments of 3, 7, or 10 days show repression (Figure 4.7A). Thus, the impact of PPARα action on NPC1L1 expression is likely to be indirect not only because nuclear receptors generally enhance expression of direct targets (transactivation),

but also because this process usually only requires several hours. Long-term activation of PPARα could theoretically repress NPC1L1 mRNA expression either by decreasing transcription of NPC1L1 or by altering the half-life of the transcript. Because NPC1L1 protein was decreased to a greater extent than mRNA, there may also be translational or post-translational effects of PPARα activation on NPC1L1. We hypothesized that if PPARα activation were changing transcription of NPC1L1, there might be a change in histone acetylation at this locus. Fenofibrate treatment, however, does not significantly alter histone-H3 acetylation at the points tested (Figure 4.7B). Although this observation does not formally exclude changes in transcription factor (or cofactor) binding or activation, it does define a region of acetylated histone-H3 enrichment and therefore presumably "open" structure of chromatin. This enrichment of acetylation (up to ~9-fold) indicates that, in the basal state, NPC1L1 is constitutively expressed in the proximal small intestine. Thus, the region beginning approximately 2500 base pairs upstream of the putative transcriptional start site represents a potential area for transcription factors to access and bind DNA to regulate expression of NPC1L1. Transcription factor binding sites that are conserved between species in this region could be important in the physiological regulation of expression.

These studies support a role for PPARα in the regulation of NPC1L1, thus expanding the list of nuclear receptors known to influence NPC1L1 expression in the intestine. These include LXRs and PPARβ, which seem to down-regulate NPC1L1, as LXR agonist treatment (T0901317, 5 days) of ApoE-KI mice on a western diet reduces
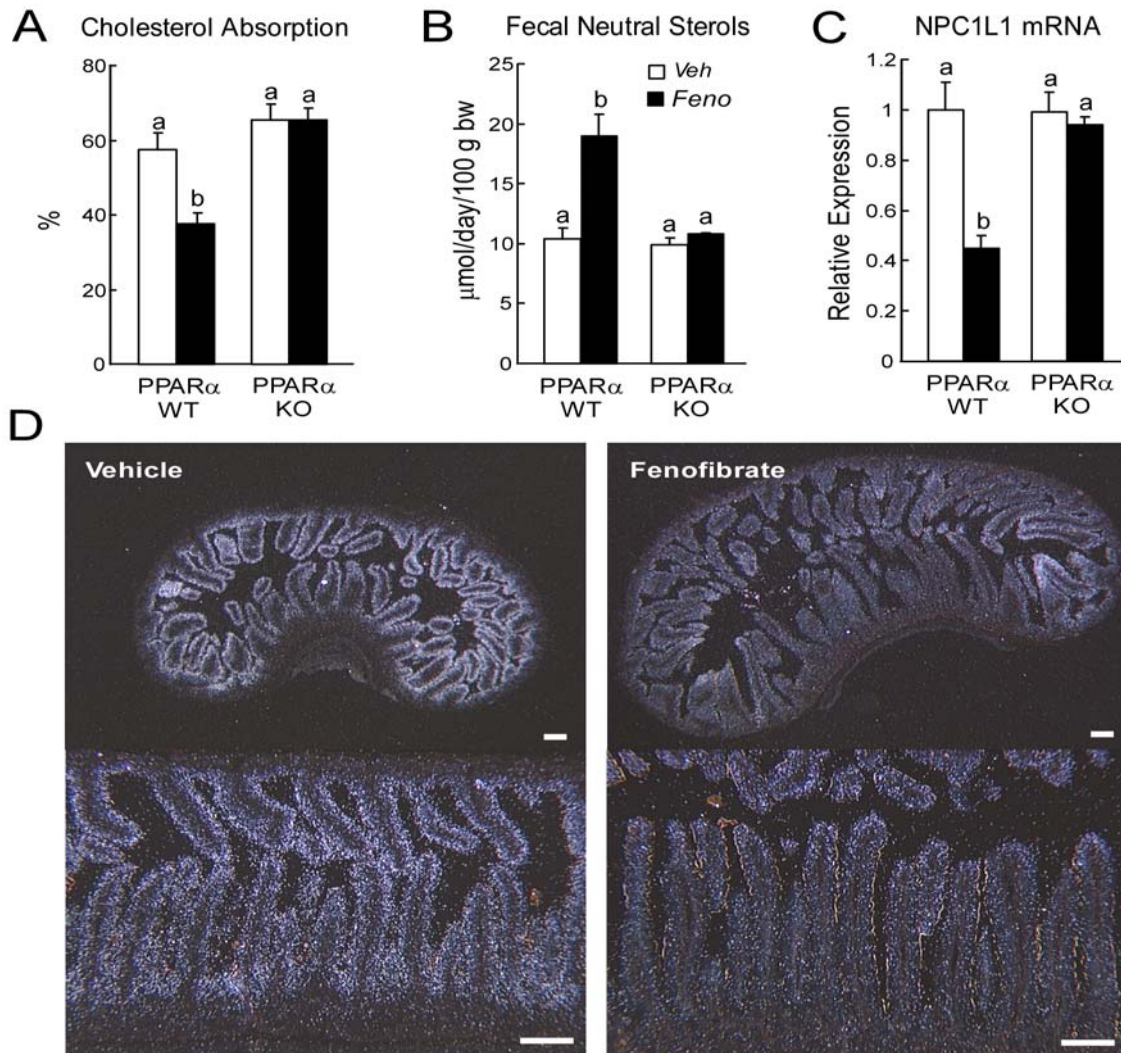
duodenal NPC1L1 mRNA expression by approximately 40 percent (Duval et al., 2006), whereas PPARβ agonist treatment (GW610742, 0.017% w/w, 8 days) of DBA/1 wild-type mice reduces NPC1L1 mRNA expression in jejunum and ileum, but not duodenum (van der Veen et al., 2005). Estrogen receptors may play a role in upregulation of NPC1L1 as administration of high-doses of 17β-estradiol (6 µg/day) to ovariectomized AKR or C57L mice increases NPC1L1 mRNA expression in duodenum and jejunum, but not ileum (Duan et al., 2006). In each of these cases and in our studies, relatively long treatment durations were used to change NPC1L1 expression; therefore, the effects on NPC1L1 by nuclear receptor agonists could be secondary to other metabolic perturbations. Nevertheless, it is clear that nuclear receptors, including PPARα, can influence NPC1L1 gene expression.

Since PPARα is known to function in the adaptive response to fasting and can also be activated by high-fat diet (Kersten et al., 1999), PPARα could potentially mediate a change in cholesterol balance in response to these and other factors. Future work aims not only to elucidate the precise molecular mechanisms downstream of PPARα activation that modulate NPC1L1 gene expression, but also the physiologic or pathophysiologic circumstances in which PPARα and other nuclear receptors might mediate changes in cholesterol absorption.

4.6 ACKNOWLEDGEMENTS

Figure 4.1 PPARα inhibits both cholesterol absorption and NPC1L1 mRNA expression in mouse small intestine. Three-month old male PPARα +/+ (PPARα WT) and PPARα -/- (PPARα KO) mice were fed powdered basal diet (Veh) or diet supplemented with fenofibrate at 800 mpk/day (Feno) for a total of 10 days. *A*, Fractional cholesterol absorption, as determined by the fecal dual-isotope method, was decreased in fenofibrate-treated wild-type mice but not in knockouts. *B*, Fecal neutral sterol excretion was increased in fenofibrate-treated wild-type mice but not knockouts. *C*, RNA was isolated from mucosa of the proximal third of small intestine of each individual animal and subjected to qPCR to ascertain the relative levels of NPC1L1 mRNA. *D*, *In situ* hybridization of jejunal sections using a probe directed at the 3' UTR of NPC1L1 shows reduced expression in female mice treated with 800 mpk fenofibrate for 10 days. (Scale Bar: 100μm) Values represent the mean ± SEM of data from 4-6 mice per group. Statistical analyses were performed by two-way ANOVA with post-hoc test; different letters indicate statistically different groups ($p < 0.05$).
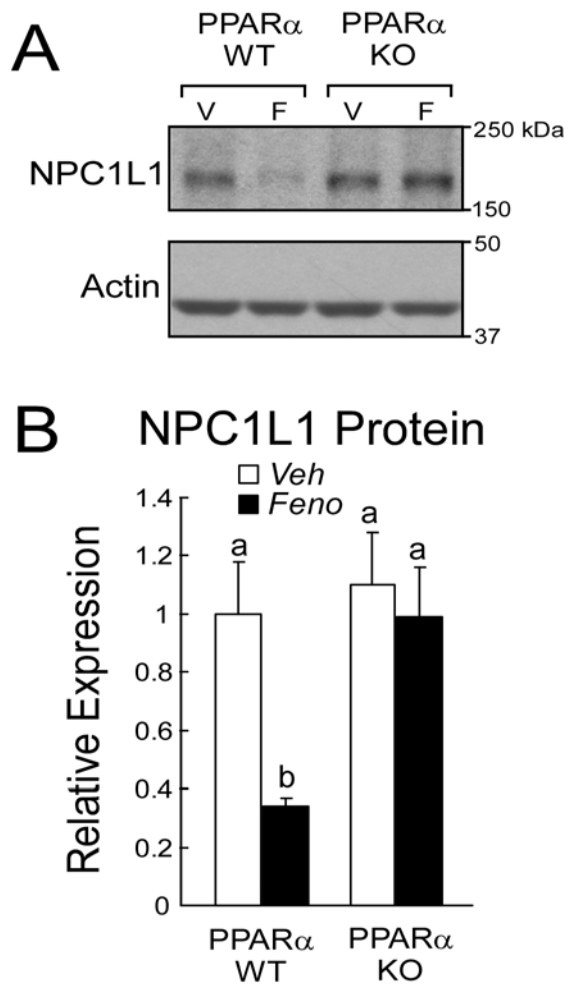
Figure 4.2 PPARα inhibits NPC1L1 protein expression in mouse small intestine.

Three-month old male PPARα +/+ (PPARα WT) and PPARα -/- (PPARα KO) mice were fed powdered basal diet (Veh) or diet supplemented with fenofibrate at 800 mpk/day (Feno) for a total of 10 days. Whole-cell protein was isolated from mucosa of the proximal third of small intestine of each individual animal. 40µg protein was loaded in each lane and resolved by SDS-PAGE, then immunoblotted with NPC1L1 and actin polyclonal antisera. A, Representative immunoblot showing one individual animal from each treatment group. B, NPC1L1 protein was quantified using OptiQuant software with actin as a loading control. Values represent the mean ± SEM of data from 4-6 mice per group. Statistical analyses were performed by two-way ANOVA (with genotype and treatment as factors) with post-hoc test; different letters indicate statistically different groups (p<0.05).
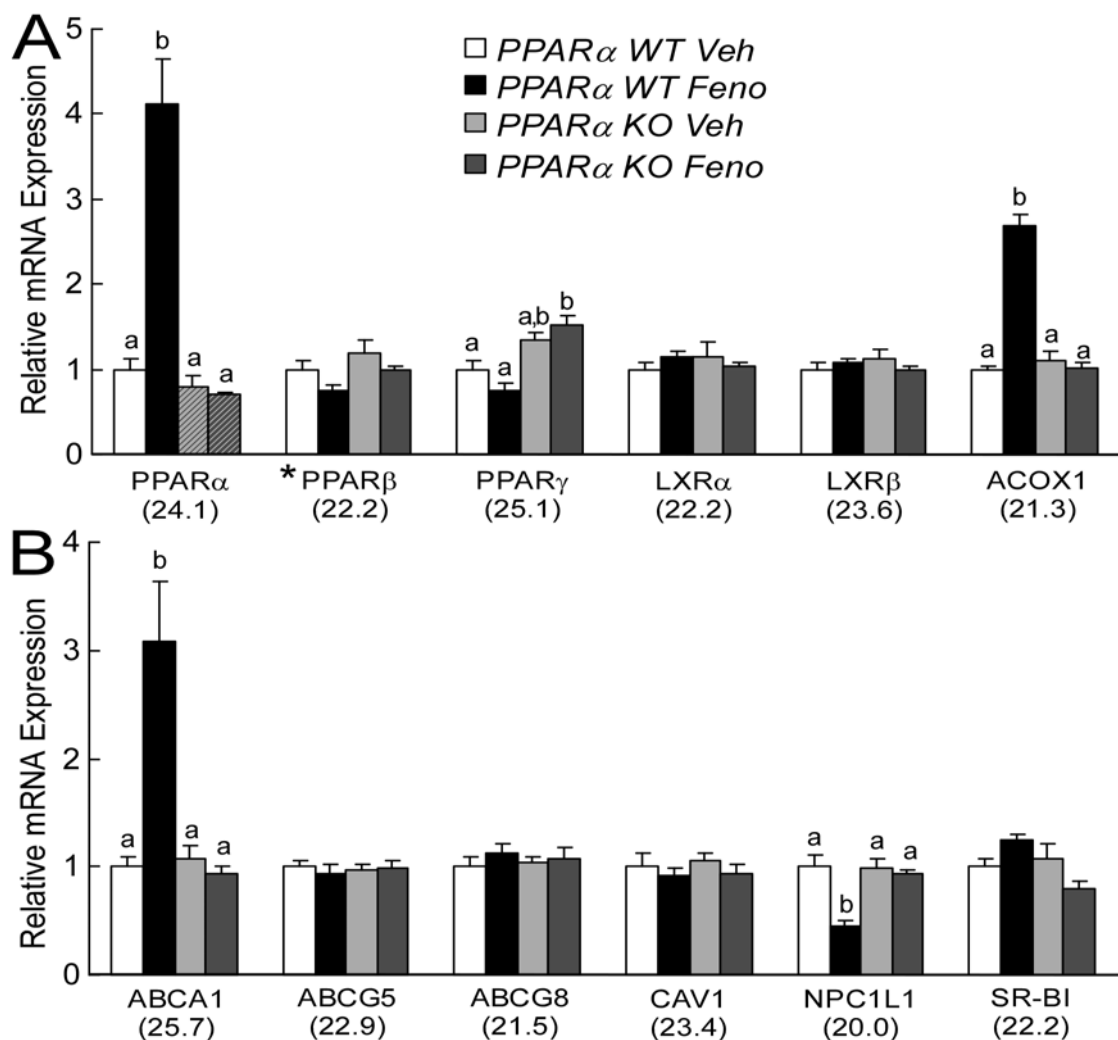
Figure 4.3 PPARa specifically regulates NPC1L1 mRNA levels, but not those of other sterol transport proteins.

Three-month old male PPARα +/+ (WT) and PPARα -/- (KO) mice were fed powdered basal diet (Veh) or diet supplemented with fenofibrate at 800 mpk/day (Feno) for a total of 10 days. RNA was isolated from mucosa of the proximal third of small intestine of each mouse and subjected to quantitative real-time PCR. A, Relative mRNA levels of PPAR and LXR isoforms, and ACOX1, a PPARα target gene. Hatched bars represent recognition of an aberrant transcript in *Pparα*-null mice. B, Relative mRNA levels for various sterol transport proteins as measured by qPCR. Values represent the mean ± SEM of data from 4-6 mice per group. Statistical analyses were performed by two-way ANOVA (with genotype and treatment as factors) with post-hoc test; different letters indicate statistically different groups (p<0.05). *Statistical evaluation of PPARß expression revealed a modest (p<0.05) decrease in mRNA due to fenofibrate, with no interaction between genotypes.
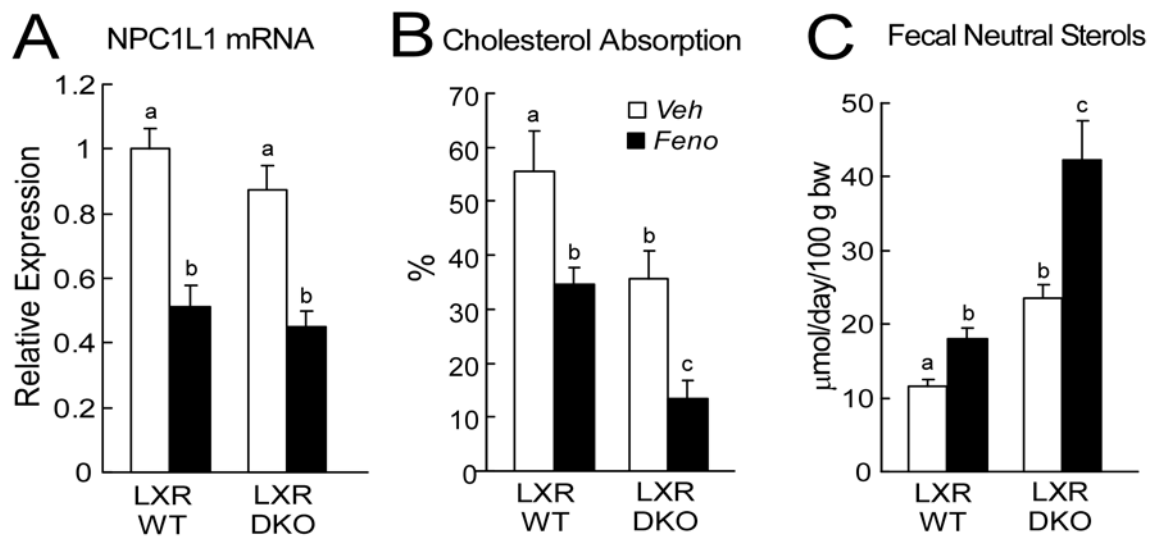
Figure 4.4 Fenofibrate inhibits cholesterol absorption and NPC1L1 expression independent of LXRs.
Three-month old female LXRα/β +/+ (LXR WT) and LXRα/β -/- (LXR DKO) were fed powdered basal diet (Veh) or diet supplemented with fenofibrate at 800 mpk/day (Feno) for a total of 7 days. *A*, RNA was isolated from mucosa of the proximal third of small intestine of each mouse and subjected to quantitative real-time PCR to determine the relative levels of NPC1L1 mRNA. *B*, Fractional cholesterol absorption, as determined by the fecal dual-isotope method, was decreased in both fenofibrate-treated wild-type mice and knockouts. *C*, Fecal neutral sterol excretion was increased in both fenofibrate-treated wild-type mice and knockouts. Values represent the mean ± SEM of data from 6 mice per group. Statistical analyses were performed by two-way ANOVA (with genotype and treatment as factors) with post-hoc test; different letters indicate statistically different groups (p<0.05).
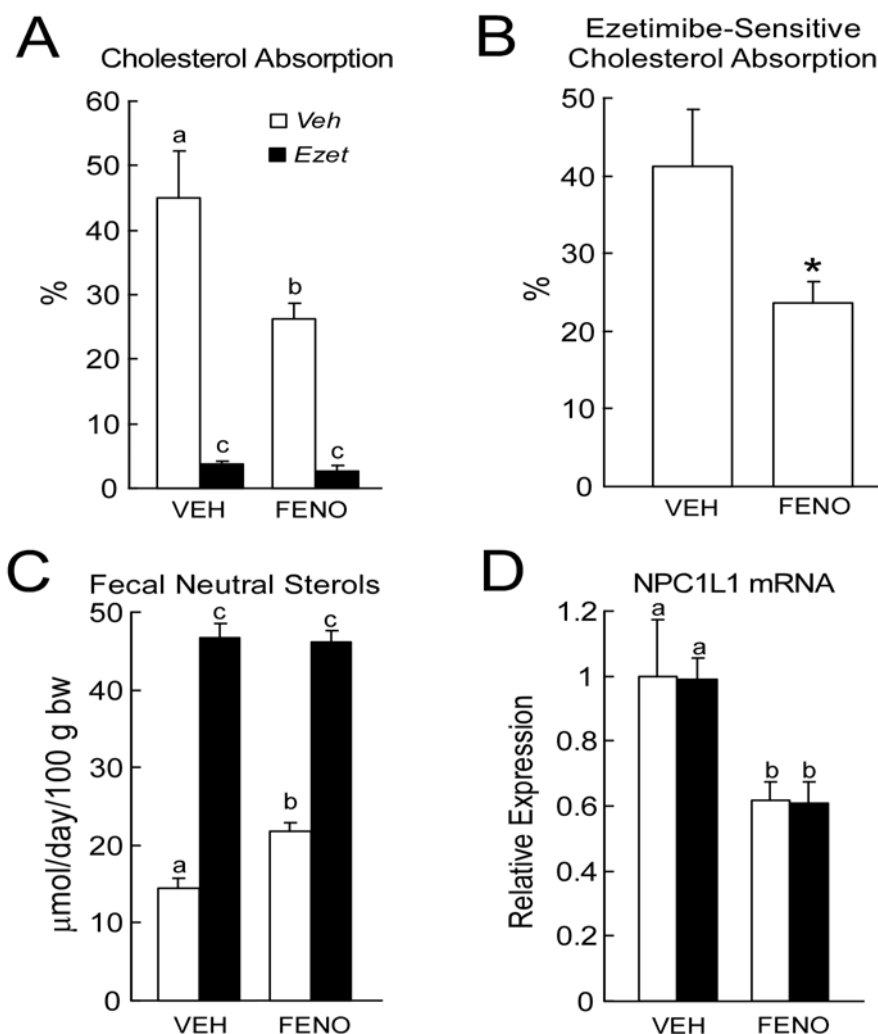
Figure 4.5 Fenofibrate impacts the ezetimibe-sensitive pathway. Three-month old male PPARα +/+ (WT) and PPARα -/- (KO) mice were fed powdered basal diet (Veh) or diet supplemented with ezetimibe (10mpk/day, Ezet), fenofibrate (800mpk/day, Feno), or both (Both) for 10 days. *A*, Fractional cholesterol absorption was decreased in all drug-treated groups relative to vehicle controls. *B*, Calculated "ezetimibe-sensitive" fractional cholesterol absorption was decreased by fenofibrate. *C*, Fecal neutral sterol excretion was increased in all drug-treated groups relative to vehicle controls. *D*, NPC1L1 mRNA was decreased in proximal small intestine by fenofibrate but not ezetimibe. Values represent the mean ± SEM of data from 5-6 mice per group. Statistical analyses were performed by two-way ANOVA (with ezetimibe and fenofibrate as factors) with post-hoc test; different letters indicate statistically different groups (p<0.05). Statistical analyses comparing 2 groups were performed by calculating two-tailed p-values; asterisks indicate statistical difference from vehicle treated controls: *, p<0.05.
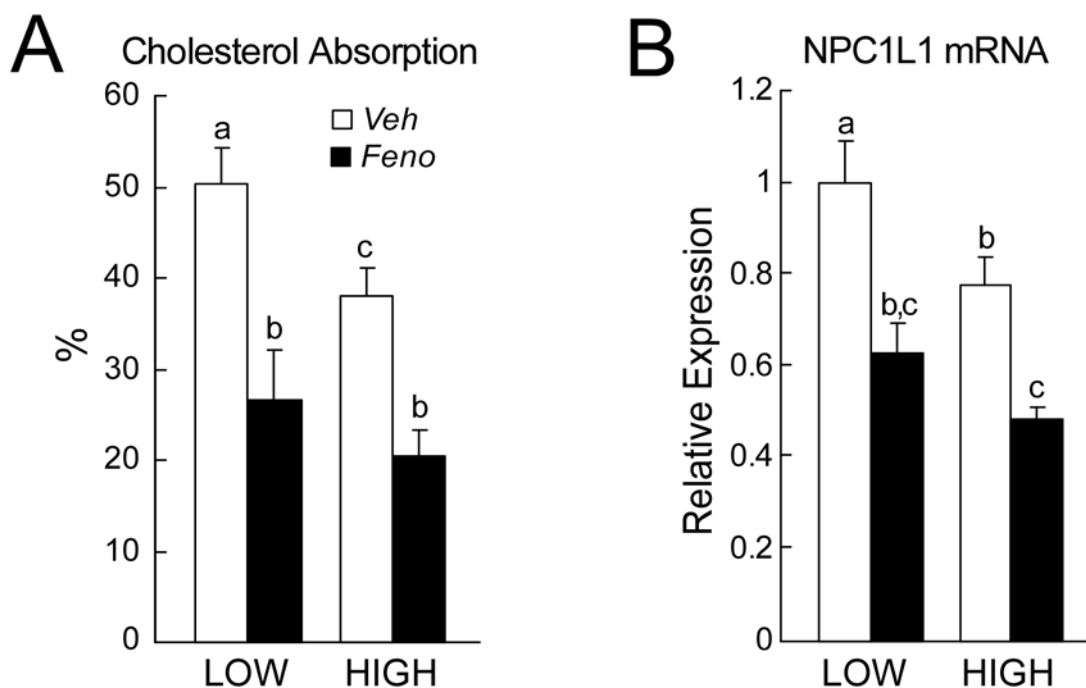
Figure 4.6 Fenofibrate inhibits cholesterol absorption and NPC1L1 mRNA expression in mice fed a high-cholesterol diet.
Three-month old female A129/Sv mice were fed powdered low-cholesterol basal diet (0.02% w/w, LOW) or high-cholesterol diet (0.2% w/w, HIGH) for 10 days. In addition, these diets were either unsupplemented (Veh) or supplemented with fenofibrate (800mpk/day, Feno). *A*, Fenofibrate-treated groups showed decreased fractional cholesterol absorption as compared to vehicle controls whether on high- or low-cholesterol diet. *B*, RNA was isolated from mucosa of the proximal third of small intestine of each individual animal and subjected to quantitative real-time PCR to ascertain the relative levels of NPC1L1 mRNA. Relative mRNA levels were measured using SYBR green chemistry with gene-specific primers (Table 4.1) and calculated by the comparative CT method using cyclophilin as the housekeeping control. NPC1L1 mRNA was decreased by fenofibrate on both high and low cholesterol diets. Values represent the mean ± SEM of data from 7-8 mice per group. Statistical analyses were performed by two-way ANOVA (with cholesterol and fenofibrate as factors) with post-hoc test; different letters indicate statistically different groups (p<0.05).
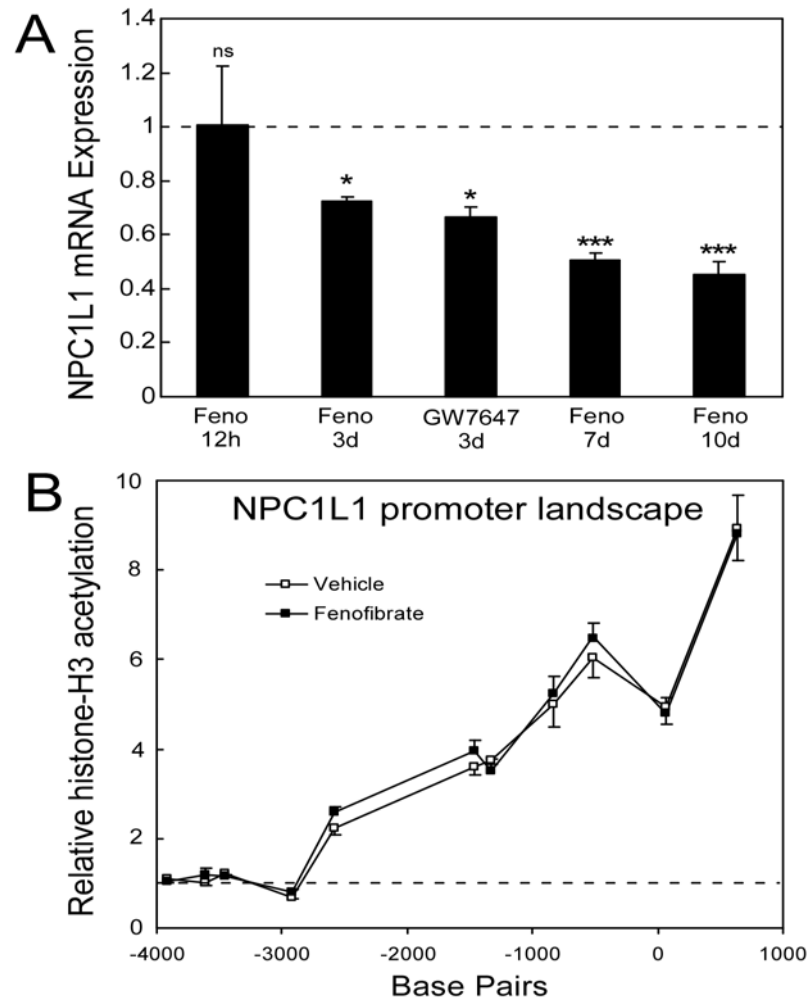
Figure 4.7 Chronic PPARα activation decreases NPC1L1 expression without altering histone-H3 acetylation at the NPC1L1 gene locus. *A*, NPC1L1 mRNA expression relative to vehicle controls from a compilation of separate studies in which mice (n=4-6) were treated with PPARα agonists for various durations including: 12h fenofibrate (800 mpk/day,diet); 3 days fenofibrate (150 mpk/day, daily gavage); 3 days GW7647 (10mpk/day, daily gavage); 7 days fenofibrate (800 mpk/day, diet); 10 days fenofibrate (800mpk/day, diet). *B*, Three-month old female A129/SvJ mice were fed powdered basal diet (Veh) or diet supplemented with fenofibrate at 800 mpk/day (Feno) for a total of 10 days. Chromatin immunoprecipitation (ChIP) assays were performed on proximal intestinal mucosa and quantified by qPCR. Data is represented as fold signal over the average value for the negative control region (average of points -3911,-3612,-3455,-2921) to correct for variable efficiency of immunoprecipitation. ChIP primer sets are defined in Table 4.2. Values represent the mean ± SEM of data from 4-6 mice per group. Statistical analyses were performed by two-tailed Student's t-test; asterisks indicate statistical difference from treated controls on the same diet: *, $p<0.05$; **, $p<0.01$; ***, $p<0.001$.

TABLE 4.1

Primer sequences used for the measurement of mouse intestinal RNA levels
by quantitative real-time PCR.

Gene	Common name	GenBank #	Primer sequences
ABCA1	ATP-binding cassette transporter A1	NM_013454	F: 5'-cgtttccgggaagtgtccta R: 5'-gctagagatgacaaggaggatgga
ABCG5	ATP-binding cassette transporter G5	NM_031884	F: 5'-tggatccaacacctctatgctaaa R: 5'-ggcaggttttctcgatgaactg
ABCG8	ATP-binding cassette transporter G8	NM_026180	F: 5'-tgcccaccttccacatgtc R: 5'- atgaagccggcagtaaggtaga
ACOX1	Acyl CoA oxidase – 1	NM_015729	F: 5'-ttgttgtccctatccgtgaga R: 5'-ggccgatatccccaacagt
CAV1	Caveolin-1	NM_007616	F: 5'-aacatctacaagcccaacaacaagg R: 5'-ggttctgcaatcacatcttcaaagtc
Cyclo	Cyclophilin	M60456	F: 5'-tggagagcaccaagacagaca R: 5'-tgccggagtcgacaatgat
LXRα	Liver X receptor α (NR1H3)	NM_013839	F: 5'-aggagtgtcgacttcgcaaa R: 5'-ctcttcttgccgcttcagttt
LXRβ	Liver X receptor β (NR1H2)	NM_009473	F: 5'-ctcccacccacgcttacac R: 5'-gccctaacctctctccactca
NPC1L1 5' set	Niemann Pick type C1-like 1	NM_207242	F: 5'-tggactggaaggaccatttcc R: 5'-gacaggtgccccgtagtca
NPC1L1 3' set	Niemann Pick type C1-like 1	NM_207242	F: 5'-ggcatgaacgccatttgc R: 5'-gcaatagccacataagactgattagg
PPARα	Peroxisome proliferator-activated receptor α (NR1C1)	NM_011144	F: 5'-cgtacggcaatggctttatc R: 5'-aacggcttcctcaggttctt
PPARβ	Peroxisome proliferator-activated receptor β (NR1C2)	NM_011145	F: 5'-ccacgagttcttgcgaagtc R: 5'-aacttgggctcaatgatgtca
PPARγ	Peroxisome proliferator-activated receptor γ (NR1C3)	NM_011146	F: 5'-caagaataccaaagtgcgatcaa R: 5'-gagctgggtctttcagaataataag
SR-BI	Scavenger receptor B-type I	NM_016741	F: 5'-tccccatgaactgttctgtgaa R: 5'-tgcccgatgcccttga
Villin	Villin	NM_009509	F: 5'-agtcccccatcttccaacaac R: 5'-tcaaacttcacctgttccacctt

Primer sequences are designed and optimized for use with the Applied Biosystems real-time PCR system (ABI7900HT).

TABLE 4.2

Primer sequences used for the measurement by qRT-PCR
of mouse NPC1L1 genomic DNA fragments following
chromatin immunoprecipitation with acetylated histone-H3 antibody.

Set#	Median nt# relative to transcriptional start site	Amplified Segment per GenBank# NT_039515	Primer sequences
1 (distal)	-3911	3134208-3134116	F: 5'-ctgtcatttcttcttttgcaatatatgtag R: 5'-aaaacctagcaatccaaatgtgtgt
2	-3612	3133905-3133820	F: 5'-gtggtggctcatacctgcaa R: 5'-ccctgtgtatcccacagatgact
3	-3455	3133746-3133665	F: 5'-agaaagaatggaaggaaggtcaga R: 5'-acatctcatccagcagtcacaaa
4	-2921	3133215-3133129	F: 5'-tgaggcaaggcgctacact R: 5'-aagttggcctgaaaaattctatgg
5	-2576	3132883-3132771	F: 5'-gcacaagaggtgggcaagac R: 5'-gctgaccaccgtgcatgtc
6	-1464	3131752-3131678	F: 5'-ccccacacaggcagtgatg R: 5'-gaagcccccaaaagcatga
7	-1326	3131617-3131537	F: 5'-ctggacagccctcgtgaga R: 5'-gccacatgaaaaccccaaga
8	-838	3131147-3131030	F: 5'-tggcatccagggagcaa R: 5'-gctcgggtgggctcaga
9	-520	3130821-3130721	F: 5'-ccaggttgggtgggacttg R: 5'-ctcctcatgcccgttctatcc
10	61	3130224-3130158	F: 5'-agctgccttaatgtgcaaactca R: 5'-ggaccaggccttggagaca
11 (proximal)	637	3129652-3129578	F: 5'-tgacagcaataaaggtcgctatct R: 5'-gtgatccaatagagtgtggctttaaa

Primer sequences are designed and optimized for use with the Applied Biosystems real-time PCR system (ABI7900HT).

CHAPTER 5

Conclusions, Implications, and Recommendations

5.1 CONCLUSIONS AND IMPLICATIONS

5.1.1 Mechanism of Cholesterol Uptake

5.1.1.1 The Identity of the Intestinal Cholesterol Permease

The initial finding that NPC1L1 was critical for intestinal cholesterol absorption and ezetimibe sensitivity (Altmann et al., 2004) was met with much criticism and controversy in the field. This was probably due to the unexpected nature of the discovery in light of strong *in vitro* evidence that other proteins are involved in cholesterol binding and transport, but could also have been partly due to the fact that direct binding of ezetimibe to NPC1L1 was not initially demonstrated. A subsequent report provided substantial evidence to support the idea that NPC1L1 is the *bona fide* target of ezetimibe (Garcia-Calvo et al., 2005), but did not yet demonstrate cholesterol binding or transport by NPC1L1. Very recently, an assay using a hepatoma cell line that stably overexpresses NPC1L1 has shown cholesterol uptake (Yu et al., 2006). In any case, NPC1L1 is at least a component of the "ezetimibe-sensitive" pathway for cholesterol absorption.

Our initial interests regarding NPC1L1 were to determine if indeed it is regulated by nuclear receptors. However, with the publication of studies suggesting that a

CAV1/ANXA2 complex was disrupted by ezetimibe and was important for cholesterol absorption (Smart et al., 2004), and the fact that a second group developed *Npc1l1*-knockout mice and observed mislocalization of CAV1 in *Npc1l1*-deficient fibroblasts, we decided to assess cholesterol homeostasis (including fractional cholesterol absorption and ezetimibe-sensitivity) in *Cav1*-knockout mice in a collaborative project with Dr. Richard Anderson. The major finding of the study was that *Cav1*-deficient animals absorb cholesterol similar to their wild-type controls and are completely sensitive to absorption blockade by ezetimibe (Chapter 2)(Valasek et al., 2005). Thus, we used genetic ablation of the CAV1/ANXA2 complex to determine its importance for intestinal cholesterol absorption. mRNA analyses suggested that the loss of CAV1 was not compensated for by an increase in CAV2 or CAV3. This also ruled out another possibility: that NPC1L1 was forming a complex with CAV1/ANXA2 (i.e. a heterotrimer or "cholesterol uptake system" (Seedorf et al., 2004)) to perform the function of enterocytic cholesterol transport. Additionally, although the expectation from our studies is that ANXA2 is unlikely to be important for cholesterol absorption, *Anxa2*-deficient mice have not yet been developed and assessed for their ability to absorb cholesterol. Thus, NPC1L1 is a key component of the cholesterol absorption machinery and is likely the long sought-after intestinal cholesterol "permease."

5.1.1.2 Mechanism of Cholesterol Transport and the Control of NPC1L1 Translocation

Precisely how NPC1L1 performs its function to allow cholesterol entry into the enterocyte (including the events immediately downstream of the plasma membrane) remains unclear. NPC1L1 is known to be a membrane protein (with 13 predicted transmembrane domains) similar to its only other family member, NPC1 (Davies et al., 2000b). There has been some controversy regarding which cellular membrane the protein resides as it has been suggested to be present in the apical brush border membrane (plasma membrane) of the enterocyte (Altmann et al., 2004) or present in intracellular membranes that co-localize with Rab5A (with no protein present on the plasma membrane) in HepG2 cells (Davies et al., 2005). A later study (Yu et al., 2006) provides a potential reconciliation to these disparate results regarding the subcellular localization of NPC1L1. They found that when stably-transfected McArdle RH7777 rat hepatoma cells were depleted of cholesterol using methyl-β-cyclodextran, NPC1L1 translocated from a perinuclear region to the cell surface. In addition, as the cells became more confluent, NPC1L1 protein was localized to an "apical-like" domain that was interpreted to be representative of canalicular localization in polarized hepatocytes *in situ*. Thus, these studies indicate the possibility that NPC1L1 shuttles between the plasma membrane and ER during import of cholesterol, although it remains to be determined whether this process exists and is physiologically relevant in the enterocyte.

One theoretical possibility for controlling the intracellular intinerary of NPC1L1 is the presence of an internal YQRL motif (within the SSD), which may serve as a plasma membrane to *trans*-Golgi network transport signal (Bos et al., 1993; Humphrey et al., 1993; Ponnambalam et al., 1994; Rothman and Wieland, 1996). It is still not known

how this sequence causes protein translocation, however mutation of this site will determine its importance for NPC1L1. Another theoretical possibility is that NPC1L1 could be sequestered in intracellular regions by proteins already known to be important for regulation of SSD-containing proteins: Insigs. When cellular cholesterol levels are high, SCAP is anchored in the ER by Insigs. Since SCAP binds to SREBP independent of cholesterol levels, SREBP is retained in the ER as well. A decrease in cellular cholesterol releases SCAP, which then chaperones SREBP to the Golgi for processing. For NPC1L1, an Insig (or Insig-like anchor protein) would bind NPC1L1 under conditions of high cholesterol retaining it in the ER (or other intracellular region), but upon depletion of cholesterol NPC1L1 would be released to go to the cytoplasm. This model is consistent with the observed behavior of NPC1L1 in response to methyl-β-cyclodextran treatment (Yu et al., 2006).

Whether intestinal cholesterol transport is vesicular or non-vesicular, the initial events in cholesterol absorption are likely to include NPC1L1 binding cholesterol and other proteins. However, direct binding of cholesterol to NPC1L1 has not yet been demonstrated. Because NPC1L1 contains a sterol-sensing domain (SSD) is it likely to bind cholesterol. Indeed, NPC1 was found to bind a photoactivatable analog of cholesterol called [(3)H]7,7-azocholestanol that was "competed away" (i.e. diminished cross-linking) using unlabeled cholesterol (Ohgami et al., 2004). SCAP was also found to bind cholesterol by way of the SSD (Radhakrishnan et al., 2004). Moreover, NPC1L1 can function to import extracellular cholesterol in cultured cells, in a manner that can be inhibited by ezetimibe (Yu et al., 2006). After binding cholesterol, NPC1L1 could

interact with proteins that direct vesicle formation and trafficking or transfer cholesterol directly to cholesterol-binding proteins. Certainly determination of protein and small molecule binding partners of NPC1L1 will greatly facilitate our understanding of these processes.

5.1.2 Dietary and Nuclear Receptor Control of NPC1L1 Expression

5.1.2.1 Dietary Regulation of NPC1L1 Expression

During the study of cholesterol homeostasis in ezetimibe-treated *Cav1*-knockout mice, we began to gain insight into the regulation of NPC1L1 mRNA expression, as it did not respond to ezetimibe treatment under these conditions. This suggested to us that NPC1L1 expression might not be sensitive to regulation by dietary cholesterol, and raised the possibility that NPC1L1 might be regulated by other factors.

The first assessment of diet-induced changes of NPC1L1 mRNA levels occurred in mice fed a basal rodent diet supplemented with 1% cholesterol and 0.5% cholic acid for 7 days; this diet caused a ~75% decrease in NPC1L1 mRNA expression in the proximal small intestine (Davis et al., 2004). In contrast, cholesterol supplementation alone in the diet generally causes <20% decrease in NPC1L1 mRNA expression (Mark Valasek, unpublished observations), and one study found no change when cholesterol was added to the diet for 4 weeks (Plosch et al., 2006).

A few studies have now looked at potential changes in NPC1L1 expression in response to plant sterol (and stanol) supplementation of the diet. In the first studies, C57Bl/6J, LDLR-/-, and ApoE-/- mice were fed a "Western-type" diet containing 20% dietary fat and 0.08% cholesterol, which was supplemented with or without 2% phytosterols for 4 weeks. Small intestinal expression of NPC1L1 mRNA was measured and found to be modestly but significantly altered by phytosterols: ~33% increased in C57Bl/6J, ~23% decreased LDLR-/-, and ~22% decreased in ApoE-/- (Calpe-Berdiel et al., 2005). However in a separate study, NPC1L1 gene expression was not changed by plant sterols or stanols in C57BL/6 mice fed a low-fat diet (6% fat) supplemented for the same duration (4 weeks) (Plosch et al., 2006). Thus, the changes are modest and inconsistent suggesting that changes in other factors, like dietary fat content and composition, may be responsible for NPC1L1 gene expression changes. Indeed, we have treated mice for 4 days with supplementation of fats (10% w/w) including: medium-chain triglyceride (MCT) oil, olive oil, and safflower oil. Under these conditions, olive and safflower oil modestly decrease (~20%) while MCT oil greatly decreases (>50%) NPC1L1 expression in the proximal small intestine relative to basal chow-fed controls.

5.1.2.2 Acute Regulation of NPC1L1 Expression by RXR Heterodimers

To test the hypothesis that nuclear receptors regulate expression of NPC1L1 in the proximal small intestine, the physiological site of cholesterol absorption, we treated mice with a library of nuclear hormone receptor agonists. We first focused on the "adopted

orphan receptors" (Chawla et al., 2001)(i.e. RXR, LXRα/β, PPARα/β/γ, FXR, PXR, CAR), as they are known to respond to dietary-derived lipophilic compounds (many derived from cholesterol), then extended our library to include mice treated with agonists for other ligand-activated nuclear receptors known to form RXR heterodimers (i.e. RAR, TR, and VDR). Very much to our surprise, NPC1L1 was downregulated exclusively by RXR in the proximal small intestine, whereas the other Niemann-Pick C proteins (NPC1 and NPC2) were not regulated by ligands for any of the "adopted orphans"(Chapter 3, data not shown). The failure of ligands for RXR partners to recapitulate the repression we observed after administration of an RXR-selective ligand suggested to us that RXR heterodimers were not involved, RXR homodimers could be modulating this effect. Moreover, this repression of expression was most likely indirect, as nuclear receptors generally transactivate primary target genes. The indirect nature of RXR-mediated repression of NPC1L1 is further supported by studies of LG268-treated intestinal explants. In this system, repression of NPC1L1 by LG268 is blocked by coadministration of either actinomycin D (which blocks pol II transcription) and cycloheximide (which blocks new protein synthesis). In contrast, LG268 induction of direct target genes of RXR heterodimers (e.g. ABCA1, SREBP-1c, etc.) is not blocked by cycloheximide. The repression of NPC1L1 mRNA corresponds to a decrease in protein in the proximal small intestine, suggesting that this regulation is likely to have physiological consequences. Indeed, when wild-type or *Lxrα/β/Fxr*-triple-knockout mice are given LG268 supplemented in the diet (6 mpk/day) there is a marked decrease in cholesterol absorption (Amy Liverman and David Mangelsdorf, unpublished

observation). Taken together, these data suggest the RXR regulation of NPC1L1 can alter cholesterol absorption independently of LXRs and FXR.

As the data suggested that an intermediate protein was needed for RXR to repress NPC1L1, we performed oligonucleotide microarray analysis on a section of proximal intestine in which NPC1L1 repression occurred. We hypothesized that LG268 would induce expression of a gene which could act to decrease RXR expression either by reducing transcription of NPC1L1 or by reducing the stability of the transcript. Because we observed a reduced amount of histone-H3 acetylation at the NPC1L1 locus which often occurs during transcriptional repression, we focused on regulation of transcription. The only obvious "inhibitors of transcription" which were upregulated on the array were SOCS3 (~3-fold) and SHP (~2-fold). We believed that SHP was unlikely to be the mediator of RXR activity for at least four reasons: (1) Acute administration of chenodeoxycholic acid (an FXR agonist) which also induces SHP had no effect on NPC1L1 mRNA expression in the proximal small intestine, (2) genetic alteration of bile acid pool size (and fecal bile acid content) had no statistical effect on NPC1L1 mRNA expression, (3) NPC1L1 was not repressed in the ileum, a known site of expression of both FXR and SHP, and (4) fractional cholesterol absorption is decreased in *Lxrα/β/Fxr*-triple-knockout mice treated with LG268 (Amy Liverman and David Mangelsdorf, unpublished observations). SOCS3 is well known to inhibit signaling events that lead to STAT phosphorylation and eventual transactivation of target genes. For example, SOCS3 is a negative regulator of leptin signaling via STAT3, however SOCS3 can inhibit signaling from various gp130-linked receptors to other STATs and also inhibit the

activity of NF-κB. Unbiased *in silico* analysis of the NPC1L1 proximal promoter region (2000 bp) for conserved transcription factor binding sites (between mouse and human) revealed an overlapping STAT and NF-κB site. The presence of this site suggests the possibility that NPC1L1 might be regulated by other factors that modulate STATs or NF-κB, including hormones, cytokines, or pro- and anti-inflammatory agents. Consistent with this hypothesis is that dexamethasone, a glucocorticoid known to directly interfere with STAT or NF-κB action, reduces NPC1L1 mRNA expression in intestinal explants after only 8 hours. The short time period may also suggest that the action is occurring directly on the NPC1L1 promoter without need for intermediate steps, although this has not yet been tested. Clearly, the regulation of NPC1L1 may be very complex, however at present SOCS3 is the most likely intermediate for RXR-mediated repression of NPC1L1. Therefore, we have discovered that both RXR and glucocorticoid receptor (GR) acutely modulate NPC1L1 expression.

5.1.2.3 "Subchronic" Regulation of NPC1L1 Expression by RXR Heterodimers

Peroxisome Proliferator-activated Receptor alpha (PPARα)

In addition to acute treatments, we also measured proximal small intestinal expression of NPC1L1 in wild-type and *Pparα*-knockout mice treated with vehicle or fenofibrate (0.5% w/w) for 7 days. To our surprise, NPC1L1 was markedly reduced in these samples (~50%). This prompted us to further investigate the role of PPARα in the

regulation of NPC1L1 and cholesterol absorption (Chapter 4). Upon surveying the literature, we realized that very little information existed regarding the impact of fibric acid derivatives or PPARα agonists on cholesterol absorption, moreover all of these studies were done prior to the discovery that NPC1L1 was critical for cholesterol absorption. One study treated rats with gemfibrozil (30 mpk, 14 days) and observed decreased cholesterol absorption (Umeda et al., 2001), while mice treated with WY-14643 (a PPARα agonist, 0.1% w/w) for 7 days also showed mildly decreased cholesterol absorption (Knight et al., 2003). To our knowledge, there are no other studies in rodent models, however two studies involving treatment with clofibrate (McNamara et al., 1980) and gemfibrozil (Vanhanen and Miettinen, 1995) demonstrated cholesterol absorption was also decreased in humans. We have shown that fenofibrate-treated wild-type (A129/SvJ) mice (0.5% w/w, 10 days) not only have decreased fractional cholesterol absorption (35-47% decrease) and increased fecal neutral sterol excretion (51-83% increase), but also have an associated decrease in the relative expression of NPC1L1 mRNA (38-55% decrease) and protein (66% decrease) in the proximal small intestine.

These findings have implications regarding the regulation of NPC1L1 expression by dietary (and other) factors and potential implications for the clinical use of fibrates. Because PPARα is known to respond to fatty acids (especially PUFAs) during fasting and high-fat diet feeding, it is possible that these factors could also influence NPC1L1 expression and cholesterol absorption via PPARα. In addition, the lipid-lowering effects of dietary administration of PUFAs could in part be attributable to regulation of NPC1L1. Our initial studies indicated that NPC1L1 expression was not changed by fasting, but was

decreased by MCT oil (data not shown); the PPARα dependency of these findings have not been determined. Because of the species-specific differences in the tissue distribution of NPC1L1 (see below), it is possible that fibrate drugs may modulate hepatic NPC1L1 expression in humans. If indeed this is the case, it could partly explain the well-known observation that fibrates increase biliary cholesterol levels. By decreasing NPC1L1 expression at the canalicular membrane (proposed site based on primate studies(Yu et al., 2006)), fibrates could reduce reclamation of cholesterol from bile thereby increasing cholesterol concentrations and predisposing patients to cholelithiasis (gallstone formation). These studies must be performed in humans, as the mouse is a poor model to study this particular phenomenon as it does not express NPC1L1 in liver. In addition, fenofibrate may be useful for sitosterolemic patients (possibly in conjunction with ezetimibe) treatment to reduce absorption and reclamation of plant sterols. Ezetimibe has already been shown to be effective for treating sitosterolemia in humans and an animal model (Salen et al., 2004; Yu et al., 2005).

Other Nuclear Receptors

Since we began our studies of the nuclear receptor regulation of NPC1L1 expression and discovered that activation of PPARα represses NPC1L1 expression, others have implicated various nuclear receptors in the regulation of NPC1L1 using "subchronic" treatment regimes. These include LXRs and PPARβ, which seem to down-regulate NPC1L1. In one study, LXR agonist treatment (T0901317, 5 days) of ApoE-KI

mice on a western diet reduces duodenal NPC1L1 mRNA expression by approximately 40 percent (Duval et al., 2006). In contrast, another study treated C57Bl/6 mice on a low-fat (~6%) diet with or without T0901317 for 4 weeks and found no substantial difference in NPC1L1 expression in any intestinal region (Plosch et al., 2006). PPARβ agonist treatment (GW610742, 0.017% w/w, 8 days) of DBA/1 wild-type mice reduces NPC1L1 mRNA expression in jejunum and ileum, but not duodenum (van der Veen et al., 2005). Estrogen receptors may play a role in upregulation of NPC1L1 as administration of high-doses of 17β-estradiol (6 µg/day) to ovariectomized AKR or C57L mice increases NPC1L1 mRNA expression in duodenum and jejunum, but not ileum (Duan et al., 2006). In each of these cases, relatively long treatment durations were used to change NPC1L1 expression, therefore the effects on NPC1L1 by nuclear receptor agonists could be secondary to other metabolic perturbations. Thus, long-term treatment using other nuclear receptor agonists might substantially impact NPC1L1 expression. We would predict that one of these nuclear receptors would be GR.

5.1.3 Other Factors Which May Regulate NPC1L1 Expression

5.1.3.1 Tissue-dependent Expression of NPC1L1

It is clear that NPC1L1 is differentially expressed in tissues with the predominant mRNA expression being in small intestine in various species including: mouse (Altmann et al., 2004; Calpe-Berdiel et al., 2005; Davies et al., 2005; MAV, data not shown),

rat (Altmann et al., 2004), and hamster (MAV, data not shown). In humans there is substantial expression in both liver and small intestine. One study of a panel of human tissues showed similar mRNA levels in liver and small intestine (Altmann et al., 2004), while another study showed that small intestinal expression of NPC1L1 was only 3-4% of that in liver (Davies et al., 2005). Along the length of the small intestine, NPC1L1 mRNA expression assumes a bell-shaped curve in rats (Altmann et al., 2004) and mice (van der Veen et al., 2005; Plosch et al., 2006; Chapter 3). In rats the mRNA expression is slightly shifted to proximal regions (and the protein even more so), which is consistent with the majority of cholesterol absorption in proximal small intestine. In mice, protein levels along the length of the intestine have not been determined.

To gain insight into factors important for tissue specific regulation of NPC1L1, we hypothesized that the protein might be co-expressed with NPC1L1. Therefore, we utilized GNF Symatlas (http://symatlas.gnf.org/SymAtlas/) to mine gene expression databases to find mouse genes highly expressed in small intestine but having low expression in all other tissues. The results included 30 genes with correlation coefficients >0.98 (data not shown), and as expected one of the genes was NPC1L1 (0.982003). The only transcription factor on the list was HNF4γ (0.985823). Although hypothetical, this observation nicely dovetails with our *in silico* analysis of conserved TFBS within the NPC1L1 promoter region (Chapter 3), which includes a putative HNF4 site, suggesting that this nuclear receptor may direct tissue-specific expression of NPC1L1.

5.1.3.1 Inflammation

The regulation of NPC1L1 has remained enigmatic, as the expectation was that NPC1L1 would behave as an SREBP-target gene, being transcriptionally induced by depletion of cellular cholesterol. Indeed, a putative SRE was described in the promoter during the initial cloning and characterization of the gene (Davies et al., 2000b). However, NPC1L1 expression does not change with ezetimibe-treatment, and is actually repressed by statin treatment (rather than induced like HMG-CoA synthase). The presence of a conserved overlapping STAT/NF-κB site in the NPC1L1 promoter region suggested the possibility that NPC1L1 might be regulated by other factors. The prediction from our studies of RXR-mediated regulation of NPC1L1 was that modulators of STAT or NF-kB activity could change NPC1L1 expression. Accordingly, treatment with a GR agonist (dexamethosone) decreases NPC1L1 expression in intestinal explants. All of the nuclear receptor agonists that down-regulate NPC1L1 are also thought to be at least mildly anti-inflammatory. Statins are believed to have anti-inflammatory effects. Recently, data was shown to suggest that a high-fat diet has anti-inflammatory effects in intestine as assessed by microarray analyses of gene expression (FASEB 2006 abstract). This reveals a common theme: inflammation. Thus, anti-inflammatories in general are likely to be able to decrease NPC1L1 expression. Conversely, it will be important to determine if known pro-inflammatory agents (e.g. cytokines, etc.) can induce NPC1L1 in intestine and alter cholesterol absorption.

Although not normally expressed in mouse liver, NPC1L1 mRNA expression can be induced ~20-fold in *Abcg5/8* transgenic mice given statins (Liqing Yu, AHA 2005 abstract). Although inflammation could be the cause, this also raises the possibility that under these conditions the SRE present in the NPC1L1 promoter (Davies et al., 2000b) is functionally active. Because these mice are presumably effluxing cholesterol (via ABCG5/8) while simultaneously being unable to synthesize new cholesterol (because of statins), they are likely to have extraordinarily low cellular levels of cholesterol. The question then becomes one of determining how the SRE is blocked under "normal" conditions.

5.1.4 Why Do We Absorb Cholesterol?

It has long been known that mammals absorb cholesterol, and that dietary cholesterol can ultimately have pathologic effects, as cholesterol-feeding of animal models can promote formation of atherosclerotic lesions (Anitschkow, 1933; Aschoff, 1907). It is also well known that mammals can synthesize cholesterol *de novo*, and therefore do not require dietary cholesterol. Animals treated with ezetimibe or made deficient in *Npc1l1*, simply upregulate hepatic sythesis in response to a drop in cholesterol absorption (Davis et al., 2001b; Davis et al., 2004). Why then do we absorb cholesterol, if too much is bad for us and we can make all we need? One consideration is that of efficiency; cholesterol is an energetically expensive molecule to generate, as it requires more than 30 enzymes to assemble 2-carbon units in such a way as to finally

form a 27-carbon molecule. Therefore, it makes sense to absorb (and reclaim) a portion of cholesterol from the small intestinal lumen. This absorbed cholesterol can then fulfill its vital roles in membrane structure, cell signaling, hormonal balance, and energy aquisition (via conversion to bile acids which promote fat absorption).

The discovery of the critical role of NPC1L1 in cholesterol absorption has opened the door for studies concerning the regulation of NPC1L1. Since factors that influence cholesterol absorption may also regulate NPC1L1 expression, existing studies regarding cholesterol absorption can be interpreted as having potential effects on NPC1L1 expression. Conversely, by studying the control of NPC1L1 expression by novel factors, we may be able to uncover the transcriptional networks that communicate whole-body or local "need" for cholesterol to the intestine so that cholesterol absorption can be altered. Thus, we may better understand *why* we absorb cholesterol by learning *what* controls cholesterol absorption.

5.2 RECOMMENDATIONS (FOR FUTURE STUDIES)

5.2.1 Regarding RXR

To better understand the precise molecular mechanism involved in RXR-mediated NPC1L1 repression, it is necessary to determine the binding partner of RXR, this cis-element in the promoter of a proposed intermediate, the identity of the intermediate, and the mode of action on the NPC1L1 promoter. This can be accomplished using both a

candidate approach, using *in vivo* chromatin immunoprecipitation assays to assay changes in transcription factor binding (e.g. STAT1, STAT3, STAT5A/B, NF-κB subunits, etc.), or an unbiased approach, using DNase footprinting assays to determine changes in protein binding to DNA along the length of the promoter. Once a site is found it can be cloned and excised for analysis in cell lines by addition of agents known to modulate transcription factors at the sites discovered to be important. Unfortunately, since enterocytic cell lines generally fail to recapitulate appropriate expression or regulation of NPC1L1, analysis of the full-length promoter will be difficult unless better models are developed. Certainly, SOCS3 promoter analysis should be performed, and could include cotransfection of nuclear receptors constructs (also Gal4 binding assays) to determine relevant RXR hetero- or homodimer involved. To further confirm that RXR is acting independently of certain RXR heterodimers, acute treatment of *Lxrα/β-*, *Fxr-*, and *Pparα*-knockout intestinal explants with LG268 can be performed. These methods should enable a better understanding of this pathway.

5.2.2 Regarding PPARα

Analysis of bile pool size and composition in fenofibrate-treated wild-type mice (and PPARα-knockouts) and cotreatment of cholic acid and fenofibrate should be performed to determine if PPARα is altering cholesterol absorption by mechanisms that augment the observed change in NPC1L1 mRNA and protein expression. The potential

therapeutic effect of fenofibrate on sitosterolemic animals (*Abcg5/8*-knockouts) should be determined, in part by measuring plasma phytosterol levels.

Candidates for transcriptional regulation of NPC1L1 by PPARα should be determined either by microarray analysis or by candidate approach. Since PPARα is known to be anti-inflammatory and repress NF-κB activity, candidate intermediates such as IκBα should be assayed by qRT-PCR to determine if they are induced by fenofibrate in small intestine.

5.2.3 Regarding Inflammation

Because of its explanatory power, the hypothesis that NPC1L1 is controlled by inflammation merits investigation. Two key questions may be asked in succession: 1) Does inflammation control cholesterol absorption? 2) If so, what effect does this have on atherogenesis?

These questions can first be tackled by investigating if various cytokines, hormones, pro- and anti-inflammatory agents, modulators of STATs and NF-kB, small molecules, etc. impact NPC1L1 expression in the intestinal explant system. If so, then a method of treating mice so that the agent reaches the intestine must be worked out for each agent under study. Various parameters of cholesterol absorption including fractional cholesterol absorption, fecal neutral sterol excretion, fecal acidic sterol excretion, bile size and composition, plasma lipids and profile, etc. could be investigated under various dietary regimes. These studies could then be carried out in ApoE-/- or

LDLR-/- mice to determine their effects on plasma cholesterol, atherogenesis, or other physiologic end points, to determine the potential physiological relevance of these changes in NPC1L1 expression and subsequent cholesterol absorption.

APPENDIX A

The Power of Real-Time PCR

A.1 ABSTRACT

In recent years real-time polymerase chain reaction (PCR) has emerged as a robust and widely used methodology for biological investigation because it can detect and quantify very small amounts of specific nucleic acid sequences. As a research tool, a major application of this technology is the rapid and accurate assessment of changes in gene expression as a result of physiology, pathophysiology, or development. This method can be applied to model systems to measure responses to experimental stimuli and to gain insight into potential changes in protein level and function. Thus, physiology can be correlated with molecular events to gain a better understanding of biological processes. For clinical molecular diagnostics, real-time PCR can be used to measure viral or bacterial loads or evaluate cancer status. Here, we discuss the basic concepts, chemistries, and instrumentation of real-time PCR and include present applications and future perspectives for this technology in biomedical sciences and in life science education.

A.2 A BRIEF HISTORY OF REAL-TIME PCR

Real-time polymerase chain reaction (PCR) is based on the revolutionary method of PCR, developed by Kary Mullis in the 1980's, which allows researchers to amplify specific pieces of DNA more than a billion-fold (Mullis, 1990; Mullis and Faloona, 1987;

170

Saiki et al., 1985). PCR-based strategies have propelled molecular biology forward by enabling researchers to manipulate DNA more easily, thereby facilitating both common procedures, such as cloning, and huge endeavors such as the Human Genome Project (Ausubel et al., 2005; Olson et al., 1989). Real-time PCR represents yet another technological leap forward that has opened up new and powerful applications for researchers throughout the world. This is in part because the enormous sensitivity of PCR has been coupled to the precision afforded by "real-time" monitoring of PCR products as they are generated.

Higuchi and coworkers at Roche Molecular Systems and Chiron Corporation accomplished the first demonstration of real-time PCR (Higuchi et al., 1992; Higuchi et al., 1993). By including a common fluorescent dye called ethidium bromide (EtBr) in the PCR reaction and running the reaction under ultraviolet light which causes EtBr to fluoresce, they could visualize and record the accumulation of DNA with a video camera. It had been known since 1966 that EtBr increases its fluorescence upon binding of nucleic acids (Le Pecq and Paoletti, 1966), but only by combining this fluorescent chemistry with PCR and real-time videography could real-time PCR be born as it was in the early 1990's. Subsequently this technology quickly matured into a competitive market, becoming commercially widespread and scientifically influential. This is evidenced by both the number of companies offering real-time PCR instrumentation (and reagents) and the rapidly increasing numbers of scientific publications pertaining to real-time PCR. Real-time PCR instrumentation was first made commercially available by Applied Biosystems in 1996 after which several other companies added new machines to

the market. Presently, Applied Biosystems, BioGene, Bioneer, Bio-Rad, Cepheid, Corbett Research, Idaho Technology, MJ Research, Roche Applied Science, and Stratagene all offer instrumentation lines for real-time PCR. A significant portion of these machines are used for academic research, and according to a 2003 survey of 406 scientists, 48% projected that they would increase the number of amplifications performed in the coming year. Increased usage of real-time PCR has translated into scientific publications. **Figure A.1** shows the number of publications in the Medline database that contain the words "real-time" and "PCR" or "real-time" and "polymerase chain reaction" in their title or abstract. In 2004 there were 3,522 such publications representing a 43% growth over 2003 in which there were 2,462 publications. The impact of real-time PCR technology on scientific literature is likely to be greater than these numbers imply, as they represent only a fraction of the total number of papers that utilize real-time PCR in their methods. Thus, real-time PCR expands the influence of PCR-based innovations and presents intriguing directions for the future of biomedical sciences (especially molecular diagnostics and molecular physiology) and life science education (Lederberg, 1993; Walker, 2002).

Widespread use has also resulted in a multiplicity of names for the technology, each with a different shade of meaning. "Real-time PCR" simply refers to amplification of DNA (by PCR) that is monitored while the amplification is occurring. The benefit of this "real-time" capability is that it allows the researcher to better determine the amount of starting DNA in the sample prior to amplification by PCR. Present day real-time methods generally involve fluorogenic probes which "light up" to show the amount of

DNA present at each cycle of PCR. "Kinetic PCR" refers to this process as well. "Quantitative PCR" or QPCR refers to the ability to quantify the starting amount of a specific sequence of DNA. This term predates real-time PCR because it can refer to any PCR procedure, including earlier gel-based endpoint assays, which attempts to quantify the starting amount of nucleic acid. Rarely one might see the term "quantitative fluorescent PCR" (or QF-PCR) to designate that the quantification was accomplished via measuring output from a fluorogenic probe, although this is redundant as all of the present chemistries for real-time PCR are fluorescent. In addition, if reverse transcriptase enzymes (see below) are used prior to PCR amplification in any of the above situations then "RT-PCR" replaces "PCR" in the term. Today, the two most common terms of "real-time" and "quantitative" are often used interchangeably or in combination, as real-time PCR is quickly becoming the method of choice to quantify nucleic acids.

A.3 THE GOAL OF REAL-TIME PCR

The basic goal of real-time PCR is to precisely distinguish and measure specific nucleic acid sequences in a sample even if there is only a very small quantity. Real-time PCR amplifies a specific target sequence in a sample then monitors the amplification progress using fluorescent technology. During amplification, how quickly the fluorescent signal reaches a threshold level correlates with the amount of original target sequence, thereby enabling quantification. In addition, the final product can be further characterized by subjecting it to increasing temperatures to determine when the double-stranded product "melts." This melting point is a unique property dependent on product

length and nucleotide composition. To accomplish these tasks, conventional PCR has been coupled to state-of-the-art fluorescent chemistries and instrumentation to become real-time PCR.

A.4 WHAT IS PCR?

At its core, real-time PCR technology utilizes conventional PCR. PCR is a procedure by which DNA can be copied and amplified (Powledge, 2004). As shown in **Figure A.2**, PCR exploits DNA polymerases to amplify specific pieces of DNA using short, sequence-specific oligonucleotides added to the reaction to act as primers. The first and most commonly used of these enzymes is Taq DNA polymerase (from _Thermus aquaticus_), while Pfu DNA polymerase (from _Pyrococcus furiosus_) is used widely because of its higher fidelity when copying DNA. Although these enzymes are subtly different, they both have two basic capabilities that make them useful for PCR: 1) they can generate new strands of DNA using a DNA template and primers, and 2) they are heat-resistant. The latter attribute is necessary because after each round of DNA copying, the resulting double-stranded DNA (dsDNA) must be "melted" into single strands by high temperatures within the reaction tube (~95ºC). The reaction is then cooled to allow the oligonucleotide primers to anneal to the now single-stranded template DNA and direct the DNA polymerase enzyme to initiate elongation by adding single complementary nucleotides to create a new complete strand of DNA. Thus dsDNA is created. This new dsDNA must then be melted apart before the next cycle of copying can occur. Therefore if the reaction works with perfect efficiency, there will be twice as

much specific dsDNA after each cycle of PCR. In reality, PCR reactions do not maintain perfect efficiency because reactants within the PCR reaction are consumed after many cycles, and the reaction will reach a plateau (**Figure A.3**). In addition, self-annealing of accumulating product may also contribute to the "plateau effect" (Wittwer et al., 1997). In fact, it is this very attribute of PCR reactions that makes real-time PCR technology so necessary. Because the reaction is able to efficiently amplify DNA only up to a certain quantity before the plateau effect, there is no way to reliably calculate the amount of starting DNA by quantifying the amount of product at the completion of the PCR reaction. That is to say, no matter how much of a specific target DNA sequence is present prior to PCR, there can be similar amounts of amplified DNA after PCR, and any distinct correlation between starting and finishing quantities is lost. Real-time PCR addresses this problem by taking advantage of the fact that DNA amplifications do occur efficiently early in the reaction process and, therefore, measures product formation during this "exponential phase" (**Figure A.3**). This measurement correlates to the amount of specific starting DNA, thereby allowing quantification.

A.5 REVERSE-TRANSCRIPTASE EXTENDS UTILITY OF REAL-TIME PCR

A major limitation of DNA polymerases (and PCR itself) is that they generally must use DNA as their template. They cannot, for example, amplify RNA in a similar manner. This problem can be overcome by another enzyme, reverse-transcriptase, which generates complementary DNA (or cDNA) from an RNA template. Reverse-transcriptases are enzymes used in nature by retroviruses, including human

immunodeficiency virus (HIV) and hepatitis C virus (HCV), to generate DNA from viral RNA. The virus-derived DNA can then be inserted into the host's genome. In the lab, reverse transcriptase is used to convert RNA to cDNA that can then be used for multiple purposes including PCR-based applications. There are several commonly used reverse transcriptases (RT) including avian myeloblastosis virus (AMV) RT, moloney-murine leukemia virus (M-MLV) RT, or engineered enzymes that enhance polymerase activity or decrease unwanted nuclease activities (e.g. Omniscript, PowerScript, StrataScript, SuperScript II, etc.). Under the appropriate reaction conditions, the relative amount of a given cDNA generated by reverse transcription is proportional to the relative amount of its RNA template. If this were not the case, measurement of cDNA quantities would have no relevance to RNA. Reliably generated cDNA can be used as the raw material for real-time PCR, thereby utilizing its precision and sensitivity to determine changes in gene expression (i.e. RNA levels). This is called real-time RT-PCR and has become the most popular method of quantitating steady-state mRNA levels (Bustin, 2000). It is most often used for two reasons: either as a primary investigative tool to determine gene expression or as a secondary tool to validate the results of DNA microarrays. Because of the precision and sensitivity of real-time RT-PCR, even subtle changes in gene expression can be detected. Thus, real-time PCR can be used to assess both DNA and RNA levels with great sensitivity and precision.

A.6 THE CHEMISTRIES OF REAL-TIME PCR

The key to real-time PCR is the ability to monitor the progress of DNA amplification in real-time. This is accomplished by specific chemistries and instrumentation. Generally, chemistries consist of special fluorescent probes in the PCR reaction (**Figure A.4**). Several types of probes exist including DNA-binding dyes like EtBr or SYBR Green I, hydrolysis probes (5' nuclease probes), hybridization probes, molecular beacons, sunrise and scorpion primers, and peptide nucleic acid (PNA) light-up probes. Each type of probe has its own unique characteristics, but the strategy for each is simple. They must link a change in fluorescence to amplification of DNA.

SYBR Green I binds to the minor groove of double-stranded DNA (dsDNA) emitting 1000-fold greater fluorescence than when it is free in solution (Figure 4A (Wittwer et al., 1997)). Therefore, the greater the amount of dsDNA present in the reaction tube, the greater the amount of DNA binding and fluorescent signal from SYBR Green I. Thus, any amplification of DNA in the reaction tube is measured. Other dsDNA-specific dyes (e.g. BEBO, YOYO-1, TOTO-1, etc.) have also been described but are not as widely used. The primary concern with the usage of any of these sequence-independent dsDNA-binding probes is specificity. To help ensure specificity, the dissociation curve of the amplified product can be analyzed to determine the melting point (**Figure A.3**). If there are two or more peaks, it suggests that more than one amplified sequence was obtained and the amplification was not specific for a single DNA target.

Hydrolysis probes (also called 5' nuclease probes because the 5' exonuclease activity of DNA polymerase cleaves the probe) offer an alternative approach to the

problem of specificity (Figure 4B). These are likely the most widely used fluorogenic probe format (Mackay, 2004) and are exemplified by TaqMan probes. In terms of structure, hydrolysis probes are sequence-specific dually fluorophore-labeled DNA oligonucleotides. One fluorophore is termed the quencher and the other is the reporter. When the quencher and reporter are in close proximity, that is they are both attached to the same short oligonucleotide, the quencher absorbs the signal from the reporter. This is an example of fluorescence resonance energy transfer (FRET; also called Förster transfer) in which energy is transferred from a "donor" (the reporter) to an "acceptor" (the quencher) fluorophore. During amplification the oligonucleotide is broken apart by the action of DNA polymerase (5' nuclease activity) and the reporter and quencher separate, allowing the reporter's energy and fluorescent signal to be liberated. Thus, destruction or hydrolysis of the oligonucleotide results in an increase of reporter signal and corresponds with the specific amplification of DNA. Examples of common quencher fluorophores include TAMRA, DABCYL, and BHQ while reporters are more numerous (e.g. FAM, VIC, NED, etc). Hydrolysis probes afford similar precision as SYBR Green I, (Wilhelm and Pingoud, 2003) but they give greater insurance regarding specificity as only sequence-specific amplification is measured. In addition, hydrolysis probes allow for simple identification of point mutations within the amplicon using melting curve analysis (see "Common Applications for Real-Time PCR" below).

There are several other variations on the reporter-quencher theme including molecular beacons, sunrise primers, and scorpion primers. They each seek to keep the reporter and quencher together prior to amplification, while separating them and

generating fluorescence signal during amplification. Another class, called hybridization probes, uses donor and acceptor fluorophores, while peptide nucleic acids (PNAs) containing thiazole orange fluorophores (called light-up probes) also emit greater signal upon binding of DNA (Svanvik et al., 2000). These do not represent an exhaustive list, as many other specific and non-specific chemistries exist. In addition, new fluorescent chemistries are continually being developed with a focus on increasing sensitivity (by increasing the signal to noise ratio) and specificity, enhancing multiplexing capabilities, and reducing cost.

A.7 THE INSTRUMENTATION OF REAL-TIME PCR

A critical requirement for real-time PCR technology is the ability to detect the fluorescent signal and record the progress of the PCR reaction. Because fluorescent chemistries require both a specific input of energy for excitation and a detection of a particular emission wavelength, the instrumentation must be able to do both simultaneously and at the desired wavelengths. Thus, the chemistries and instrumentation are intimately linked.

At present, there are three basic ways in which real-time instrumentation can supply the excitation energy for fluorophores: by lamp, light emitting diode (LED), or laser (**Figure A.5**). Lamps are classified as broad-spectrum emission devices while LEDs and lasers are narrow-spectrum. Instruments that utilize lamps (tungsten halogen or quartz tungsten halogen) may also include filters to restrict the emitted light to specific excitation wavelengths. Instruments using lamps include Applied Biosystem's ABI

Prism 7000, Stratagene's Mx4000 and Mx3000P, and Bio-Rad's iCycler iQ. LED systems include Roche's LightCycler, Cepheid's SmartCycler, Corbett's Rotor-Gene, and MJ Research's DNA Engine Opticon 2. The ABI Prism 7900HT is the sole machine to use a laser for excitation.

To collect data, the emission energies must also be detected at the appropriate wavelengths. Detectors include charge-coupled device (CCD) cameras, photomultiplier tubes (PMTs), or other types of photodetectors. Narrow wavelength filters or channels are generally employed to allow only the desired wavelength(s) to pass to the photodetector to be measured. Usually multiple discrete wavelengths can be measured at once which allows for multiplexing, i.e. running multiple assays in a single reaction tube.

Another portion of the instrumentation consists of a thermocycler to carry out PCR. Of particular importance for real-time PCR is the ability of the thermocycler to maintain a consistent temperature among all sample wells, as any differences in temperature could lead to different PCR amplification efficiencies. This is accomplished by using a heating block (Peltier-based or resistive), heated air, or a combination of the two. As one might expect, heating blocks generally change temperature more slowly than heated air, resulting in longer thermocycling times. For example, Roche's LightCycler models utilizing heated air can perform 40 cycles in 30 minutes while Applied Biosystem's ABI Prism 7900HT utilizing a Peltier-based heating block takes 1 hour 45 minutes. For further details on real-time PCR instrumentation, resources include "Real Time PCR: An Essential Guide" (Edwards et al., 2004) for a side-by-side

comparison or the respective manufacturer's website for the most up-to-date model information.

Real-time instrumentation certainly would not be complete without appropriate computer hardware and data acquisition and analysis software. Software platforms try to simplify analysis of real-time PCR data by offering graphical output of assay results including amplification and dissociation (melting point) curves (**Figure A.3**). The amplification curve gives data regarding the kinetics of amplification of the target sequence, while the dissociation curve reveals the characteristics of the final amplified product.

A.8 ADVANTAGES AND LIMITATIONS OF REAL-TIME PCR QUANTITATION

There are many methods in molecular biology for measuring quantities of target nucleic acid sequences. However most of these methods exhibit one or more of the following shortcomings; they are time-consuming, labor-intensive, insufficiently sensitive, non-quantitative, require the use of radioactivity, or have a substantial probability of cross contamination (Reischl et al., 2002). These methods include but are not limited to, Northern and Southern hybridizations, HPLC, scintillation proximity assay (SPA), PCR-enzyme-linked immunosorbent assay (PCR-ELISA), RNase protection assay (RPA), *in situ* hybridization, and various gel electrophoresis PCR-endpoint systems.

Real-time PCR has distinct advantages over these earlier methods for several reasons. Perhaps the most important is its ability to quantify nucleic acids over an

extraordinarily wide dynamic range (at least 5 log units). This is coupled to extreme sensitivity allowing for detection of less than 5 copies (perhaps only 1 copy in some cases) of a target sequence, making it possible to analyze small samples like clinical biopsies or miniscule lysates from laser capture microdissection (LCM). With appropriate internal standards and calculations, mean variation coefficients are <1-2%, allowing reproducible analysis of subtle gene expression changes even at low levels of expression (Klein, 2002; Luu-The et al., 2005). In addition, all real-time platforms are relatively quick, with some affording high-throughput automation. Finally, real-time PCR is performed in a closed reaction vessel that requires no post-PCR manipulations, thereby minimizing chances for cross contamination in the laboratory.

However, there are several limitations to real-time PCR methods. The majority of these are present in all PCR or RT-PCR-based techniques. Real-time PCR is susceptible to PCR inhibition by compounds present in certain biological samples. For example, clinical and forensic uses for real-time PCR may be affected by inhibitors found in certain body fluids such as hemoglobin or urea (Wilson, 1997). Food microbiological applications may encounter organic and phenolic inhibitors (Wilson, 1997). To circumvent this problem, alternative DNA polymerases (e.g. Tfl, Pwo, Tth, etc.) which are resistant to particular inhibitors can be used. Other limitations primarily concern real-time PCR-based analysis of gene expression (Bustin, 2000, 2002; Bustin and Nolan, 2004). Because of the necessary use of RNA in an extra enzymatic step, more problems have opportunity to occur. RNA itself is extremely labile as compared to DNA, and therefore isolation must be carefully performed to ensure both the integrity of the RNA

itself and the removal of contaminating nucleases, genomic DNA, and RT or PCR inhibitors. This can be a problem with any sample source, but clinical samples are of special concern as inconsistencies in sample size, collection, storage, and transport can lead to variable quality of RNA templates. Conversion of RNA to cDNA during the RT reaction is also subject to variability because multiple RT enzymes with different characteristics exist, and different classes of oligonucleotides (e.g. random, poly-dT, or gene-specific primers) can be used to prime reverse transcription.

Probably the biggest present limitation of real-time PCR, however, is not inherent in the technology, but rather resides in human error: improper assay development, incorrect data analysis, or unwarranted conclusions. In our experience using real-time PCR for gene expression analysis, real-time PCR primer sets must be designed and validated by stringent criteria to ensure specificity and accuracy of the results (**Figure A.3**). For microbiology, false positives or negatives must be considered when designing an assay to detect pathogens. Amplification and melting curves must be visually inspected while independent calculations based on these curves should be double-checked for accuracy. Real-time PCR gene expression analysis measures mRNA levels and, therefore, only suggests possible changes in protein levels or function rather than demonstrating them. And although there is a tight connection between gene expression and gene product function (Brown and Botstein, 1999), this is certainly not always the case, and formal demonstration may be needed for a given research project. Of course, conclusions based on data derived from real-time PCR are best utilized when the biological context is well understood (Bustin, 2002).

A.9 COMMON APPLICATIONS FOR REAL-TIME PCR

A.9.1 Relative and Absolute Quantitation of Gene Expression

To evaluate gene expression, RNA must first be isolated from the samples to be studied. After isolation, the RNA is linearly converted to cDNA which is used for real-time PCR. Amplification curves are graphed by the software to help determine the "cycle time" at which fluorescence reaches a threshold level (C_T; **Figure A.3**). This C_T value is inversely proportional to the amount of specific nucleic acid sequence in the original sample. Both relative and absolute quantitation of gene expression utilize the C_T value to quantitate cDNA and thereby determine gene expression. In a perfectly efficient PCR reaction, the amount of amplified product doubles each cycle. Therefore, a difference of 1 between sample C_T's means that the sample with the lower C_T value had double the target sequence of the other sample; a change in C_T of 2 means a 4-fold difference; a change in C_T of 3 means an 8-fold difference, and so on ($\Delta C_T = 2^\wedge - \Delta C_T$ fold change).

Relative quantitation measures changes in the steady-state levels of a gene of interest relative to an invariate control gene. Housekeeping genes (e.g. cyclophilin, glyceraldehyde-3-phosphate dehydrogenase (GAPDH), ribosomal protein 36B4, β-actin, 18S ribosomal RNA, transferrin receptor, etc.) (Dheda et al., 2004) that are not expected to change under the experimental conditions serve as a convenient internal standard. Because the absolute quantity of the internal standard is not known, only relative changes can be determined by this method. This may not pose a problem for most research projects because fold-change may be informative irrespective of the absolute value. The

limitations of this approach include lack of absolute quantitation and necessity for unchanging housekeeping genes as internal standards.

Absolute quantitation attempts a more ambitious task to measure the actual nucleic acid copy number in a given sample. This requires a sample of known quantity (copy number) of the gene of interest that can be diluted to generate a standard curve. This is an external "absolute" standard. Unknown samples are compared to the standard curve for absolute quantitation (Kuhne and Oschmann, 2002). The primary limitation to this approach is the necessity of obtaining an independent reliable standard for each gene to be analyzed then running concurrent standard curves during each assay.

A.9.2 Validation of DNA Microarray Results

Because of the reliability of real-time PCR, many researchers use the above relative or absolute quantitation of gene expression to validate and corroborate the results of printed DNA microarrays or oligonucleotide arrays (e.g. Affymetrix GeneChip). Arrays are used because they allow a researcher to look in an "unbiased" fashion at how experimental manipulation might affect any of the thousands of genes present on the array. Some arrays purport to contain the entire "genome" of a model organism and thus can theoretically be probed to comprehensively determine changes in expression within the entire "transcriptome." The problem is that there can be artifacts, and it is often difficult to get reliable quantitative data or adequate statistical power with present array technology. Thus, many researchers choose real-time PCR as a supporting technique to validate and better quantitate the most interesting candidate genes from their arrays.

A.9.3 Counting Bacterial, Viral, or Fungal Loads

Real-time PCR can distinguish specific sequences from a complex mixture of DNA. Because of this, it is useful for determining the presence and quantity of pathogen-specific or other unique sequences within a sample.

A.9.4 Identification of Mutations (or SNPs) by Melting Curve Analysis

Real-time PCR is ideally suited for analysis of mutations, including single nucleotide polymorphisms (SNPs), often replacing other techniques such as sequencing, single strand conformation polymorphism (SSCP) assays, and restriction fragment length polymorphism (RFLP) analysis (Edwards et al., 2004). To detect mutations in the sequence, melting curve analysis is automatically done on the amplified product (amplicon) immediately after PCR thermocycling and fluorescence is measured. Although any of the above described fluorescent chemistries will work for detection of mutations, hybridization probes are often used. After PCR is complete, the hybridization probes are attached to the amplicon in tandem, allowing energy to transfer from the donor to acceptor fluorophore which emits a signal. As the temperature of the reaction vessel increases during the melting curve analysis, the donor probe will dissociate, resulting in a decrease of fluorescence. If there are any mutations in the amplicon (in the hybridization region), the donor probe will bind less strongly and dissociate at a lower temperature. Thus, mutations can easily be detected by observing a shift in the melting point of the PCR product. This type of analysis can also be used for genotyping individuals or experimental organisms (i.e. allelic discrimination).

A.10 FIELDS OF REAL-TIME PCR APPLICATION

Because of the power of real-time PCR applications, it is already used in many different fields within biomedical research and molecular diagnostics.

A.10.1 Biomedical Research

Real-time PCR has become quite commonplace in basic research within the biomedical sciences. Any time gene expression data is desired for a particular research project, real-time PCR is likely to be used. Therefore, real-time PCR has impacted a wide variety of topics of study, and the examples of gene expression analyses are innumerable. However, there are additional applications that are particularly useful to basic research. Real-time PCR can be used for genotyping knock-out, knock-in, and transgenic mouse models or for determining efficacy of gene knockdown and delivery methods in animals or cell culture systems. Using real-time PCR's capability of allelic discrimination, detection of single nucleotide polymorphisms (SNPs) that may predispose individuals to particular diseases can be determined in populations, thereby facilitating epidemiological studies.

A.10.2 Molecular Diagnostics

Clinical microbiology diagnostic laboratories can use real-time PCR to detect changes in viral load. Because viral load and disease severity are related, real-time PCR can measure disease progression and efficacy of antiviral therapies. Mutation analyses using melting curves enable individual and epidemiological studies of viral co-infections or quasispecies (Mackay et al., 2002).

Real-time PCR most notably benefits patients when used to detect and identify bacteria (Mackay, 2004). Quick and early detection allows the clinician to immediately prescribe better targeted antibiotic therapies and could in the long-term help reduce the use of broad-spectrum antibiotics which may encourage emergence of antibiotic-resistant strains. Real-time PCR has been used to detect *Mycobacterium tuberculosis*, *Legionella pneumophila*, *Listeria monocytogenes*, and *Neisseria gonorrhoeae* (Ballard et al., 2000; Cleary et al., 2003; Lunge et al., 2002; Whiley et al., 2002). Mutation (melting curve) analysis has been able to monitor antibiotic resistance among *Staphylococcus aureus*, *S. epidermidis*, *Helicobacter pylori*, *Enterococcus faecalis*, and *E. faecium* (Gibson et al., 1999; Martineau et al., 2000; Woodford et al., 2002). This technology has been extended to quickly detect spores of *Bacillus anthracis*, the well-known causative agent of anthrax and potential weapon of biological warfare (Makino et al., 2001).

Real-time PCR is revolutionizing microbiological diagnostics because of the sensitivity of detection and specificity for determination of variants. In addition, there may be substantial time and cost savings over traditional culture methods for determining the quantity of a given pathogen in a clinical specimen. In fact, the Mayo Clinical Microbiology Laboratory has decreased the analytical turnaround time for 6 different pathogens from a range of 1-14 days by traditional methods to 30-50 minutes using real-time PCR and has obtained these results with similar or better sensitivities (Reischl et al., 2002). Of course, there are limitations. Real-time PCR will measure DNA from both live and dead pathogens while traditional culture methods focus on measuring live pathogens

(Hein et al., 2001). Accordingly, assays for particular pathogens must be responsibly designed and strictly evaluated before conclusions can be made (Klein, 2002).

The ability to identify specific DNA sequences is also critical in clinical oncology. For example, real-time PCR can be used to detect and sometimes quantify chromosomal translocations or their fusion gene transcripts present in a patient sample for use in determination of minimum residual disease (MRD) or disease progression. This technique has been used to detect MRD in patients by measuring the AML-1/MTG8 fusion gene product of acute myeloblastic leukemia (Krauter et al., 2001); several gene product rearrangements of acute lymphoblastic leukemia (Pongers-Willemse et al., 1998); or patient response to interferon-α treatment by measuring the BCR-ABL fusion gene product of chronic myeloid leukemia (Barthe et al., 2001). Real-time PCR can also be used to determine DNA copy number which can lead to malignancy (Ginzinger et al., 2000), or be used to analyze gene expression in solid tumors using very small specimens like fine-needle aspirates (Ohnmacht et al., 2001). Such sensitive and precise detection may prove useful not just for better understanding of cancer and tumor biology but also for determining more efficacious therapeutic strategies and better stratification of a patient's risk for recurrence of disease.

Real-time PCR can be used to aid drug discovery and characterization by determining the kinetics of target gene expression in response to drugs and the response of transporters or metabolizing enzymes which facilitate distribution or disposal (Brazeau, 2004).

A.11 FUTURE APPLICATIONS AND PERSPECTIVES

Any need for fast and precise measurement of small amounts of nucleic acids represents a potential future niche for real-time PCR-based innovations. As machines become faster, cheaper, smaller, and easier to use through competition, standardized assay development, and advances in microfluidics (Mitchell, 2001), optics, and thermocycling, more in-field application needs are likely to be filled. In the commercial food industry and agriculture, real-time PCR will likely see expanded use for detection and identification of microbes, parasites, or genetically modified organisms (GMOs). Forensics will benefit from real-time PCR's sensitivity, specificity, and speed, especially because time is crucial to many criminal investigations and specimen size may be limiting. Reduced cost and increased portability open the door for diagnosis of diseases in remote areas along with on-site epidemiological studies and may facilitate the transfer of needed scientific technologies to developing countries, thereby contributing to their "scientific capacity" (Harris, 2004). Since the demand to measure gene expression is unlikely to wane as long as biomedical science is thriving, new generations of real-time PCR machines are likely to be developed. Much like computers, earlier generations of machines should be relatively inexpensive and therefore increase global access to the technology. Hopefully, this technology will enter the classroom to enable life science educators to better equip students and encourage them to consider careers in science. Teaching real-time PCR could be used both as a platform to introduce key concepts in molecular biology as well as a chance to give students confidence by successfully learning and implementing scientifically relevant skills. This would be a great way to

increase hands-on learning, which may be a key component to improving biology education in the United States (Stokstad, 2001).

Real-time PCR generates a focused look at the "transcriptome," enabling researchers to better understand the transcriptional programs that underlie physiology, pathophysiology, and development. Understanding gene expression narrows the gap in our knowledge between the "instructions" (the genome) and the "functions" (gene products) of biology. The evolution of the science and technology of molecular biology can be viewed chronologically as epochs hallmarked by the maturation of study of particular biomolecules. Extensive, and in some ways comprehensive, analysis of DNA (genomics) was first realized in the Human Genome Project. Now analysis of RNA expression profiles (transcriptomics) is reaching maturity. The imminent future promises great leaps forward in the analysis of proteins (proteomics), whose technology is the most rapidly growing, and in the analysis of biological lipids or metabolic intermediates (lipomics or metabolomics, respectively). Hopefully, the pieces of the biomolecular puzzle can be put together, leading to a more holistic understanding of biology. To form a coherent picture, however, parallel advances in data acquisition, compilation, and analysis will be necessary to help deal with the enormity of data. The promise of such extensive knowledge of biological systems is staggering, but will certainly require dedicated individuals in all biomedical fields to figure out how best to utilize the new technologies and the information produced by them.

A.12 AN EXAMPLE OF REAL-TIME PCR FOR RELATIVE QUANTITATION OF GENE EXPRESSION: ACTIVATION OF PPARα ENHANCES EXPRESSION OF ADIPONECTIN RECEPTORS IN LIVER

The superfamily of nuclear receptors include ligand-activated transcription factors which can respond to hormonal or metabolic ligands. Since these proteins regulate the transcription of target genes and thereby change mRNA levels, their activities are particularly amenable to study by the methodology of real-time RT-PCR.

The peroxisome-proliferator activated receptors (PPARs) α, β (δ), and γ are members of the nuclear receptor superfamily and known to be activated by endogenous saturated and unsaturated long-chain fatty acids, eicosanoids, and prostaglandins. In addition, two classes of antidiabetic agents are known to bind PPARs: fibrates (e.g. fenofibrate, known clinically as Lofibra or Tricor) bind PPARα, while the thiazolidinediones (TZDs; e.g. rosiglitazone, known clinically as Avandia) bind PPARγ. The binding of these drugs activates the respective transcription factor to enhance transcription of target genes and effect a physiological response.

Since PPARα activation favors fatty acid oxidation in tissues (esp. liver and heart), it may enhance insulin sensitivity by reducing intracellular fatty acid accumulation. PPARγ activation favors storage of lipids in adipose tissue, thereby protecting the rest of the body from lipid overload and insulin resistance (Ferre, 2004). Activation of PPARs may also enhance insulin sensitivity in other ways. For example, PPARγ is known to upregulate adiponectin (Brand et al., 2003; Ye et al., 2003). Adiponectin is considered to be an "adipocytokine" as it is made exclusively by adipose

tissue then secreted into circulation. Plasma adiponectin levels appear to be inversely correlated with obesity and insulin resistance. Adiponectin action on tissues became better understood when two receptors for adiponectin were recently identified (Yamauchi et al., 2003). Adiponectin receptor 1 (AdipoR1) is expressed ubiquitously but most highly in skeletal muscle, whereas AdipoR2 is primarily expressed in liver (Yamauchi et al., 2003). Since the adiponectin system is already implicated in enhancing insulin sensitivity, we wanted to know if insulin sensitization by PPARs could in part be due to their potential effects on adiponectin receptor expression.

In these experiments, we sought to determine the impact of various nuclear receptor agonists (drugs) and a gene knockout (genes) on the expression of adiponectin receptors in liver. First, mice were fed standard chow supplemented with 30mpk LG268 (RXR), 0.5%(w/w) fenofibrate (PPARα), 150mpk troglitazone (PPARγ), 0.05%(w/w) prenenolone-16α-carbonitrile (PXR), 3mpk TCPOBOP (CAR), 0.5%(w/w) chenodeoxycholic acid (FXR), 50mpk T1317 (LXR), or 30mpk LG268 + 50mpk T1317 (RXR+LXR) for 12 hours. Second, both wild-type and PPARα-knockout mice were fed a standard chow with or without 0.5% (w/w) fenofibrate for 7 days. Tissues were harvested, RNA extracted, and real-time PCR performed to determine relative abundance of mRNA (Kurrasch et al., 2004) and calculations were done using the comparative C_T method (User Bulletin No. 2, Perkin Elmer Life Sciences). Shown in **Figure A.6** is data procured by analyzing expression in individual livers (triplicate measurement) in each group (n=3-4) and expressed as mean +/- SEM. Thus, the standard error reflects biological variation in addition to measurement variation. In the first experiment,

AdipoR1 mRNA levels were mildly increased by activation of RXR and PPARα (1.34+/-0.15 and 1.70+/-0.12 fold) as were AdipoR2 mRNA levels (1.70+/-0.07 and 2.31+/-0.24). Notably, the PPARγ agonist had no effect. In the second experiment, AdipoR1 and AdipoR2 mRNA expression are increased 1.91+/-0.05 and 3.28+/-0.10 fold, respectively, in wild-type animals treated with fenofibrate. No increase was observed for either gene in treated PPARα-knockout animals. Similar results were observed in livers of mice treated with another PPARα agonist, GW7647, by oral gavage (2 doses of 5mpk over 14 hours; data not shown, (Lander et al., 2001)).

These results demonstrate that fenofibrate enhances adiponectin receptor expression in liver by a PPARα-dependent mechanism and suggest that fenofibrate may enhance insulin sensitivity by increasing adiponectin action on liver. Further investigation is needed to determine if PPARα is acting directly on the promoters of AdipoR1 and AdipoR2 genes in liver cells or indirectly by some other means (e.g. changes in metabolism). Also, this result is consistent with the therapeutic potential of PPARα/γ dual agonists (Brand et al., 2003; Ye et al., 2003).

This example is a testimony to the power of real-time PCR in elucidating molecular events that underlie physiology. By applying a single methodology, that of real-time PCR, to a drug-treated mouse knockout model, we were able to gain insight into novel molecular mechanisms potentially involved in insulin sensitization. Obviously, the ability to precisely detect relative changes in gene expression is a valuable tool for studying any number of physiological, pathophysiological, and developmental models.

Thus, real-time PCR can be a powerful first step in many biomedical research projects and programs.

A.13 ACKNOWLEDGEMENTS
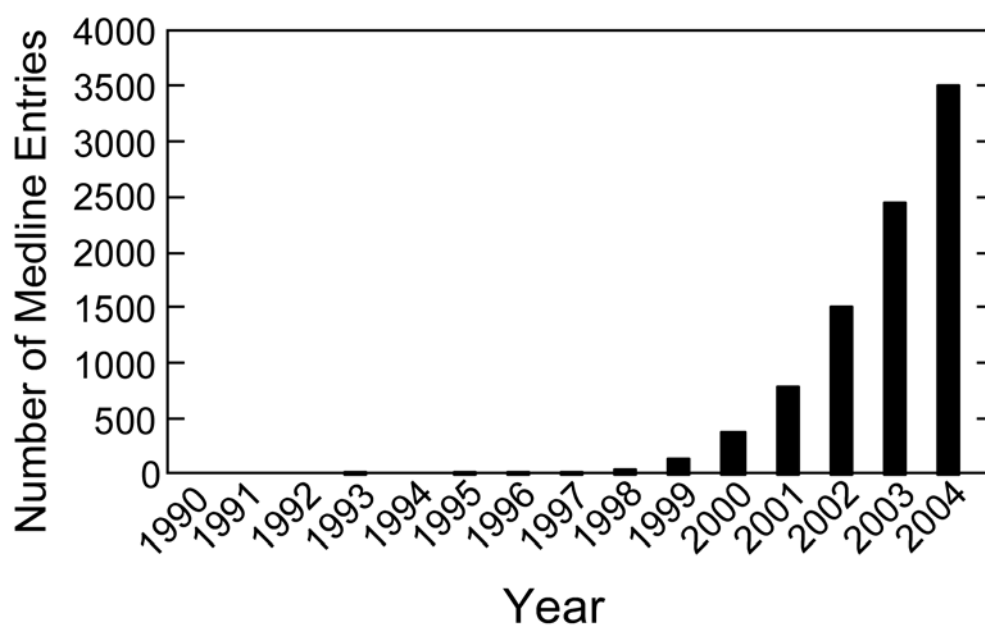
Figure A.1 The growing use of real-time PCR. The number of publications in the Medline database that contain the words "real-time" and "PCR" or "real-time" and "polymerase chain reaction" in their title or abstract for the years 1990 to 2004.
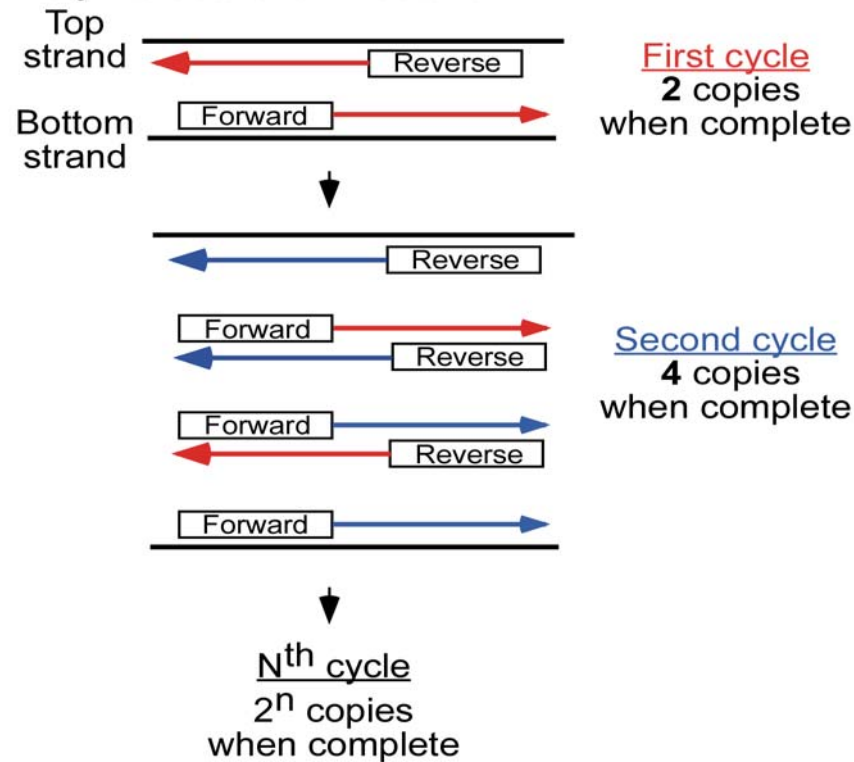
A. Polymerase chain reaction

B. Reverse transcription (RNA ➤ ssDNA)
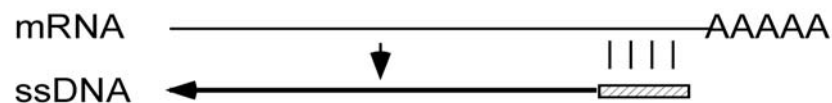
Figure A.2 The enzyme reactions that make real-time PCR possible. *A*, The polymerase chain reaction is depicted. High temperatures are used to "melt" dsDNA into its top and bottom strands. This mixture is cooled in the presence of sequence-specific primers (denoted as forward and reverse) that anneal to their targets, and an optimal temperature is then applied to allow elongation of complementary DNA (arrows) by the action of DNA polymerase to complete a cycle. This is repeated numerous times and, if no reagents are limiting, 2n copies of the desired DNA fragment can be obtained. *B*, As DNA polymerase does not utilize RNA as a template, the conversion of RNA to DNA can be achieved using the enzyme reverse-transcriptase.
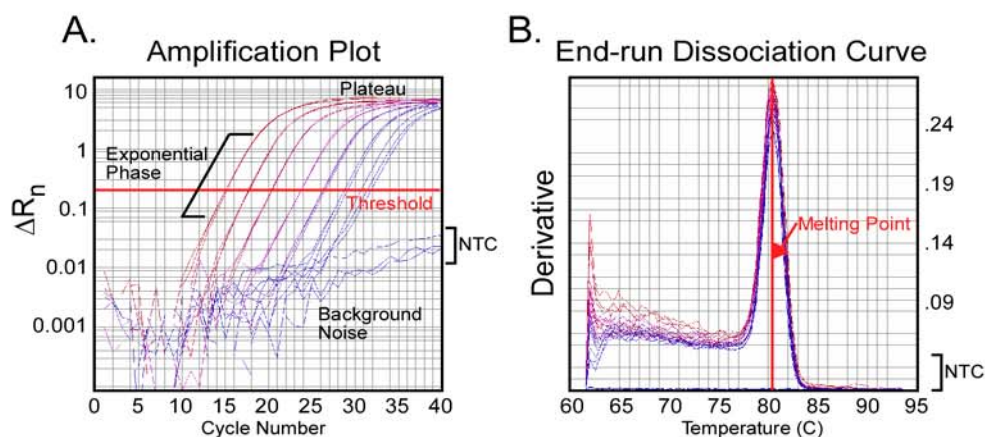
Figure A.3 Typical real-time PCR results. *A*, The amplification plot illustrates the increase in fluorescent reporter signal (Y-axis, note the log scale) with each PCR cycle (X-axis). The Y-axis units, DRn, actually reflect reporter signal normalized to a passive reference dye in the reaction buffer. The curves seen with a no-template control (NTC) that lacks added DNA, show that the primers alone do not generate a signal, and that the reagents used in this assay showed no DNA contamination. *B*, The dissociation curve for this analysis shows a single, sharp peak suggesting that only a specific PCR product was generated with this set of primers.

A. SYBR Green I

520
480
520
480

B. Taqman probe

Q
R
R
Q
Taq
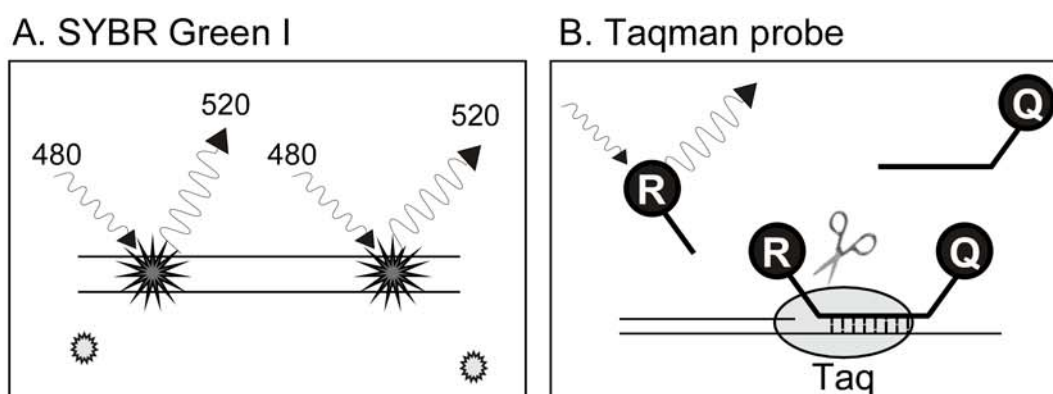
Figure A.4 Real-time PCR chemistries. *A*, SYBR Green I fluoresces (absorbing light of 480 nm wavelength and emitting light of 520 nm) when associated with dsDNA. *B*, Other detection formats often utilize compatible fluorphores. Shown in this example is the Taqman probe, which contains a reporter fluorophore (R) that emits at a wavelength absorbed by the quencher fluorophore (Q). During PCR amplification, the DNA polymerase (Taq) cleaves the probe thus liberating the reporter from the quencher and allowing for measurable fluorescence.
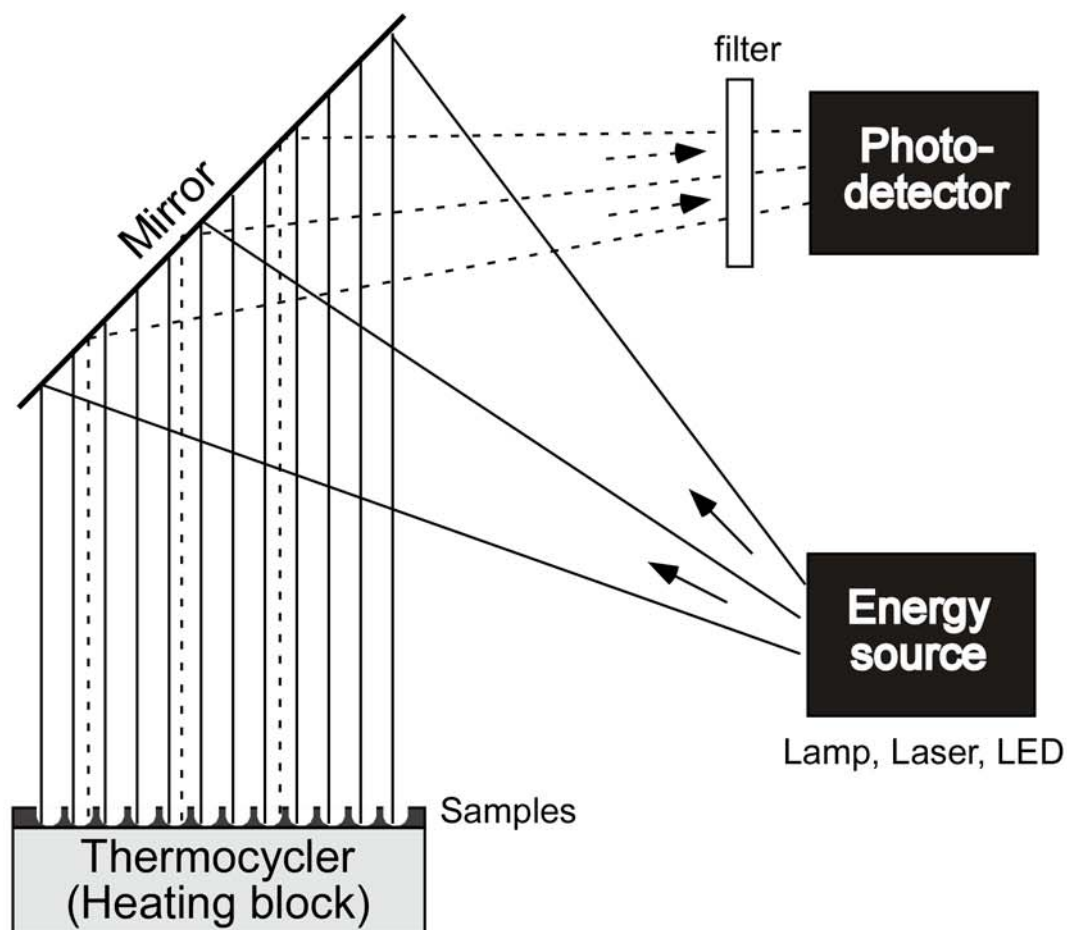
Figure A.5 Real-time PCR hardware. Samples are placed in a thermocycler which controls temperatures required for each cycle of PCR. The samples are exposed to excitation energy and the resulting fluorescence is measured by a photodetector with each cycle.
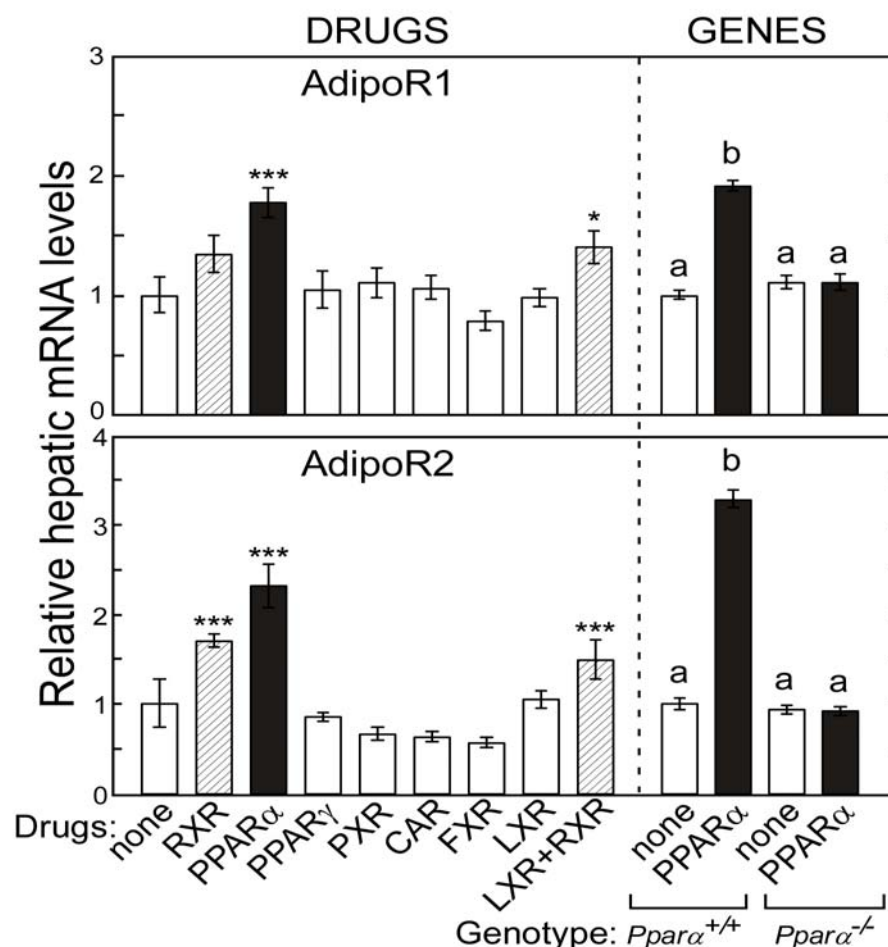
Figure A.6 An example of real-time PCR analysis. Mice received drugs that specifically activate various nuclear hormone receptors (listed on the X-axis). Liver RNA was prepared and the RNA levels for the adiponectin receptors, AdipoR1 and AdipoR2, were measured using an ABI Prism 7900HT system, the SYBR Green I method, and target-specific primers: AdipoR1-forward: 5'cagtgggaccggtttgc and AdipoR1-reverse: 5'aagccaagtcccaggaacac; AdipoR2-forward: 5'aacgaatggaagagtttgtttgtaa and AdipoR2-reverse: 5'gtagcacatcgtgagggatca. Full details of the method can be found in (25) and cyclophilin was used as the invariate housekeeping gene. In the left panel it is revealed that only PPARα (black bars) and it dimeric partner RXR (hatched bars) elicit an increase in hepatic AdipoR1 and R2 mRNA levels when compared to the control group (*p<0.05, ***p<0.001). In the right panel, the importance of PPARα is highlighted, since in mice lacking this nuclear hormone receptor (*Pparα-/-*) the fibrate drug fails to work. (By ANOVA, groups sharing a common letter designation are not different).

APPENDIX B

CELF6 Gene Expression is Regulated by Retinoid X Receptor in Mouse Small Intestine

B.1 ABSTRACT

CUG-binding protein and embryonic lethal abnormal vision-type RNA-binding protein 3-like factor 6 (CELF6) and other CELF family members have previously been shown to regulate exon inclusion via muscle-specific splicing enhancers (MSEs) in minigene studies. In contrast, little is known about the regulation of CELF6 gene expression itself. Here, we confirm that CELF6 mRNA is highly expressed in brain, but also expressed at lower levels in other tissues. We show that steady-state levels of CELF6 mRNA are dose-dependently enhanced (more than 10-fold) in mouse small intestine by administration of LG268, a selective retinoid X receptor (RXR) agonist, whereas agonists for other nuclear receptors do not recapitulate this effect. LG268 retains the ability to induce intestinal CELF6 expression in mice lacking farnesoid X receptor (FXR) and liver X receptors (LXRs). Thus, CELF6 gene expression can be modulated by selective activation of a member of the nuclear receptor superfamily, RXR.

B.2 INTRODUCTION

Although it was expected that the human genome might contain as many as 150,000 genes, largely based on the number of expressed-sequence clusters (mRNAs), the actual number of genes is probably closer to 32,000 (Lander et al., 2001; Venter et al., 2001). The difference is likely explained by the prevalence of alternative splicing of

mRNA and the generation of multiple protein isoforms from a single gene. In fact, as much as 40%-60% of genes are believed to be alternatively spliced, leading to the large diversity of the human proteome (Modrek and Lee, 2002; Roberts and Smith, 2002).

Pre-mRNA splicing is an essential step in the expression of most genes containing intronic sequences. Although introns are transcribed into the pre-mRNA, they must first be removed to allow the translation of mRNA. Splicing is regulated by conserved sequences at the intron-exon borders and is facilitated by a variety of RNA and protein splicing factors. Because pre-mRNAs typically contain multiple introns, exons can be joined in a variety of ways to create protein diversity from a single gene. The importance of regulated splicing is evident in cases where alterations in authentic protein isoforms are associated with disease (Li et al., 2001a; Musunuru, 2003; Sironi et al., 2003). For example, alternative splicing plays in the etiology of insulin resistance associated with myotonic dystrophy. In patients with myotonic dystrophy there is an expansion of CUG repeats in myocytes and the expression of CUG-binding protein (CUG-BP) is also increased (Philips et al., 1998). The increased expression of CUG-BP is thought to contribute to alternative splicing of the insulin receptor leading to the production of an insulin insensitive receptor splice variant that lacks exon 11 (Savkur et al., 2001; Savkur et al., 2004).

Although a large number of genes that undergo alternative splicing are known, relatively few *cis*- and *trans*-acting factors involved in this process have been identified. Furthermore, characterization of the target mRNAs of *trans*-acting factors is in its infancy. Alternative splicing occurs constitutively, but also appears to occur in a tissue-

and cell-specific manner, suggesting regulated expression of splicing proteins results in the formation of multiple protein isoforms with potentially different biological functions.

A super-family of RNA binding proteins (RBP) has been defined containing a conserved domain known as the RNA recognition motif (RRM). The RRM is composed of a 80-90 amino acid domain that contains two highly conserved sequences termed the ribonucleoprotein 1 (RNP1) and RNP2 motifs that have been shown to specifically interact with RNA (Kenan et al., 1991). CUG-BP, a member of the RBP superfamily, is also a member of a conserved family of proteins known the CELF (CUG-BP and ETR-3 Like Factor) family of RNA binding proteins. CELF proteins have roles in modulating alternative splicing, RNA editing, and mRNA translation (Gromak et al., 2003; Mukhopadhyay et al., 2003; Singh et al., 2004; Timchenko et al., 1999). The human genome contains six CELF paralogs. Based on phylogenetic analysis, CELF proteins belong to one of two subfamilies: one containing CUG-BP and ETR-3 and the other containing CELF3, 4, 5, and 6 (Ladd et al., 2004). Members of the CELF family are themselves alternatively spliced to produce multiple protein isoforms (Good et al., 2000; Ladd et al., 2001).

The expression of CELF mRNA varies considerably. CUG-BP and CELF4 are widely expressed, whereas CELF3 and CELF5 are expressed primarily in the brain. Based on an RNA dot blot, CELF6 is expressed in the brain, kidney, and testis, but also found at lower levels in other tissues such as the intestine, spleen, and thymus (Ladd et al., 2004).

The binding sequences responsible for targeting pre-mRNAs for alternative splicing by CUG-BP and ETR3 are usually U/G-rich motifs located within introns in the vicinity of intron/exon junctions (Gromak et al., 2003; Suzuki et al., 2002). Furthermore, all CELF family members can promote alternative splicing from these U/G-rich motifs. ETR-3 can also bind AU-rich sequences and, in the case of apolipoprotein B, inhibit the post-transcriptional C$\rightarrow$U editing normally present in the small intestine that generates a truncated protein involved in lipid absorption (Anant et al., 2001).

CELF proteins have been detected in both the nucleus and cytoplasm, suggesting that subcellular localization may influence protein function and/or activity. In the nucleus, the protein is likely involved in pre-mRNA splicing, or perhaps RNA editing (Anant et al., 2001). CELF proteins are also found in the cytoplasm and likely play a role in the regulation of translation and mRNA stability (Ladd and Cooper, 2004).

The retinoid X receptors (RXRα, RXRβ, and RXRγ) are members of the nuclear hormone receptor superfamily of transcription factors (Mangelsdorf and Evans, 1995). They are often referred to as "master regulators", as they are required as heterodimeric partners for a large subgroup of the receptor superfamily (i.e., with PPARs, LXRs, FXR, PXR, CAR, TR, VDR, RAR, NGFIB, and NURR1, (Chawla et al., 2001)). RXRs have also been shown to function as homodimers in cell-based systems, although the role of RXR homodimers *in vivo* remains controversial. RXRs are soluble receptor proteins containing a central DNA-binding domain and a carboxy-terminal ligand-binding domain. It is generally accepted that the RXRs reside in the nucleus of cells, associated with specific enhancer elements in the vicinity of their target genes. In the absence of

ligand, RXRs associate with co-repressors that maintain neighboring target genes in the "off" position. Upon binding ligand, RXRs undergo a conformational change thereby releasing associated corepressor proteins and recruiting coactivators that allow the receptor to communicate with the general transcription machinery to regulate target gene expression.

Little is known about factors controlling the tissue-specific expression of CELF family members. In particular, it is not known what factors influence the tissue-specific expression of CELF6, and in what tissues CELF6 may be expressed or regulated. Here, we have identified that RXR is a regulator of CELF6 gene expression in the adult mouse intestine.

B.3 MATERIALS AND METHODS

B.3.1 Animal Experiments

FXR and LXRα/β knockout mice were generated as previously described (Peet et al., 1998; Repa et al., 2000c; Sinal et al., 2000). Mice were maintained on a cereal-based rodent diet (Teklad Diet #7001, Madison, WI) that contains 0.02% (w/w) cholesterol and 4% total lipid, unless otherwise noted. For some experiments, mice were fed the powdered form of this diet with or without supplementation of various nuclear receptor agonists, including: 30 mg/kg/day LG268 [retinoid X receptor (RXR)], 0.5% (wt/wt) fenofibrate (PPAR-α), 150 mg/kg/day troglitazone (PPAR-γ), 0.05% (wt/wt) prenenolone-16α-carbonitrile [pregnane X receptor (PXR)], 3 mg/kg/day TCPOBOP (constitutive androstane receptor), 0.5% (wt/wt) chenodeoxycholic acid (farnesoid X

receptor), 50 mg/kg/day T1317 [liver X receptor (LXR)], or 30 mg/kg/day LG268 + 50 mg/kg/day T1317 (RXR+LXR). The calculated quantities of dietary drug supplement assume a food consumption rate of 160 g of diet/day/kg body weight. Other agonists were administered by oral gavage as a suspension in 1% methylcellulose 1% Tween-80 and dosed twice over 14h. These include: 5 mg/kg GW0742 (PPARβ/δ), 1 mg/kg triiodothyronine (T_3) [thyroid hormone receptor (TR)], 50μg/kg 4-[(E)-2-(5,6,7,8-tetrahydro-5,5,8,8-tetramethyl-2-naphthalenyl)-1-propenyl] benzoic acid (TTNPB) [retinoic acid receptor (RAR)], and 75 μg/kg 1α,25-dihydroxyvitamin D_3 [vitamin D receptor (VDR)]. Mice were housed in a temperature-controlled environment with 12 hour light/dark cycles with free access to food and water. Tissues were harvested at the end of the dark cycle, thus mice were in a fed-state at the time of study. Experiments were approved by the Institutional Animal Care and Use Committee of the University of Texas Southwestern Medical Center at Dallas.

B.3.2 Islet Isolation and Culture

Pancreatic islets were isolated as previously described (Lacy and Kostianovsky, 1967; Scharp et al., 1973). Mouse cell lines, βTC6 and αTC1, were purchased from American Type Culture Collection and maintained according to their recommendations. Briefly, βTC6 were maintained in Dulbecco's Modified Eagle's Medium (DMEM) containing 4mM L-glutamine, 4.5g/L glucose, 1.5g/L sodium bicarbonate, 1mM sodium pyruvate, and supplemented with 15% heat-inactivated fetal bovine serum (FBS), and were subcultivated 1:4 every two or three days with renewal of media. αTC1 cells were maintained in DMEM containing 4mM L-glutamine, 3g/L glucose, 1.5g/L sodium

bicarbonate, 15mM HEPES, 0.1mM non-essential amino acids, 0.02% bovine serum albumin, and supplemented with 10% FBS, and similarly subcultivated.

B.3.3 Preparation of Samples for RNA Isolation

Mice were anesthetized and exsanguinated via the descending vena cava. Various tissues were harvested then immediately frozen in liquid nitrogen then stored at -85 °C. For small intestine, the entire length was removed, cut into three sections of equal length (the proximal third denoted as duodenum, middle third as jejunum, and distal third as ileum), then flushed with ice-cold phosphate-buffered saline. The sections were slit lengthwise, and the mucosae were gently scraped, then frozen in liquid nitrogen and stored. Total RNA was isolated from tissue samples by homogenization in RNA STAT-60 (Tel-Test Inc.) followed by manufacturer's extraction protocol. RNA concentrations were determined by absorbance at 260 nm.

B.3.4 RNA Measurement

B.3.4.1 Northern Analysis

Equal quantities of total RNA from the samples of each group were pooled, and poly(A)+ RNA was purified using oligo(dT)-cellulose columns (Pharmacia Biotech). mRNA (5 μg/lane) was size fractionated on a 1% formaldehyde-agarose gel and transferred to nylon membrane (Zetaprobe, Bio-Rad) for probing with ^{32}P-labeled cDNA for CELF6 (nt 2034-2334, Genbank accession no. ***NM_175235***).

B.3.4.2 Quantitiative Real Time PCR

Quantitiative real time (qRT)-PCR was performed using an Applied Biosystems Prism 7900HT sequence detection system as described (Kurrasch et al., 2004; Valasek and Repa, 2005). Briefly, total RNA was treated with DNase I (RNase-free, Roche Molecular Biochemicals), and reverse-transcribed with random hexamers using SuperScript II (Invitrogen) to generate cDNA. Primers for each gene were designed using Primer Express Software (PerkinElmer Life Sciences) and validated by analysis of template titration and dissociation curves. Primer sequences are available upon request. Each qRT-PCR contained (final volume of 10 µl) 25 ng of reverse-transcribed RNA, each primer at 150 nM, and 5 µl of 2X SYBR Green PCR Master Mix (Applied Biosystems), and each sample was analyzed in triplicate. Results were evaluated by the comparative C_T method (User Bulletin No. 2, PerkinElmer Life Sciences) using cyclophilin as the invariant control gene. Two qPCR primer sets for CELF6 and one for CUGBP1 were designed and validated [26]:(CELF6-1, forward 5'-gctctgcctcaacaacaaagag-3' and reverse 5'-tcctgaggcaggtgatagatga-3'; CELF6-2: forward 5'-atctttcctatgcaagcgtgtct-3' and reverse 5'-cacacaccacttctaagctgaaca-3'; CUGBP1, forward 5'-gcaatgcaccaagcacaaa-3' and reverse 5'-ggtgtcggcaaactttacca-3'). Both CELF6 sets were found to give similar results. In addition northern blots gave similar pattern as CELF6 qPCR in a control experiment (data not shown). RNA levels are expressed relative to those obtained for the wild-type mice fed the basal diet and reflect the average ± S.E. for *n* = 4-6 animals per group.

B.3.4.3 In Situ Hybridization

Segments of jejunum (13-18 cm from pyloric sphincter) were harvested and fixed overnight in 4% paraformaldehyde. Segments were paraffin-embedded, sectioned, then *in situ* hybridization was performed by using ^{35}S-labeled sense and antisense riboprobes against CELF6 (nucleotides 42-1424; GenBank Accession #NM_175235). Slides were exposed at 4°C for 6 weeks. Sections hybridized with the sense probe gave no signal above background.

B.3.5 Statistical Analysis of Data

Data are reported as the mean ± S.E.M. for the specified number of animals. GraphPad Prism 4 or InStat 3 software (GraphPad, San Diego, CA) was used to perform all statistical analyses. If unequal standard deviations between groups were indicated by Bartlett's test, log transformation was performed prior to statistical analysis. One-way analysis of variance (ANOVA) was used along with appropriate post-hoc tests as described in the figure legends. Different letters indicate statistically different groups. Asterisks represent the following statistical differences: $^{*}, p < 0.05$; $^{**}, p < 0.01$; $^{***}, p < 0.001$.

B.4 RESULTS AND DISCUSSION

To confirm previous data suggesting that CELF6 is abundantly expressed in the brain (Ladd et al., 2004), we measured relative expression of CELF6 mRNA by quantitative real-time PCR (qPCR) analysis in a panel of tissues harvested from 3 month old male A129/SvJ mice in a fed state (Figure B.1A). Indeed, CELF6 was most highly

expressed in hypothalamus and whole brain (C_T=23.2 and 25.5, respectively), but was also expressed in pancreatic islets, and to a lesser degree, the small intestine (duodenum, jejunum, and ileum), colon, and adrenal gland (C_T from 29-31). Residual expression was also noted in heart. Similar expression as heart was observed for lung, spleen, kidney, skeletal muscle (quadriceps), white and brown adipose tissue, and peritoneal macrophages, while no signal was detected for liver (data not shown). Because of the abundant expression in isolated islets, we wanted to gain insight into the cell type which might be expressing this gene, and therefore tested expression in mouse pancreatic alpha-cell and beta-cell lines. As shown in Figure B.1A, both the α- and β-cell lines express CELF6 mRNA suggesting that this may be the case *in vivo* as well. To corroborate our qPCR results, we performed *in situ* hybridization on brain and intestine. Coronal sections of wild-type mouse brain hybridized with antisense riboprobes directed at CELF6 mRNA displayed clearly enhanced expression in the dentate gyrus (dg), hippocampus (hc), and habenulae (hn), with lower levels of expression in other regions including the hypothalamus (Figure B.1B, data not shown). In contrast, no signal was observed in jejunum with the same riboprobe and exposure time utilized for brain sections (data not shown). This difference in detection is likely due to the greater sensitivity of qPCR as compared to in situ hybridization. Thus, CELF6 mRNA is differentially expressed in tissues (Ladd et al., 2004).

To determine if nuclear receptors could acutely regulate expression of CELF6, we treated mice for 12 h with various nuclear receptor agonists supplemented in a basal diet. The nuclear receptor agonists included: 30 mg/kg LG268 [retinoid X receptor (RXR)],

0.5% (wt/wt) fenofibrate (PPAR-α), 150 mg/kg troglitazone (PPAR-γ), 0.05% (wt/wt) prenenolone-16α-carbonitrile [pregnane X receptor (PXR)], 3 mg/kg TCPOBOP (constitutive androstane receptor), 0.5% (wt/wt) chenodeoxycholic acid (farnesoid X receptor), 50 mg/kg T1317 [liver X receptor (LXR)], or 30 mg/kg LG268 + 50 mg/kg T1317 (RXR+LXR). After tissue harvesting, RNA was isolated from both a high-expressing (i.e. whole brain) and a low-expressing tissue (i.e. duodenum), and CELF6 mRNA expression was assessed by qPCR. CELF6 mRNA was not significantly altered in whole brain by any of the agonists tested (Figure B.2C). Suprisingly, CELF6 mRNA was robustly induced in duodenum (~7 fold) in mice treated with an RXR-specific agonist, LG268, by itself, or in combination with an LXR agonist, T1317 (Figure B.2A). Since the LXR agonist alone did not statistically effect the expression of CELF6 mRNA as compared to vehicle-treated controls, we conclude that the induction of CELF6 is due to the specific activation of RXR. Because RXR is known to promiscuously heterodimerize with a subset of nuclear receptors to transactivate target genes (Mangelsdorf and Evans, 1995), we expected one of the other nuclear receptor agonists to recapitulate induction of CELF6 expression in a similar manner as the RXR-specific agonist thereby revealing the heterodimer responsible for induction. Since agonists for PPARα, PPARγ, PXR, CAR, FXR, and LXR failed to induce CELF6, we additionally treated mice overnight with agonists for PPARβ/δ, thyroid hormone receptor (TR), retinoic acid receptor (RAR), and vitamin D receptor (VDR). These agonists did not induce CELF6 expression (data not shown), suggesting that RXR could either be (1) acting as a homodimer, (2) heterodimerizing with another binding partner already known

to bind RXRs (e.g. NURR1, NGF-IB), or (3) utilizing an unknown partner or mechanism. In any case, RXR activation was sufficient to induce CELF6 in a tissue-dependent manner in the adult mouse.

To further investigate the role of RXR in CELF6 regulation, mice were treated with a range of LG268 doses (0-30mpk) for 10 days, and duodenal CELF6 mRNA expression was assessed. CELF6 was markedly induced by all doses of LG268, including the lowest dose (Figure B.3A, 4.45±0.73 to 11.82±1.30 fold as compared to vehicle), whereas a related family member, CUGBP1, shows no significant induction. The dose-dependent induction of CELF6 expression suggests the possibility that CELF6 is being directly regulated by RXR. To determine if LG268 could induce CELF6 in other portions of the small intestine, mice were maintained on a chow diet containing 0.2% cholesterol and supplemented with or without LG268 for 12h. LG268 rapidly induces CELF6 expression along the entire length of the intestine (Figure B.3B). Because FXR:RXR and LXR:RXR permissive heterodimers are known to play important roles in intestinal physiology, we wanted to definitively exclude involvement of these nuclear receptors in modulation of CELF6 by RXR ligand administration. To do this we treated FXR, LXRα/β, and triple knockouts with LG268 (30 mpk) for 10 days. LG268 was able to induce CELF6 gene expression in all genotypes (Figure B.4), which is consistent with an independent role for RXR.

Our data indicate that selective activation of RXR is capable of inducing gene expression of CELF6, at least in adult mouse intestine. Although we observed no change in adult brain upon stimulation with LG268, it is tempting to speculate that RXR may

regulate CELF6 expression in the developing brain. RXR is known to play a role during development of the mouse brain and may possibly be activated by endogenous ligands. Putative endogenous ligands for RXRs include 9-*cis*-retinoic acid (Heyman et al., 1992), docosahexanoic acid (de Urquiza et al., 2000), and phytanic acid (Lemotte et al., 1996). While there is still controversy as to whether these are true physiologic ligands, it is clear that activated RXR is detectable during embryonic development (Luria and Furlow, 2004; Solomin et al., 1998).

Elucidation of the precise role(s) of CELF6 in the intestine could lead to a better understanding of the development and physiology of the gastrointestinal tract. Thus, the establishment of a link between RXR and CELF6-dependent regulation of intestinal physiology provides a tool for understanding CELF6 function, but could also in principle lead to drug development for various gastrointestinal disorders. Indeed, the approach of "reverse endocrinology" has yielded a number of drug therapies that target nuclear receptors (Shulman and Mangelsdorf, 2005). To specifically target RXRs, high-affinity ligands called rexinoids have been developed and are now being tested clinically for their utility in regulating hyperproliferative disorders, such as throat and neck cancers, and psoriasis (Miller et al., 1997).

Here, we have shown that selective activation RXR robustly enhances expression of CELF6 mRNA in adult mouse small intestine. To our knowledge, this represents the first description of nuclear receptor regulation of an RNA-binding protein and thus is a new mode by which nuclear receptors could influence development and/or physiology.

B.5 ACKNOWLEDGEMENTS
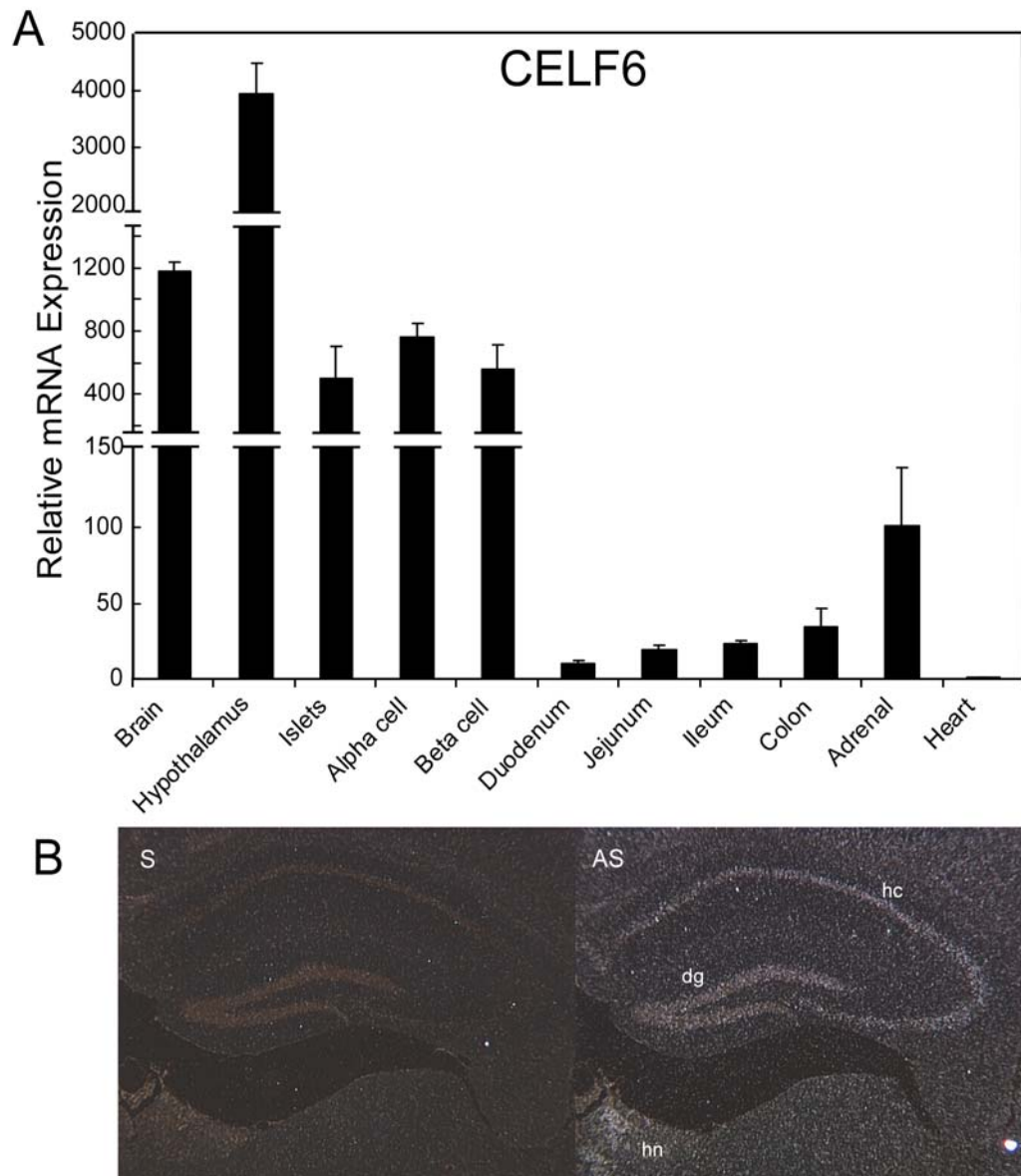
Figure B.1 Tissue-dependent Expression of CELF6. *A*, Three month old male A129/SvJ mice were sacrificed and tissues harvested and islets were isolated. Alpha cells and beta cells represent data from the aTC1 and ßTC6 mouse cell lines, respectively. RNA was extracted and subjected to qPCR (see materials and Methods) to determine expression of CELF6 mRNA relative to a housekeeping gene, cyclophilin. Data are represented as mean±S.E.M of fold change as compared to expression in heart (n=4). *B*, In situ hybridization of coronal sections of mouse brain using sense (S) and antisense (AS) 35S riboprobes directed against nt of CELF6 mRNA. Whereas no signal above background was observed in the sense controls, antisense probes detected specific expression in the hippocampus (hc), dentate gyrus (dg), and habenulae (hn), with lower levels throughout the brain.
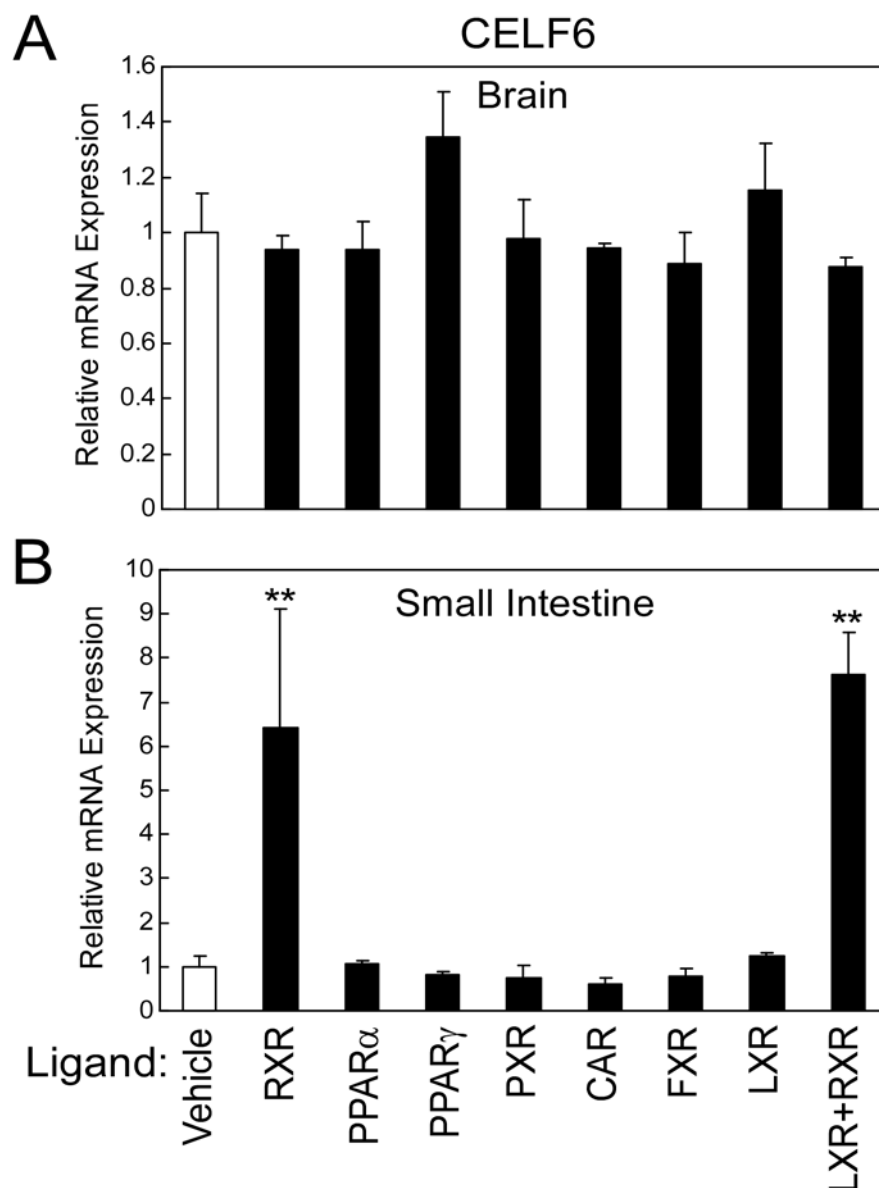
Figure B.2 Activation of RXR Induces CELF6 Expression in Duodenum but not Brain. Various nuclear receptor agonists were administered to three month old male A129/SvJ mice for 12 hours. Insert drugs. Tissues were harvested, then RNA was isolated and subjected to qPCR. *A*, Brain expression of CELF6 mRNA relative to cyclophilin. *B*, Duodenal expression of CELF6 mRNA relative to cyclophilin. CELF6 was strongly induced by RXR and LXR+RXR, but not by others. Values represent the mean ± SEM of data from 4 mice per group. Statistical analyses were performed by one-way ANOVA with Dunnett's post-hoc test. The asterisks denote significant difference as compared to vehicle treated controls: **$P<0.01$.
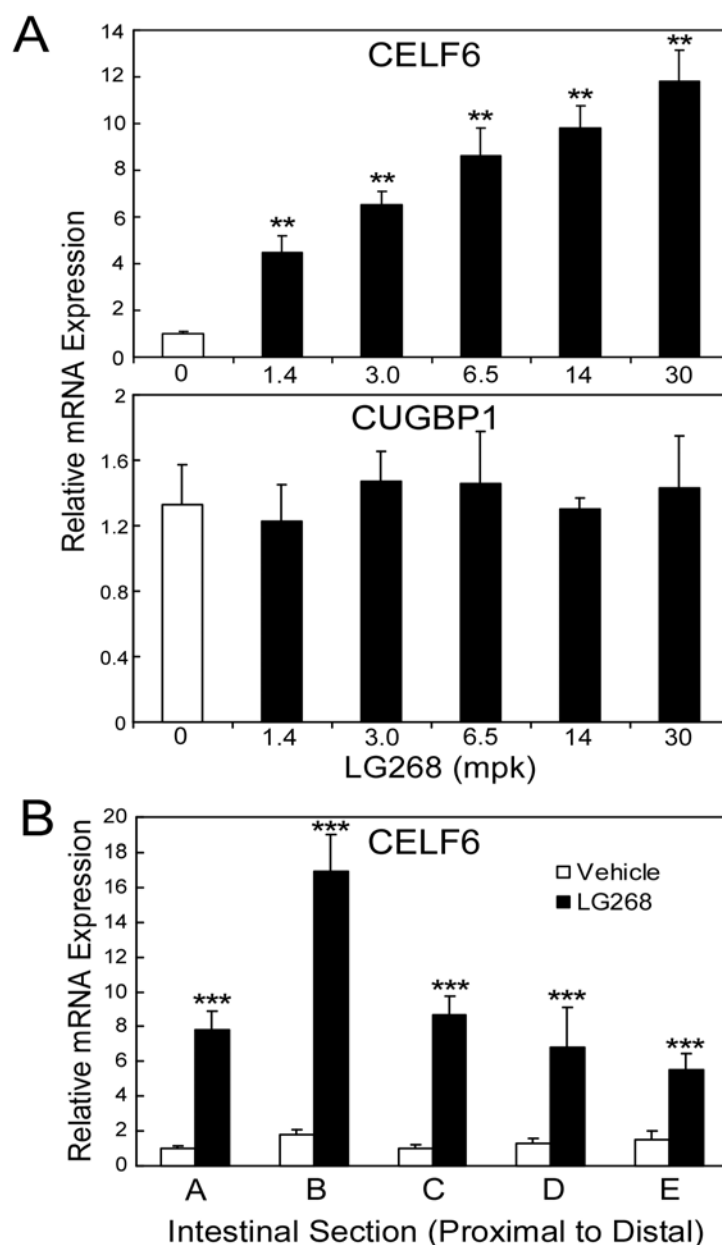
Figure B.3 LG268 Induces CELF6 Expression in a Dose-dependent Manner and Along the Entire Length of the Small Intestine. *A*, CELF6 and CUGBP1 expression in duodenum after different doses of LG268 were administered for 10 days. *B*, CELF6 mRNA expression along the the entire length of small intestine. Small intestines were divided into fifths from vehicle and LG268 animals then assayed for gene expression by qPCR. Values represent the mean ± SEM of data from 4-5 mice per group. Statistical analyses were performed by one-way ANOVA with Dunnett's or Student-Newman-Keuls post-hoc test. Asterisks denote significant difference as compared to vehicle treated controls of the same intestinal segment (**, $p < .01$; ***, $p < .001$).
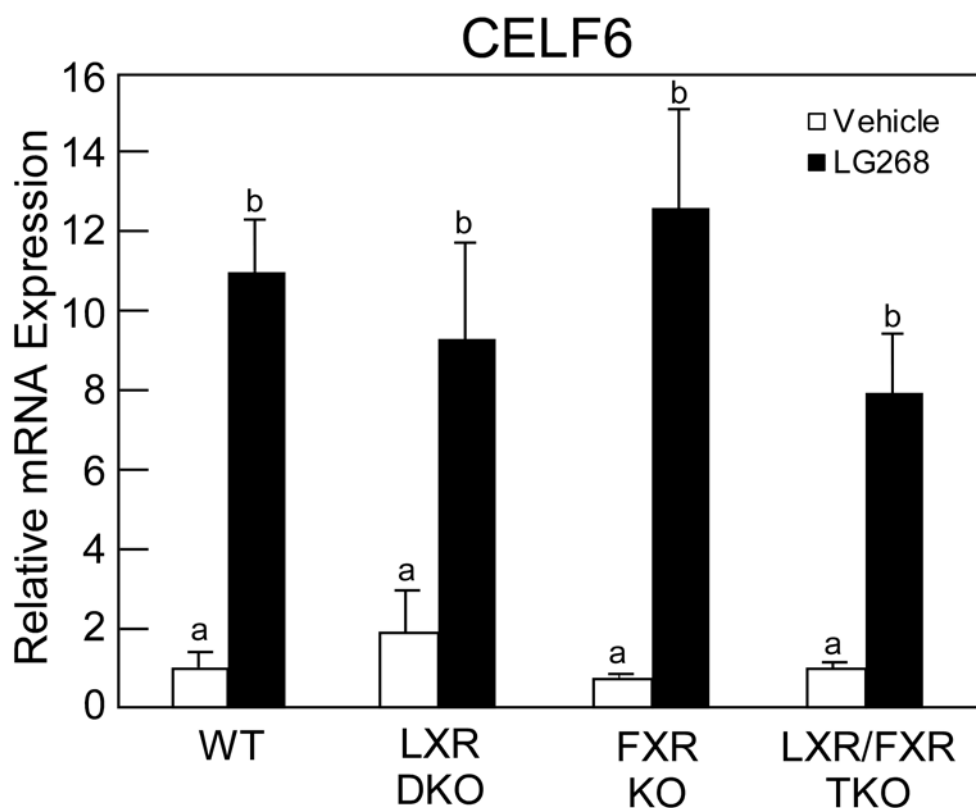
Figure B.4 LG268 Induces CELF6 Independent of FXR and LXR. Male wild-type, FXR knockout, LXRα/β double knockout, or triple knockout mice were given LG268 (6 mpk) supplemented in diet for 10 days, then qPCR was used to determine duodenal expression of CELF6 mRNA. Values represent the mean ± SEM of data from 4-8 mice per group. Statistical analyses were performed by one-way ANOVA with Student-Newman-Keuls post-hoc test. Different letters indicate statistically different groups (p<.001).

BIBLIOGRAPHY

A, I.J., Tan, N.S., Gelman, L., Kersten, S., Seydoux, J., Xu, J., Metzger, D., Canaple, L., Chambon, P., Wahli, W*., et al.* (2004). In vivo activation of PPAR target genes by RXR homodimers. The EMBO journal *23*, 2083-2091.

Adkins, J.C., and Faulds, D. (1997). Micronised fenofibrate: a review of its pharmacodynamic properties and clinical efficacy in the management of dyslipidaemia. Drugs *54*, 615-633.

Altmann, S.W., Davis, H.R., Jr., Yao, X., Laverty, M., Compton, D.S., Zhu, L.J., Crona, J.H., Caplen, M.A., Hoos, L.M., Tetzloff, G*., et al.* (2002). The identification of intestinal scavenger receptor class B, type I (SR-BI) by expression cloning and its role in cholesterol absorption. Biochim Biophys Acta *1580*, 77-93.

Altmann, S.W., Davis, H.R., Jr., Zhu, L.J., Yao, X., Hoos, L.M., Tetzloff, G., Iyer, S.P., Maguire, M., Golovko, A., Zeng, M*., et al.* (2004). Niemann-Pick C1 Like 1 protein is critical for intestinal cholesterol absorption. Science *303*, 1201-1204.

Anant, S., Henderson, J.O., Mukhopadhyay, D., Navaratnam, N., Kennedy, S., Min, J., and Davidson, N.O. (2001). Novel role for RNA-binding protein CUGBP2 in mammalian RNA editing. CUGBP2 modulates C to U editing of apolipoprotein B mRNA by interacting with apobec-1 and ACF, the apobec-1 complementation factor. JBiolChem *276*, 47338-47351.

Anitschkow, N. (1933). Experimental atherosclerosis in animals (New York, Macmillan).

Armbrecht, H.J., Boltz, M.A., and Kumar, V.B. (2002). Development of a vitamin D-responsive organ culture system for adult and old rat intestine. Digestive diseases and sciences *47*, 2831-2838.

Aschoff, L. (1907). Ein Beitrag zur Myelinfrage. Verhandleneen der Duetschen Patholoaischen GeseIlschaft *10*, 166-170.

Ausubel, F.M., Brent, R., Kingston, R.E., Moore, D.D., Seidman, J.G., Smith, J.A., and Struhl, K., eds. (2005). Current Protocols in Molecular Biology (Hoboken, NJ, John Wiley & Sons, Inc.).

Ballard, A.L., Fry, N.K., Chan, L., Surman, S.B., Lee, J.V., Harrison, T.G., and Towner, K.J. (2000). Detection of Legionella pneumophila using a real-time PCR hybridization assay. J Clin Microbiol *38*, 4215-4218.

Banerjee, S., Smallwood, A., Chambers, A.E., and Nicolaides, K. (2003). Quantitative recovery of immunoreactive proteins from clinical samples following RNA and DNA isolation. Biotechniques *35*, 450-452, 454, 456.

Barthe, C., Mahon, F.X., Gharbi, M.J., Faberes, C., Bilhou-Nabera, C., Hochhaus, A., Reiffers, J., and Marit, G. (2001). Expression of interferon-alpha (IFN-alpha) receptor 2c at diagnosis is associated with cytogenetic response in IFN-alpha-treated chronic myeloid leukemia. Blood *97*, 3568-3573.

Bennett, M.K., Ngo, T.T., Athanikar, J.N., Rosenfeld, J.M., and Osborne, T.F. (1999). Co-stimulation of promoter for low density lipoprotein receptor gene by sterol regulatory element-binding protein and Sp1 is specifically disrupted by the yin yang 1 protein. J Biol Chem *274*, 13025-13032.

Benoit, G., Malewicz, M., and Perlmann, T. (2004). Digging deep into the pockets of orphan nuclear receptors: insights from structural studies. Trends in cell biology *14*, 369-376.

Berge, K.E., Tian, H., Graf, G.A., Yu, L., Grishin, N.V., Schultz, J., Kwiterovich, P., Shan, B., Barnes, R., and Hobbs, H.H. (2000). Accumulation of dietary cholesterol in sitosterolemia caused by mutations in adjacent ABC transporters. Science *290*, 1771-1775.

Bjorkhem, I. (2002). Do oxysterols control cholesterol homeostasis? J Clin Invest *110*, 725-730.

Bos, K., Wraight, C., and Stanley, K.K. (1993). TGN38 is maintained in the trans-Golgi network by a tyrosine-containing motif in the cytoplasmic domain. The EMBO journal *12*, 2219-2228.

Brand, C.L., Sturis, J., Gotfredsen, C.F., Fleckner, J., Fledelius, C., Hansen, B.F., Andersen, B., Ye, J.M., Sauerberg, P., and Wassermann, K. (2003). Dual PPARalpha /gamma activation provides enhanced improvement of insulin sensitivity and glycemic control in ZDF rats. Am J Physiol Endocrinol Metab *284*, E841-854.

Brazeau, D.A. (2004). Combining genome-wide and targeted gene expression profiling in drug discovery: microarrays and real-time PCR. Drug Discov Today *9*, 838-845.

Brooks-Wilson, A., Marcil, M., Clee, S.M., Zhang, L.H., Roomp, K., van Dam, M., Yu, L., Brewer, C., Collins, J.A., Molhuizen, H.O.*, et al.* (1999). Mutations in ABC1 in Tangier disease and familial high-density lipoprotein deficiency. Nat Genet *22*, 336-345.

Brown, M.S., and Goldstein, J.L. (1986). A receptor-mediated pathway for cholesterol homeostasis. Science *232*, 34-47.

Brown, M.S., and Goldstein, J.L. (1997). The SREBP pathway: regulation of cholesterol metabolism by proteolysis of a membrane-bound transcription factor. Cell *89*, 331-340.

Brown, P.O., and Botstein, D. (1999). Exploring the new world of the genome with DNA microarrays. Nat Genet *21*, 33-37.

Brunham, L.R., Kruit, J.K., Iqbal, J., Fievet, C., Timmins, J.M., Pape, T.D., Coburn, B.A., Bissada, N., Staels, B., Groen, A.K.*, et al.* (2006). Intestinal ABCA1 directly contributes to HDL biogenesis in vivo. J Clin Invest *116*, 1052-1062.

Buhman, K.K., Accad, M., Novak, S., Choi, R.S., Wong, J.S., Hamilton, R.L., Turley, S., and Farese, R.V., Jr. (2000). Resistance to diet-induced hypercholesterolemia and gallstone formation in ACAT2-deficient mice. Nature medicine *6*, 1341-1347.

Burnett, D.A., Caplen, M.A., Davis, H.R., Jr., Burrier, R.E., and Clader, J.W. (1994). 2-Azetidinones as inhibitors of cholesterol absorption. J Med Chem *37*, 1733-1736.

Bustin, S.A. (2000). Absolute quantification of mRNA using real-time reverse transcription polymerase chain reaction assays. J Mol Endocrinol *25*, 169-193.

Bustin, S.A. (2002). Quantification of mRNA using real-time reverse transcription PCR (RT-PCR): trends and problems. J Mol Endocrinol *29*, 23-39.

Bustin, S.A., and Nolan, T. (2004). Pitfalls of quantitative real-time reverse-transcription polymerase chain reaction. J Biomol Tech *15*, 155-166.

Calpe-Berdiel, L., Escola-Gil, J.C., Ribas, V., Navarro-Sastre, A., Garces-Garces, J., and Blanco-Vaca, F. (2005). Changes in intestinal and liver global gene expression in response to a phytosterol-enriched diet. Atherosclerosis *181*, 75-85.

Cao, G., Yang, G., Timme, T.L., Saika, T., Truong, L.D., Satoh, T., Goltsov, A., Park, S.H., Men, T., Kusaka, N*., et al.* (2003). Disruption of the caveolin-1 gene impairs renal calcium reabsorption and leads to hypercalciuria and urolithiasis. The American journal of pathology *162*, 1241-1248.

Carstea, E.D., Morris, J.A., Coleman, K.G., Loftus, S.K., Zhang, D., Cummings, C., Gu, J., Rosenfeld, M.A., Pavan, W.J., Krizman, D.B*., et al.* (1997). Niemann-Pick C1 disease gene: homology to mediators of cholesterol homeostasis. Science *277*, 228-231.

Chawla, A., Repa, J.J., Evans, R.M., and Mangelsdorf, D.J. (2001). Nuclear receptors and lipid physiology: opening the X-files. Science *294*, 1866-1870.

Chianale, J., Vollrath, V., Wielandt, A.M., Amigo, L., Rigotti, A., Nervi, F., Gonzalez, S., Andrade, L., Pizarro, M., and Accatino, L. (1996). Fibrates induce mdr2 gene expression and biliary phospholipid secretion in the mouse. Biochem J *314 (Pt 3)*, 781-786.

Christiansen-Weber, T.A., Voland, J.R., Wu, Y., Ngo, K., Roland, B.L., Nguyen, S., Peterson, P.A., and Fung-Leung, W.P. (2000). Functional loss of ABCA1 in mice causes severe placental malformation, aberrant lipid distribution, and kidney glomerulonephritis as well as high-density lipoprotein cholesterol deficiency. The American journal of pathology *157*, 1017-1029.

Clader, J.W. (2004). The discovery of ezetimibe: a view from outside the receptor. J Med Chem *47*, 1-9.

Clader, J.W., Berger, J.G., Burrier, R.E., Davis, H.R., Domalski, M., Dugar, S., Kogan, T.P., Salisbury, B., and Vaccaro, W. (1995). Substituted (1,2-diarylethyl)amide acyl-CoA:cholesterol acyltransferase inhibitors: effect of polar groups on in vitro and in vivo activity. J Med Chem *38*, 1600-1607.

Cleary, T.J., Roudel, G., Casillas, O., and Miller, N. (2003). Rapid and specific detection of Mycobacterium tuberculosis by using the Smart Cycler instrument and a specific fluorogenic probe. J Clin Microbiol *41*, 4783-4786.

Cohen, J.C., Boerwinkle, E., Mosley, T.H., Jr., and Hobbs, H.H. (2006a). Sequence variations in PCSK9, low LDL, and protection against coronary heart disease. N Engl J Med *354*, 1264-1272.

Cohen, J.C., Pertsemlidis, A., Fahmi, S., Esmail, S., Vega, G.L., Grundy, S.M., and Hobbs, H.H. (2006b). Multiple rare variants in NPC1L1 associated with reduced sterol absorption and plasma low-density lipoprotein levels. Proc Natl Acad Sci U S A *103*, 1810-1815.

Davies, J.P., Chen, F.W., and Ioannou, Y.A. (2000a). Transmembrane molecular pump activity of Niemann-Pick C1 protein. Science *290*, 2295-2298.

Davies, J.P., Levy, B., and Ioannou, Y.A. (2000b). Evidence for a Niemann-pick C (NPC) gene family: identification and characterization of NPC1L1. Genomics *65*, 137-145.

Davies, J.P., Scott, C., Oishi, K., Liapis, A., and Ioannou, Y.A. (2005). Inactivation of NPC1L1 causes multiple lipid transport defects and protects against diet-induced hypercholesterolemia. J Biol Chem *280*, 12710-12720.

Davis, H.R., Jr., Compton, D.S., Hoos, L., and Tetzloff, G. (2001a). Ezetimibe, a potent cholesterol absorption inhibitor, inhibits the development of atherosclerosis in ApoE knockout mice. Arterioscler Thromb Vasc Biol *21*, 2032-2038.

Davis, H.R., Jr., Pula, K.K., Alton, K.B., Burrier, R.E., and Watkins, R.W. (2001b). The synergistic hypocholesterolemic activity of the potent cholesterol absorption inhibitor, ezetimibe, in combination with 3-hydroxy-3-methylglutaryl coenzyme a reductase inhibitors in dogs. Metabolism *50*, 1234-1241.

Davis, H.R., Jr., Zhu, L.J., Hoos, L.M., Tetzloff, G., Maguire, M., Liu, J., Yao, X., Iyer, S.P., Lam, M.H., Lund, E.G.*, et al.* (2004). Niemann-Pick C1 Like 1 (NPC1L1) is the intestinal phytosterol and cholesterol transporter and a key modulator of whole-body cholesterol homeostasis. J Biol Chem *279*, 33586-33592.

Dawson, P.A., Haywood, J., Craddock, A.L., Wilson, M., Tietjen, M., Kluckman, K., Maeda, N., and Parks, J.S. (2003). Targeted deletion of the ileal bile acid transporter eliminates enterohepatic cycling of bile acids in mice. J Biol Chem *278*, 33920-33927.

Dawson, P.A., Hubbert, M., Haywood, J., Craddock, A.L., Zerangue, N., Christian, W.V., and Ballatori, N. (2005). The heteromeric organic solute transporter alpha-beta, Ostalpha-Ostbeta, is an ileal basolateral bile acid transporter. J Biol Chem *280*, 6960-6968.

de Urquiza, A.M., Liu, S., Sjoberg, M., Zetterstrom, R.H., Griffiths, W., Sjovall, J., and Perlmann, T. (2000). Docosahexaenoic acid, a ligand for the retinoid X receptor in mouse brain. Science *290*, 2140-2144.

Desvergne, B., and Wahli, W. (1999). Peroxisome proliferator-activated receptors: nuclear control of metabolism. Endocrine reviews *20*, 649-688.

Dhe-Paganon, S., Duda, K., Iwamoto, M., Chi, Y.I., and Shoelson, S.E. (2002). Crystal structure of the HNF4 alpha ligand binding domain in complex with endogenous fatty acid ligand. J Biol Chem *277*, 37973-37976.

Dheda, K., Huggett, J.F., Bustin, S.A., Johnson, M.A., Rook, G., and Zumla, A. (2004). Validation of housekeeping genes for normalizing RNA expression in real-time PCR. Biotechniques *37*, 112-114, 116, 118-119.

Dietschy, J.M., and Turley, S.D. (2001). Cholesterol metabolism in the brain. Current opinion in lipidology *12*, 105-112.

Drobnik, W., Lindenthal, B., Lieser, B., Ritter, M., Christiansen Weber, T., Liebisch, G., Giesa, U., Igel, M., Borsukova, H., Buchler, C.*, et al.* (2001). ATP-binding cassette transporter A1 (ABCA1) affects total body sterol metabolism. Gastroenterology *120*, 1203-1211.

Duan, L.P., Wang, H.H., Ohashi, A., and Wang, D.Q. (2006). Role of intestinal sterol transporters Abcg5, Abcg8, and Npc1l1 in cholesterol absorption in mice: gender and age effects. Am J Physiol Gastrointest Liver Physiol *290*, G269-276.

Duval, C., Touche, V., Tailleux, A., Fruchart, J.C., Fievet, C., Clavey, V., Staels, B., and Lestavel, S. (2006). Niemann-Pick C1 like 1 gene expression is down-regulated by LXR activators in the intestine. Biochem Biophys Res Commun *340*, 1259-1263.

Edwards, K., Logan, J., and Saunders, N., eds. (2004). Real-Time PCR: An Essential Guide (Norfolk, UK, Horizon Bioscience).

Ferland, S., and Hugon, J.S. (1979a). Organ culture of adult mouse intestine. I. Morphological results after 24 and 48 hours of culture. In vitro *15*, 278-287.

Ferland, S., and Hugon, J.S. (1979b). Organ culture of adult mouse intestine. II. Mitotic activity, DNA synthesis and cellular migration after 24 and 48 hours of culture. In vitro *15*, 288-293.

Ferre, P. (2004). The biology of peroxisome proliferator-activated receptors: relationship with lipid metabolism and insulin sensitivity. Diabetes *53 Suppl 1*, S43-50.

Field, F.J., Born, E., Murthy, S., and Mathur, S.N. (1998). Caveolin is present in intestinal cells: role in cholesterol trafficking? J Lipid Res *39*, 1938-1950.

Frick, M.H., Elo, O., Haapa, K., Heinonen, O.P., Heinsalmi, P., Helo, P., Huttunen, J.K., Kaitaniemi, P., Koskinen, P., Manninen, V.*, et al.* (1987). Helsinki Heart Study: primary-prevention trial with gemfibrozil in middle-aged men with dyslipidemia. Safety of treatment, changes in risk factors, and incidence of coronary heart disease. N Engl J Med *317*, 1237-1245.

Fu, Y., Hoang, A., Escher, G., Parton, R.G., Krozowski, Z., and Sviridov, D. (2004). Expression of caveolin-1 enhances cholesterol efflux in hepatic cells. J Biol Chem *279*, 14140-14146.

Fuchs, M., Ivandic, B., Muller, O., Schalla, C., Scheibner, J., Bartsch, P., and Stange, E.F. (2001). Biliary cholesterol hypersecretion in gallstone-susceptible mice is associated

with hepatic up-regulation of the high-density lipoprotein receptor SRBI. Hepatology *33*, 1451-1459.

Garcia-Calvo, M., Lisnock, J., Bull, H.G., Hawes, B.E., Burnett, D.A., Braun, M.P., Crona, J.H., Davis, H.R., Jr., Dean, D.C., Detmers, P.A*., et al.* (2005). The target of ezetimibe is Niemann-Pick C1-Like 1 (NPC1L1). Proc Natl Acad Sci U S A *102*, 8132-8137.

Gibson, J.R., Saunders, N.A., Burke, B., and Owen, R.J. (1999). Novel method for rapid determination of clarithromycin sensitivity in Helicobacter pylori. J Clin Microbiol *37*, 3746-3748.

Ginzinger, D.G., Godfrey, T.E., Nigro, J., Moore, D.H., 2nd, Suzuki, S., Pallavicini, M.G., Gray, J.W., and Jensen, R.H. (2000). Measurement of DNA copy number at microsatellite loci using quantitative PCR analysis. Cancer Res *60*, 5405-5409.

Good, P.J., Chen, Q., Warner, S.J., and Herring, D.C. (2000). A family of human RNA-binding proteins related to the Drosophila Bruno translational regulator. JBiolChem *275*, 28583-28592.

Gromak, N., Matlin, A.J., Cooper, T.A., and Smith, C.W. (2003). Antagonistic regulation of alpha-actinin alternative splicing by CELF proteins and polypyrimidine tract binding protein. RNA *9*, 443-456.

Grundy, S.M., Cleeman, J.I., Merz, C.N., Brewer, H.B., Jr., Clark, L.T., Hunninghake, D.B., Pasternak, R.C., Smith, S.C., Jr., and Stone, N.J. (2004). Implications of recent clinical trials for the National Cholesterol Education Program Adult Treatment Panel III guidelines. Circulation *110*, 227-239.

Grundy, S.M., and Vega, G.L. (1987). Fibric acids: effects on lipids and lipoprotein metabolism. Am J Med *83*, 9-20.

Grundy, S.M., Vega, G.L., Yuan, Z., Battisti, W.P., Brady, W.E., and Palmisano, J. (2005). Effectiveness and tolerability of simvastatin plus fenofibrate for combined hyperlipidemia (the SAFARI trial). Am J Cardiol *95*, 462-468.

Guo, Q., Wang, P.R., Milot, D.P., Ippolito, M.C., Hernandez, M., Burton, C.A., Wright, S.D., and Chao, Y. (2001). Regulation of lipid metabolism and gene expression by fenofibrate in hamsters. Biochim Biophys Acta *1533*, 220-232.

Hajri, T., Ferezou, J., Laruelle, C., and Lutton, C. (1995). Crilvastatin, a new 3-hydroxy-3-methylglutaryl-coenzyme A reductase inhibitor, inhibits cholesterol absorption in genetically hypercholesterolemic rats. European journal of pharmacology *286*, 131-136.

Harris, E. (2004). Building scientific capacity in developing countries. EMBO Rep *5*, 7-11.

Hauser, H., Dyer, J.H., Nandy, A., Vega, M.A., Werder, M., Bieliauskaite, E., Weber, F.E., Compassi, S., Gemperli, A., Boffelli, D.*, et al.* (1998). Identification of a receptor mediating absorption of dietary cholesterol in the intestine. Biochemistry *37*, 17843-17850.

Hein, I., Klein, D., Lehner, A., Bubert, A., Brandl, E., and Wagner, M. (2001). Detection and quantification of the iap gene of Listeria monocytogenes and Listeria innocua by a new real-time quantitative PCR assay. Res Microbiol *152*, 37-46.

Heyman, R.A., Mangelsdorf, D.J., Dyck, J.A., Stein, R.B., Eichele, G., Evans, R.M., and Thaller, C. (1992). 9-cis retinoic acid is a high affinity ligand for the retinoid X receptor. Cell *68*, 397-406.

Higgins, M.E., Davies, J.P., Chen, F.W., and Ioannou, Y.A. (1999). Niemann-Pick C1 is a late endosome-resident protein that transiently associates with lysosomes and the trans-Golgi network. Mol Genet Metab *68*, 1-13.

Higuchi, R., Dollinger, G., Walsh, P.S., and Griffith, R. (1992). Simultaneous amplification and detection of specific DNA sequences. Biotechnology (N Y) *10*, 413-417.

Higuchi, R., Fockler, C., Dollinger, G., and Watson, R. (1993). Kinetic PCR analysis: real-time monitoring of DNA amplification reactions. Biotechnology (N Y) *11*, 1026-1030.

Horton, J.D., Goldstein, J.L., and Brown, M.S. (2002). SREBPs: activators of the complete program of cholesterol and fatty acid synthesis in the liver. J Clin Invest *109*, 1125-1131.

Howles, P.N., Carter, C.P., and Hui, D.Y. (1996). Dietary free and esterified cholesterol absorption in cholesterol esterase (bile salt-stimulated lipase) gene-targeted mice. J Biol Chem *271*, 7196-7202.

Humphrey, J.S., Peters, P.J., Yuan, L.C., and Bonifacino, J.S. (1993). Localization of TGN38 to the trans-Golgi network: involvement of a cytoplasmic tyrosine-containing sequence. The Journal of cell biology *120*, 1123-1135.

Huuskonen, J., Vishnu, M., Pullinger, C.R., Fielding, P.E., and Fielding, C.J. (2004). Regulation of ATP-binding cassette transporter A1 transcription by thyroid hormone receptor. Biochemistry *43*, 1626-1632.

Ioannou, Y.A. (2000). The structure and function of the Niemann-Pick C1 protein. Mol Genet Metab *71*, 175-181.

Ishibashi, S., Schwarz, M., Frykman, P.K., Herz, J., and Russell, D.W. (1996). Disruption of cholesterol 7alpha-hydroxylase gene in mice. I. Postnatal lethality reversed by bile acid and vitamin supplementation. J Biol Chem *271*, 18017-18023.

Iyer, S.P., Yao, X., Crona, J.H., Hoos, L.M., Tetzloff, G., Davis, H.R., Jr., Graziano, M.P., and Altmann, S.W. (2005). Characterization of the putative native and recombinant rat sterol transporter Niemann-Pick C1 Like 1 (NPC1L1) protein. Biochim Biophys Acta *1722*, 282-292.

Janowski, B.A., Grogan, M.J., Jones, S.A., Wisely, G.B., Kliewer, S.A., Corey, E.J., and Mangelsdorf, D.J. (1999). Structural requirements of ligands for the oxysterol liver X receptors LXRalpha and LXRbeta. Proc Natl Acad Sci U S A *96*, 266-271.

Janowski, B.A., Willy, P.J., Devi, T.R., Falck, J.R., and Mangelsdorf, D.J. (1996). An oxysterol signalling pathway mediated by the nuclear receptor LXR alpha. Nature *383*, 728-731.

Jaye, M. (2003). LXR agonists for the treatment of atherosclerosis. Curr Opin Investig Drugs *4*, 1053-1058.

Johnson, R.L., Rothman, A.L., Xie, J., Goodrich, L.V., Bare, J.W., Bonifas, J.M., Quinn, A.G., Myers, R.M., Cox, D.R., Epstein, E.H., Jr*., et al.* (1996). Human homolog of patched, a candidate gene for the basal cell nevus syndrome. Science *272*, 1668-1671.

Jolley, C.D., Dietschy, J.M., and Turley, S.D. (1999). Genetic differences in cholesterol absorption in 129/Sv and C57BL/6 mice: effect on cholesterol responsiveness. The American journal of physiology *276*, G1117-1124.

Kallen, J.A., Schlaeppi, J.-M., Bitsch, F., Geisse, S., Geiser, M., Delhon, I., and Fournier, B. (2002). X-Ray Structure of the hROR[alpha] LBD at 1.63 A: Structural and Functional Data that Cholesterol or a Cholesterol Derivative Is the Natural Ligand of ROR[alpha]. Structure *10*, 1697-1707.

Karlsen, A.E., Heding, P.E., Frobose, H., Ronn, S.G., Kruhoffer, M., Orntoft, T.F., Darville, M., Eizirik, D.L., Pociot, F., Nerup, J*., et al.* (2004). Suppressor of cytokine signalling (SOCS)-3 protects beta cells against IL-1beta-mediated toxicity through inhibition of multiple nuclear factor-kappaB-regulated proapoptotic pathways. Diabetologia *47*, 1998-2011.

Keech, A., Simes, R.J., Barter, P., Best, J., Scott, R., Taskinen, M.R., Forder, P., Pillai, A., Davis, T., Glasziou, P*., et al.* (2005). Effects of long-term fenofibrate therapy on cardiovascular events in 9795 people with type 2 diabetes mellitus (the FIELD study): randomised controlled trial. Lancet *366*, 1849-1861.

Kenan, D.J., Query, C.C., and Keene, J.D. (1991). RNA recognition: towards identifying determinants of specificity. Trends BiochemSci *16*, 214-220.

Kersten, S., Seydoux, J., Peters, J.M., Gonzalez, F.J., Desvergne, B., and Wahli, W. (1999). Peroxisome proliferator-activated receptor alpha mediates the adaptive response to fasting. J Clin Invest *103*, 1489-1498.

Klein, D. (2002). Quantification using real-time PCR technology: applications and limitations. Trends Mol Med *8*, 257-260.

Klett, E.L., Lu, K., Kosters, A., Vink, E., Lee, M.H., Altenburg, M., Shefer, S., Batta, A.K., Yu, H., Chen, J*., et al.* (2004). A mouse model of sitosterolemia: absence of Abcg8/sterolin-2 results in failure to secrete biliary cholesterol. BMC medicine [electronic resource] *2*, 5.

Klett, E.L., and Patel, S.B. (2004). Biomedicine. Will the real cholesterol transporter please stand up. Science *303*, 1149-1150.

Klucken, J., Buchler, C., Orso, E., Kaminski, W.E., Porsch-Ozcurumez, M., Liebisch, G., Kapinsky, M., Diederich, W., Drobnik, W., Dean, M*., et al.* (2000). ABCG1 (ABC8), the human homolog of the Drosophila white gene, is a regulator of macrophage cholesterol and phospholipid transport. Proc Natl Acad Sci U S A *97*, 817-822.

Knight, B.L., Patel, D.D., Humphreys, S.M., Wiggins, D., and Gibbons, G.F. (2003). Inhibition of cholesterol absorption associated with a PPAR alpha-dependent increase in ABC binding cassette transporter A1 in mice. J Lipid Res *44*, 2049-2058.

Ko, Y.G., Liu, P., Pathak, R.K., Craig, L.C., and Anderson, R.G. (1998). Early effects of pp60(v-src) kinase activation on caveolae. Journal of cellular biochemistry *71*, 524-535.

Kok, T., Bloks, V.W., Wolters, H., Havinga, R., Jansen, P.L., Staels, B., and Kuipers, F. (2003). Peroxisome proliferator-activated receptor alpha (PPARalpha)-mediated regulation of multidrug resistance 2 (Mdr2) expression and function in mice. Biochem J *369*, 539-547.

Kramer, W., Girbig, F., Corsiero, D., Pfenninger, A., Frick, W., Jahne, G., Rhein, M., Wendler, W., Lottspeich, F., Hochleitner, E.O*., et al.* (2005). Aminopeptidase N (CD13) is a molecular target of the cholesterol absorption inhibitor ezetimibe in the enterocyte brush border membrane. J Biol Chem *280*, 1306-1320.

Kramer, W., Glombik, H., Petry, S., Heuer, H., Schafer, H., Wendler, W., Corsiero, D., Girbig, F., and Weyland, C. (2000). Identification of binding proteins for cholesterol absorption inhibitors as components of the intestinal cholesterol transporter. FEBS letters *487*, 293-297.

Krauter, J., Heil, G., and Ganser, A. (2001). The AML1/MTG8 Fusion Transcript in t(8;21) Positive AML and its Implication for the Detection of Minimal Residual Disease; Malignancy. Hematol *5*, 369-381.

Krylova, I.N., Sablin, E.P., Moore, J., Xu, R.X., Waitt, G.M., MacKay, J.A., Juzumiene, D., Bynum, J.M., Madauss, K., Montana, V*., et al.* (2005). Structural analyses reveal phosphatidyl inositols as ligands for the NR5 orphan receptors SF-1 and LRH-1. Cell *120*, 343-355.

Kuhne, B.S., and Oschmann, P. (2002). Quantitative real-time RT-PCR using hybridization probes and imported standard curves for cytokine gene expression analysis. Biotechniques *33*, 1078, 1080-1072, 1084 passim.

Kurrasch, D.M., Huang, J., Wilkie, T.M., and Repa, J.J. (2004). Quantitative real-time polymerase chain reaction measurement of regulators of G-protein signaling mRNA levels in mouse tissues. Methods Enzymol *389*, 3-15.

Lacy, P.E., and Kostianovsky, M. (1967). Method for the isolation of intact islets of Langerhans from the rat pancreas. Diabetes *16*, 35-39.

Ladd, A.N., Charlet, N., and Cooper, T.A. (2001). The CELF family of RNA binding proteins is implicated in cell-specific and developmentally regulated alternative splicing. MolCell Biol *21*, 1285-1296.

Ladd, A.N., and Cooper, T.A. (2004). Multiple domains control the subcellular localization and activity of ETR-3, a regulator of nuclear and cytoplasmic RNA processing events. JCell Sci *117*, 3519-3529.

Ladd, A.N., Nguyen, N.H., Malhotra, K., and Cooper, T.A. (2004). CELF6, a member of the CELF family of RNA-binding proteins, regulates muscle-specific splicing enhancer-dependent alternative splicing. JBiolChem *279*, 17756-17764.

Lammert, F., and Wang, D.Q. (2005). New insights into the genetic regulation of intestinal cholesterol absorption. Gastroenterology *129*, 718-734.

Lander, E.S., Linton, L.M., Birren, B., Nusbaum, C., Zody, M.C., Baldwin, J., Devon, K., Dewar, K., Doyle, M., FitzHugh, W*., et al.* (2001). Initial sequencing and analysis of the human genome. Nature *409*, 860-921.

Lange, Y., Ye, J., and Strebel, F. (1995). Movement of 25-hydroxycholesterol from the plasma membrane to the rough endoplasmic reticulum in cultured hepatoma cells. J Lipid Res *36*, 1092-1097.

Lauvrak, S.U., Hollas, H., Doskeland, A.P., Aukrust, I., Flatmark, T., and Vedeler, A. (2005). Ubiquitinated annexin A2 is enriched in the cytoskeleton fraction. FEBS letters *579*, 203-206.

Le Pecq, J.B., and Paoletti, C. (1966). A new fluorometric method for RNA and DNA determination. Anal Biochem *17*, 100-107.

Lederberg, J. (1993). What the double helix (1953) has meant for basic biomedical science. A personal commentary. Jama *269*, 1981-1985.

Lee, M.H., Lu, K., Hazard, S., Yu, H., Shulenin, S., Hidaka, H., Kojima, H., Allikmets, R., Sakuma, N., Pegoraro, R.*, et al.* (2001). Identification of a gene, ABCG5, important in the regulation of dietary cholesterol absorption. Nat Genet *27*, 79-83.

Lee, S.S., Pineau, T., Drago, J., Lee, E.J., Owens, J.W., Kroetz, D.L., Fernandez-Salguero, P.M., Westphal, H., and Gonzalez, F.J. (1995). Targeted disruption of the alpha isoform of the peroxisome proliferator-activated receptor gene in mice results in abolishment of the pleiotropic effects of peroxisome proliferators. Mol Cell Biol *15*, 3012-3022.

Lehmann, J.M., Kliewer, S.A., Moore, L.B., Smith-Oliver, T.A., Oliver, B.B., Su, J.L., Sundseth, S.S., Winegar, D.A., Blanchard, D.E., Spencer, T.A.*, et al.* (1997). Activation of the nuclear receptor LXR by oxysterols defines a new hormone response pathway. J Biol Chem *272*, 3137-3140.

Lemotte, P.K., Keidel, S., and Apfel, C.M. (1996). Phytanic acid is a retinoid X receptor ligand. European journal of biochemistry / FEBS *236*, 328-333.

Li, D., Bachinski, L.L., and Roberts, R. (2001a). Genomic organization and isoform-specific tissue expression of human NAPOR (CUGBP2) as a candidate gene for familial arrhythmogenic right ventricular dysplasia. Genomics *74*, 396-401.

Li, W.P., Liu, P., Pilcher, B.K., and Anderson, R.G. (2001b). Cell-specific targeting of caveolin-1 to caveolae, secretory vesicles, cytoplasm or mitochondria. Journal of cell science *114*, 1397-1408.

Li, Y., Choi, M., Cavey, G., Daugherty, J., Suino, K., Kovach, A., Bingham, N.C., Kliewer, S.A., and Xu, H.E. (2005). Crystallographic identification and functional characterization of phospholipids as ligands for the orphan nuclear receptor steroidogenic factor-1. Molecular cell *17*, 491-502.

Liang, G., Yang, J., Horton, J.D., Hammer, R.E., Goldstein, J.L., and Brown, M.S. (2002). Diminished hepatic response to fasting/refeeding and liver X receptor agonists in mice with selective deficiency of sterol regulatory element-binding protein-1c. J Biol Chem *277*, 9520-9528.

Liu, P., Rudick, M., and Anderson, R.G. (2002). Multiple functions of caveolin-1. J Biol Chem *277*, 41295-41298.

Loftus, S.K., Morris, J.A., Carstea, E.D., Gu, J.Z., Cummings, C., Brown, A., Ellison, J., Ohno, K., Rosenfeld, M.A., Tagle, D.A.*, et al.* (1997). Murine model of Niemann-Pick C disease: mutation in a cholesterol homeostasis gene. Science *277*, 232-235.

Loots, G.G., and Ovcharenko, I. (2004). rVISTA 2.0: evolutionary analysis of transcription factor binding sites. Nucleic Acids Res *32*, W217-221.

Lu, K., Lee, M.H., Hazard, S., Brooks-Wilson, A., Hidaka, H., Kojima, H., Ose, L., Stalenhoef, A.F., Mietinnen, T., Bjorkhem, I.*, et al.* (2001a). Two genes that map to the STSL locus cause sitosterolemia: genomic structure and spectrum of mutations involving sterolin-1 and sterolin-2, encoded by ABCG5 and ABCG8, respectively. Am J Hum Genet *69*, 278-290.

Lu, T.T., Makishima, M., Repa, J.J., Schoonjans, K., Kerr, T.A., Auwerx, J., and Mangelsdorf, D.J. (2000). Molecular basis for feedback regulation of bile acid synthesis by nuclear receptors. Molecular cell *6*, 507-515.

Lu, T.T., Repa, J.J., and Mangelsdorf, D.J. (2001b). Orphan nuclear receptors as eLiXiRs and FiXeRs of sterol metabolism. JBiolChem *276*, 37735-37738.

Lund, E.G., Xie, C., Kotti, T., Turley, S.D., Dietschy, J.M., and Russell, D.W. (2003). Knockout of the cholesterol 24-hydroxylase gene in mice reveals a brain-specific mechanism of cholesterol turnover. J Biol Chem *278*, 22980-22988.

Lunge, V.R., Miller, B.J., Livak, K.J., and Batt, C.A. (2002). Factors affecting the performance of 5' nuclease PCR assays for Listeria monocytogenes detection. J Microbiol Methods *51*, 361-368.

Luria, A., and Furlow, J.D. (2004). Spatiotemporal retinoid-X receptor activation detected in live vertebrate embryos. Proc Natl Acad Sci U S A *101*, 8987-8992.

Luu-The, V., Paquet, N., Calvo, E., and Cumps, J. (2005). Improved real-time RT-PCR method for high-throughput measurements using second derivative calculation and double correction. Biotechniques *38*, 287-293.

Machleidt, T., Li, W.P., Liu, P., and Anderson, R.G. (2000). Multiple domains in caveolin-1 control its intracellular traffic. The Journal of cell biology *148*, 17-28.

Mackay, I.M. (2004). Real-time PCR in the microbiology laboratory. Clin Microbiol Infect *10*, 190-212.

Mackay, I.M., Arden, K.E., and Nitsche, A. (2002). Real-time PCR in virology. Nucleic Acids Res *30*, 1292-1305.

Makino, S.I., Cheun, H.I., Watarai, M., Uchida, I., and Takeshi, K. (2001). Detection of anthrax spores from the air by real-time PCR. Lett Appl Microbiol *33*, 237-240.

Makishima, M., Okamoto, A.Y., Repa, J.J., Tu, H., Learned, R.M., Luk, A., Hull, M.V., Lustig, K.D., Mangelsdorf, D.J., and Shan, B. (1999). Identification of a nuclear receptor for bile acids. Science *284*, 1362-1365.

Mallordy, A., Besnard, P., and Carlier, H. (1993). Research of an in vitro model to study the expression of fatty acid-binding proteins in the small intestine. Molecular and cellular biochemistry *123*, 85-92.

Mangelsdorf, D.J., and Evans, R.M. (1995). The RXR heterodimers and orphan receptors. Cell *83*, 841-850.

Mardones, P., Quinones, V., Amigo, L., Moreno, M., Miquel, J.F., Schwarz, M., Miettinen, H.E., Trigatti, B., Krieger, M., VanPatten, S.*, et al.* (2001). Hepatic cholesterol and bile acid metabolism and intestinal cholesterol absorption in scavenger receptor class B type I-deficient mice. J Lipid Res *42*, 170-180.

Martineau, F., Picard, F.J., Lansac, N., C, M.i.q.m., Roy, P.H., Ouellette, M., and Bergeron, M.G. (2000). Correlation between the resistance genotype determined by multiplex PCR assays and the antibiotic susceptibility patterns of Staphylococcus aureus and Staphylococcus epidermidis. Antimicrob Agents Chemother *44*, 231-238.

Mazzariol, A., Cornaglia, G., and Nikaido, H. (2000). Contributions of the AmpC beta-lactamase and the AcrAB multidrug efflux system in intrinsic resistance of Escherichia coli K-12 to beta-lactams. Antimicrob Agents Chemother *44*, 1387-1390.

McNamara, D.J., Davidson, N.O., Samuel, P., and Ahrens, E.H., Jr. (1980). Cholesterol absorption in man: effect of administration of clofibrate and/or cholestyramine. J Lipid Res *21*, 1058-1064.

Miller, V.A., Benedetti, F.M., Rigas, J.R., Verret, A.L., Pfister, D.G., Straus, D., Kris, M.G., Crisp, M., Heyman, R., Loewen, G.R.*, et al.* (1997). Initial clinical trial of a selective retinoid X receptor ligand, LGD1069. J Clin Oncol *15*, 790-795.

Mitchell, P. (2001). Microfluidics--downsizing large-scale biology. Nat Biotechnol *19*, 717-721.

Modrek, B., and Lee, C. (2002). A genomic view of alternative splicing. NatGenet *30*, 13-19.

Moreau, R.A., Whitaker, B.D., and Hicks, K.B. (2002). Phytosterols, phytostanols, and their conjugates in foods: structural diversity, quantitative analysis, and health-promoting uses. Progress in lipid research *41*, 457-500.

Mukhopadhyay, D., Houchen, C.W., Kennedy, S., Dieckgraefe, B.K., and Anant, S. (2003). Coupled mRNA stabilization and translational silencing of cyclooxygenase-2 by a novel RNA binding protein, CUGBP2. MolCell *11*, 113-126.

Mullis, K.B. (1990). The unusual origin of the polymerase chain reaction. Sci Am *262*, 56-61, 64-55.

Mullis, K.B., and Faloona, F.A. (1987). Specific synthesis of DNA in vitro via a polymerase-catalyzed chain reaction. Methods Enzymol *155*, 335-350.

Murakami, S., Nakashima, R., Yamashita, E., and Yamaguchi, A. (2002). Crystal structure of bacterial multidrug efflux transporter AcrB. Nature *419*, 587-593.

Murata, M., Peranen, J., Schreiner, R., Wieland, F., Kurzchalia, T.V., and Simons, K. (1995). VIP21/caveolin is a cholesterol-binding protein. Proc Natl Acad Sci U S A *92*, 10339-10343.

Musunuru, K. (2003). Cell-specific RNA-binding proteins in human disease. Trends CardiovascMed *13*, 188-195.

Nakamura, Y., Takayama, N., Minamitani, T., Ikuta, T., Ariga, H., and Matsumoto, K. (2000). Primary structure, genomic organization and expression of the major secretory protein of murine epididymis, ME1. Gene *251*, 55-62.

Neufeld, E.B., Wastney, M., Patel, S., Suresh, S., Cooney, A.M., Dwyer, N.K., Roff, C.F., Ohno, K., Morris, J.A., Carstea, E.D.*, et al.* (1999). The Niemann-Pick C1 protein resides in a vesicular compartment linked to retrograde transport of multiple lysosomal cargo. J Biol Chem *274*, 9627-9635.

Nielsen, L.B., Stender, S., and Kjeldsen, K. (1993). Effect of lovastatin on cholesterol absorption in cholesterol-fed rabbits. Pharmacology & toxicology *72*, 148-151.

Nissinen, M., Gylling, H., Vuoristo, M., and Miettinen, T.A. (2002). Micellar distribution of cholesterol and phytosterols after duodenal plant stanol ester infusion. Am J Physiol Gastrointest Liver Physiol *282*, G1009-1015.

Ohgami, N., Ko, D.C., Thomas, M., Scott, M.P., Chang, C.C., and Chang, T.Y. (2004). Binding between the Niemann-Pick C1 protein and a photoactivatable cholesterol analog requires a functional sterol-sensing domain. Proc Natl Acad Sci U S A *101*, 12473-12478.

Ohnmacht, G.A., Wang, E., Mocellin, S., Abati, A., Filie, A., Fetsch, P., Riker, A.I., Kammula, U.S., Rosenberg, S.A., and Marincola, F.M. (2001). Short-term kinetics of tumor antigen expression in response to vaccination. J Immunol *167*, 1809-1820.

Olson, M., Hood, L., Cantor, C., and Botstein, D. (1989). A common language for physical mapping of the human genome. Science *245*, 1434-1435.

Orso, E., Broccardo, C., Kaminski, W.E., Bottcher, A., Liebisch, G., Drobnik, W., Gotz, A., Chambenoit, O., Diederich, W., Langmann, T.*, et al.* (2000). Transport of lipids from golgi to plasma membrane is defective in tangier disease patients and Abc1-deficient mice. Nat Genet *24*, 192-196.

Ortlund, E.A., Lee, Y., Solomon, I.H., Hager, J.M., Safi, R., Choi, Y., Guan, Z., Tripathy, A., Raetz, C.R., McDonnell, D.P.*, et al.* (2005). Modulation of human nuclear receptor LRH-1 activity by phospholipids and SHP. Nature structural & molecular biology *12*, 357-363.

Palmer, R.H. (1985). Effects of fenofibrate on bile lipid composition. Arteriosclerosis *5*, 631-638.

Parini, P., Davis, M., Lada, A.T., Erickson, S.K., Wright, T.L., Gustafsson, U., Sahlin, S., Einarsson, C., Eriksson, M., Angelin, B.*, et al.* (2004). ACAT2 is localized to hepatocytes and is the major cholesterol-esterifying enzyme in human liver. Circulation *110*, 2017-2023.

Parks, D.J., Blanchard, S.G., Bledsoe, R.K., Chandra, G., Consler, T.G., Kliewer, S.A., Stimmel, J.B., Willson, T.M., Zavacki, A.M., Moore, D.D.*, et al.* (1999). Bile acids: natural ligands for an orphan nuclear receptor. Science *284*, 1365-1368.

Patel, S.B., Salen, G., Hidaka, H., Kwiterovich, P.O., Stalenhoef, A.F., Miettinen, T.A., Grundy, S.M., Lee, M.H., Rubenstein, J.S., Polymeropoulos, M.H.*, et al.* (1998). Mapping a gene involved in regulating dietary cholesterol absorption. The sitosterolemia locus is found at chromosome 2p21. J Clin Invest *102*, 1041-1044.

Peet, D.J., Turley, S.D., Ma, W., Janowski, B.A., Lobaccaro, J.M., Hammer, R.E., and Mangelsdorf, D.J. (1998). Cholesterol and bile acid metabolism are impaired in mice lacking the nuclear oxysterol receptor LXR alpha. Cell *93*, 693-704.

Peters, J.M., Hennuyer, N., Staels, B., Fruchart, J.C., Fievet, C., Gonzalez, F.J., and Auwerx, J. (1997). Alterations in lipoprotein metabolism in peroxisome proliferator-activated receptor alpha-deficient mice. J Biol Chem *272*, 27307-27312.

Philips, A.V., Timchenko, L.T., and Cooper, T.A. (1998). Disruption of splicing regulated by a CUG-binding protein in myotonic dystrophy. Science *280*, 737-741.

Pineda Torra, I., Jamshidi, Y., Flavell, D.M., Fruchart, J.C., and Staels, B. (2002). Characterization of the human PPARalpha promoter: identification of a functional nuclear receptor response element. Molecular endocrinology (Baltimore, Md *16*, 1013-1028.

Plosch, T., Bloks, V.W., Terasawa, Y., Berdy, S., Siegler, K., Van Der Sluijs, F., Kema, I.P., Groen, A.K., Shan, B., Kuipers, F.*, et al.* (2004). Sitosterolemia in ABC-transporter G5-deficient mice is aggravated on activation of the liver-X receptor. Gastroenterology *126*, 290-300.

Plosch, T., Kok, T., Bloks, V.W., Smit, M.J., Havinga, R., Chimini, G., Groen, A.K., and Kuipers, F. (2002). Increased hepatobiliary and fecal cholesterol excretion upon activation of the liver X receptor is independent of ABCA1. J Biol Chem *277*, 33870-33877.

Plosch, T., Kruit, J.K., Bloks, V.W., Huijkman, N.C., Havinga, R., Duchateau, G.S., Lin, Y., and Kuipers, F. (2006). Reduction of cholesterol absorption by dietary plant sterols and stanols in mice is independent of the abcg5/8 transporter. J Nutr *136*, 2135-2140.

Pongers-Willemse, M.J., Verhagen, O.J., Tibbe, G.J., Wijkhuijs, A.J., de Haas, V., Roovers, E., van der Schoot, C.E., and van Dongen, J.J. (1998). Real-time quantitative PCR for the detection of minimal residual disease in acute lymphoblastic leukemia using junctional region specific TaqMan probes. Leukemia *12*, 2006-2014.

Ponnambalam, S., Rabouille, C., Luzio, J.P., Nilsson, T., and Warren, G. (1994). The TGN38 glycoprotein contains two non-overlapping signals that mediate localization to the trans-Golgi network. The Journal of cell biology *125*, 253-268.

Powledge, T.M. (2004). The polymerase chain reaction. Advances in physiology education *28*, 44-50.

Radhakrishnan, A., Sun, L.P., Kwon, H.J., Brown, M.S., and Goldstein, J.L. (2004). Direct binding of cholesterol to the purified membrane region of SCAP: mechanism for a sterol-sensing domain. Molecular cell *15*, 259-268.

Rawson, R.B. (2003). The SREBP pathway--insights from Insigs and insects. Nature reviews *4*, 631-640.

Razani, B., Combs, T.P., Wang, X.B., Frank, P.G., Park, D.S., Russell, R.G., Li, M., Tang, B., Jelicks, L.A., Scherer, P.E.*, et al.* (2002). Caveolin-1-deficient mice are lean, resistant to diet-induced obesity, and show hypertriglyceridemia with adipocyte abnormalities. J Biol Chem *277*, 8635-8647.

Reischl, U., Wittwer, C.T., and Cockerill, F., eds. (2002). Rapid cycle real-time PCR: methods and applications; microbiology and food analysis (New York, Springer-Verlag).

Remaley, A.T., Rust, S., Rosier, M., Knapper, C., Naudin, L., Broccardo, C., Peterson, K.M., Koch, C., Arnould, I., Prades, C.*, et al.* (1999). Human ATP-binding cassette transporter 1 (ABC1): genomic organization and identification of the genetic defect in the original Tangier disease kindred. Proc Natl Acad Sci U S A *96*, 12685-12690.

Repa, J.J., Berge, K.E., Pomajzl, C., Richardson, J.A., Hobbs, H., and Mangelsdorf, D.J. (2002a). Regulation of ATP-binding cassette sterol transporters ABCG5 and ABCG8 by the liver X receptors alpha and beta. J Biol Chem *277*, 18793-18800.

Repa, J.J., Buhman, K.K., Farese, R.V., Jr., Dietschy, J.M., and Turley, S.D. (2004a). ACAT2 deficiency limits cholesterol absorption in the cholesterol-fed mouse: impact on hepatic cholesterol homeostasis. Hepatology *40*, 1088-1097.

Repa, J.J., Buhman, K.K., Farese, R.V., Jr., Dietschy, J.M., and Turley, S.D. (2004b). ACAT2 deficiency limits cholesterol absorption in the cholesterol-fed mouse: impact on hepatic cholesterol homeostasis. Hepatology *40*, 1088-1097.

Repa, J.J., Dietschy, J.M., and Turley, S.D. (2002b). Inhibition of cholesterol absorption by SCH 58053 in the mouse is not mediated via changes in the expression of mRNA for ABCA1, ABCG5, or ABCG8 in the enterocyte. JLipid Res *43*, 1864-1874.

Repa, J.J., Dietschy, J.M., and Turley, S.D. (2002c). Inhibition of cholesterol absorption by SCH 58053 in the mouse is not mediated via changes in the expression of mRNA for ABCA1, ABCG5, or ABCG8 in the enterocyte. J Lipid Res *43*, 1864-1874.

Repa, J.J., Liang, G., Ou, J., Bashmakov, Y., Lobaccaro, J.M., Shimomura, I., Shan, B., Brown, M.S., Goldstein, J.L., and Mangelsdorf, D.J. (2000a). Regulation of mouse sterol regulatory element-binding protein-1c gene (SREBP-1c) by oxysterol receptors, LXRalpha and LXRbeta. Genes Dev *14*, 2819-2830.

Repa, J.J., Lund, E.G., Horton, J.D., Leitersdorf, E., Russell, D.W., Dietschy, J.M., and Turley, S.D. (2000b). Disruption of the sterol 27-hydroxylase gene in mice results in hepatomegaly and hypertriglyceridemia. Reversal by cholic acid feeding. JBiolChem *275*, 39685-39692.

Repa, J.J., and Mangelsdorf, D.J. (2002). The liver X receptor gene team: potential new players in atherosclerosis. Nature medicine *8*, 1243-1248.

Repa, J.J., Turley, S.D., Lobaccaro, J.A., Medina, J., Li, L., Lustig, K., Shan, B., Heyman, R.A., Dietschy, J.M., and Mangelsdorf, D.J. (2000c). Regulation of absorption and ABC1-mediated efflux of cholesterol by RXR heterodimers. Science *289*, 1524-1529.

Repa, J.J., Turley, S.D., Quan, G., and Dietschy, J.M. (2005). Delineation of molecular changes in intrahepatic cholesterol metabolism resulting from diminished cholesterol absorption. J Lipid Res *46*, 779-789.

Roberts, G.C., and Smith, C.W. (2002). Alternative splicing: combinatorial output from the genome. CurrOpinChemBiol *6*, 375-383.

Rosen, H., Reshef, A., Maeda, N., Lippoldt, A., Shpizen, S., Triger, L., Eggertsen, G., Bjorkhem, I., and Leitersdorf, E. (1998). Markedly reduced bile acid synthesis but maintained levels of cholesterol and vitamin D metabolites in mice with disrupted sterol 27-hydroxylase gene. J Biol Chem *273*, 14805-14812.

Rosenblum, S.B., Huynh, T., Afonso, A., Davis, H.R., Jr., Yumibe, N., Clader, J.W., and Burnett, D.A. (1998). Discovery of 1-(4-fluorophenyl)-(3R)-[3-(4-fluorophenyl)-(3S)-hydroxypropyl]-(4S)-(4 -hydroxyphenyl)-2-azetidinone (SCH 58235): a designed, potent, orally active inhibitor of cholesterol absorption. J Med Chem *41*, 973-980.

Rothberg, K.G., Heuser, J.E., Donzell, W.C., Ying, Y.S., Glenney, J.R., and Anderson, R.G. (1992). Caveolin, a protein component of caveolae membrane coats. Cell *68*, 673-682.

Rothman, J.E., and Wieland, F.T. (1996). Protein sorting by transport vesicles. Science *272*, 227-234.

Rubins, H.B., Robins, S.J., Collins, D., Fye, C.L., Anderson, J.W., Elam, M.B., Faas, F.H., Linares, E., Schaefer, E.J., Schectman, G.*, et al.* (1999). Gemfibrozil for the secondary prevention of coronary heart disease in men with low levels of high-density lipoprotein cholesterol. Veterans Affairs High-Density Lipoprotein Cholesterol Intervention Trial Study Group. N Engl J Med *341*, 410-418.

Russell, D.W. (1999). Nuclear orphan receptors control cholesterol catabolism. Cell *97*, 539-542.

Russell, D.W., and Setchell, K.D. (1992). Bile acid biosynthesis. Biochemistry *31*, 4737-4749.

Saiki, R.K., Scharf, S., Faloona, F., Mullis, K.B., Horn, G.T., Erlich, H.A., and Arnheim, N. (1985). Enzymatic amplification of beta-globin genomic sequences and restriction site analysis for diagnosis of sickle cell anemia. Science *230*, 1350-1354.

Salen, G., Horak, I., Rothkopf, M., Cohen, J.L., Speck, J., Tint, G.S., Shore, V., Dayal, B., Chen, T., and Shefer, S. (1985). Lethal atherosclerosis associated with abnormal plasma and tissue sterol composition in sitosterolemia with xanthomatosis. J Lipid Res *26*, 1126-1133.

Salen, G., Shefer, S., Nguyen, L., Ness, G.C., Tint, G.S., and Shore, V. (1992). Sitosterolemia. J Lipid Res *33*, 945-955.

Salen, G., von Bergmann, K., Lutjohann, D., Kwiterovich, P., Kane, J., Patel, S.B., Musliner, T., Stein, P., and Musser, B. (2004). Ezetimibe effectively reduces plasma plant sterols in patients with sitosterolemia. Circulation *109*, 966-971.

Savkur, R.S., Philips, A.V., and Cooper, T.A. (2001). Aberrant regulation of insulin receptor alternative splicing is associated with insulin resistance in myotonic dystrophy. NatGenet *29*, 40-47.

Savkur, R.S., Philips, A.V., Cooper, T.A., Dalton, J.C., Moseley, M.L., Ranum, L.P., and Day, J.W. (2004). Insulin receptor splicing alteration in myotonic dystrophy type 2. AmJHumGenet *74*, 1309-1313.

Scharp, D.W., Kemp, C.B., Knight, M.J., Ballinger, W.F., and Lacy, P.E. (1973). The use of ficoll in the preparation of viable islets of langerhans from the rat pancreas. Transplantation *16*, 686-689.

Schultz, J.R., Tu, H., Luk, A., Repa, J.J., Medina, J.C., Li, L., Schwendner, S., Wang, S., Thoolen, M., Mangelsdorf, D.J.*, et al.* (2000). Role of LXRs in control of lipogenesis. Genes Dev *14*, 2831-2838.

Schwarz, M., Russell, D.W., Dietschy, J.M., and Turley, S.D. (1998). Marked reduction in bile acid synthesis in cholesterol 7alpha-hydroxylase-deficient mice does not lead to diminished tissue cholesterol turnover or to hypercholesterolemia. J Lipid Res *39*, 1833-1843.

Seedorf, U., Engel, T., Lueken, A., Bode, G., Lorkowski, S., and Assmann, G. (2004). Cholesterol absorption inhibitor Ezetimibe blocks uptake of oxidized LDL in human macrophages. Biochem Biophys Res Commun *320*, 1337-1341.

Sever, N., Yang, T., Brown, M.S., Goldstein, J.L., and DeBose-Boyd, R.A. (2003). Accelerated degradation of HMG CoA reductase mediated by binding of insig-1 to its sterol-sensing domain. Molecular cell *11*, 25-33.

Shelton, J.M., Lee, M.H., Richardson, J.A., and Patel, S.B. (2000). Microsomal triglyceride transfer protein expression during mouse development. J Lipid Res *41*, 532-537.

Shimano, H., Horton, J.D., Hammer, R.E., Shimomura, I., Brown, M.S., and Goldstein, J.L. (1996). Overproduction of cholesterol and fatty acids causes massive liver enlargement in transgenic mice expressing truncated SREBP-1a. J Clin Invest *98*, 1575-1584.

Shrivastava, A., and Calame, K. (1994). An analysis of genes regulated by the multi-functional transcriptional regulator Yin Yang-1. Nucleic Acids Res *22*, 5151-5155.

Shulman, A.I., Larson, C., Mangelsdorf, D.J., and Ranganathan, R. (2004). Structural determinants of allosteric ligand activation in RXR heterodimers. Cell *116*, 417-429.

Shulman, A.I., and Mangelsdorf, D.J. (2005). Retinoid x receptor heterodimers in the metabolic syndrome. N Engl J Med *353*, 604-615.

Sinal, C.J., Tohkin, M., Miyata, M., Ward, J.M., Lambert, G., and Gonzalez, F.J. (2000). Targeted disruption of the nuclear receptor FXR/BAR impairs bile acid and lipid homeostasis. Cell *102*, 731-744.

Singh, G., Charlet, B., Han, J., and Cooper, T.A. (2004). ETR-3 and CELF4 protein domains required for RNA binding and splicing activity in vivo. Nucleic Acids Res *32*, 1232-1241.

Sironi, M., Cagliani, R., Comi, G.P., Pozzoli, U., Bardoni, A., Giorda, R., and Bresolin, N. (2003). Trans-acting factors may cause dystrophin splicing misregulation in BMD skeletal muscles. FEBS Lett *537*, 30-34.

Smart, E.J., De Rose, R.A., and Farber, S.A. (2004). Annexin 2-caveolin 1 complex is a target of ezetimibe and regulates intestinal cholesterol transport. Proc Natl Acad Sci U S A *101*, 3450-3455.

Smart, E.J., Ying, Y., Donzell, W.C., and Anderson, R.G. (1996). A role for caveolin in transport of cholesterol from endoplasmic reticulum to plasma membrane. J Biol Chem *271*, 29427-29435.

Solomin, L., Johansson, C.B., Zetterstrom, R.H., Bissonnette, R.P., Heyman, R.A., Olson, L., Lendahl, U., Frisen, J., and Perlmann, T. (1998). Retinoid-X receptor signalling in the developing spinal cord. Nature *395*, 398-402.

Srikumar, R., Kon, T., Gotoh, N., and Poole, K. (1998). Expression of Pseudomonas aeruginosa multidrug efflux pumps MexA-MexB-OprM and MexC-MexD-OprJ in a multidrug-sensitive Escherichia coli strain. Antimicrob Agents Chemother *42*, 65-71.

Stangl, H., Hyatt, M., and Hobbs, H.H. (1999). Transport of lipids from high and low density lipoproteins via scavenger receptor-BI. J Biol Chem *274*, 32692-32698.

Stehlin, C., Wurtz, J.M., Steinmetz, A., Greiner, E., Schule, R., Moras, D., and Renaud, J.P. (2001). X-ray structure of the orphan nuclear receptor RORbeta ligand-binding domain in the active conformation. The EMBO journal *20*, 5822-5831.

Steinberg, S.J., Ward, C.P., and Fensom, A.H. (1994). Complementation studies in Niemann-Pick disease type C indicate the existence of a second group. Journal of medical genetics *31*, 317-320.

Stokstad, E. (2001). Reintroducing the intro course. Science *293*, 1608-1610.

Sudhop, T., Lutjohann, D., Kodal, A., Igel, M., Tribble, D.L., Shah, S., Perevozskaya, I., and von Bergmann, K. (2002). Inhibition of intestinal cholesterol absorption by ezetimibe in humans. Circulation *106*, 1943-1948.

Sudhop, T., Lutjohann, D., and von Bergmann, K. (2005). Sterol transporters: targets of natural sterols and new lipid lowering drugs. Pharmacol Ther *105*, 333-341.

Suzuki, H., Jin, Y., Otani, H., Yasuda, K., and Inoue, K. (2002). Regulation of alternative splicing of alpha-actinin transcript by Bruno-like proteins. Genes Cells *7*, 133-141.

Svanvik, N., Westman, G., Wang, D., and Kubista, M. (2000). Light-up probes: thiazole orange-conjugated peptide nucleic acid for detection of target nucleic acid in homogeneous solution. Anal Biochem *281*, 26-35.

Temel, R.E., Lee, R.G., Kelley, K.L., Davis, M.A., Shah, R., Sawyer, J.K., Wilson, M.D., and Rudel, L.L. (2005). Intestinal cholesterol absorption is substantially reduced in mice deficient in both ABCA1 and ACAT2. J Lipid Res *46*, 2423-2431.

Thurnhofer, H., and Hauser, H. (1990). Uptake of cholesterol by small intestinal brush border membrane is protein-mediated. Biochemistry *29*, 2142-2148.

Timchenko, N.A., Welm, A.L., Lu, X., and Timchenko, L.T. (1999). CUG repeat binding protein (CUGBP1) interacts with the 5' region of C/EBPbeta mRNA and regulates translation of C/EBPbeta isoforms. Nucleic Acids Res *27*, 4517-4525.

Trauner, M., and Boyer, J.L. (2003). Bile salt transporters: molecular characterization, function, and regulation. Physiological reviews *83*, 633-671.

Trigatti, B.L., Anderson, R.G., and Gerber, G.E. (1999). Identification of caveolin-1 as a fatty acid binding protein. Biochem Biophys Res Commun *255*, 34-39.

Tseng, T.T., Gratwick, K.S., Kollman, J., Park, D., Nies, D.H., Goffeau, A., and Saier, M.H., Jr. (1999). The RND permease superfamily: an ancient, ubiquitous and diverse family that includes human disease and development proteins. Journal of molecular microbiology and biotechnology *1*, 107-125.

Tugwood, J.D., Issemann, I., Anderson, R.G., Bundell, K.R., McPheat, W.L., and Green, S. (1992). The mouse peroxisome proliferator activated receptor recognizes a response element in the 5' flanking sequence of the rat acyl CoA oxidase gene. The EMBO journal *11*, 433-439.

Turley, S.D., Daggy, B.P., and Dietschy, J.M. (1991). Cholesterol-lowering action of psyllium mucilloid in the hamster: sites and possible mechanisms of action. Metabolism *40*, 1063-1073.

Turley, S.D., Daggy, B.P., and Dietschy, J.M. (1994a). Psyllium augments the cholesterol-lowering action of cholestyramine in hamsters by enhancing sterol loss from the liver. Gastroenterology *107*, 444-452.

Turley, S.D., Daggy, B.P., and Dietschy, J.M. (1996). Effect of feeding psyllium and cholestyramine in combination on low density lipoprotein metabolism and fecal bile acid excretion in hamsters with dietary-induced hypercholesterolemia. J Cardiovasc Pharmacol *27*, 71-79.

Turley, S.D., and Dietschy, J.M. (1980). Effects of clofibrate, cholestyramine, zanchol, probucol, and AOMA feeding on hepatic and intestinal cholesterol metabolism and on biliary lipid secretion in the rat. J Cardiovasc Pharmacol *2*, 281-297.

Turley, S.D., and Dietschy, J.M. (2003). Sterol absorption by the small intestine. Current opinion in lipidology *14*, 233-240.

Turley, S.D., Herndon, M.W., and Dietschy, J.M. (1994b). Reevaluation and application of the dual-isotope plasma ratio method for the measurement of intestinal cholesterol absorption in the hamster. J Lipid Res *35*, 328-339.

Uittenbogaard, A., Everson, W.V., Matveev, S.V., and Smart, E.J. (2002). Cholesteryl ester is transported from caveolae to internal membranes as part of a caveolin-annexin II lipid-protein complex. J Biol Chem *277*, 4925-4931.

Uittenbogaard, A., Ying, Y., and Smart, E.J. (1998). Characterization of a cytosolic heat-shock protein-caveolin chaperone complex. Involvement in cholesterol trafficking. J Biol Chem *273*, 6525-6532.

Umeda, Y., Kako, Y., Mizutani, K., Iikura, Y., Kawamura, M., Seishima, M., and Hayashi, H. (2001). Inhibitory action of gemfibrozil on cholesterol absorption in rat intestine. J Lipid Res *42*, 1214-1219.

Vaccaro, W., Amore, C., Berger, J., Burrier, R., Clader, J., Davis, H., Domalski, M., Fevig, T., Salisbury, B., and Sher, R. (1996). Inhibitors of acyl CoA:cholesterol acyltransferase. J Med Chem *39*, 1704-1719.

Valasek, M.A., and Repa, J.J. (2005). The power of real-time PCR. Advances in physiology education *29*, 151-159.

Valasek, M.A., Weng, J., Shaul, P.W., Anderson, R.G., and Repa, J.J. (2005). Caveolin-1 is not required for murine intestinal cholesterol transport. J Biol Chem *280*, 28103-28109.

van der Veen, J.N., Kruit, J.K., Havinga, R., Baller, J.F., Chimini, G., Lestavel, S., Staels, B., Groot, P.H., Groen, A.K., and Kuipers, F. (2005). Reduced cholesterol absorption upon PPARdelta activation coincides with decreased intestinal expression of NPC1L1. J Lipid Res *46*, 526-534.

Van Heek, M., France, C.F., Compton, D.S., McLeod, R.L., Yumibe, N.P., Alton, K.B., Sybertz, E.J., and Davis, H.R., Jr. (1997). In vivo metabolism-based discovery of a potent cholesterol absorption inhibitor, SCH58235, in the rat and rhesus monkey through the identification of the active metabolites of SCH48461. The Journal of pharmacology and experimental therapeutics *283*, 157-163.

Vanhanen, H., Kesaniemi, Y.A., and Miettinen, T.A. (1992). Pravastatin lowers serum cholesterol, cholesterol-precursor sterols, fecal steroids, and cholesterol absorption in man. Metabolism *41*, 588-595.

Vanhanen, H.T., and Miettinen, T.A. (1995). Cholesterol absorption and synthesis during pravastatin, gemfibrozil and their combination. Atherosclerosis *115*, 135-146.

Vanier, M.T., Duthel, S., Rodriguez-Lafrasse, C., Pentchev, P., and Carstea, E.D. (1996). Genetic heterogeneity in Niemann-Pick C disease: a study using somatic cell hybridization and linkage analysis. Am J Hum Genet *58*, 118-125.

Varban, M.L., Rinninger, F., Wang, N., Fairchild-Huntress, V., Dunmore, J.H., Fang, Q., Gosselin, M.L., Dixon, K.L., Deeds, J.D., Acton, S.L.*, et al.* (1998). Targeted mutation reveals a central role for SR-BI in hepatic selective uptake of high density lipoprotein cholesterol. Proc Natl Acad Sci U S A *95*, 4619-4624.

Venkateswaran, A., Repa, J.J., Lobaccaro, J.M., Bronson, A., Mangelsdorf, D.J., and Edwards, P.A. (2000). Human white/murine ABC8 mRNA levels are highly induced in lipid-loaded macrophages. A transcriptional role for specific oxysterols. J Biol Chem *275*, 14700-14707.

Venter, J.C., Adams, M.D., Myers, E.W., Li, P.W., Mural, R.J., Sutton, G.G., Smith, H.O., Yandell, M., Evans, C.A., Holt, R.A.*, et al.* (2001). The sequence of the human genome. Science *291*, 1304-1351.

Walker, N.J. (2002). A technique whose time has come. Science *296*, 557-559.

Wang, H., Chen, J., Hollister, K., Sowers, L.C., and Forman, B.M. (1999). Endogenous bile acids are ligands for the nuclear receptor FXR/BAR. Molecular cell *3*, 543-553.

Wang, H.H., Afdhal, N.H., Gendler, S.J., and Wang, D.Q. (2004). Lack of the intestinal Muc1 mucin impairs cholesterol uptake and absorption but not fatty acid uptake in Muc1-/- mice. Am J Physiol Gastrointest Liver Physiol *287*, G547-554.

Wang, H.H., and Wang, D.Q. (2005). Reduced susceptibility to cholesterol gallstone formation in mice that do not produce apolipoprotein B48 in the intestine. Hepatology *42*, 894-904.

Wang, L., Walia, B., Evans, J., Gewirtz, A.T., Merlin, D., and Sitaraman, S.V. (2003a). IL-6 induces NF-kappa B activation in the intestinal epithelia. J Immunol *171*, 3194-3201.

Wang, Z., Benoit, G., Liu, J., Prasad, S., Aarnisalo, P., Liu, X., Xu, H., Walker, N.P., and Perlmann, T. (2003b). Structure and function of Nurr1 identifies a class of ligand-independent nuclear receptors. Nature *423*, 555-560.

Wellington, C.L., Walker, E.K., Suarez, A., Kwok, A., Bissada, N., Singaraja, R., Yang, Y.Z., Zhang, L.H., James, E., Wilson, J.E*., et al.* (2002). ABCA1 mRNA and protein distribution patterns predict multiple different roles and levels of regulation. Laboratory investigation; a journal of technical methods and pathology *82*, 273-283.

Werder, M., Han, C.H., Wehrli, E., Bimmler, D., Schulthess, G., and Hauser, H. (2001). Role of scavenger receptors SR-BI and CD36 in selective sterol uptake in the small intestine. Biochemistry *40*, 11643-11650.

Whiley, D.M., LeCornec, G.M., Mackay, I.M., Siebert, D.J., and Sloots, T.P. (2002). A real-time PCR assay for the detection of Neisseria gonorrhoeae by LightCycler. Diagn Microbiol Infect Dis *42*, 85-89.

Wilhelm, J., and Pingoud, A. (2003). Real-time polymerase chain reaction. Chembiochem *4*, 1120-1128.

Willson, T.M., Brown, P.J., Sternbach, D.D., and Henke, B.R. (2000). The PPARs: from orphan receptors to drug discovery. J Med Chem *43*, 527-550.

Wilson, I.G. (1997). Inhibition and facilitation of nucleic acid amplification. Appl Environ Microbiol *63*, 3741-3751.

Wisely, G.B., Miller, A.B., Davis, R.G., Thornquest, J.A.D., Johnson, R., Spitzer, T., Sefler, A., Shearer, B., and Moore, J.T. (2002). Hepatocyte Nuclear Factor 4 Is a Transcription Factor that Constitutively Binds Fatty Acids. Structure *10*, 1225-1234.

Wittwer, C.T., Herrmann, M.G., Moss, A.A., and Rasmussen, R.P. (1997). Continuous fluorescence monitoring of rapid cycle DNA amplification. Biotechniques *22*, 130-131, 134-138.

Woodford, N., Tysall, L., Auckland, C., Stockdale, M.W., Lawson, A.J., Walker, R.A., and Livermore, D.M. (2002). Detection of oxazolidinone-resistant Enterococcus faecalis and Enterococcus faecium strains by real-time PCR and PCR-restriction fragment length polymorphism analysis. J Clin Microbiol *40*, 4298-4300.

Xie, Y., Newberry, E.P., Young, S.G., Robine, S., Hamilton, R.L., Wong, J.S., Luo, J., Kennedy, S., and Davidson, N.O. (2006). Compensatory increase in hepatic lipogenesis in mice with conditional intestine-specific Mttp deficiency. J Biol Chem *281*, 4075-4086.

Yamauchi, T., Kamon, J., Ito, Y., Tsuchida, A., Yokomizo, T., Kita, S., Sugiyama, T., Miyagishi, M., Hara, K., Tsunoda, M.*, et al.* (2003). Cloning of adiponectin receptors that mediate antidiabetic metabolic effects. Nature *423*, 762-769.

Ye, J.M., Iglesias, M.A., Watson, D.G., Ellis, B., Wood, L., Jensen, P.B., Sorensen, R.V., Larsen, P.J., Cooney, G.J., Wassermann, K.*, et al.* (2003). PPARalpha /gamma ragaglitazar eliminates fatty liver and enhances insulin action in fat-fed rats in the absence of hepatomegaly. Am J Physiol Endocrinol Metab *284*, E531-540.

Young, S.G., Cham, C.M., Pitas, R.E., Burri, B.J., Connolly, A., Flynn, L., Pappu, A.S., Wong, J.S., Hamilton, R.L., and Farese, R.V., Jr. (1995). A genetic model for absent chylomicron formation: mice producing apolipoprotein B in the liver, but not in the intestine. J Clin Invest *96*, 2932-2946.

Yu, L., Bharadwaj, S., Brown, J.M., Ma, Y., Du, W., Davis, M.A., Michaely, P., Liu, P., Willingham, M.C., and Rudel, L.L. (2006). Cholesterol-regulated translocation of NPC1L1 to the cell surface facilitates free cholesterol uptake. J Biol Chem *281*, 6616-6624.

Yu, L., Hammer, R.E., Li-Hawkins, J., Von Bergmann, K., Lutjohann, D., Cohen, J.C., and Hobbs, H.H. (2002a). Disruption of Abcg5 and Abcg8 in mice reveals their crucial role in biliary cholesterol secretion. Proc Natl Acad Sci U S A *99*, 16237-16242.

Yu, L., Li-Hawkins, J., Hammer, R.E., Berge, K.E., Horton, J.D., Cohen, J.C., and Hobbs, H.H. (2002b). Overexpression of ABCG5 and ABCG8 promotes biliary cholesterol secretion and reduces fractional absorption of dietary cholesterol. J Clin Invest *110*, 671-680.

Yu, L., von Bergmann, K., Lutjohann, D., Hobbs, H.H., and Cohen, J.C. (2005). Ezetimibe normalizes metabolic defects in mice lacking ABCG5 and ABCG8. J Lipid Res *46*, 1739-1744.

Yu, L., York, J., von Bergmann, K., Lutjohann, D., Cohen, J.C., and Hobbs, H.H. (2003). Stimulation of cholesterol excretion by the liver X receptor agonist requires ATP-binding cassette transporters G5 and G8. J Biol Chem *278*, 15565-15570.

VITAE

Mark Andrew Valasek was born in Sacramento, California, on May 3, 1977, the son of Linda Carol Valasek and Gary Mark Valasek. After graduating as valedictorian from Northwest High School, Cincinnati, OH in 1995, he entered Texas A&M University, College Station, Texas, as a Robert C. Byrd and President's Endowed Scholar, and a National Merit Finalist. He received the degree of Bachelor of Science in Molecular and Cell Biology in August 1999, with cum laude honors from Texas A&M University. During the next two years, Mark was employed as a laboratory technician and married Jeri Amanda Matcek on May 20, 2000. He entered University of Texas Southwestern Medical Center at Dallas in August 2001 and was accepted into the Medical Scientist Training Program a year later. His first child, Ruby Josephine, was born on St. Patrick's Day, March 17, 2004, and his second child, Andrew Pershing, was born on April 24, 2006.

Permanent Address: 4024 Willow Leaf Ct.
                     Dallas, TX 75212-1670